Alfred-Wegener-Institut für Polar- und Meeresforschung Bremerhaven

On the copepod response to iron-induced phytoplankton blooms in the Southern Ocean

Dissertation
zur Erlangung des akademischen Grades eines
Doktors der Naturwissenschaften
-Dr. rer. nat.-

Fachbereich 2 (Biologie/Chemie)
Universität Bremen

vorgelegt von
Sören Krägefsky

November 2008

1. Gutachter: Prof. Dr. Ulrich Bathmann

Alfred-Wegener-Institut für Polar- und Meeresforschung, Bremerhaven u.
Universität Bremen

2. Gutachter: Prof. Dr. Dieter Wolf-Gladrow

Alfred-Wegener-Institut für Polar- und Meeresforschung, Bremerhaven u.
Universität Bremen

Danksagung

Ich danke Prof. Dr. Ulrich Bathmann, daß er mir die Möglichkeit zur Promotion gab und mich sehr unterstützt hat, sowie Prof. Dr. Dieter Wolf-Gladrow, dem zweiten Betreuer dieser Promotion.

Danken möchte ich Freunden und Kollegen für die Bereitstellung von Daten, für Diskussionen und die viele kleinen und großen Hilfen. Besonders nennen möchte ich: Phillip Assmy, Boris Ciesewski, Gaby David, Corinna Dubischar, Lars Friedrichs, Bettina Fach, Lena v. Harbou, Christian Hamm, Joachim Henjes, Sandra Jansen, Christine Klaas, Karoline Klinck, Gerald Langer, Harry Leach, Barbara Niehoff, Helga Schwarz und Volker Strass. Prof. Dr. Victor Smetacek danke ich für die begeisternden Diskussionen während meines Studiums der Meeresbiologie. Mein Dank gilt den Kapitänen und Mannschaften aller Polarsternexpeditionen.

Danken möchte ich meiner Familie für ihre Unterstützung und Geduld.

Contents

1 Summary

This thesis investigates the response of copepods to increased phytoplankton abundance during two mesoscale iron-fertilisation experiments in the Southern Ocean (EisenEx in austral spring 2001 and EIFEX in austral autumn 2004), focussing on the copepods vertical migration behaviour.

The horizontal and vertical distribution of zooplankton was surveyed by acoustic methods (multi-frequency echosounder Simrad EK60), which generated data with high spatial and temporal resolution. In addition to the acoustic measurements and to identify acoustic scatterer, net samples were taken and analysed. Mathematical models which take into account the copepod behaviour and the prevailing current regimes were developed and used to interpret the population dynamics during the experiments. To assess trophic interaction within the pelagic ecosystem, ingestion rates of the dominant copepod species were measured during both experiments. During EIFEX, faecal pellet production, egg production and gut content of copepods were investigated in addition. The combination of these diverse methods provided new insights in the behaviour of copepods.

Diatom dominated phytoplankton blooms developed during both experiments within the fertilised patches. In response to the increased phytoplankton concentration, the distribution patterns of the copepods changed as follows: During EisenEx, the abundance of *Oithona similis*, a small, non diurnal migrating copepod species, increased strongly within the food-rich upper layer in the central area of the fertilised patch. The corresponding mathematical simulation study showed that most of this increase can be explained by the vertical migration behaviour of *O. similis*: Within the fertilised area during EisenEx, *O. similis* shifted its vertical distribution towards the phytoplankton enriched surface layer, while the population showed a deeper vertical distribution in the non-fertilised areas characterized by low food concentration. The deep-dwelling behaviour of *O. similis* enhances the drift out of unproductive regions and increases the chance of getting advected from a low to a high food environment. In contrast, during EIFEX, no significant change in vertical

migration of *O. similis* was observed. Here, in contrast to EisenEx, diatoms with long spines (*Chaetoceros spp.*) and heavily silicified diatoms (*Fragilariopsis kerguelensis*) dominated within the phytoplankton community. Previous studies indicate that small copepods such as *O. similis* have difficulties to feed on such diatoms.

Diel vertical migration was observed for larger copepods, such as *Ctenocalanus citer*, *Calanus simillimus*, *Rhincalanus gigas* and *Metridia lucens*. During both experiments, EisenEx and EIFEX, the acoustic survey showed that diel migrating copepods and maybe other zooplankton decreased their daytime residence inside the bloom areas. Shallow migrating species reduced their amplitude of diel vertical migration (DVM) by tens and deep migrating species by up to more than 150 metres. Similar to the effects observed in *Oithona similis*, the simulation study showed that the changes in migration behaviour of diel migrating species led to a retention of individuals inside phytoplankton-rich areas, and can largely explain the observed increase in abundance in the fertilised area, especially during EIFEX.

Further simulation results showed, that improvements in food acquisition, which could be achieved by changes in migratory behaviour, can be very substantial. The nutritional benefit gained inside the phytoplankton bloom was also reflected by data from egg production experiments. The percentage of adult females of *Rhincalanus gigas* producing eggs increased during the development of the bloom from 0 to 90%. Accordingly, faecal pellet production increased significantly during bloom development. The observed migration behaviour can be considered as a food finding strategy to cope with the strongly seasonal and horizontal patchy food supply.

Zooplankton can strongly influence fluxes of carbon and nutrients after iron fertilisation in the Southern Ocean. The mechanisms mentioned above caused both an accumulation of copepods and increased feeding pressure during the experiments. However, copepod abundances did not increase suddenly, but gradually. Accordingly, feeding pressure increased only gradually and allowed bloom formation of the phytoplankton, which encountered substantial feeding pressure, but could, due to higher growth rates, increase its biomass. Gut content analyses showed that strongly armoured diatom frustules (*Fragilariopsis kerguelensis*) or species having long spines (*Chaetoceros spp.*), were readily ingested by larger copepods during EIFEX, in contrast, *O. similis* seemed not to be able to feed on these diatoms. The faecal pellet concentration within the surface layer was not substantially higher than daily production of faecal pellets, thus, no significant accumulation of faecal pellets occurred. This observation suggests in the context with further field data that organic faecal

matter was largely degraded and respired in the surface layer.

The results of the present thesis show, that a combination of classical methods of zooplankton research with high-resolution acoustic methods and mathematical simulations can contribute significantly to a better understanding of pelagic ecosystems.

2 Zusammenfassung

Diese Dissertation untersucht die Reaktion von Copepoden auf die Entwicklung einer Blüte während zweier mesoskaliger Eisendüngungsexperimente im Südozean – EisenEx im Süd-Frühling 2001 und EIFEX im Süd-Herbst 2004. Ein Schwerpunkt dieser Untersuchungen ist dabei das vertikale Wanderverhalten der Copepoden.

Die Untersuchung der horizontalen und der vertikalen Zooplankton-Verteilung wurde mit akustischen Methoden durchgeführt (Multi-Frequenz Echolot Simrad EK 60), wodurch eine hohe zeitliche und räumliche Auflösung erreicht werden konnte. Zusätzlich zu den so gewonnenen Daten und für die Identifikation der Rückstreuer wurden Netzfänge untersucht. Mathematische Simulationsmodelle, die das Verhalten der Copepoden und die vorherrschenden Strömungsregimes berücksichtigen, wurden entwickelt und genutzt, um die Populationsdynamik in den Experimenten zu interpretieren. Für die Abschätzung der Geschehnisse im Pelagial wurden zusätzlich während beider Experimente Ingestionsraten dominanter Copepoden bestimmt. Während EIFEX wurden darüber hinaus Experimente zur Kotballenproduktion und zur Eiproduktion sowie Untersuchungen von Copepoden-Darminhalten durchgeführt. Durch die Kombination dieser verschiedenen methodischen Ansätze konnten neue Erkenntnisse über das Verhalten von Copepoden gewonnen werden.

Während beider Eisendüngungsexperimente entwickelten sich in den eisengedüngten Gebieten Phytoplanktonblüten, die von Diatomeen dominiert wurden. Die Verteilungsmuster der Copepoden als Reaktion auf die erhöhte Phytoplanktonabundanz veränderten sich folgendermaßen:

Während EisenEx erhöhte sich die Abundanz von *Oithona similis*, einer kleinen, nicht täglich wandernden Copepodenart, in der futterreichen Deckschicht im Zentrum des gedüngten Gebietes sehr stark. Die entsprechende Simulationsstudie zeigte, daß ein großer Teil dieses Anstiegs durch das vertikale Migrationsverhalten von *O. similis* erklärt werden kann: Innerhalb des gedüngten Gebiets von EisenEx veränderte *O. similis* seine Tiefenverteilung hinein in die futterreiche Deckschicht, während die Population in den ungedüngten Gebieten mit geringeren Phytoplanktonkonzentrationen eine tiefere Verteilung zeigte. Der Aufenthalt in tieferen Wasserschichten

führt, entsprechend der Simulationsstudie, zu einer erhöhten Verdriftung aus unproduktiven Gebieten und erhöht so die Chance der Copepoden, von futterarmen in futterreiche Gebiete verdriftet zu werden. Während EIFEX wurde keine signifikante Migrations-Reaktion von *O. similis* beobachtet. Während dieses Experiments dominierten im Gegensatz zu EisenEx Diatomeen mit langen, dornigen Fortsätzen das Phytoplankton. Verschiedene Studien weisen darauf hin, daß *O. similis* nicht fähig ist, diese Diatomeen effizient zu verwerten.

Ein tägliches Wanderverhalten wurde für größere Copepoden beobachtet, etwa für *Ctenocalanus citer*, *Calanus simillimus*, *Rhincalanus gigas* und *Metridia lucens*. Während beider Experimente, EisenEx und EIFEX, zeigten die akustischen Untersuchungen, daß täglich wandernde Copepoden und möglicherweise andere Zooplankter ihre Tagesaufenthaltstiefe in Gebieten mit hoher Phytoplankton-Konzentration verringerten. Flach wandernde Arten verringerten ihre Wanderungsamplituden um einige 10 Meter, während tief wandernde Arten ihre Wanderungsamplitude bis um 150 m reduzierten. Ähnlich wie im oben genannten Fall von *O. similis* zeigte die Simulationsstudie, daß die beobachtete Änderung des Wanderverhaltens der täglich wandernden Arten zu einer Retention von Tieren in den futterreichen Gebieten führte und somit der größte Teil des im Untersuchungsgebiet beobachteten Abundanzanstiegs der Copepoden, insbesondere während EIFEX, erklärt werden kann.

Die Ergebnisse der Simulationsstudie stellten des weiteren heraus, daß der Nahrungsgewinn, der durch das veränderte Wanderverhalten erzielt werden konnte, sehr bedeutend ist. Dieser starke Ernährungsvorteil innerhalb des Blütengebiets zeigte sich während EIFEX unter anderem auch in den Eiproduktionsmessungen: Die Anzahl der Eier produzierenden Weibchen von *Rhincalanus gigas* erhöhte sich im Verlauf der Blütenentwicklung von 0 auf 90%. Auch die Kotballenproduktion stieg während der Blütenentwicklung signifikant an. Die beschriebenen Veränderungen im Wanderungsverhalten der Copepoden können als eine effektive Strategie zur Futterfindung angesehen werden, um mit den Bedingungen eines stark saisonal abhängigen und horizontal sehr fleckenhaften Futterangebots zurechtzukommen.

Das Zooplankton kann große Bedeutung für die Flüsse von Kohlenstoff und Nährsalzen nach einer Eisendüngung im Südozean haben. Durch die oben genannten Mechanismen kam es während der Eisendüngungsexperimente zu einer Anreicherung von Zooplankton sowie einer Erhöhung des Fraßdruckes. Die Abundanz der Copepoden im Blütengebiet stieg jedoch nicht abrupt, sondern graduell an. Somit stieg auch der damit einhergehende höhere Fraßdruck nur graduell und ermöglichte dem Phytoplankton aufgrund höherer Wachstumsraten, trotz eines substantiellen

Fraßdruckes von Copepoden und anderen Zooplanktern, Blütenkonzentration zu erreichen. Die Analysen von Copepoden-Darminhalten zeigten, daß stark verkieselte Diatomeen-Schalen (*Fragilariopsis kerguelensis*) oder lange Borsten (*Chaetoceros spp.*), die vermutlich eine effektive Ingestion durch kleine Copepoden wie *O. similis* verhindern, während EIFEX keine fraßmindernde Wirkung auf größere Copepoden hatten. Die Kotballenkonzentrationen in der Deckschicht überstiegen nicht deutlich die tägliche Kotballenproduktion, d.h. es fand keine bedeutende Akkumulation von Kotballen statt. Dieser Befund deutet im Kontext weiterer Felddaten darauf hin, daß der größte Teil des Kotmaterials in der Deckschicht zersetzt und veratmet wurde.

Die Ergebnisse der vorliegenden Arbeit zeigen, daß die Kombination klassischer Methoden der Zooplanktonforschung mit hoch-auflösenden akustischen Methoden und mathematischen Simulationen maßgeblich zum besseren Verständnis pelagischer Ökosysteme beitragen können.

3 General Introduction

3.1 Short introduction to copepods

Copepods are very ancient aquatic crustacean. They may have originated in the Cambrian (Schminke 2007), even earlier than the insects, which made their first appearance in the Devonian 400 million years ago. Compared to the insects with more than 900,000 known species (Grimaldi & Engel 2005), a low number of roughly 20,000 copepod species is described at present (http://invertebrates.si.edu/copepod, Fig. 3.1). Nearly half of them lives in parasitic relationship with other animals (Huys & Boxhall 1991). However, while insects outnumber by far the rest of the terrestrial fauna (Eisner & Wilson 1977), copepods still outnumber the insects (Boxhall 1989, Schminke 2007). They successfully exploited allmost all aquatic habitats on earth and are found in all salinity and temperature regimes from fresh- to hypersaline water and from hot deep sea vents (Heptner & Ivanenko 2002) to sea ice (Schnack-Schiel et al. 2001). Copepods are found even in moist forest litter where they can form an important component of the cryptic microfauna (Fiers & Ghenne 2000). Copepods, in short, "occur wherever there is water as a liquid" (Schminke 2007).

Pelagic copepods, most of them having a body length of 0.5 to 2 mm, dominate the zooplankton communities in most areas of the world ocean (Longhurst 1985). In the Polar Oceans they clearly constitute the majority of the zooplankton biomass (Mumm 1993, Voronina 1998, Pakhomov et al. 2000).

In general, they are omnivorous and feed on a wide variety of food items, though the morphology of their mandibular gnathobases often shows specialisations (Michels & Schnack-Schiel 2008), which allow for effective handling of certain prey organisms or to overcome the prey's protection (e.g. strongly silicified diatom frustules). Copepods are well known for their feeding selectivity (Kiørboe 1996, Meyer-Harms et al. 1999, Irigoien et al. 2000). In structuring the phyto- and microzooplankton communities through grazing, they do not only have a direct but also an indirect effect on the cycling of carbon and nutrients in the world's oceans.

The biogeochemical fluxes in the sea modify and regulate the climate on earth,

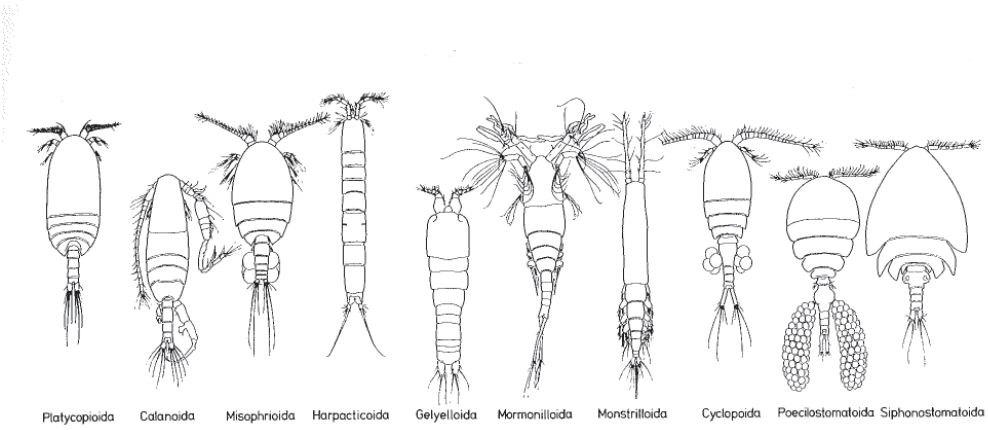

Figure 3.1: Morphology variation in the old 10 Copepod orders (after Huys & Boshall 1991). The order Poecilostomatoida has been recently moved to Cyclopoida. While *Oithona similis* belong to the Cyclopoida, all other copepods discussed in this study are calanoid copepods.

and in view of the drastic changes in earth's climate it is even more crucial to understand the impact of copepods in more detail. This includes for example how copepods successfully exploit their oceanic environment and how they cope with the strongly seasonal and patchy food supply in the mostly food-poor and cold Southern Ocean. Biological and physical processes particularly in this ocean are of crucial importance to climate regulation (Falkowski et al. 1998).

Form and features of the body construction of copepods are discussed by different authors to explain their successful colonisation of the pelagic realm and their dominance. Verity and Smetacek (1996) propose that the shape of the cephalothorax of copepods is selected by flight ability, allowing for effective predation avoidance. Turbidity in the ancient ocean is suggested by Marcotte (1999) and Bradford-Grieve (2002) as the driving force in evolution of copepod body features such as a miniaturised body form and highly sensitive sensory organelles, which allow for non-visual sensory perception. These body features are believed to have allowed for development of effective foraging strategies and predator avoidance mechanisms in the turbid environment but may still provide the basis of success in the modern ocean.

Copepods are able to swim at non-transient swimming velocities on the order of several body lengths s^{-1} while maximum velocities of several tens of mm s^{-1} are reached during escape responses (Genin et al. 2005). Their different motion behaviours imply drastic changes in relative importance of viscous to inertial forces, with shifts from low Reynolds numbers of 10^{-2} during the generation of a feeding current to Reynolds numbers up to 10^3 during escape responses (Yen 2000, van

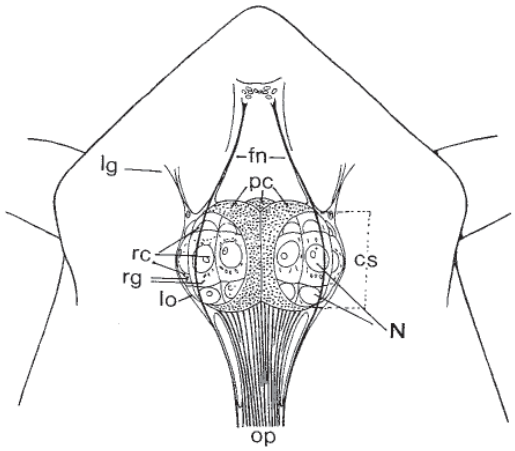

Figure 3.2: Dorsal view of the eye of a calanoid copepod (*Eucalanus elongatus*) (after Vaissiere 1961 & Dussart & Defaye 1995). cs = crystalline sphere; fn = frontal nerve; lg = ligament; lo = lateral ocellus; N = nucleus, op = optical nerve; rc = rentina cell; rg = refringent granule; pc = pigmentary cell;

Duren & Videler 2003).

Copepods perceive hydromechanical and chemical signals from prey and predator in their surrounding. Their actual motion behaviour affects these perception abilities (Bundy et al. 1998, Visser 2001), but likewise their own conspicuousness due to the hydromechanical disturbances generated by the copepod's movements (Tiselius & Jonsson 1990, Kaartvedt & Jørstadt 1996). Predator avoidance and feeding thus are essentially linked, and a switch between different prey organisms may include the switch in feeding and motional mode (Kiørboe et al 1996).

Besides sensing of their near field environment by highly sensitive mechano- and chemoreception, the sensing of copepods includes photoreception, with a so-called nauplius eye in case of calanoid copepods (Fig. 3.2). This eye is sited in the median region of the anterior cephalosome and consists of three juxtaposed ocelli, with 8 to 10 photoreceptor cells in each ocellus. The morphology of this eye varies between species, but copepods generally are considered capable of only rudimentary spatial vision (Dussart & Defaye 1995).

In the aquatic realm, light carries information not only about the near surrounding but as well as on time, vertical position of the animal and the water column content the light has passed through. The intensity and spectral composition of the underwater light field changes periodically over the year and time of day and shows a strong vertical gradient. This gradient is due the selective attenuation of solar irra-

diation in water and depends highly on the concentration of phytoplankton, yellow substances, detritus and other particle (Ragni & D'Alcala 2004). Phytoplankton causes a wavelength specific light attenuation and thus qualitative (spectral composition) and quantitative (intensity) changes in the downwelling light (Platt et al. 1994).

The spectral sensitivity of copepods is sparsely investigated. Wavelength sensitive photoresponses are observed for diel migrating copepod species (Stearns & Forward 1984, Cohen & Forward 2002) and for copepods exposed to simulated bioluminescent flashes (Buskey & Swift 1985). Recent observations with the calanoid freshwater copepod *Diaptomus nevadensis* suggest true color vision (Goodell 2008). Further investigation in the photoreception abilities of copepods may add valuably to the limited knowledge of their sensing capabilities as one feature of the copepod's body construction allowing for successful exploitation of the oceanic realm.

Some particular features of the extreme oceanic environment of the Southern Ocean are outlined in the following.

3.2 The Southern Ocean

The Southern Ocean (SO) is unique among the world's oceans and links all of them. The circulation of the SO is characterized by the Antarctic Circumpolar Current (ACC) which flows eastwards through the southern portions of the Atlantic, Indian, and Pacific Oceans. This broad ring of cold water maintains the thermal isolation of the continent.

The ACC is the largest oceanic current system on earth and the only one that completely circumflows the globe. Narrow, high-speed currents up to 50 cm s^{-1} are associated with a number of circumpolar fronts, which correspond to water mass boundaries, and are separated by broad, rather quiescent zones with current speeds less than 20 cm s^{-1}. Poleward of the ACC, cyclonic gyres are found in the embayments of the Weddell Sea and Ross Sea that contribute to a westward flowing coastal current. To the north, the Southern Ocean is bounded by the Polar Frontal Zone (or Antarctic Convergence) where the cold Antarctic surface waters meet warmer Subantarctic waters (Orsi et al. 1995). The water temperature in the Southern Ocean declines from north to south, but is generally low. North in the vicinity of the Polar Front, the sea surface temperature varies between 3°C and 5°C in summer and between 1°C and 2°C in winter. Towards the continent the sea surface temperature decreases down to -1.8°C (Orsi et al. 1995).

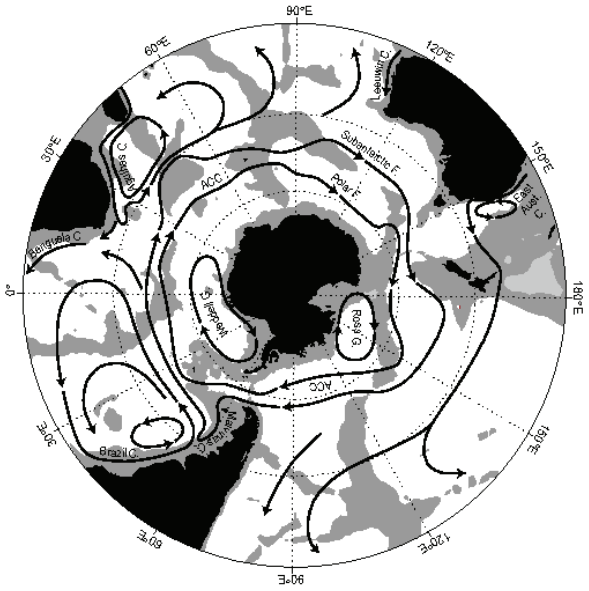

Figure 3.3: Schematic map of major currents in the southern hemisphere oceans south of 20°S. Two major fronts of the Antarctic Circumpolar Current (ACC), the Subantarctic Front and Polar Front, are shown, as well as the Weddell Sea and Ross Sea Gyres. Depths shallower than 3500 m are shaded in gray. (after Rintoul et al. 2001)

Hence the Southern Ocean is strongly zonal, and consists of distinct circumpolar bands that differ in physical and chemical parameters. These bands are mostly associated with distinct pattern in abundance and species composition of phyto- and zooplankton communities. Relatively high phytoplankton productivity and biomass is observed in the frontal regions of the ACC, but the overall production is low (Sullivan et al. 1993, Moore & Abbot 2000, Pakhomov et al. 2000, Strass et al. 2002, Pollard et al. 2002, Figure 1). The bulk of the macronutrients nitrate and phosphate which enter the euphotic zone with up-welling deep water in the south are returned unused to the ocean interior at the Polar Frontal Zone. In this region the surface water that has travelled north across the ACC mixes with Sub-Antarctic water and sinks to intermediate depths, contributing to the global overturning circulation (Falkoswki et al. 1998, Sarmiento et al. 2004).

The Southern Ocean is the largest of three major HNLC (High Nutrient Low Chlorophyll) regions of the world oceans. The inefficient use of the macronutrients in these regions is in striking contrast to other regions of the world oceans where nutrients are exhausted in the surface mixed layers over much of the growth season. Low light levels in the deep mixed layers, strong grazing pressure on phytoplankton and iron deficiency were proposed to limit the primary production in the HNLC

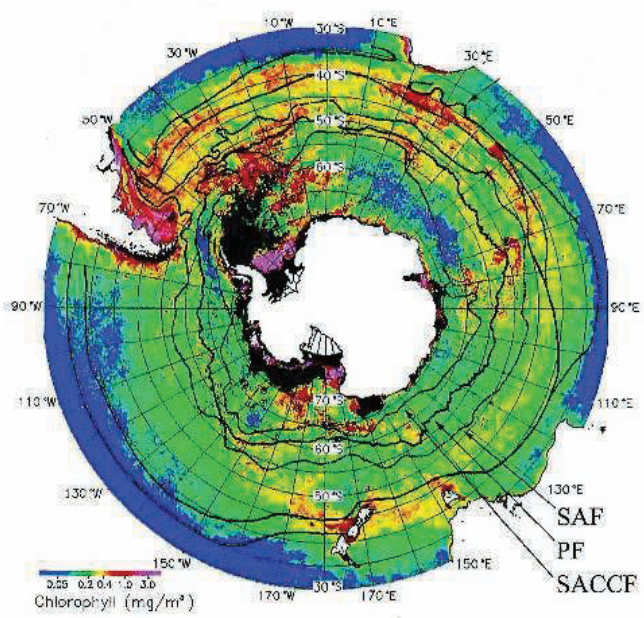

Figure 3.4: Mean chlorophyll concentration derived from SeaWiFS observations during austral summer (December 1997 through February 1998) and mean location of the major Southern Ocean fronts (after Moore & Abbott 2000). SACCF = Southern Antarctic Circumpolar Current Front; PF = Polarfront; SAF = Subantartic Front

regions (Martin 1990, Chisholm & Morel 1991).

Iron is found in bioavailable form in trace amounts in the oceans, but is an essential element of many key enzyme systems of phytoplankton (e.g. chlorophyll, redox systems). It had required the development of ultraclean techniques in the 1980's to allow for reliable measurement of the concentration of this micronutrient in the sea. These measurements followed by twelve mesoscale iron fertilisation experiments conducted since the mid-1990s, have now clearly demonstrated that iron is a main determinant of phytoplankton productivity in HNLC regions (Boyd et al. 2007). Its limiting control was suggested as early as the 1930's (Gran 1931, Hart 1934).

Non-limiting supply of iron which allow for the development of phytoplankton blooms is restricted to the continental shelf regions, where waters come in contact with sediments, and to local areas of the open Southern Ocean. Far off the continent, iron is released from melting icebergs (Raiswell et al. 2008), may be supplied by upwelling of iron-enriched sub-surface waters in frontal regions (de Baar et al. 1995), and is deposited by wind-blown dust (Jickells et al. 2005). Thus the iron supply in the Southern Ocean is sporadically and locally restricted.

Dust deposits seem to be the main source of iron in the open sea. In the modern

Southern Ocean the atmospheric dust supply is low and originates from small dust sources in Argentina, Australia and South Africa (Jickells et al. 2005). In his famous 'iron hypothesis', Martin (1990) postulated that an increased dust transport during last glaciation had increased primary production in the present HNLC regions, and this had caused a significant drawdown of atmospheric carbon dioxide (CO_2) and long-term carbon sequestering due to its export to the deep-sea. According to Martin (1990), artificial iron fertilisation would have similary, strong climate relevant effects.

In the Southern Ocean four artificial (SOIREE: Boyd & Law 2001, EisenEx: Smetacek 2001, SOFeX: Coale et al. 2004, EIFEX: Bathmann 2005) and one natural iron fertilisation experiment (KEOPS: Blain & Trull 2008) have been performed (Bathmann submitted). The iron fertilisation experiment EisenEx was conducted in austral spring 2000. The experiment was carried out in Lagrangian manner within a cyclonic eddy (approximately 120 km wide) shed by the Antarctic Polar Front (APF). An area of about 40 km^2 around a drifting buoy was fertilised with 4 tonnes of acidified iron sulphate solution ($FeSO_4$) on three occasions at intervals of 8 days. The European iron fertilisation experiment EIFEX was also conducted in the Atlantic sector of the Southern Ocean on RV Polarstern (2° E, 49° S), but took place later in the year during autumn 2004. An area of ca. 150 km^2 around a drifting buoy was fertilised with seven tons of $FeSO_4$. A second fertilisation was made 14 days later. During both EisenEx and EIFEX a diatom bloom developed in the iron fertilsed area.

However, though iron is a strong limiting factor for phytoplankton growth, the composition of the phyto- and zooplankton community, their growth and production and the degree of carbon recycling or vertical export out of the surface layer is determined by a set of physical and biological factors. Those interacting factors include iron concentration, light intensity and silicate concentration as shown for areas north of the Polar frontal zone (Frank et al. 2000, Pollard et al. 2002, Strass et al. 2002, de Baar 2005). There are conflicting observations concerning the degree of light limitation of phytoplankton growth, but most species have apparently developed a high efficiency to use the low light levels in the deeply mixed surface layers of the Southern Ocean (Mitchell et al. 1991, Tilzer 1994, Timmermanns et al. 2001, de Baar et al. 2005, Hoffmann 2008).

While species specific light constraints of growth seems to play a less important role in determination of the phytoplankton species composition, grazing is assumed to have a great effect under iron-deplete and iron-replete conditions (e.g. Hoffmann et al. 2008, Smetacek et al. 2004). Differences in the grazing impact on the different

phytoplankton species may strongly affect the functioning of the biological carbon pump, as the different phytoplankton species contribute differently to CO_2 uptake and carbon export to the deep sea. However, there is very limited knowledge about this topic and how the prey specific grazing mortality changes during transition between a low-phytoplankton to a bloom situation.

3.3 Outline of this thesis

Mesoscale iron-fertilisation experiments are a highly valuable tool for studying the behaviour of copepods which allows them to cope with the low food environment in the Southern Ocean with only sporadic and local increase in food concentration during bloom events. Besides field studies, modelling techniques have been used in this thesis as an additional investigation method to elucidate copepod impact and response during plankton blooms in the Southern Ocean.

The findings of EisenEx and EIFEX give new insight in the behavioural strategies of copepods and their possible impact on the biogeochemical cycling in the Southern Ocean. Their vertical migration behaviour, which is investigated and addressed as a food finding strategy in **manuscript 1 and 2** of this thesis, and the food switching behaviour which is discussed in this context and dealt with in **manuscript 5**, should cause significant quantitative and qualitative changes in grazing impact. Direct effects of copepod grazing on the biogeochemical cycling due to their consumption of phyto- and microzooplankton and their faecal pellet production are investigated and discussed in **manuscript 3 and 6**.

This thesis includes six separate manuscripts in total, considering different aspects of the investigation:

Manuscript 1 investigates the vertical migration behaviour of the small copepod *Oithona similis*, which does not migrate diurnally but shifted its depth distribution towards the food enriched surface layer in the phytoplankton bloom area. The effects of this migration behaviour are explored by a simulation study, using a Langrangian individual based modelling approach.

Manuscript 2 investigates the acoustically detected migration behaviour of diel migrating copepods, which adjusted their daytime residence in response to changing phytoplankton concentration in the surface layer during EisenEx and EIFEX. Also here, a Langrangian individual based modelling approach is used to explore the effects on the food gain of an individual copepod and on the horizontal distribution of the copepods in relation to the phytoplankton patch.

Manuscript 3 examines the development in copepod biomass, abundance, species and stage composition and ingestion rates inside and outside the iron-fertilised area during EIFEX. The vertical and horizontal zooplankton distribution was surveyed by net sampling and by acoustic measurements. Acoustic measurements are correlated to copepod biomass and are compared to the chlorophyll distribution. Published results of EisenEx are summarized and discussed in the context of the findings during both iron-fertilisation experiments.

Manuscript 4 analyses the reproductive response the large copepod *Rhincalanus gigas* to the build up of the phytoplankton bloom during EIFEX, by examining egg production rates and the maturation state of the gonads.

Manuscript 5 investigates the diet of three Antarctic copepods, *Calanus simillimus*, *Rhincalanus gigas* and *Pleuromamma robusta*, by means of gut content analysis of copepod individuals caught in- and outside the bloom area during EIFEX.

Manuscript 6 analyses the impact of faecal pellets to carbon sequestering during EIFEX by a combination of faecal pellet production experiments and determination of the faecal pellet standing stock in different depth strata inside and outside the bloom area.

4 List of Manuscripts

4.1 List of Manuscripts

This thesis is based on following manuscripts, partly submitted or already published. The contribution of the authors is specified on the following page.

1. **Krägefsky, S.**, Bathmann, U., Strass, V, Wolf-Gladrow, D. (in press) Response of small copepods to an iron-induced phytoplankton bloom - a model to address the mechanisms of aggregation. Marine Ecology Progress Series

2. **Krägefsky, S.**, Bathmann, U., Wolf-Gladrow, D. (to be submitted) On the migratory response of diel migrating copepods during two iron-fertilisation experiments (EisenEx and EIFEX)

3. **Krägefsky, S.**, Harbou, L. v., Jansen, S., Bathmann, U. (to be submitted) Copepod response to iron-induced diatom blooms in the Southern Ocean (EisenEx and EIFEX)

4. Jansen, S., Klaas, C., **Krägefsky, S.**, Harbou, L. v., Bathmann, U. (2006) Reproductive response of the copepod Rhincalanus gigas to an iron-induced phytoplankton bloom in the Southern Ocean. Polar Biology 29: 1039-1044

5. Kruse, S., Jansen, S., **Krägefsky, S.**, Bathmann, U. (accepted) Gut content analyses of three dominant Antarctic copepod species during an induced phytoplankton bloom (EIFEX). Marine Ecology

6. Jansen, J., Henjes, J., Friedrichs, L., **Krägefsky, S.**, Bathmann, U. (manuscript) Fate of copepod faecal pellets during an iron induced phytoplankton bloom (EIFEX) in the Southern Ocean

4.2 Contributions of the authors

Manuskript 1
Das Konzept zu dieser Simulationsstudie wurde von mir erstellt. Das Modell (Individual based model) wurde von mir entwickelt, implementiert und die Ergebnisse in Zusammenarbeit mit den Koautoren ausgewertet. Die Erstellung des Manuskripts erfolgte unter der Mitarbeit der Koautoren.

Manuskript 2
Das Konzept zu dieser Simulationsstudie wurde von mir erstellt. Das Modell (Individual based model) wurde von mir entwickelt, implementiert und die Ergebnisse in Zusammenarbeit mit den Koautoren ausgewertet. Die akustischen Felddaten, die in das Model eingehen, sind von mir erhoben und ausgewertet worden. Bei der Erhebung anderer Felddaten habe ich zum Teil mitgewirkt. Die Erstellung des Manuskripts erfolgte unter der Mitarbeit der Koautoren.

Manuskript 3
Ich habe die Akustikdaten erhoben, Netzbeprobung und die Datenauswertung in Zusammenarbeit mit den Koautoren durchgeführt. Ich habe das Manuskript in Zusammenarbeit mit den Koautoren verfasst.

Manuskript 4
S. Jansen hat das Konzept entwickelt und die Versuche durchgeführt. Die Zooplanktonbeprobung erfolgte durch alle Autoren. Das Manuskript wurde gemeinsam unter Federführung von S. Jansen verfasst.

Manuskript 5
Das Konzept wurde gemeinsam durch die Autoren entwickelt. S. Kruse hat den Darminhalt der Copepoden analysiert. Die Datenauswertung und die Erstellung des Manuskripts erfolgte gemeinsam unter Federführung von S. Kruse.

Manuskript 6
Das Konzept wurde gemeinsam durch die Autoren entwickelt. S. Jansen hat die Experimente durchgeführt. Die Datenauswertung und die Erstellung des Manuskripts erfolgte gemeinsam unter Federführung von S. Jansen.

5 Manuscript 1

Response of small copepods to an iron-induced phytoplankton bloom - a model to address the mechanisms of aggregation

S. Krägefsky[1], U. Bathmann[1], V. Strass[1], D. Wolf-Gladrow[1]

Alfred Wegener Institute for Polar and Marine Research, Am Handelshafen 12, 27570 Bremerhaven, Germany

We investigated the causes of a large increase in abundance of small copepods, in particular *Oithona similis*, that was observed during the iron fertilisation experiment EisenEx in the Southern Ocean. *Oithona* individuals showed a pronounced migratory response, by which they shifted their vertical distribution towards the progressively phytoplankton enriched surface layer in the bloom area, while outside, in the area with dilute food concentration, a substantial number of individuals resided in deeper layers. This deep-dwelling behaviour effected an increased drift relative to scarce food in the surface layer, whereas upward migration led to a gradual accumulation of animals in the bloom area. Our simulation study takes into account the particular flow field and the migratory response of *Oithona* and shows that it can explain most of the abundance increase of *Oithona* observed during EisenEx. The migratory behaviour of *Oithona* may be considered as a food finding strategy to cope with the patchy, mostly poor food environment of the Southern Ocean.

1 Introduction

Ocean currents of different spatiotemporal scales keep pelagic organisms in permanent motion. Some currents are short transient features, other circulation patterns like mesoscale eddies and meanders last for weeks or months. Large scale, persistent currents are part of the global ocean circulation, of which the Antarctic Circumpolar Current (ACC) has the largest transport ($\approx$ 130 Sv). Current speeds within the ACC can exceed 0.5 m s^{-1}.

The ACC governs the circulation of the Southern Ocean, which is the largest high nutrient - low chlorophyll (HNLC) region on earth. The phytoplankton production is strongly limited by low iron availability (Boyd et al. 2007). Blooms of large phytoplankton, whose occurrence is regionally and seasonally restricted, strongly increase phytoplankton biomass locally above the background of pico- and nanophytoplankton (Smetacek et al. 1990). These typically are mesoscale blooms and develop and decay on the time scale of weeks (Moore & Abbott 2002).

Total metazoan biomass in the Southern Ocean is dominated by copepods (Voronina 1998), whose life cycles are on the order of several months to years in this environment (Atkinson 1998, Schnack-Schiel 2001). Single phytoplankton blooms thus cover a short fraction of their generation times.

Copepods feature swimming speeds up to many body lengths per second, but still drift with the ocean currents without the ability to move against them by own horizontal movements. Vertical differences in the oceanic flow field cause a depth dependency of their drift, and vertical movements may cause significant changes in drift direction and speed.

There is increasing evidence that copepods and various other planktonic animals are able to utilise these differences to maintain their horizontal distribution or to move in a certain direction by means of their vertical migration (Bosch & Taylor 1973, Peterson et al. 1978, Kimmerer & McKinnon 1987, Batchelder et al. 2002, Emsley et al. 2005). Vertical migration as well increases or decreases the drift divergence between organisms or particles located at different depth, e. g. between migrating copepods and food items in the surface layer.

Hardy and Gunther (1935) raised this topic for the first time to explain an anti-correlated spatial distribution of phytoplankton and crustaceans found during the Discovery expedition 1926-1927 to the South Georgia whaling grounds. They hypothesised an exclusion of crustacean zooplankton from phytoplankton rich areas due to an increased drift divergence induced by an active avoidance of phytoplank-

ton dense layers. Contradictory to the supposed avoidance behaviour, however, copepods and other crustacean were attracted by abundant phytoplankton in the verification experiments done by Bainbridge (1953), whose findings thus reverse the exclusion hypothesis.

Mesoscale iron fertilisation during in situ experiments induced mesoscale phytoplankton blooms in HNLC areas. During six of twelve experiments a rise in the abundance of copepods was observed in the bloom areas. The experiments covered observation periods of 5 to 37 days, and were conducted under different abiotic conditions (Boyd et al. 2007).

During two iron fertilisation experiments in the ACC, EisenEx (Cisewski et al. 2005) and EIFEX (Strass et al. 2005), the experimental set-up provided nearly ideal conditions for surveying the response of copepods and other zooplankton to the experimentally raised food concentration in the fertilised patch. Both experiments were conducted within the nearly closed circulation of a mesoscale eddy. Hence over the course of the experiments the zooplankton within the experimental area remained nearly unaffected by an exchange with zooplankton from adjacent water.

During these fertilisation experiments, an increase of up to two to three times in the abundance of diurnally and non-diurnal vertical migrating copepods was detected inside the phytoplankton bloom area over the course of the experiments (Henjes 2007 et al., Krägefsky unpublished results). The aim of this model study is to explore the impact of the observed migratory response of non-diurnal migrating copepods in different flow fields. The question is addressed, whether and to what extent copepods utilise vertical differences in current speed and direction to their benefit to increase their food gain.

2 Model description

A Lagrangian individual based model (IBM) is used to track copepods. These copepods are exposed to different flow regimes, which are simplified representations of those at the experimental site during EisenEx and EIFEX. Individuals in the model are representative of a number of neighbouring copepods in the field. Their motional behaviour is prescribed to force a characteristic vertical distribution of copepods outside and a gradual vertical redistribution inside a bloom area accordant to the field findings during EisenEx. Basically, it forced an upward migration of individuals towards the progressively food-enriched surface layer.

The simulations account for the migratory response of adults and copepodites of

the genus *Oithona*, in particular *Oithona similis*, which clearly dominated the fraction of small-sized copepods in terms of abundance and biomass during EisenEx and EIFEX (Henjes et al. 2007). Their stage-specific development, which was observed over the course of these experiments, indicates no advanced recruitment into and within copepodite stages inside the bloom areas (Wend 2005). Consequently, the simulations do not account for copepod growth and mortality. The model study assesses the magnitude of changes in horizontal copepod distribution as solely caused by directional vertical migration of copepod individuals, drifting in a vertical sheared flow field (Fig. 1).

The path followed by a copepod individual (i) at location $\vec{X}_i$ is given by

$$\frac{d\vec{X}_i}{dt} = \vec{U}_i \tag{1}$$

$\vec{U}_i$, the actual velocity of a copepod, results from superposition of directional ($\vec{u}_{d_i}$) and random ($\vec{u}_{r_i}$) copepod motion and copepod drift with ocean currents ($\vec{u}_{m_i}$).

$$\vec{U}_i = \vec{u}_{d_i} + \vec{u}_{r_i} + \vec{u}_{m_i} \tag{2}$$

Subscript i, which denotes a single copepod, is dropped in the following. The active motion is assumed to be at a constant speed V_A. Its vertical directionality is determined by the attraction factor g_z, within a value range of -1 (moving upward at speed V_A) and 1 (moving downward at speed V_A) (see *Directionality of copepod motion*),

$$\vec{u}_d = \begin{pmatrix} 0 \\ 0 \\ V_A\, g_z \end{pmatrix} \tag{3}$$

The active motion includes an isotropically distributed random component. Its share is reduced by the copepod's directionality,

$$\vec{u}_r = \begin{pmatrix} V_A\,(1-|g_z|)\sin(\vartheta)\cos(\varphi) \\ V_A\,(1-|g_z|)\sin(\vartheta)\sin(\varphi) \\ V_A\,(1-|g_z|)\cos(\vartheta) \end{pmatrix} \tag{4}$$

The angles $\vartheta(0 \le \vartheta \le \pi)$ and $\varphi(0 \le \varphi < 2\pi)$ are chosen randomly at each time step. If $R(0,1)$ is a random variable of uniform distribution on the unit interval, φ and ϑ are given by $\varphi = 2\pi R(0,1)$ and $\vartheta = \arccos(1 - 2R(0,1))$, respectively.

Copepod individuals drift with horizontal currents, their respective drift velocity is given by

$$\vec{u}_m = \begin{pmatrix} u_s + u_{im} \\ v_{im} \\ 0 \end{pmatrix} \quad (5)$$

Copepod drift is determined by stationary flow (u_s) and flow components due to inertial oscillations (u_{im} and v_{im}). Given the copepods ability to maintain their position or to swim against vertical currents and mixing, we did not account for these vertical components of the flow field, for simplicity (see *Flow field and model geometry*).

2.1 Directionality of copepod motion

Motional behaviour of copepod individuals affects prey perception and likewise own conspicuousness. It is thus essentially linked to food gathering and predator avoidance (Tiselius and Jonsson 1990, Kaartvedt et al. 1996). Motion of a copepod individual in the model represents the displacement of the centre of mass of a number of neighbouring copepods in the field. It is assumed that this displacement is directional within a stimuli gradient due to frequent movements of individuals towards (or away from) the stimuli.

We abstract from the particular predator avoidance and foraging behaviour of individual copepods, which are addressed by other copepod IBM studies (Wiggert et al. 2005, Woodson et al. 2007). Formulation of the motional behaviour of individuals thus has a descriptive character. It forces the observed redistribution of *Oithona* within the bloom area during EisenEx, and may help to explain the absence of pronounced vertical redistribution during EIFEX.

During EisenEx a net upward migration of individuals towards and redistribution within the progressively food-enriched surface layer led to an increasingly correlated depth distribution of *Oithona* with microzooplankton and diatoms. Correlation between *Oithona* and microzooplankton declined after the middle of the experiment with diminishing abundance of a fraction of microzooplankton (e. g. dinoflagellates), which initially had increased during EisenEx (Henjes et al. 2007). In contrast, after its increase the correlation between diatom and *Oithona* depth distribution stayed constant at high values inside the fertilized patch, while there was a weak to moderate correlation in the non-fertilised area throughout the experiment (see Fig.

2).

Microzooplankton may have remained an important fraction of the diet of *Oithona* still in the bloom situation throughout the experiment (see *Discussion*). However, exclusive use of diatoms as trigger of the local attraction of *Oithona* individuals seems to be appropriate for the model purpose.

Repulsion of *Oithona* is supposed to be caused by other *Oithona* individuals and by an avoidance of the near surface layer. Attraction and repulsion of copepods is defined by the field Φ as a function of diatom carbon concentration (F; Eq. 10), local copepod density (ϱ_{zoo}) and residence depth (z), as

$$\Phi(\mathrm{x,y,z,t}) = \alpha F - \beta \varrho_{zoo} - \gamma e^{-z/z_a} \tag{6}$$

2.1.1 Attraction by diatoms

The remote prey perception ability of *Oithona* is assumed to be biased towards larger immobile particles and motile prey (Visser 2001). The floristic shift towards large diatoms, which happened during EisenEx and other iron fertilisation experiments, thus likely had potentiated attraction by diatoms. For the sake of simplicity, however, no size-dependent attraction is introduced in the model, but is assumed to be proportional to the local diatom carbon concentration (F). Its attraction is weighted by the attraction coefficient α (Eq. 6) (see *Diatom distribution*).

2.1.2 Surface avoidance

The vertical field distribution of *Oithona* further indicates an avoidance of the near surface layer. With this behaviour *Oithona* may reduce the risk of visual predation and avoid a high-turbulent environment which affects their prey perception (Maar et al. 2006). Light and thus visibility, and in many cases near surface turbulence, decays exponentially with depth (Anis & Moum 1995). Accordingly, we prescribe surface avoidance in general form by an exponential declining quantity (e^{-z/z_a}) that is determined by the decay length $\mathrm{z_a}$, independent of the actual light field and temporal changes inside the fertilised patch. We assume a constant $\mathrm{z_a} = 10$ m, thus the quantity is 1 at the surface, decays to about 0.5 at 7 m depth and is less then 0.15 at 20 m. Surface avoidance is weighted by the surface avoidance coefficient γ (Eq. 6).

2.1.3 Repulsion due to other individuals

Like other copepods, *Oithona* individuals possess a sensitive remote sensing ability. They use hydromechanic signals to detect prey and predators (Svensen & Kiørboe 2000). We assume that the presence of other individuals causes hydromechanic disturbances that potentially mask prey signals and may induce escape reactions. Predominance of hydromechanic disturbances should effect a net repulsion of animals out of a local volume, and thus act to disperse individuals within the water column. We introduce a repulsion term assuming proportionality to the local *Oithona* density (ϱ_{zoo}) and weight the repulsive effects by the repulsion coefficient β (Eq. 6).

A model individual represents an invariant number of neighbouring copepods in the field ($\mathrm{N_{oit}\,L^{-1}}$) within the range $\pm$dx/2, $\pm$dy/2 and $\pm$dz/2 around its actual position. Model individuals are initially uniformly distributed (ϱ_{o}), and $\mathrm{N_{oit}\,L^{-1}}$ corresponds to the mean *Oithona* density in the field within the depth range covered by the model domain (0 - 160 m). During EisenEx the corresponding *Oithona* density was 9 individuals $\mathrm{L^{-1}}$ including adults and copepodites in the non-fertilised area.

For the purpose of generalization , dependency on the actual field abundance is dropped and ϱ_{zoo} is given as relative abundance by use of the initial abundance (ϱ_{o}) as reference. Thus the local copepod density initially is $\varrho_{\mathrm{zoo}} = 1$ throughout the model domain.

2.1.4 Attraction factor $\mathrm{g_z}$

Net directional displacement of copepod individuals which are located in a small volume with a vertical gradient of attractive or repulsive stimuli is assumed to be along or against the gradient, respectively. The horizontal components of the gradient of Φ, which defines local attraction or repulsion in our model (Eq. 6), are much smaller than the vertical component, and are neglected. The vertical component $\partial\Phi/\partial\mathrm{z}$ is used to define the attraction factor $\mathrm{g_z}$, which by use of the hyperbolic tangent function is limited to the range of -1 to 1.

$$\mathrm{g_z}(\mathrm{x,y,z,t}) = \tanh\left(\frac{\epsilon}{2}\frac{\partial\Phi}{\partial\mathrm{z}}\right) \tag{7}$$

The attraction factor $\mathrm{g_z}$ forces a directional up- or downward motion of copepod individuals in the model and proportionally reduces the share of random motion ($\vec{\mathrm{u}}_{\mathrm{r}}$) (see Eq. 3, 4). The constant scaling parameter ($\epsilon = 10$) determines the slope of the response curve and is chosen arbitrarily.

2.2 Swimming speed

Actual activity of neighbouring copepods covers different patterns of motion. In feeding experiments *Oithona similis* showed low sinking of the order of 0.1 mm s^{-1} and rapid escape and food gathering jumps at a velocity of $\sim$ 14 mm s^{-1} (Svensen and Kiørboe 2000). Accounting for the low frequency of jumps ($\sim$ 8 jumps min^{-1}) and jump length ($\sim$ 2 mm), the observed motion (sinking and jumping) equates to a nominal speed of about 0.4 mm s^{-1}. Uchima and Hirano (1988) found a nominal swimming speed of *Oithona davisae* of roughly 0.7 mm s^{-1}, e. g. leaping and paddling forward. Activity may be higher in the stimuli rich oceanic environment. Nevertheless, we assume slow constant motion of the model individuals at speed V_A in the range of 0.5 to 1 mm s^{-1}, during different model runs.

2.3 Flow field and model geometry

The flow field at the experimental site during EisenEx and EIFEX was governed by the quasi-steady geostrophic eddy circulation. Superimposed fluctuations were mainly associated with tides and inertial oscillations. During both experiments the patch with the iron-induced diatom bloom circled around the eddy centre. Under the assumption of an ideal symmetric eddy circulation, the copepod drift in relation to the bloom patch is accurately modelled within a channel flow.

Stationary flow along the channel is defined by means of geostrophic velocity profiles derived from deep CTD-profiles (Conductivity Temperature and Depth probe) measured during EisenEx. During EIFEX, measurements with an Acoustic Doppler Current Profiler (ADCP) attached to a buoy, which was drifting with the fertilised patch, provide direct measurements of the vertical shear of the flow field along its path. Measurements were low-pass filtered to remove tidal components and fluctuations caused by inertial oscillations. The depth-dependent stationary flow in the x-direction, $u_s(z)$, is defined using the mean velocity magnitude of residual flow in the EIFEX case, while v_s and w_s are zero (Fig. 1a).

Flow fluctuations superimposed on the stationary flow field are taken into account by defining an idealised inertial motion:

$$\begin{aligned} u_{im}(z,t) &= V_H \times \sin\left(2\Omega \sin\left(\frac{2\pi}{360} \times lat\right) \times t\right) \\ &\quad \times \left(0.5 - 0.5 \times \tanh\left(h_t^{-1}(z - z_{mt})\right)\right) \end{aligned} \tag{8}$$

and

$$\begin{aligned} \mathrm{v_{im}}\left(\mathrm{z,t}\right) &= V_H \times \cos\left(2\Omega \sin\left(\frac{2\pi}{360} \times lat\right) \times t\right) \\ &\quad \times \left(0.5 - 0.5 \times \tanh\left(\mathrm{h_t^{-1}}\left(\mathrm{z - z_{mt}}\right)\right)\right) \end{aligned} \tag{9}$$

The respective time dependent velocity components at the surface are given by the amplitude, V_H, and the second factor of the equation. The third factor defines the depth dependency, with $\mathrm{z_{mt}}$ denoting for the depth of the mixed layer (see Tab. 1).

The drift of copepod individuals is treated as a movement relative to the upper patch centre which is fixed in the model runs. The patch centre is located at the middle of the channel-like model domain. The model domain is bounded by the vertical planes $-by$ and $+by$ along the channel and by $-bx$ and $+bx$ perpendicular to it (Fig. 1b). In- and outflow conditions of copepod individuals at these boundaries are defined as follows.

Drift differences on the order of kilometres per day between deep-dwelling copepods and the phytoplankton patch within the surface layer are comparatively moderate in proportion to the length of the patch trajectory around the eddy centre (in the range of 200 – 300 km). Despite circular trajectories in the eddy flow field, deep-dwelling individuals did not drift a second time into the bloom area within the time-frame of the experiments. For modelling purposes, there is thus no need to track the path of copepod individuals outside the area covered by the model domain. Individuals permanently leave the model domain at the boundaries $-bx$ and $+bx$.

Inflow of individuals into the model domain has to sustain a characteristic out-patch distribution of copepods, which ensures a characteristic flow of deep-dwelling copepods towards the bloom area. It rises gradually during the simulation and corresponds to a dynamic equilibrium of repulsive and attractive effects (see *Model sensitivity*).

A steady state distribution develops during an initialisation period as a result of vertical migration of inward-drifting copepods, which initially pass through an area with permanently low diatom concentration. Depending on direction of the stationary flow ($\mathrm{u_s}$), the respective areas are left to $-bx_e$ or right to $+bx_e$. These are inner planes at which we sample the actual inward flow of copepod individuals. A correspondent actual inflow of new individuals into the model domain is forced at the outer boundary $-bx$ or $+bx$, respectively. It keeps recent changes in copepod

distribution and allows for further changes during the drift of new individuals passing through the area.

The flow component that determines the copepod drift ($\vec{u}_m$) in the y-direction is oscillatory or zero, if we account for inertial motion (Eq. 9) or not, respectively. Individuals which exit at $-by$ or $+by$ are wrapped around and enter the model domain at the opposite side.

2.4 Diatom distribution

Diatom stock is not a prognostic variable in the model. The simulated diatom distribution follows the observed progression in the field (Assmy et al. 2007), but with the following simplifications: In the horizontal model plane the bloom area has a circular or elliptical shape. We omit small-scale field variability and assume a horizontal bell-shaped diatom distribution. For the vertical, we assume a uniform distribution in the mixed layer and a sharp decline in concentration below.

The diatom distribution (F) is given in terms of diatom carbon concentration [μmol C L^{-1}]:

$$F(x, y, z, t) = (C_0 + (C_s(t) - C_0) \times f_h) \times f_v + C_{sub} \tag{10}$$

In this equation $C_o = 0.74$ μmol C $L^{-1}$is the surface diatom carbon concentration in the non-fertilised area. The time-dependent diatom carbon concentration at the patch centre $C_s(t)$ follows the increase of its mean concentration in the upper 50 meter over the course of EisenEx (Figure 1a).

The horizontal pattern of diatom distribution is determined by f_h, specifying a bell-shaped distribution,

$$f_h = e^{-\frac{\pi^2}{2}(\frac{x^2}{a^2}+\frac{y^2}{b^2})} \tag{11}$$

The semimajor axis, a, and semininor axis, b, give the extent of the bloom area, which increases in time. Simulating a circular bloom area (a = b), these are equal to the patch radius, $r_p(t)$ (Eq. 12). If an elliptical bloom area is simulated, a(t) is identical to $r_p(t)$, while a constant a/b ratio is kept.

The bloom area spreads in time. We assume a constant dilution time scale $\tau = 10$ d, which characterizes the spreading of the fertilised patch during EisenEx and other iron-fertilisation experiments (Boyd et al. 2007). Patch spreading is given by an increasing patch radius,

$$r_p(t) = r_{p0}\sqrt{e^{t/\tau}} \tag{12}$$

Vertical decline of surface diatom carbon concentration is determined by f_v, defined as

$$f_v = 0.5 - 0.5 \times \tanh(h_t^{-1}(z - z_{mt})) \tag{13}$$

The steepness of the concentration decline at the mixed layer base is regulated by the slope factor h_t, which is set to a constant value of $h_t = 15$ m in all simulations.

Substantial numbers of diatoms were observed below the mixed layer during EisenEx and EIFEX, without temporal trend or differences between the fertilised and non-fertilised area. Diatom carbon concentration found at 150 m amounted to 8 – 24% of surface concentration outside and 1-5% at the highest diatom concentration inside the bloom area during EisenEx (Assmy et al. 2007).

To fit the observed field distribution, we add a share which is constant in time, C_{sub}, to the variable share of the diatom distribution (Eq. 10). C_{sub} defines a profile with zero concentration in the upper layer and sharp concentration increase towards the bottom of the mixed layer. The concentration reaches a maximum below the mixed layer and declines linearly beneath with increasing depth. For simplicity, we assume a constant concentration reached at 160 m (vertical extent of the model domain) in all simulations, which is chosen to match the field distribution during EisenEx (Fig. 1a). It is equivalent to a percentage of 18% and 3% relative to the surface concentration outside and the highest diatom carbon concentration inside the bloom area, respectively.

$$C_{sub} = 0.45 \times \left(1 - 0.7 \times \frac{z - z_{mt}}{Z_{max} - z_{mt}}\right) \times \left(0.5 + 0.5 \tanh\left(h_t^{-1}(z - z_{mt})\right)\right) \tag{14}$$

2.5 Initialisation

The development of a diatom patch is initiated after a spin up time of 7 model days. During this time a steady state vertical distribution of *Oithona* individuals is reached under the low diatom 'outpatch' condition (see *Flow field and model geometry*). After initialisation the simulation spans a period of 21 days, corresponding to the duration of the iron fertilization experiment EisenEx. A definition of the model parameters and range of values used are listed in Table 1.

3 Results

The stochastic and directional motion of copepod individuals modifies the overall vertical copepod distribution in time. Distributional changes are represented in the following in terms of the development of the correlation coefficient between diatom carbon and copepod depth distribution. This vertical correlation is denoted by c_v, the horizontal correlation of copepod and diatom carbon distribution by c_h. If not otherwise stated c_v refers to the vertical correlation at the patch centre ($r \leq 1000$ m) followed by a parenthesised c_v value referring to the entire inpatch area.

The horizontal distribution of copepods is given in terms of a relative abundance that refers to the initial abundance per unit area. The characteristic relative abundance within the outpatch area thus is 1. Changes in copepod abundance within a certain depth interval are referenced to the corresponding mean outpatch abundance and are given as percent change.

Uncertainty in the determination of the actual depth distribution in the field (see Discussion) requires consideration of a characteristic range of vertical steady state distributions outside and migratory responses of Oithona inside the bloom area, forced by varying attraction (α) and repulsion weights (β, γ). This range is characterized by a relatively stable increase in abundance at the patch centre (see *Model sensitivity*).

3.1 Reference run

In terms of the diatom attraction weight (α) and repulsion coefficient (β), the range of values at which a moderately varying abundance increase is observed is centred at $\alpha = 4$ and $\beta = 2$, if the surface avoidance weight is $\gamma = 1.5$. These settings are used for a reference simulation, by which a strong directional response along the diatom gradient is forced and a pronounced directionality of copepod motion due to repulsion by other individuals. Swimming speed of copepods is assumed to be $V_A = 1\,\mathrm{mm\,s^{-1}}$.

The vertical extent of the food rich layer ($z_{mt} = 70$ m) and the flow field are given with regard to the situation during the iron fertilisation experiment EisenEx. Inertial oscillations with an amplitude $V_H = 0.2\,\mathrm{m\,s^{-1}}$ are superimposed on the geostrophic flow field.

Using this set of parameters the vertical correlation between copepods and diatom carbon (c_v) increases asymptotically to 0.83 at the patch centre and 0.77 within the entire inpatch area, respectively, which is close to the lower limit of c_v derived from

observations during EisenEx (Fig. 2). After the initialisation period a constant c_v value of 0.67 is reached in the outpatch area. This value represents the upper limit of c_v within the low-food environment during EisenEx (Fig. 2).

During the initialisation period the homogenous initial copepod distribution changes towards a higher number of animals within the diatom enriched layer until a steady state distribution is reached (Fig. 3a). In the patch there is a continuous copepod immigration into the diatom rich layer, which is supplied by an inward drift of animals from surroundings in deeper layers and their subsequent upward vertical migration (Fig. 3b). Supply of deep-dwelling individuals counters the depletion of *Oithona* stock below the mixed layer in the patch area. Its decrease is moderate and exceeds a percentage decrease of 50% relative to the abundance outside the patch only towards the end of the experiment. In contrast, the number of *Oithona* individuals at the patch centre ($r \leq 1000$ m) gradually increases by 150% in the mixed layer and by 70% in total (160m) relative to the outpatch abundance.

The horizontal copepod and diatom distribution is highly correlated after day 5 in the fertilised area ($c_h > 0.9$, progression not shown here). Significant abundance increase of *Oithona* in the diatom rich surface layer (> 15%) is limited to an area enclosed by a radius of about 0.6 r_p around the patch centre at day 21. Consequently, net abundance increase (0 - 160 m) is limited to the inner part of the patch area where the increase in diatom carbon concentration exceeds approximately 20 % of its increment at the patch centre (Fig. 4 a, b).

3.2 Sensitivity study

3.2.1 Effects of varying α, β and γ

For the sensitivity study the weights α, β and γ have been changed in the range of 0.5 - 8, 0 - 4 and 1 - 2, respectively, while keeping all other parameters constant and equal to their standard values (Table 2). With increasing diatom attraction coefficient (α) the vertical steady state outpatch distribution of *Oithona* shows a progressively increased abundance within the upper layer and depletion below (Fig. 5a). In the patch, copepod abundance within the diatom rich layer steeply increases with increasing diatom attraction coefficient (α) by a maximum of 150% at an α value of 4 (Fig. 5b). With further increase of α the relative abundance increase is gradually weakened towards 90% at an α of 8, corresponding to a $\alpha : \beta$ ratio of 4 (Fig. 5b).

With increasing repulsion coefficient (β) the vertical steady state outpatch dis-

tribution of *Oithona* shows a progressively declining number of individuals within the mixed layer and changes towards a homogenous vertical distribution (Fig. 5c). Inpatch abundance within the diatom rich layer increases by 50% at a β of 0.5 ($\alpha : \beta = 8$) and steeply rises towards a maximal increase at a $\alpha : \beta$ ratio of 2 by 150% (Fig. 5d). With further increment of β the abundance increase is gradually weakened towards 110% at a β of 4, corresponding to a $\alpha : \beta$ ratio of 1 (Fig. 5d).

The progression of the net abundance increase (0 - 160 m) is dampened in relation to the increase within the mixed layer. Within a range of α and β weights, corresponding to a $\alpha : \beta$ ratio of 1 - 4, the total abundance increase varies from 50% to 70%. The abundance below the mixed layer is reduced by 30% relative to the outpatch abundance at a $\alpha : \beta$ ratio of 1, however, declines within this range towards a nearly complete exhaustion with increasing $\alpha : \beta$ ratio. (Fig. 5 b, Fig. 5 d).

Changing the surface avoidance coefficient (γ) within a range of 1 - 2 has a minor effect on the model outcome . The vertical correlation between food and copepod distribution declines at the patch centre from $c_v = 0.87$ to 0.80 and outside the patch from $c_v = 0.69$ to 0.65 with increasing γ (Table 2). Abundance increase at the patch centre does not change significantly within the mixed layer and in total (0 - 160 m), respectively (Table 2).

3.2.2 Effects of varying mixed layer depth

The effect of different mixed layer depths was explored within the z_{mt} range of 20 - 120 m, which affects the vertical diatom distribution (see Diatom distribution) and the profile of inertial motion (Eq. 8) in the model. Other settings were retained unchanged with respect to the reference simulation.

The steady state distribution of *Oithona* which develops outside the patch is changed with changing depth of the mixed layer. Mean ϱ_{zoo} within the mixed layer increases from 1.25 to 1.4 when z_{mt} changes from 20 to 50 m, and decreases again with increasing z_{mt} towards 1.18 for a depth of 120 m (Fig. 6 a). Mean ϱ_{zoo} below the mixed layer decreases nearly linearly from 0.95 to 0.45 within the z_{mt} range from 20 – 120 m (Fig. 6 a).

The percentage increase in copepod abundance which is observed within the mixed layer at the patch centre relative to the respective outpatch abundance is reduced nearly linearly with increasing z_{mt} (Fig. 6b, triangles). Maximum percentage increase is 250% within the shallowest mixed layer (20 m). The minimum percentage

increase is 50%, reached within the deepest mixed layer (120 m).

The net abundance increase (0 - 160 m) rises towards a maximum increase of about 70% for z_{mt} in the range 40 to 80 m (Fig. 6b, filled circles). Within this range the abundance below the mixed layer declines nearly linearly with increasing z_{mt}, and shows a percentage decrease relative to the respective outpatch abundance of 20% for a z_{mt} of 40 m and more than 70% for a z_{mt} of 80 m (Fig. 6b, open circles).

The correlation coefficient of the vertical diatom carbon and animal distribution, c_v, follows the progression of net abundance increase within the bloom area. It increases towards 0.75 and subsequently declines again towards 0.6. Within the outpatch area c_v increases asymptotically with deepening mixed layer depth towards 0.75 (Table 2). The horizontal correlation coefficient of diatom carbon and copepod distribution (c_h) is only weakly affected by different mixed layer depths and varies in the range from 0.87 to 0.91 at day 21 (Table 2).

3.2.3 Effects of copepod swimming speed

Along with a lower swimming speed, V_A, deep-dwelling animals have a reduced probability of entering the shallower transition zone between food depleted and food enriched layer, where upward migration is forced along a steep diatom gradient.

Using a swimming speed of 0.5 mm s^{-1} (as compared to 1 mm s^{-1} in the reference run), c_v increases towards 0.87 in the patch centre and 0.79 within the entire food patch area, respectively, and is 0.71 outside the patch (Table 2). The horizontal copepod and diatom carbon distribution is highly correlated ($c_h > 0.9$) after day 7, which is slightly delayed with respect to the reference run. The abundance increase of *Oithona* is weakened towards a percentage increase of 130% and 60% relative to the outpatch abundance within the mixed layer and in total (0 - 160 m), respectively (Table 2).

3.2.4 Effects of different flow fields

To explore the impact of inertial oscillation, this flow component is simulated without stationary flow ($u_s(z) = 0$). The correlation between vertical copepod and diatom carbon distribution, c_v, approaches a value of 0.83 in the patch centre and 0.75 in the total bloom area after two weeks, c_v is 0.67 in the outpatch area (Table 2). The horizontal distribution of copepods and diatom carbon is highly correlated and peaked at 0.94 at day 6, but gradually decreases towards 0.85 at day 21 (Table 2). Percentage increase in copepod abundance at the patch centre is 140% within

the diatom rich layer relative to the outpatch abundance. Net abundance increased by 50% (0 - 160 m) until day 16 (Table 2).

Inertial oscillation causes a wobbling of the surface layer. The resultant circular displacement of the diatom patch changes the local vertical gradients of diatom concentration and copepod abundance inside the bloom area and in its periphery. The actual migration behaviour of a deep-dwelling individual is subject to the steepness of these gradients (Fig. 7a). Upward migration is increasingly forced with increasing surface diatom concentration when diatom attraction outweighs the repulsive effects of other individuals. This dependency causes a net displacement of copepods along the horizontal diatom gradient towards the centre of the bloom area (Fig.7b). Net abundance increase within the bloom area is gained from the surroundings and depends on the ratio of the area affected by the wobbling diatom patch to the diatom patch area itself, A_i. Regarding a circular food patch, A_i is given by

$$A_i = \frac{(r_p + r_i)^2}{r_p^2} \tag{15}$$

as a function of the food patch radius, r_p, and radius of inertial oscillation, r_i. In the simulations r_i is ca. 1850 m and the area ratio is about 1.5, 1.3 and 1.2 for patch areas of 300, 600 and 1200 km^2, respectively.

Inertial oscillation which is superimposed on a stationary flow field contributes significantly to the abundance increase inside the bloom area and causes deflection of the paths of copepod individuals towards the patch centre line (Fig. 7c).

Simulating the EisenEx flow field without inertial oscillation, c_v increases towards 0.81 at day 11 at the patch centre and towards 0.73 in the total bloom area, c_v is about 0.67 outside the patch. The increase of c_h is weakened and flattened in comparison to the reference simulation with inertial oscillation. It approaches 0.82 towards day 11 after fertilisation. *Oithona* abundance increases at the patch centre by 115% and 40% within the mixed layer and over 160 m, respectively, compared to an increase by 150% and 70% with superimposed inertial oscillations (Tab. 2).

In a further simulation, we investigate the effects caused by the differences in the stationary EisenEx and EIFEX flow fields. In the simulation considering the EIFEX flow field with superimposed inertial oscillations, c_v increases towards 0.8 and 0.75 at the patch centre and in the total bloom area, respectively, and is about 0.67 in the outpatch area. The horizontal correlation between copepod and diatom carbon distribution approaches 0.93 towards day 8 after fertilisation. *Oithona* abundance in the centre of the bloom area increases by 145% within the mixed layer and shows

net increase (160 m) by 65% (Fig. 4 c), which is slightly less than the respective increases in the EisenEx flow field.

3.2.5 Effects of diatom patch extent

To explore the impact of the diatom patch dimension and shape, firstly r_p is doubled compared to the reference run, the surface area thus is increased by a factor of four. The patch radius increases to 20 km at day 21 in the respective model runs. Within the EisenEx flow field and retaining other parameters unchanged with respect to the reference simulation, c_v is slightly reduced and increases towards 0.82 at the centre and 0.73 within the total bloom area (Table 2). The horizontal correlation of diatom and copepod distribution varies periodically with inertial oscillations and peaks at day 11 with a c_h of 0.8 ($\pm$0.015) and gradually decreases thereafter to 0.74 at day 21. The relative copepod abundance at the patch centre is raised by 120% and 45% within the mixed layer and over 160 m, respectively (Table 2). Like the results of the reference run, net abundance increase is limited to the inner part of the patch area where the increase in diatom concentration exceeds approximately 20% of its increment at the patch centre. However, there is a strong depletion of animals inside the food patch upstream at a distance $> r_p/2$. The doubling of the patch radius leads to a reduced increase in copepod abundance at the patch centre which is equivalent to 88% and 86% of the increase during the reference simulation within the mixed layer and over 160 m, respectively.

Prescribing an elliptical shape for the diatom patch (semimajor axis (a) /semiminor axis (b) = 0.5, a = 20 km at day 21) and aligning the semimajor axis (a) in the direction of the stationary flow, c_v increases to about 0.82 at the centre and 0.7 within the total bloom area (Table 2). The horizontal correlation is maximal at day 12 ($c_h = 0.88$) and declines thereafter towards 0.83 (day 21) while it varies periodically. The copepod abundance at the patch centre is raised by 140% and 60% within the mixed layer and over 160 m, respectively, equivalent to an increase of about 96% and 94%, respectively, relative to the increase in the reference run (Table 2).

3.3 EIFEX

In order to approximate the field situation during EIFEX, a mixed layer depth of 120 m and a final patch radius of 20 km (day 21) is simulated. During the model run c_v is 0.75 outside the patch, c_v increases to 0.8 at day 10 at the centre of the

bloom area but declines again towards 0.76 at day 21. Within the total bloom area it decreases continuously to 0.59. Horizontal correlation between diatom carbon concentration and *Oithona* abundance, c_h, increases to 0.82 at day 14 and decline thereafter towards 0.78 (day 21) while varying periodically with inertial oscillations. The copepod abundance at the patch centre shows a percentage increase of 35% relative to the outpatch abundance within the mixed layer and a net increase by 20% (160 m, Fig. 4 d).

4 Discussion

In this simulation study, we have explored the magnitude of changes in horizontal copepod distribution which are caused by directional vertical migration in a bloom area in the vertical sheared flow fields at the sites of the iron fertilisation experiments EisenEx and EIFEX.

4.1 EisenEx field findings and simulation results

During EisenEx, *Oithona* was sampled at the discrete depths of 10, 20, 40, 60, 80, 100 and 150 m at 5 outpatch and 13 inpatch stations with a Niskin bottle with a sampling volume of 12 L. Estimates of the abundance in different depth strata are based on trapezoidal integration of the estimates at the discrete sampling depths (Henjes et al. 2007). The mean outpatch abundance of *Oithona* copepodites and adults was 9 individuals L^{-1} (0 - 150 m), which corresponds to $\varrho_{zoo} = 1$ in the simulation study.

The vertical distribution of *Oithona* was centred below or near the bottom of the mixed layer outside the fertilised area. The depth-integrated abundance over the depth range 60 – 150 m and 80 – 150 m, respectively, amounted to 60 % (30 – 95%) and 30 % (20 – 55%) on average of the integrated abundance in the upper 60 m of the water column. The relative amount of deep-dwelling copepods (60 – 150 m) was 75% on average without the first outpatch station with a comparable shallow *Oithona* distribution.

The integrated abundances equate to a mean outpatch concentration of ca. 13.5 individuals L^{-1} in the upper 60 m. Generally, the single abundance estimates showed large variability. Sampled abundance varied in the range of 3 - 25, 3 - 25, 1.8 - 7.2 and 0 – 5.6 individuals L^{-1} at 60, 80, 100 and 150 m outside the patch, while the mean abundance was 15, 11, 3.8 and 1.7 individuals L^{-1}, respectively (Fig. 8).

The simulated vertical outpatch distribution corresponds approximately to the mean abundances sampled at different depths during EisenEx if a food attraction coefficient $\alpha = 6$ and a repulsion coefficient $\beta = 2$ is used (Fig. 8). However, in view of the mean vertical distribution without the first outpatch station, this simulated vertical distribution may underestimate the proportion of individuals which reside near below the surface layer.

Compared to EisenEx, large number of *Oithona* individuals were sampled during EIFEX at 150 m (11 individuals L^{-1} on average) and even at depths of 200 and 250 m (see below). This large number of markedly deep-dwelling individuals could imply that the sparse vertical resolution and the very small sampling volume had caused an underestimate of the number *Oithona* individuals below 100 m during EisenEx. Consequently, in the simulation study we account for a range of vertical *Oithona* distributions outside the patch.

Whether very deep-dwelling *Oithona* ($>$ 150 m) respond with upward migration below a phytoplankton bloom or whether they occasionally re-enter the upper 150 m of the water column is unknown and not covered by the simulation study.

At the patch centre, *Oithona* individuals migrated into the phytoplankton-rich surface layer. A transient downward displacement of individuals occurred after two storm events (at the end of the first and the second week of EisenEx). The strong decrease in abundance below the mixed layer at the patch centre which is shown in simulations (e.g. α =6, $\beta = 2$) was only observed at single stations.

The number of *Oithona* individuals at patch centre increased by up to 15 individuals L^{-1} in the upper 60 m of the water column over the course of EisenEx. This increase is 1.5-times the integrated outpatch abundance (m^{-2}) in the deeper layer between 60 – 150 m and 3-times the integrated abundance over the depth range 80 – 150 m. Sampling suggests net increase of up to 7 individuals L^{-1} (0 -150 m), which would correspond to an increase by 80% of the mean outpatch abundance, but maybe is not properly assessed due to the low vertical resolution. Moreover, *Oithona* was only sampled near or at the centre of the phytoplankton patch. Sampling thus gives no information about the horizontal distribution pattern of *Oithona* within the fertilised area.

The simulation results show a quite stable net increase in *Oithona* abundance at the patch centre by approximately 70% of the outpatch abundance in the $\alpha : \beta$ ratio range of 2-3 (Fig. 5b,c). Simulation results with an elliptical shaped patch approximating the field situation during EisenEx show little less abundance increase compared to the standard patch simulation (Tab. 2). In both cases a significant

abundance increase is limited to the central patch area and show maximal increase at the patch centre. In the simulation with α =6 and $\beta = 2$ (a/b=0.5; Tab. 2), the net abundance increase is by ca. 60% at the patch centre and by 25% on average in the area where the surface diatom carbon concentration are more than two-fold increased relative to the outpatch (180 km^2). The respective abundance increases are by ca. 110% and by 60% in the mixed layer.

4.1.1 Effects of the model simplifications

In the field, storm events forced deepening of the mixed layer depth over the course of EisenEx from 30 - 40 m at the very beginning of the experiment to 80 - 90 m at the end (Cisewski et al. 2005). The depth distribution of the diatoms observed during EisenEx would correspond to a vertical diatom distribution in a simulation with variable z_{mt}, increasing from ca. 60 m to 80 m. In the simulation, shallowing (60 m) or deepening (80 m) of z_{mt} shows converse effects on the abundance increase within the mixed layer and abundance decrease below (Fig. 6), and a constant mixed layer depth ($z_{mt} = 70$ m) is assumed as a standard in the simulation study for simplicity.

A circular diatom patch which increases in extent towards a final diameter of 20 km (day 21) is used as standard in the simulation study. The diatom patch had a variable, elongated shape during EisenEx, with a larger patch extent aligned to the stationary flow (Bakker et al. 2005). Shape and area increase of the diatom patch may be well approximated by an elliptically shaped patch that increases in extent towards a final length of 40 km and final width of 20 km ($\tau = 10$ d; a/b = 0.5; a = 20 km at day 21).

Simulation results show a minor effect of an increased patch length on the abundance increase in the bloom area (see *Effects of diatom patch extent*). Net abundance increase at the patch centre and abundance increase within the mixed layer amounted to 94% and 96% of the respective increments during the reference run with a standard patch.

The small impact of an increased patch length is due to the effects of inertial motion, which gives rise to a net displacement of animals towards the patch centre (see *Effects of different flow fields*). This net displacement of *Oithona* individuals within the patch and from the surroundings can take place along smallest patch dimension (semiminor axis), because of the circular relative motion of deep-dwelling copepods and the surface layer.

Inertial motion is caused by transient wind events which set water in motion, that continues to move in a circular trajectory subject to the Coriolis force. Rapid changes of strong winds produce the largest oscillations. During EisenEx inertial motion was forced by a sequence of strong wind events, and showed periods of intensification and decay and furthermore showed vertical variability. In the model, we define an idealised inertial motion and assume a characteristic, constant amplitude, V_H, and an invariable vertical extent (constant z_{mt}).

The simulated flow field is a major simplification of the actual flow field at the experimental site, which in reality gives rise to more complex pattern of copepod redistribution. The model simplification, however, may lead to a substantial underestimate of the area which was covered by the relative displacement of phytoplankton patch and subsurface layer and thus of the number of copepods which can enter the food-rich surface layer from below.

4.1.2 Uncertainties in field data and interpretation

In view of the number of small copepods sampled at 100 m and 150 m, Henjes et al. (2007) conclude that their abundance increase in the phytoplankton bloom area could not be explained by upward migration alone. Differences in the conclusions drawn by Henjes et al. (2007) and by this study are partly due to a different interpretation of the field abundance data, which shows high variability but was sampled with low resolution. Furthermore, Henjes et al. (2007) assume similar high abundance increase as observed at the patch centre for a wide extent of the fertilised area, while the simulation study shows maximum increase at the patch centre and an abundance gradient within the patch. The different assessment, however, is also due to a different estimate of the area swept over by the patch and of the depth range in which substantial inflow of *Oithona* individuals occurs below the patch.

The simulation study shows that especially the displacement of the surface layer relative to the deeper layer, which is caused by surface currents (e.g. inertial oscillations), allows for a large abundance increase which explains most of the estimated increase during EisenEx. Thus besides inflow of individuals well below the mixed layer (e.g. $>$ 100 m) whose drift is mainly determined by the stationary flow field, the accumulation of *Oithona* in a bloom area should critically depend on the number of those deep-dwelling copepods which reside in proximity to the base of the mixed layer.

In view of the flow field simplification in the model and the possible underestimate

of the number of markedly deep-dwelling *Oithona* individuals during EisenEx, the simulation results should be considered as conservative estimates of the abundance increase that could have been caused by migratory response of *Oithona.*The much more complex displacement of the surface layer relative to deeper layer in the real flow field may also partly explain why a strong decrease in *Oithona* abundance below the phytoplankton-rich layer at the patch centre was only observed at single stations in the field. However, it has to be assumed that the low sampling resolution and the strong variability in abundance did not allow to resolve properly shifts in the abundance of *Oithona* below the mixed layer.

The composition of the developmental stages of *Oithona* indicates no advanced recruitment into copepodite stages inside the bloom area of EisenEx (Wend 2005). However, such growth signal could have been masked by the gradual accumulation of vertically immigrating copepods.Thus higher recruitment rates may have added to the observed increase in abundance of *Oithona* copepodites and adults during EisenEx.

4.2 EIFEX

During EIFEX, a large number of *Oithona* were sampled at 150 m and even at 200 and 250 m, showing mean abundances of 11, 7 and 6 individuals L^{-1}, respectively. About half of this individuals belonged to the species *Oithona similis*. No clear vertical and subsequent horizontal redistribution of *Oithona* was observed during EIFEX (Henjes, pers. communication), which in part can be explained by the very deep vertical extent of the phytoplankton-enriched surface layer in accordance with the simulation results. However, we suppose that *Oithona* was less attracted by the long-spined diatom species which dominated the EIFEX phytoplankton bloom.

4.3 Southern Ocean environment

Ward and Hirst (2006) found the abundance and fecundity rates of *Oithona similis* to be strongly related to temperature and depth-integrated chlorophyll *a* in the Southern Ocean, and found further indication of food limitation. These findings are in agreement with findings for other copepod species (e.g. Shreeve et al. 2002, Jansen et al. 2006).

Southern Ocean copepods have to cope with a strongly seasonal, patchy and overall dilute food environment. Most copepod species shift their diet towards an omnivorous feeding before and after the growth season, while diatoms dominate the

diet in summer (Atkinson 1998, Pasternak & Schack-Schiel 2001). In the growth season, transient mesoscale phytoplankton blooms strongly increase the phytoplankton biomass locally and cause high horizontal patchiness of the food environment (Smetacek et al 1990, Strass et al. 2002, Moore & Abbott 2002). Copepods have to face with periods of food shortage even in the growth season and need to utilise a wider range of food items to survive under the different conditions of food supply during their life span.

Oithona similis is known to feed on a variety of food items, including nauplii of other copepod species, microzooplankton, fecal pellets, diatoms and other phytoplankton (Lampitt 1978, Hopkins 1985, Gonzales & Smetacek 1994, Atkinson 1998, Castellani et al. 2005). Ambush feeding behaviour and body construction bias the prey perception ability of *Oithona* towards motile prey and larger immobile particles (Visser 2001), while a beneficial diet is restricted to food items which they are able to ingest with an effort that match the particular nutritional gain.

Considerable difference in this respect even among diatoms of the same size class and biased perception ability may be reasons for conflicting reports on diet and feeding preference of *Oithona*. The rare dietary studies may be additionally biased by the investigation methods and by seasonal effects. They show diatoms as preferred food in the spring, summer and autumn (gut content analysis; Hopkins 1985, Hopkins 1987, Hopkins & Torres 1989), substantial amount of diatoms but preference for motile prey in the pre- bloom and post-bloom situation (gut content analysis and feeding experiments; Atkinson 1995, Atkinson 1996), but also no confirmation for feeding on diatoms in the summer (fatty acid composition; Kattner et al. 2003).

Utilisation of a variety of food items likewise gives copepods the ability to prolong their residence periods in the deeper unproductive water column. It allows for the development of a food finding strategy that includes deep-dwelling behaviour in areas with low surface phytoplankton concentration, which causes an increased drift out of areas with rare food in the surface layer. Thus deep-dwelling would be a suitable mechanism for copepods to increase the chance of getting advected from a low to a high food environment. Given the wide range of possible food of *Oithona*, the nutritional detriment during deep-dwelling periods should be moderate compared to the food gain due to an increased probability to be subsequently exposed to a food rich environment.

In view of the vertical distribution of potential food items (e.g. Klaas 2001) the nutritional detriment should be especially small for deep-dwelling individuals that reside in proximity to the base of the mixed layer. Also these copepods are displaced

great distances relative to the surface layer due to surface currents that cause not only wobbling but also non-circular displacement of the surface layer in the field. Whether *Oithona* individuals that reside near below the mixed layer particularly benefit from their migration behaviour cannot be addressed with this simple model.

The strong migratory response of deep-dwelling copepods towards the progressively phytoplankton enriched surface inside the bloom area during EisenEx is consistent with the food finding strategy discussed above and provides a strong nutritional benefit for *Oithona* individuals. In contrast, dominance of long-spined diatoms likely prevents an effective feeding on diatoms by *Oithona* in the bloom area of EIFEX. The very deep extent of the phytoplankton-enriched layer and less attraction by the dominant diatom species may have caused the absence of significant vertical and subsequent horizontal redistribution of *Oithona* during this experiment.

4.4 Conclusion

A rise in copepod abundance was observed during six of twelve mesoscale iron fertilisation experiments. The experiments were conducted during different seasons and under different environmental abiotic conditions (like temperature). During most of the experiments, which covered observation periods of 5 to 37 days, phytoplankton blooms were induced which were dominated by diatoms, but variable in species composition and abundance (Boyd et al. 2007).

A significant reproductive response may increase copepod abundance in warm environments which support short life cycles. This seems to have happened during IronEx II, conducted in the warm equatorial Pacific (Rollwagen Bollens and Landry 2000).

A lower mortality of copepod nauplii stages, caused e.g. by a diet shift of omnivorous predators in phytoplankton blooms, may lead to an increase in number of copepodites relative to the outpatch. Such mechanism is discussed by Tsuda et al. (2006) to explain part of the crustacean abundance increase during the SERIES experiment.

Only during some iron fertilisation experiments were the sampling gear and procedure adequate to resolve abundance in different depth strata and thus a vertical animal redistribution. Differences of the residence depth of non-diurnal and diurnal migrating copepods between inside and outside the phytoplankton bloom area were observed during IronExII (Rollwagen Bollens & Landry 2000), EisenEx (Henjes 2007), SERIES (Sastri & Dower 2006, Tsuda et al. 2006) and EIFEX (Krägefsky

unpublished results).

The migratory behaviour of *Oithona* individuals can explain most of their abundance increase observed during EisenEx. The findings add to the increasing evidence that copepods are able to utilise the vertical differences in current speed and direction to affect their drift to their own benefit, here to increase their food gain in a patchy food environment with low background food concentration.

Acknowledgments

We thank J. Henjes for providing abundance data of Oithona and B. Fach, H. Leach and two anonymous referees for valuable suggestions for improvement of the manuscript.

Parameter	Definition	Units	Value
V_H	Velocity amplitude of inertial oscillation	$\mathrm{m\,s^{-1}}$	0.2
V_A	Swimming speed of copepod	$\mathrm{m\,s^{-1}}$	0.0005 - 0.001
Ω	Angular velocity of rotation of earth	$\mathrm{rad\,s^{-1}}$	7.29×10^{-5}
lat	Latitude	$^\circ$	-48
h_t	slope factor	m	15
z_{mt}	mixed layer depth	m	20 - 120
$\mathrm{Z_{max}}$	vertical extent of the model domain	m	160
τ	dilution time scale	d	10
α	food attraction coefficient	$\mathrm{m^2\,s^{-2}\,\mu M^{-1}}$	0.5 - 8
β	repulsion coefficient	$\mathrm{m^2\,s^{-2}}$	0 - 4
γ	surface avoidance coefficient	$\mathrm{m^2\,s^{-2}}$	1 - 2
ϵ	scaling factor	$\mathrm{m^{-1}\,s^2}$	10
$\mathrm{z_a}$	decaying length	m	10
ϑ	zenith	rad	0 - π
φ	azimuth	rad	0 - 2π

Table 1: Definition and parameter range

α	β	γ	z_{mt}	V_A	V_H	flow field	a/b day 21 [10^4m]	cv_{in}	cv_{inC}	cv_{out}	ch	copepod increase (160 m)	copepod increase (z_{mt})
4	**2**	**1.5**	**70**	**0.001**	**0.2**	**EE**	**1/1**	**0.77**	**0.84**	**0.66**	**0.92**	**1.70**	**2.52**
4	2	1.5	70	0.001	0	EE	1/1	0.73	0.80	0.67	0.82	1.45	2.17
0.5	2	1.5	70	0.001	0.2	EE	1/1	0.18	0.43	0.04	0.82	1.11	1.38
1	2	1.5	70	0.001	0.2	EE	1/1	0.41	0.64	0.19	0.87	1.25	1.72
2	2	1.5	70	0.001	0.2	EE	1/1	0.63	0.75	0.4	0.9	1.46	2.19
3	2	1.5	70	0.001	0.2	EE	1/1	0.73	0.83	0.57	0.91	1.61	2.45
6	2	1.5	70	0.001	0.2	EE	1/1	0.78	0.85	0.76	0.93	1.72	2.34
8	2	1.5	70	0.001	0.2	EE	1/1	0.74	0.79	0.78	0.92	1.55	1.91
4	0.5	1.5	70	0.001	0.2	EE	1/1	0.70	0.79	0.83	0.85	1.40	1.50
4	0.75	1.5	70	0.001	0.2	EE	1/1	0.75	0.78	0.85	0.9	1.55	1.80
4	1	1.5	70	0.001	0.2	EE	1/1	0.79	0.81	0.84	0.91	1.65	2.08
4	1.5	1.5	70	0.001	0.2	EE	1/1	0.78	0.80	0.78	0.92	1.69	2.38
4	3	1.5	70	0.001	0.2	EE	1/1	0.68	0.78	0.48	0.91	1.56	2.37
4	4	1.5	70	0.001	0.2	EE	1/1	0.60	0.75	0.38	0.91	1.41	2.10
4	2	1	70	0.001	0.2	EE	1/1	0.77	0.87	0.69	0.92	1.70	2.54
4	2	2	70	0.001	0.2	EE	1/1	0.76	0.80	0.65	0.92	1.69	2.51
4	2	1.5	20	0.001	0.2	EE	1/1	0.60	0.73	0.36	0.87	1.38	3.49
4	2	1.5	30	0.001	0.2	EE	1/1	0.68	0.73	0.46	0.90	1.49	3.25
4	2	1.5	40	0.001	0.2	EE	1/1	0.73	0.78	0.55	0.91	1.64	3.22
4	2	1.5	50	0.001	0.2	EE	1/1	0.75	0.78	0.61	0.91	1.70	3.02
4	2	1.5	90	0.001	0.2	EE	1/1	0.72	0.82	0.71	0.90	1.49	1.92
4	2	1.5	120	0.001	0.2	EE	1/1	0.62	0.77	0.76	0.88	1.30	1.44
4	2	1.5	70	0.001	0.2	EF	1/1	0.75	0.80	0.67	0.93	1.65	2.45
4	2	1.5	70	0.0005	0.2	EE	1/1	0.79	0.87	0.71	0.90	1.59	2.3
4	2	1.5	70	0.001	0.2	NOG	1/1	0.75	0.83	0.67	0.86	1.52	2.4
4	2	1.5	70	0.001	0.2	EE	2/2	0.73	0.81	0.66	0.75	1.46	2.22
4	2	1.5	70	0.001	0.2	EE	2/1	0.75	0.82	0.66	0.84	1.59	2.42
4	2	1.5	70	0.001	0.2	NOG	2/2	0.7	0.82	0.66	0.68	1.22	1.95
6	2	1.5	70	0.001	0.2	EE	2/1	0.75	0.79	0.76	0.86	1.57	2.15
4	2	1.5	120	0.001	0	EF	2/2	0.59	0.76	0.75	0.78	1.21	1.35

Table 2: Model results. a/b ratio of semi-major and semi-minor axes, given the food patch extent and shape at day 21. EE = EisenEx. EF = EIFEX. NOG = no geostrophic flow. cv_{in} = vertical correlation of copepods and diatom carbon (c_v) at day 21 in total impatch area, $cv_{inC} = c_v$ at the patch centre ($r < 1000$ m) and $cv_{out} = c_v$ in the outpatch. c_h = horizontal correlation of copepods and diatom carbon at day 21. See also Table 1 for parameter definition. Copepod increase is given in terms of increase relative to the outpatch abundance (steady state distribution) in total and within the mixed layer, which, for example, is 1.7 fold and 2.52 fold, respectively, in the refernce run.

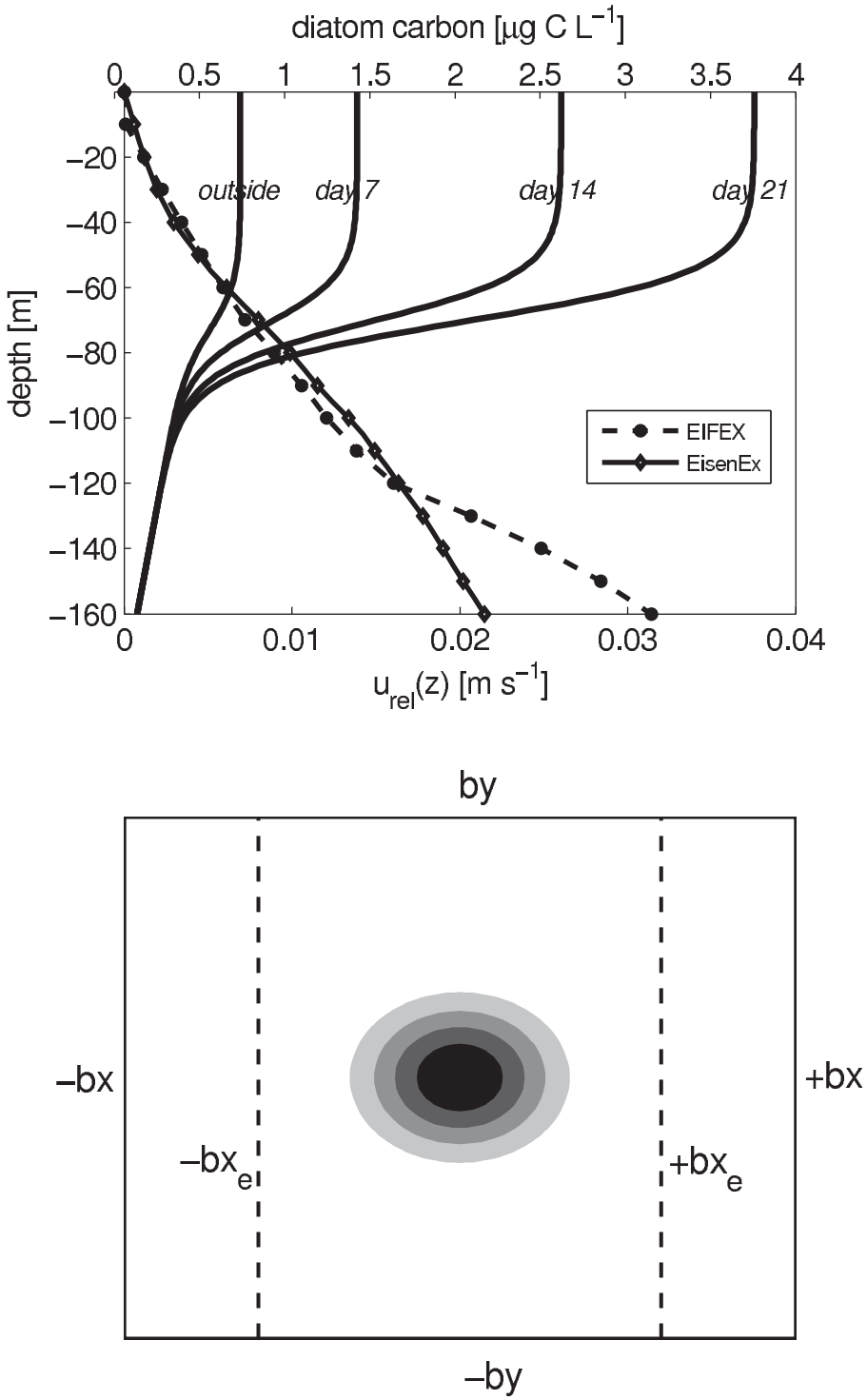

Figure 1: a.) Profiles of the carbon concentration outside the bloom area and at day 7, 14 and 21 inside the bloom area (solid lines) and depth dependent drift velocity of copepods relative to the upper patch centre (u_{rel}(z)). b.) Sketch of the model domain with the outer boundaries $-bx$, $+bx$, $-by$ and $+bx$ and the inner planes $-bx_e$ and $+bx_e$, grey-black shadings marks the diatom carbon concentration (black mark the highest concentration).

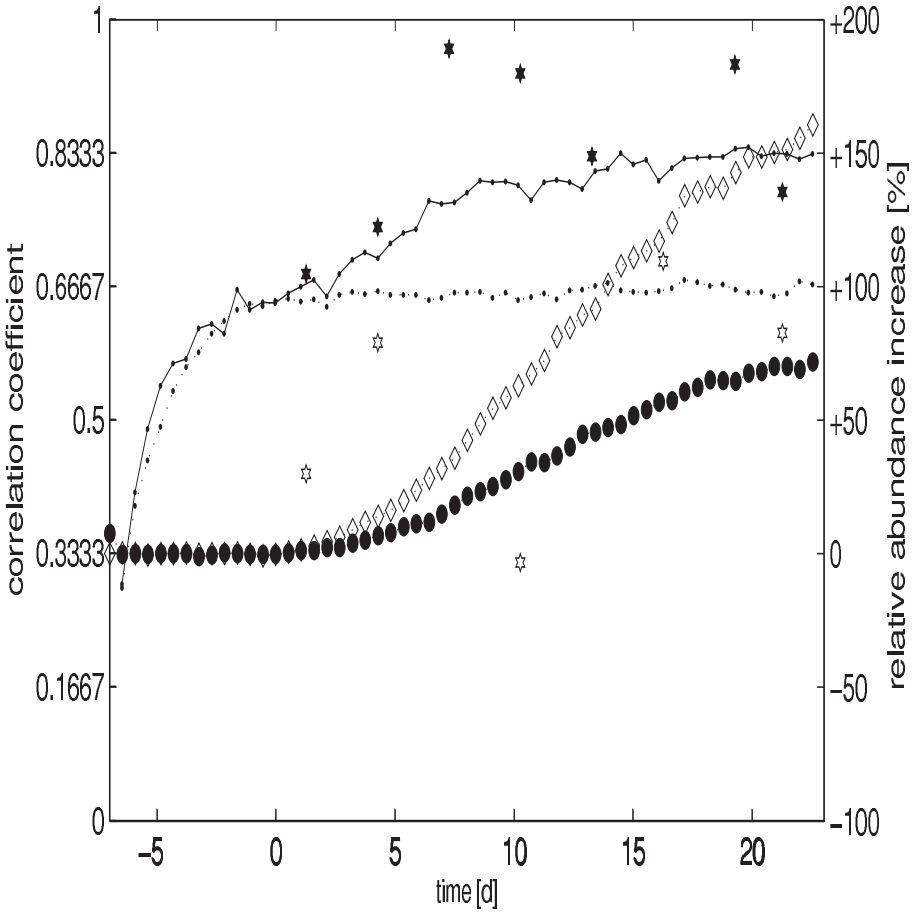

Figure 2: Modelled temporal development of relative copepod abundance at the patch centre, given as percental increase relative to outpatch abundance within the mixed layer (diamonds) and over 160 m (filled circles). Dotted lines represent the temporal development of correlation coefficient between vertical copepod and food distribution (in terms of diatom carbon concentration) in the outpatch area (dashed line) and at the patch centre (continuous line). The development of vertical correlation during EisenEx (field situation) is given by open (outpatch) and filled (inpatch) stars (three-day mean)

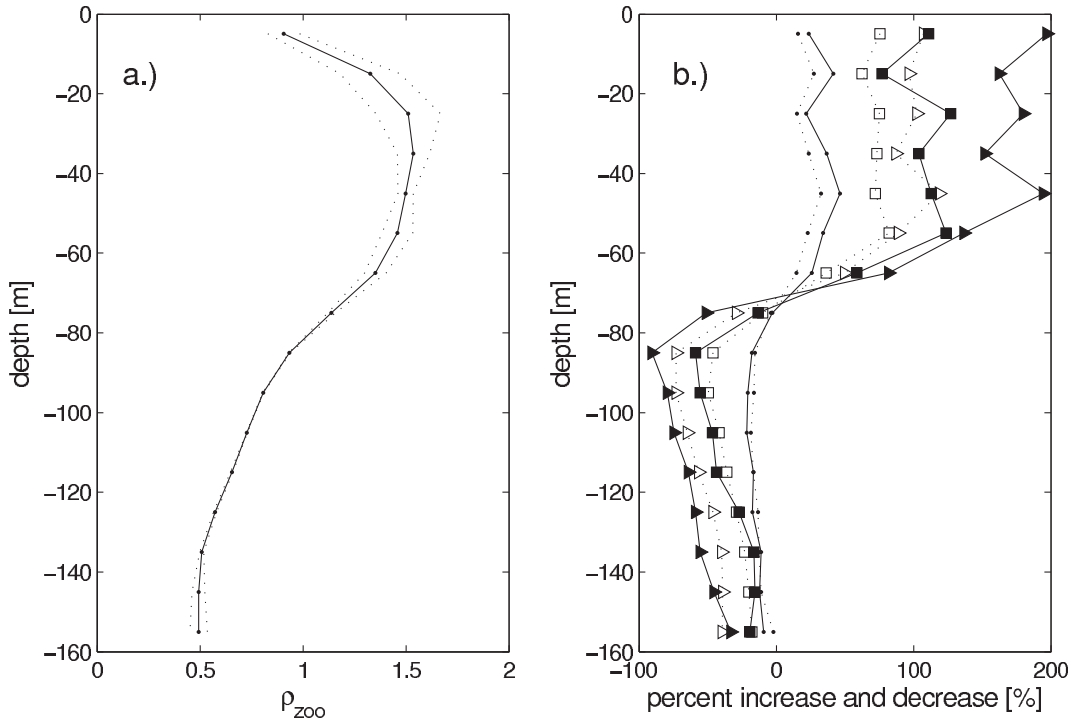

Figure 3: a.) Mean vertical distribution of copepods in the outpatch area after the initialisation period during the reference run (solid line). Dotted lines represent one standard deviation. b.) Relative depth dependent copepod abundance increase and decrease at the patch centre (solid lines, filled markers; $r \leq 1000\,m$) and central inpatch area ($< r_p/2$) (dotted lines) at day 7 (points), 14 (squares) and 21(triangles) relative to the vertical outpatch distribution.

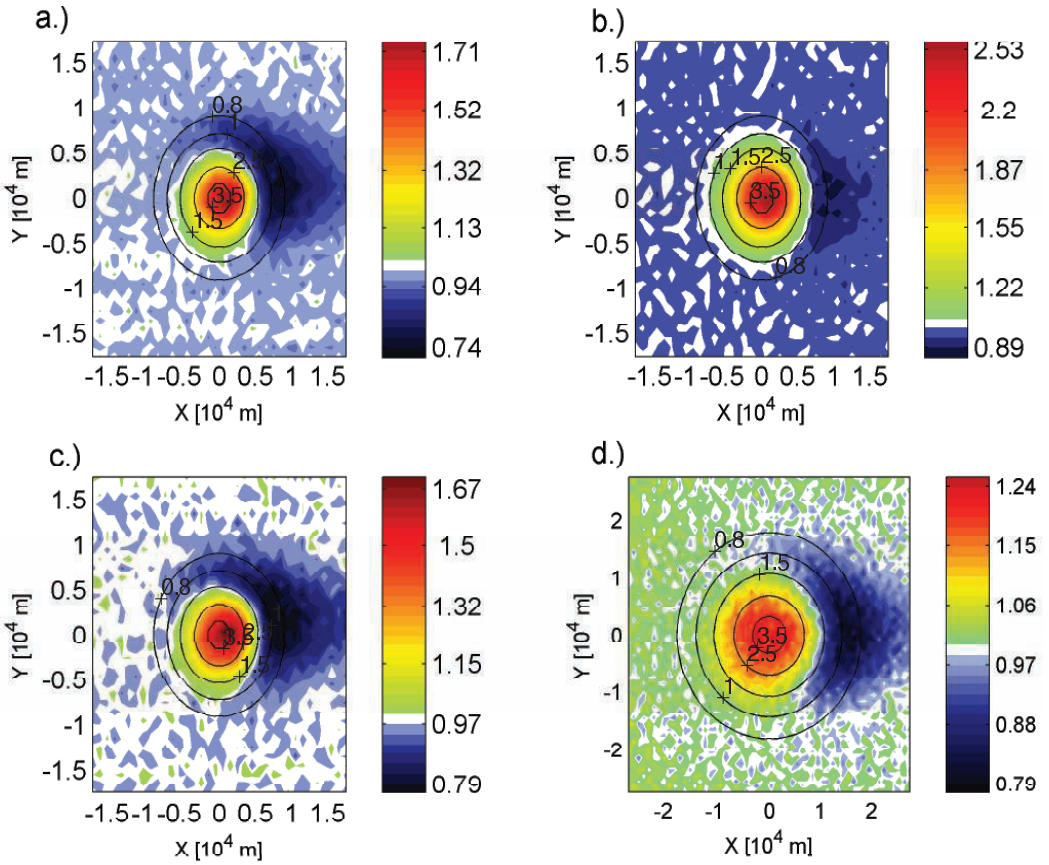

Figure 4: Horizontal copepod distribution at day 21 after fertilisation during the reference run, given in terms of the realtive copepod increase within the total water column (160 m) (a) and the mixed layer (b), respectively, referenced to the outpatch (steady state distribution). Surface diatom carbon concentration [μmol C L^{-1}] is indicated by isolines . c) Horizontal copepod distribution at day 21 (160 m) within the EIFEX flow field, using otherwise unchanged model settings. d.) Resulting distribution using the EIFEX flow, a mixed layer depth of 120 m, and a doubled patch radius.

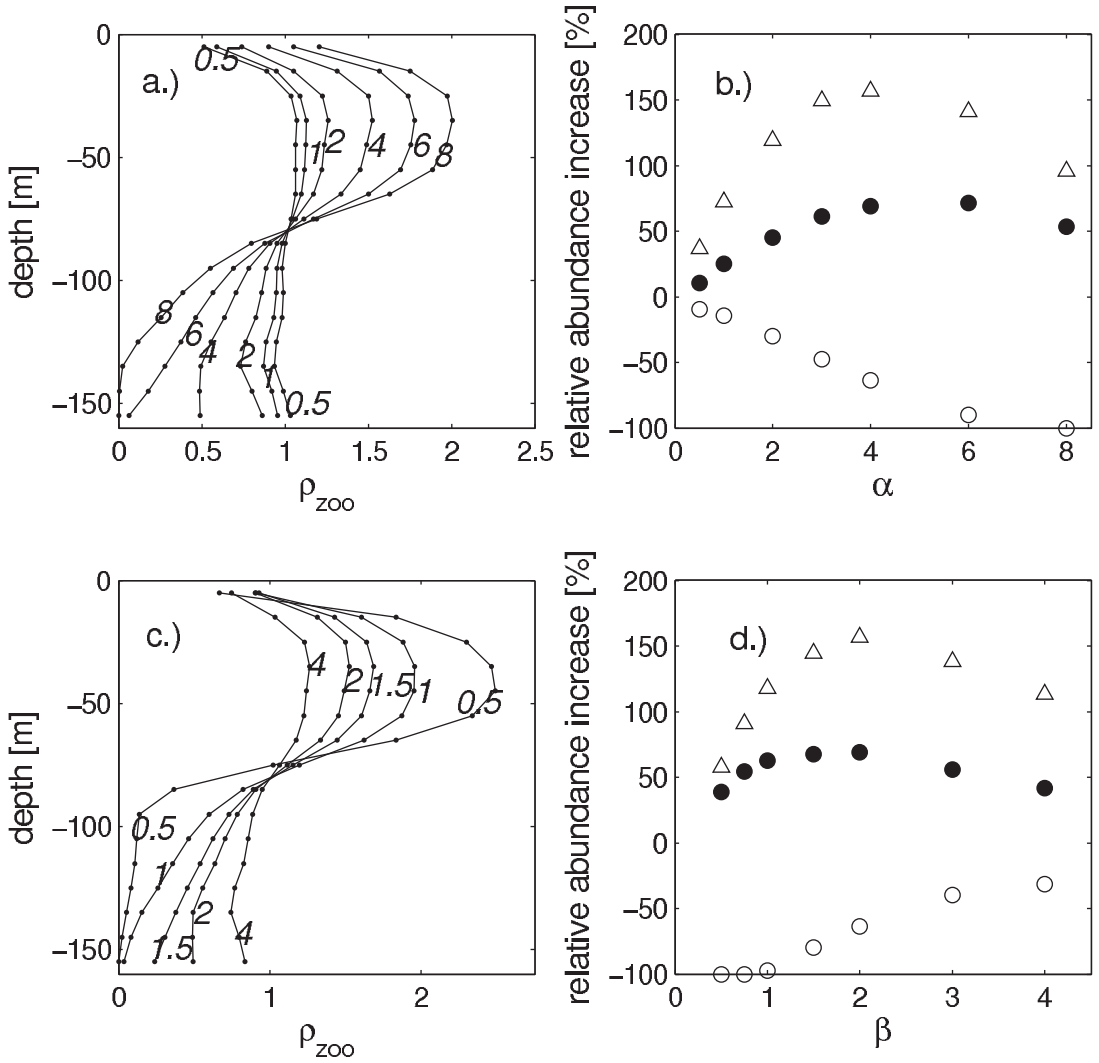

Figure 5: Sensitivity study: a.) mean vertical animal distribution (steady state) outside the patch dependent on food attraction coefficient (α). The single profiles are marked by the respective α-value. b.) Relative abundance increase at the patch centre at day 21 in the mixed layer (triangles), below the mixed layer (open circles) and over 160 m (filled circles), relative to the respective outpatch abundance and plotted against α. c.) and d.) analogous plots for varying repulsion coefficient (β).

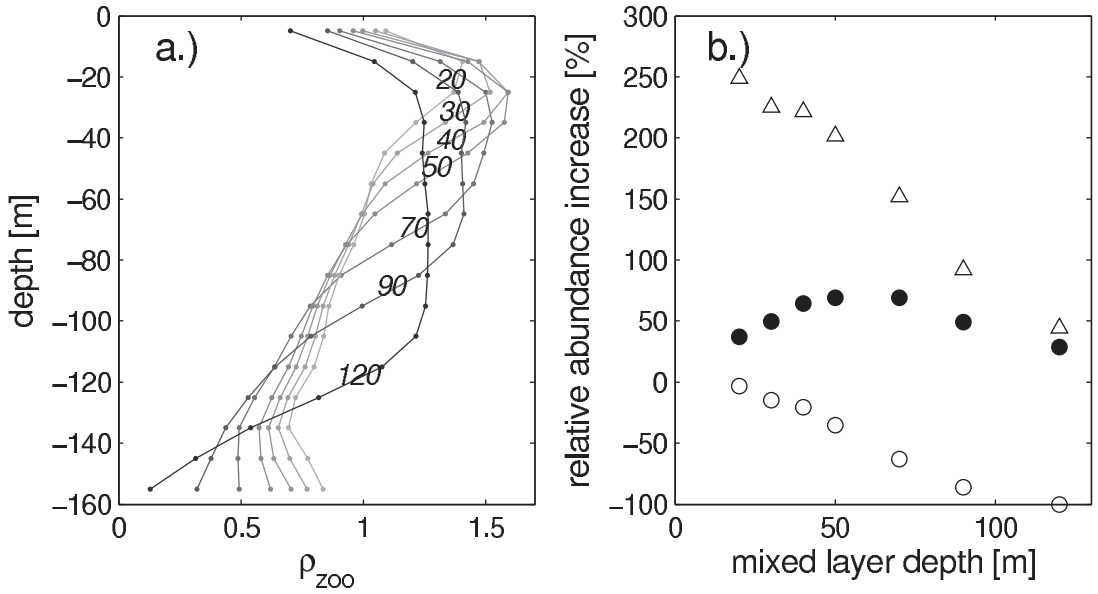

Figure 6: Sensitivity study: a.) mean vertical animal distribution (steady state) outside the patch dependent on mixed layer depth (20, 30, 40, 50, 70, 90, 120 m). b.) Relative copepod abundance increase in the patch centre at day 21 in the mixed layer (triangles), below the mixed layer (open circles) and over 160 m (filled circles) dependent on the mixed layer depth, relative to the respective outpatch abundance. Except depth of mixed layer, settings remained unchanged with respect to the reference run.

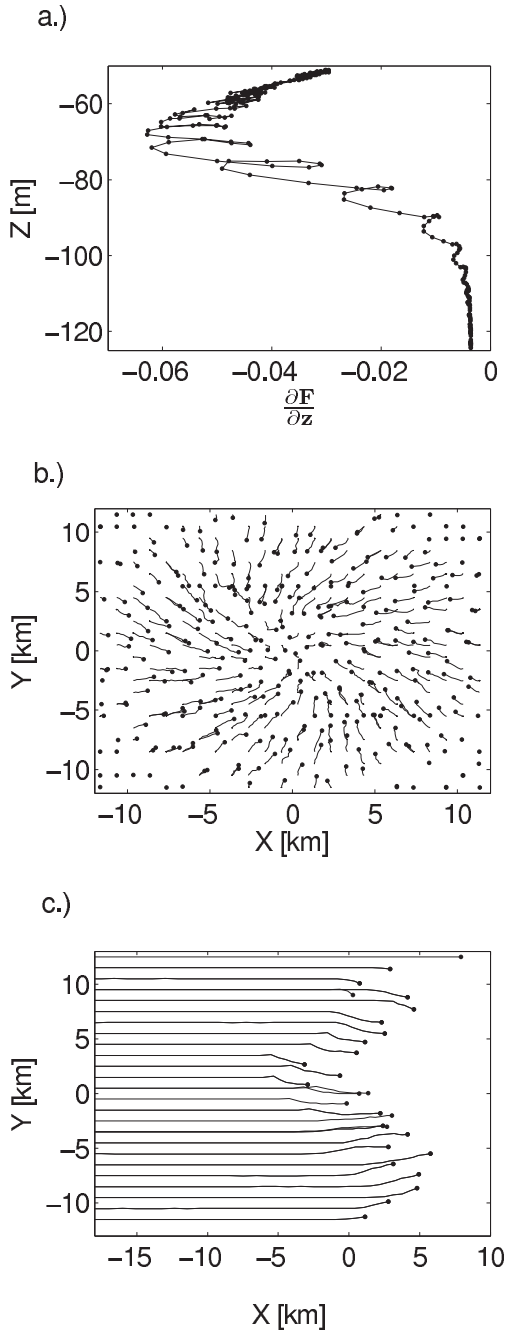

Figure 7: a.) Ascent of a copepod individual triggered by the steepness of the food gradient. b.) Net horizontal displacement of animals that show such migratory behaviour in a flow field governed by inertial oscillation, illustrated by the path of different individuals (solid line) and their final horizontal position (filled circle). c.) Paths of ascending copepods in a flow field that is governed by geostrophic flow and inertial oscillation. Their paths show a deflection along the horizontal food gradient. Paths in b.) and c.) are given as an average position over one period of inertial oscillation.

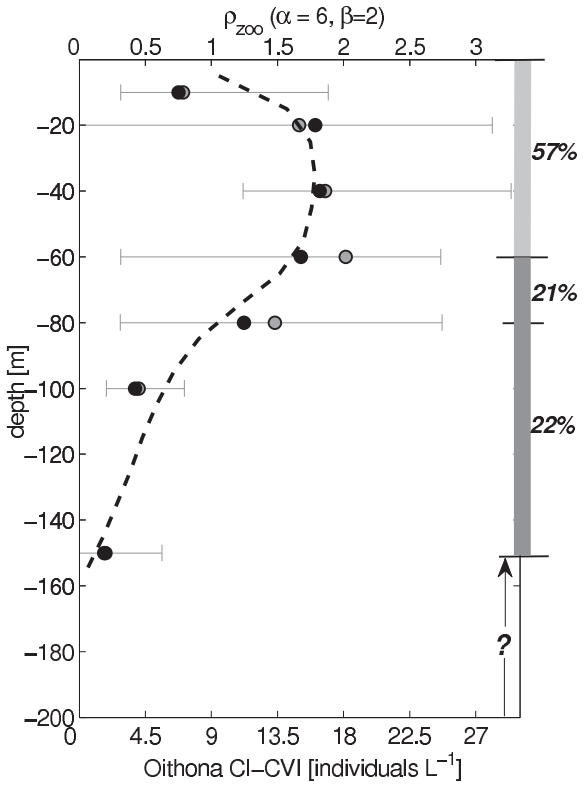

Figure 8: Mean abundance of *Oithona* sampled at different depths during EisenEx outside the phytoplankton patch including (black circle) and excluding (gray circle) the first oupatch station. The simulated mean vertical distribution are shown by the black dashed line for food attraction coefficient $\alpha = 6$ and repulsion coefficient $\beta = 2$. Gray horizontal bars indicate the minimum and maximum abundances of *Oithona* sampled at the discrete sampling depth. Percentage of *Oithona* individuals found on average at outpatch stations (excluding the first station) in the upper 0-60 m, 60 - 80 m, 80 - 150 m of the total individuals in upper 0 - 150 m is given on the right hand side of the graph.

References

[1] Anis, A. and Moum, J.N. Surface wave-turbulence interactions: Scaling $\epsilon(z)$ near the sea surface. *J Phys Oceanogr*, 25(9):2025–2045, 1995.

[2] Assmy, P., Henjes, J., Klaas, C., and Smetacek, V. Mechanisms determining species dominance in a phytoplankton bloom induced by iron fertilization experiment EisenEx in the Southern Ocean. *Deep-Sea Res Part I*, 54:340–384, 2007.

[3] Atkinson, A. Omnivory and feeding selectivity in five copepod species during spring in the Bellinghausen Sea, Antarctica. *ICES J Mar Sci*, 52:385–396, 1995.

[4] Atkinson, A. Subantarctic coepepods in an oceanic, low chlorophyll environment: ciliate predation, food selectivity and impact on prey populations. *Mar Ecol Prog Ser*, 130:85–96, 1996.

[5] Atkinson, A. Life cycle strategies of epipelagic copepods in the Southern Ocean. *J Mar Syst*, 15(1-4):289–311, 1998.

[6] Bainbridge, R. Studies on the interrelationships of zooplankton and phytoplankton. *J Mar Biol Ass U K*, 32:385–447, 1953.

[7] Bakker, D.C.E., Bozec, Y., Nightingale, P.D.], Goldson, L., Messias, M-J.and de Baar, H.J.W., Liddicoat, M., Skjelvan, I., Strass, V., and Watson, A.J. Iron and mixing affect biological carbon uptake in SOIREE and EisenEx, two Southern Ocean iron fertilisation experiments. *Deep-Sea Res I*, 52:1001–1019, 2005.

[8] Batchelder, H. P., Edwards, C. A., and Powell, T. M. Individual-based models of copepod populations in costal upwelling regions: implications of physiologically and evironmentally influenced diel vertical migration on demograhic success and nearshore retention. *Prog Oceanogr*, 53:307–333, 2002.

[9] Bosch, H. F. and Taylor, W. R. Diurnal vertical migration of an eustuarine cladoceran *Podon polyphemoides* in the Cheasapeake Bay. *Mar Biol*, 10:172–181, 1973.

[10] Boyd, P. W., Jickells, T., Law, C. S., Blain, S., Boyle, E. A., Buesseler, K. O., Coale, K. H., Cullen, J. J., de Baar, H. J. W., Follows, M., Harvey, M., Lancelot,

C., Levasseur, M., Owens, N. P. J., Pollard, R., Rivkin, R. B., Sarmiento, J., Schoemann, V., Smetacek, V., Takeda, S., Tsuda, A., Turner, S., and Watson, A. J. Mesoscale Iron Enrichment Experiments 1993-2005: Synthesis and Future Directions. *Science*, 315(5812):612–617, 2007.

[11] Castellani, C., Irigoien, X. and Harris, R.P., and Lampitt, R.S. Feeding and egg production of *Oithona similis* in the North Atlantic. *Mar Ecol Prog Ser*, 288:173–182, 2005.

[12] Cisewski, B., Strass, V. H., and Prandke, H. Upper-ocean vertical mixing in the Antarctic Polar Front Zone. *Deep-Sea Res Part II*, 52(9-10):1087–1108, 2005.

[13] Emsley, S. M., Tarling, G. A., and Burrows, M. T. The effect of vertical migration strategy on retention and dispersion in the Irish Sea during spring-summer. *Fish Oceanogr*, 14(3):161–174, 2005.

[14] Genin, A., Jaffe, J. S., Reef, R., Richter, C., and Franks, P. J. S. Swimming Against the Flow: A Mechanism of Zooplankton Aggregation. *Science*, 308(5723):860–862, 2005.

[15] Gonzales, H.E. and Smetacek, V. The possible role of the cyclopoid copepod Oithona in retarding the flux of zooplankton faecal material. *Mar Ecol Prog Ser*, 113:233–246, 1994.

[16] Hardy, A. C. and Gunther, E. R. The plankton of the South Georgia whaling grounds and adjacent waters, 1926-1927. *Disc Rep*, 11:1–456, 1935.

[17] Henjes, J., Assmy, P., Klaas, C., Verity, P., and Smetacek, V. Response of microzooplankton (protists and small copepods) to an iron-induced phytoplankton bloom in the Southern Ocean (EisenEx). *Deep-Sea Res Part I*, 54:363–384, 2007.

[18] Hopkins, T.L. Food web of an Antarctic midwater ecosystem. *Mar Biol*, 89:197–212, 1985.

[19] Hopkins, T.L. Midwater food web in Mc Murdo Sound, Ross Sea, Antarctica. *Mar Biol*, 96:93–106, 1987.

[20] Hopkins, T.L. and Torres, J.J. Midwater food web in the vicinity of a marginal ice zone in the western Weddel Sea. *Deep-Sea Res*, 36:542–560, 1989.

[21] Jansen, S., Klass, C., Krägefsky, S., Harbou, L.v., and Bathmann, U. Reproductive response of the copepod *Rhincalanus gigas* to an iron-induced phytoplankton bloom in the Southern Ocean. *Polarl Biol*, 29:1039–1044, 2006.

[22] Kaartvedt, S., Olsen, E., and Jørstad, T. Effects of copepod foranging behaviour on predation risk: An experimental study of the predatory copepod *Paraeuchaeta norvegica* feeding on *Acartia clausi* and *A. tonsa* (copepoda). *Limnol Oceanogr*, 42(1):164–170, 1996.

[23] Kattner, G., Albers, C., Graeve, M., and Schnack-Schiel, S.B. Fatty acid and alcohol composition of small polar copepods, Oithona and Oncaea: indication on feeding modes. *Polar Biol*, 26:666–671, 2003.

[24] Kimmerer, W. and McKinnon, A. Zooplankton in a marine bay. II. Vertical migration to maintain horizontal distribution. *Mar Ecol Prog Ser*, 41:53–60, 1987.

[25] Klaas, C. Spring distribution of larger (>64 μm) protozoans in the Atlantic sector of the Southern Ocean. *Deep-Sea Res I*, 48:1627–1649, 2001.

[26] Lampitt, M.R. Carnivorous feeding by a small marine copepod. *Limnol Oceanogr*, 23:1228–1230, 1978.

[27] Maar, M., Visser, A. W. andNielsen, T. G., Stips, A., and Saito, H. Turbulence and feeding behaviour affect the vertical distributions of *Oithona similis* and *Microsetella norwegica*. *Mar Ecol Prog Ser*, 313:157–172, 2006.

[28] Moore, J. K. and Abbott, M. R. Surface chlorophyll concentrations in relation to the Antarctic Polar Front: seasonal and spatial patterns from satellite observations. *J Mar Syst*, 37(1-3):69–86, 2002.

[29] Pasternak, A.F. and Schnack-Schiel, S.B. Feeding patterns of dominant Antarctic copepods: an interplay of diapause, selectivity, and availability of food. *Hydrobiologia*, 453/454:25–36, 2001.

[30] Peterson, W. T., Miller, C. B., and Hituchinson, A. Zonation and maintenance of copepod populations in the Oregon upwelling zone. *Deep-Sea Res Part A*, 26A:467–494, 1978.

[31] Rollwagen Bollens, G.C. and Landry, M.R. Biological response to iron fertilization in the eastern equatorial Pacific (IronEx II). II. Mesozooplankton abundance, biomass, depth distribution and grazing. *Mar Ecol Prog Ser*, 201:43–56, 2000.

[32] Sastri, A. R. and Dower, J. F. Mesozooplankton community response during the SERIES iron enrichment experiment in the subarctic NE Pacific. *Deep-Sea Res Part II*, 53(20-22):2268–2280, 2006.

[33] Schnack-Schiel, S. B. Aspects of the study of the life cycles of Antarctic copepods. *Hydrobiologia*, 453/454:9–24, 2001.

[34] Schnack-Schiel, S.B. Aspects of the study of the life cycles of Antarctic copepods. *Hydrobiologia*, 453/454:9–24, 2001.

[35] Shreeve, R.S., Ward, P., and Whitehouse, M.J. Copepod growth and development around South Georgia: relationships with temperature, food, krill. *Mar Ecol Prog Ser*, 233:169–183, 2002.

[36] Smetacek, V., Scharek, R., and Nöthig, E. M. Seasonal and regional variation in the pelagial and its relationship to the life history cycle of krill. In K. Kerry and G. Hempel, editors, *Antartic ecosystems: Ecological change and conservation*, pages 103–114. Springer Verlag, Berlin, 1990.

[37] Strass, V., Cisewski, B., Gonzalez, S., Leach, H., Loquay, K-D., Prandke, H., Rohr, H., and Thomas, M. The physical setting of the European Iron Fertilisation experiment 'EIFEX' in the Southern Ocean. *Reports on Polar and Marine Research*, 500:15–46, 2005.

[38] Strass, V.H., Naveira Garabato, A.C., Pollard, R.T., Fischer, H.I., Hense, I., Allen, J.T., Read, J.F., Leach, H., and Smetacek, V. Mesoscale frontal dynamics: shaping the environment of primary production in the Antarctic Circumpolar Current. *Deep-Sea Res Part II*, 49:3735–3769, 2002.

[39] Svensen, C. and Kiørboe, T. Remote prey detection in *Oithona similis*: hydromechanical versus chemical cues. *J Plankton Res*, 22(6):1155–1166, 2000.

[40] Tiselius, P. and Jonsson, P. R. Foranging behaviour of six calanoid copepods: observations and hydromechanic analysis. *Mar Ecol Prog Ser*, 66:23–33, 1990.

[41] Tsuda, A., Saito, H., Nishioka, J., Ono, T., Noiri, Y., and Kudo, I. Mesozooplankton response to iron enrichment during the diatom bloom and bloom decline in SERIES (NE Pacific). *Deep-Sea Res Part II*, 53(20-22):2281–2296, 2006.

[42] Uchima, M. and Hirano, R. Swimming behaviour of the marine copepod *Oithona davisae*: internal control and search for environment. *Mar Biol*, 99:47–56, 1988.

[43] Visser, A. W. Hydromechanical signals in the plankton. *Mar Ecol Prog Ser*, 222:1–24, 2001.

[44] Voronina, N.M. Comparative abundance and distribution of major filter-feeders in the Antarctic pelagic zone. *J Mar Syst*, 17(1-4):375–390, 1998.

[45] Ward, P. and Hirst, A.G. *Oithona similis* in a high latitude ecosystem: abundance, distribution and temperature limitation of fecundity rates in a sac spawning copepod. *Mar Biol*, 151:1099–1110, 2007.

[46] Wend, B. Stage development of *Oithona similis* (Copepods: Cyclopoida) during EisenEx. Master's thesis, University Bremen, 2005.

[47] Wiggert, J.D., Haskell, A.G.E., Paffenhöfer, G.A., Hofmann, E.E., and Klinck, J.M. The role of feeding behaviour in sustaining copepod populations in the tropical ocean. *J Plankton Res*, 10:1013–1031, 2005.

[48] Woodson, C.B., Webster, D.R., Weissburg, M.J., and Yen, J. The prevalence and implications of copepods behavioral responses to oceanographic gradients and biological patchiness. *Integrative and Comparative Biology*, doi:10.1093/icb/icm091:1–16, 2007.

6 Manuscript 2

On the migratory response of diel migrating copepods during two iron-fertilisation experiments (EisenEx and EIFEX)

S. Krägefsky[1*], U. Bathmann[1], D. Wolf-Gladrow[1]

Alfred Wegener Institute for Polar and Marine Research, Am Handelshafen 12, 27570 Bremerhaven, Germany

The vertical migration behaviour of copepods was surveyed with acoustic methods and net sampling during the two iron-fertilisation experiments EisenEx and EIFEX in the Southern Ocean. Diel migrating copepods responded to the changing phytoplankton concentration in the surface layer and decreased their daytime residence depth with increasing phytoplankton concentration. The observed migration behaviour causes drift of copepods out of regions with dilute food concentration, but increases their retention in phytoplankton-rich areas. The behaviour can be considered as a food finding strategy to cope with the patchy, mostly food poor environment of the Southern Ocean. In this simulation study we take the particular flow fields and the observed diel vertical migration behaviour into account to investigate the effects on the horizontal copepod distribution and the individual food gain. The migratory response can explain most of the large abundance increase of diel migrating copepods in the bloom area during EIFEX and might explain their apparent increase during EisenEx. The simulation results further highlight the strong nutritional benefit gained by the copepod individuals.

*Corresponding author: Soeren.Kraegefsky@awi.de

1 Introduction

Copepods are small aquatic crustaceans and probably the most numerous metazoan animals on earth (Schminke 2007). They play an important role in marine food webs and biogeochemical cycling of carbon and nutrients in the sea. Copepods are abundant even in extreme environments, and dominate the total metazoan biomass in the cold and mostly food-poor Southern Ocean as well as in wide areas of the world ocean (Voronina 1998). Yet there is limited knowledge about their behavioural strategies to cope with the Southern Ocean environment, which is characterized by strongly seasonal and horizontal patchy food supply.

Complex sensing of their environment is always involved during feeding, predator avoidance and motional behaviour of copepods (Tiselius and Jonsson 1990, Kaartvedt and Jørstad 1996). In the near field, their sensing ability is rooted in their hydrodynamic and chemical sensory sensitivity (Visser 2001). Photoreception plays an important role in their diel vertical migration (DVM) (e.g. Russel 1926, Stearns & Forward 1984), during which they leave the well-illuminated surface layer and migrate tens and up to hundreds of metres towards a deeper daytime residence.

While it is nowadays widely accepted that avoidance of visual predators is the main reason why animals undertake DVM (Hays 2003), Hardy and Gunther (1935) had addressed vertical migration as a mechanism at disposal of planktonic animals to use vertical differences in the oceanic flow field. Use of the sheared flow field would allow them to drift great distances relative to the surface, which they cannot achieve by own horizontal movements.

In fact, there is increasing evidence, mainly from the research in tidal and estuarine environments, that planktonic animals can actively effect their drift by vertical migration e.g. to maintain their horizontal distribution (Bosch & Taylor 1973, Isaac et al. 1974, Peterson et al. 1978, Kimmerer & McKinnon 1987, Hill 1998, Batchelder et al. 2002, Emsley et al. 2005). Diel migrating species may regulate their drift by complete cessation of their vertical migration, for example, under favourable food condition in the surface layer as well as through deepening or shallowing of their daytime residence to effect a transport out of unproductive regions and their maintenance in food-rich areas.

In the Southern Ocean and other regions of the world oceans, the phytoplankton productivity is limited by iron supply, and increases strongly after iron fertilisation during mesoscale experiments (Boyd et al. 2007). These field experiments are a highly valuable tool for studying the response of copepods and other zooplank-

ton to an increased food supply in their mostly food poor environment. The first evidence for a vertical migration response in an experimentally induced mesoscale phytoplankton bloom was given during the iron fertilisation experiment IronExII (Rollwagen Bollens and Landry 2001).

The iron fertilisation experiments EisenEx (Cisewski et al. 2005) and EIFEX (Strass et al. 2005) which were carried out in the Southern Ocean were conducted within mesoscale eddies, and thus provide ideal condition for studying the zooplankton response unaffected by an exchange from adjacent waters. Changes in horizontal and vertical zooplankton distribution were surveyed by multi-frequency acoustic measurements with a scientific echosounder (Simrad EK60) with a very high spatial and temporal resolution, and by net and water rosette sampling.

During EisenEx and EIFEX, the copepods responded to the increased phytoplankton concentration inside the bloom area by vertical migration towards the phytoplankton maxima (non-diurnal migrating copepods) and by shallowing of their residence depth during day (DVM participants), respectively. The migratory response of non-diurnal migrating small copepods is addressed in Krägefsky et al. (in press). It is shown that their migratory response in the vertically sheared flow field at the experimental site can explain most of their abundance increase observed during EisenEx. The aim of the current model study is to explore the effects of changing DVM pattern shown by the different copepod species during EisenEx and EIFEX. We investigate the extent to which their migratory behaviour in response to the phytoplankton concentration account for the observed abundance increase of copepods, and address the potential increase in the individual food gain.

2 Model description

A Lagrangian individual based model is used to track copepods. These copepods are exposed to different flow regimes, which are simplified representations of those at the experimental sites during EisenEx and EIFEX. Individuals in the model are representative of a number of neighbouring copepods in the field. They migrate vertically in accordance to the DVM pattern shown by different copepod species during EisenEx and EIFEX (see *Parameter settings*).

The path followed by a copepod individual (i) at location $\vec{X}_i$ is given by

$$\frac{d\vec{X}_i}{dt} = \vec{U}_i \tag{1}$$

$\vec{U}_i$, the actual velocity of a copepod, results from superposition of directional ($\vec{u}_{d_i}$) and random ($\vec{u}_{r_i}$) copepod motion and copepod drift with ocean currents ($\vec{u}_{m_i}$):

$$\vec{U}_i = \vec{u}_{d_i} + \vec{u}_{r_i} + \vec{u}_{m_i} \tag{2}$$

Subscript i, which denotes an individual copepod, is dropped in the following. The active motion ($u_d + u_r$) is assumed to be at a constant speed V_A, which equals the maximum swimming speed required to migrate vertically in accordance with the prescribed DVM pattern. The vertical directionality of an copepod individual is determined by the directionality factor g_z, within a value range of -1 (moving upward at speed V_A) and 1 (moving downward at speed V_A) (see *Vertical migration behaviour*),

$$\vec{u}_d = \begin{pmatrix} 0 \\ 0 \\ V_A\ g_z \end{pmatrix} \tag{3}$$

The active motion includes an isotropically distributed random component. Its magnitude is reduced by the copepods directional motion,

$$\vec{u}_r = \begin{pmatrix} V_A\ (1 - |g_z|) \sin(\vartheta) \cos(\varphi) \\ V_A\ (1 - |g_z|) \sin(\vartheta) \sin(\varphi) \\ V_A\ (1 - |g_z|) \cos(\vartheta) \end{pmatrix} \tag{4}$$

The angles $\vartheta (0 \leq \vartheta \leq \pi)$ and $\varphi (0 \leq \varphi < 2\pi)$ are chosen randomly at each time step. If $R(0,1)$ is a random variable of uniform distribution on the unit interval, φ and ϑ are given by $\varphi = 2\pi R(0,1)$ and $\vartheta = \arccos(1 - 2R(0,1))$, respectively.

Copepod individuals drift with horizontal currents, their respective drift velocity is given by

$$\vec{u}_m = \begin{pmatrix} u_s + u_{im} \\ v_{im} \\ 0 \end{pmatrix} \tag{5}$$

Copepod drift is determined by stationary flow (u_s) and flow components due to inertial oscillation (u_{im} and v_{im}; see *Flow field and model geometry*).

2.1 Vertical migration behaviour

We model the vertical migration behaviour of different copepod species. All of them showed normal diel vertical migration during EisenEx and EIFEX. They descended at dawn from their shallower night time residence towards a deeper day time residence and re-ascended at dusk. The different species maintained a constant residence depth during night inside and outside the bloom area, but stayed at an increasingly shallower depth at day time with increasing phytoplankton concentration.

The migration behaviour of copepods was surveyed with acoustic measurements by comparing the detected actual residence depth with chlorophyll concentration measured at the surface during transects (see *Parameter settings*). With this method we did not consider the actual vertical extent of the phytoplankton-enriched layer and the concentration variability within it. However, particularly for the deeper sound scattering layers which were less affected by a superposition of different backscattering signals, the observed day-time residence was mostly well correlated with the surface chlorophyll concentration. The migratory response of the copepods to changing phytoplankton concentration was widely independent of changes in solar irradiation during the daytime (Fig. 2-4), while generally shallowing of the daytime residence may have occurred during days with low daily average irradiation (e.g. very cloudy days).

Phytoplankton causes wavelength-specific light attenuation in the water (Platt et al. 1994), and causes decreasing intensity of downwelling light and changes in its spectral composition with increasing concentration. These quantitative and qualitative changes could have been both used as a cue for migration response. Changes in the underwater light field below the mixed layer, however, were not investigated during the experiments.

For modelling purpose, the maximal day time migration depth, z_{max}, shown by the copepod individuals in- and outside the phytoplankton bloom area is well described as a function of the surface chlorophyll *a* concentration and the deviation from the day time residence of individuals under low chlorophyll condition:

$$z_{max}(\text{chla}) = \alpha \times z_{ref} \times \frac{\text{chla}_{ref}}{\text{chla}} + \beta \times z_{ref} \times \left(1 - \frac{\text{chla}_{ref}}{\text{chla}}\right) \qquad (6)$$

z_{ref} denotes for the maximum migration depth at a low reference surface chlorophyll *a* concentration, which is choosen to be chla_{ref}= 0.5 μg chla L^{-1} in view of the lowest concentration measured during EisenEx outside the fertilised area, while in all simulations the outpatch surface chlorophyll concentration is 0.56 μg chla L^{-1}.

The first factor in Eq. (6) describes a shallowing response which is proportional to the increasing chlorophyll *a* concentration, while the second factor counteracts the shallowing proportional to the deviation from z_{ref}. The shallowing response weight (α) and the retentive weight (β) specify the respective impact of the factors to model the field results.

Individuals of the same species are distributed over a certain depth range. The centre of their vertical distribution is denoted in following as the preferential residence depth (z_{pref}), it changes in time and depend on the local surface chlorophyll *a* concentration (Eq. 14):

$$z_{pref}(t,\ chla) = z_{min} + f_{nDVM}(t) \times (z_{max}(chla) - z_{min}) \tag{7}$$

In this equation z_{min} is the preferential residence depth at night and $f_{nDVM}(t)$ a function which describes a normalised migration pattern (Fig 1c) that characterizes the pattern of normal DVM performed during EisenEx or EIFEX, respectively.

The directionality of a copepod individual in the model depends on the difference between its actual (z_i) and the preferential residence depth (z_{pref}) and the dispersion range I_z, and is given in terms of the directionality factor g_z (Eq. 4):

$$g_z(x, y, z, t) := \begin{cases} \left(\frac{z_i - z_{pref}}{I_z}\right) & |z_i - z_{pref}| \leq I_z \\ 1 & (z_i - z_{pref}) > I_z \\ -1 & (z_i - z_{pref}) < -I_z \end{cases} \tag{8}$$

DVM participation

During EisenEx and EIFEX, the copepods changed the amplitude of their DVM but continued to leave the surface layer during day time despite increased food concentrations in the surface layer. However, a high number of deep-dwelling *Metridia lucens* and *Rhincalanus gigas* individuals, which did not migrate towards the surface layer during day, were found during EIFEX in areas with low phytoplankton concentration. The proportion of individuals of both species, found in the upper 160 m (*M. lucens*) and 100 m (*R. gigas*; see *Parameter settings*) during darkness, respectively, increased with increasing phytoplankton concentration (Fig. 5). Linear regression analysis of the relationship between the surface chlorophyll concentration (chla [μg chl a L^{-1}]) and proportion of ascended individuals (P_{asc}) gives

$$P_{asc} = 0.167 \times chla + 0.30 \tag{9}$$

($r^2 = 0.86$) for *M. lucens* (CIII-CVI) and

$$P_{asc} = 0.138 \times chla + 0.26 \tag{10}$$

($r^2 = 0.53$) for *R. gigas* (CII-CVI).

Regression slopes are not significantly different if young copepodite stage of *R. gigas* are included or exluded.

The observed relationships suggests a food triggered DVM (re-)initiation for *R. gigas* and *M. lucens*. The impact of a triggered DVM participation is investigated by two special simulations runs. We use the standard DVM parameter settings which are assumed to characterize the DVM pattern of *R. gigas* and *M. lucens* (see *Parameter settings*), respectively, and simulate a changing proportion of ascending individuals (DVM participants). For this purpose, we introduce an ascend probability, p_A, which is the probability that a deep-dwelling copepod participates in DVM:

$$p_A = \kappa_a \times chla_i + p_{ba} \tag{11}$$

The coefficient κ_a weight the impact of the chlorophyll *a* concentration on the ascend behaviour of copepod individuals, whereas $chla_i$ denotes for the chlorophyll *a* concentration copepods are exposed to in the surface layer or were exposed to during their last stay. p_{ba} defines a basic ascend probability, translating to a minimal proportion of ascending animals.

2.2 Flow field and model geometry

The flow field at the experimental site during EisenEx and EIFEX was governed by the quasi-steady geostrophic eddy circulation. Superimposed fluctuations were mainly associated with tides and inertial oscillations (Cisewski et al. 2005, Strass et al. 2005). During both experiments a patch with an iron-induced diatom bloom moved around the eddy centre. Under the assumption of an ideal symmetric eddy circulation, the copepod drift in relation to the bloom patch is accurately modelled within a channel flow.

For the EisenEx simulations, the flow along the channel is defined by means of geostrophic velocity profiles derived from deep CTD-profiles (Conductivity Temperature and Depth probe). During EIFEX an Acoustic Doppler Current Profiler (ADCP) was attached to a buoy which was drifting with the fertilised patch, pro-

viding direct measurements of the vertical shear of the flow field along its path. Measurements were low-pass filtered to remove tidal components and fluctuations caused by inertial oscillations. Depth-dependent stationary flow in the x-direction, $u_s(z)$, is defined using the mean velocity magnitude of residual flow in the EIFEX case, while v_s and w_s are zero (Fig. 1a).

We account additionally for superimposed fluctuations of the stationary flow field by an idealised inertial motion, which is defined as

$$\begin{aligned} u_{im}(z,t) &= V_H \times \sin\left(2\Omega \sin\left(\frac{2\pi}{360} \times lat\right) \times t\right) \\ &\quad \times \left(0.5 - 0.5 \times \tanh\left(h_t^{-1}(z - z_{mt})\right)\right) \end{aligned} \tag{12}$$

and

$$\begin{aligned} v_{im}(z,t) &= V_H \times \cos\left(2\Omega \sin\left(\frac{2\pi}{360} \times lat\right) \times t\right) \\ &\quad \times \left(0.5 - 0.5 \times \tanh\left(h_t^{-1}(z - z_{mt})\right)\right) \end{aligned} \tag{13}$$

The respective time dependent velocity components at the surface are given by the amplitude, V_H, and the second factor of the equation. The third factor defines the depth dependency (see Tab. 1).

The motion of copepod individuals is treated as relative movement referenced to the upper patch centre which is fixed in the model runs. The patch centre is located at the middle of the channel-like model domain, which is sketched and discussed in detail in Krägefsky et al. (in press). The model domain is bounded by the vertical planes $-by$ and $+by$ along the channel and by $-bx$ and $+bx$ perpendicular to it. In- and outflow conditions of copepod individuals at these boundaries are defined as follows.

The drift difference between a deep migrating copepod and the phytoplankton patch was on the order of kilometres per day during EisenEx and EIFEX, while the patch moved around the eddy centre on a circular path with a length of 200 – 300 km. Consequently, copepods did not drift a second time into the bloom area over the course of the experiments despite circular trajectories in the eddy flow field. For modelling purposes, there is thus no need to track the path of copepod individuals outside the area covered by the model domain. Individuals permanently leave the model domain at the boundaries $-bx$ and $+bx$.

Inward drifting copepods initially pass through an area with permanently low chlorophyll *a* concentration, right to $-bx$ or left to $+bx$, dependent on the net drift direction ($u_{rel}(z)$). Within these areas we define an inner plane,$-bx_e$ or $+bx_e$, respectively, at which we sample the actual inward flow of copepod individuals. A correspondent actual inflow of new individuals into the model domain is forced at the outer boundary $-bx$ or $+bx$, respectively, keeping a characteristic outpatch distribution.

The flow component which determines copepod drift ($\vec{u}_m$) in y-direction is oscillating if we account for inertial motion or is zero if not. Individuals which exit at $-by$ or $+by$ are wrapped around and enter the model domain at the opposite side.

2.3 Phytoplankton distribution

The phytoplankton stock is not a prognostic variable in the model. Simulated phytoplankton distribution follows the observed progression in the field (Gervais 2002, Assmy et al. 2007), but with the following simplifications: Simplifying its variable shape in the field, the bloom area has a circular shape in the model domain. We omit small-scale field variability and assume a horizontal bell-shaped chlorophyll distribution [μg Chl a L^{-1}]:

$$F(x, y, t) = Chl_0 + (Chl_s(t) - Chl_0) \times e^{-\frac{\pi^2}{2}\frac{(x^2+y^2)}{r_p^2}} \quad (14)$$

The surface chlorophyll *a* concentration in the non-fertilised area ($Chl_0 = 0.56$ μg Chl a L^{-1}) and its progression in the patch centre, $Chl_s(t)$, is given in order to characterise the bloom development during both EIFEX and EisenEx (Fig. 1b). It implies a decline of the bloom after a time frame of 30 days, which exceeds the survey period of EisenEx. The bloom area spreads in time, prescribed by the patch radius, $r_p(t)$, with respect to the EisenEx and EIFEX situation, respectively (Fig. 1b).

2.4 Parameter Settings

The acoustic monitoring of the periodic vertical displacement of distinct sound scattering layers is a prominent tool to survey DVM behaviour of pelagic organisms with a high temporal and spatial resolution (Fig. 2). During EisenEx and EIFEX the acoustic survey showed response of shallow and deep migrating species to the increased phytoplankton concentration inside the bloom area. The acoustic mea-

surements were effectively restricted to the upper 200 m of the water column during EisenEx even for measurements with 70 kHz. During EIFEX, the effective measuring range was down to about 400 m (70 kHz), giving the ability to survey properly the migratory response of deep migrating species. Shallow migrants reduced their DVM amplitude by tens of metres and deep migrants by up to more than 150 metre, respectively (Fig. 2).

Their migratory response to the increased phytoplankton concentration is surveyed by tracking shifts in the vertical position of scattering layers during the period of maximal DVM amplitude along transects through the bloom area and the surrounding (Fig. 2). A response model is fitted to the data, solving for the shallow response weight, α, and the retentive weight, β, by relating the local migration amplitude to the surface chlorophyll concentration according Eq. 6 (Fig. 3).

The comparison with net samples shows a high correlation between acoustic measurements (normalised mean volume backscattering strength measured at 70 and 120 kHz) and copepod biomass for EIFEX (Krägefsky et al. in prep.). A low number of comparable net hauls did not allow such comparison for EisenEx. However, copepods clearly dominated the zooplankton biomass during both experiments (Krägefsky et al. in prep.). Other zooplankton, like amphipods and euphausids were sampled in low abundances, however, were probably undersampled due to net avoidance and a patchy distribution. Particularly during day-time larger zooplankton seem to have added significantly to the acoustic backscattering in the upper water column. They may have contributed to overall vertical migration response in the phytoplankton bloom area, in direct response or indirectly by following responding copepods as prey organisms.

The coarse vertical resolution of the net sampling during EIFEX (0 - 25, 25 - 50, 50 - 100, 100 - 160, 160 - 400 m) did not allow to derive phytoplankton dependent changes of the daytime residence of the different copepod species and stages from net samples. The migratory response of shallow migrants occurred mainly within the net sampling interval 50 - 100 m, while the depth range of the daytime residence of the deep migrating species was only covered by a single sampling interval (160 - 400 m). For this reason, the effects of the acoustically observed migration responses are investigated systematically covering the range of shallow, intermediate and deep migration.

During EisenEx and EIFEX, *Calanus simillimus* and the smaller *Ctenocalanus citer* clearly dominated the fraction of shallow diel migrating copepods with a daytime residence near the phytoplankton-enriched surface layer. *C. simillimus* and

particularly *C. citer* were highly abundant but are very weak scatters of sound.

Here it is assumed that the migration response of both *C. simillimus* and *C. citer* can be derived from the acoustic measurements due to their own contribution to the sound scattering in the layer of shallow migrating species and/or due to the backscattering of larger predators which prey on them. The sound scattering layer of shallow migrating species was highly patchy due to the superposition of backscattering signals of different, apparently also larger species and showed occasionally a two-layer structure during EIFEX. Clear observations of migratory response were restricted to measurements along transects with a steep horizontal gradient in surface chlorophyll concentration after the phytoplankton had reached high concentrations inside the bloom areas of EisenEx and EIFEX (Fig. 2). The migration behaviour of *C. simillimus* and *C. citer* during EisenEx is characterized by DVM parameter set PS1 ($z_{ref} = 125$ m, $\alpha = 1$, $\beta = 0.46$; see Fig. 3a). Here and in the following PSn denotes for the Parameter sets for shallow migranting species, PIn for intermediate and PDn for deep migranting species.

The migration pattern of *C. simillimus* and *C. citer* strongly overlapped also during EIFEX, showing, however, smaller migration amplitudes compared to the EisenEx situation. Differences in the vertical distribution of young and older stages observed in net samples suggest smaller migration amplitude of early copepodite stages of *C. simillimus*. Based on the acoustic observations and their vertical distribution observed in net samples, the migration behaviour of *C. simillimus* and *C. citer* during EIFEX is assumed to be approximatly given by DVM parameter set PS2 and for young stages of *C. simillimus* by PS3. PS2 defines a day-time residence of 100 m (z_{ref}) at the low reference chlorophyll concentration and a moderate migratory response to increased phytoplankton concentration ($\alpha = 1$, $\beta = 0.46$), while PS3 define a very shallow maximal day-time residence ($z_{ref} = 70$ m) and weaker migratory response ($\alpha = 1$, $\beta = 0.5$).

The migration behaviour of deep migrating species is simulated using DVM parameter sets PD1 and PD2 (Fig. 3b,c), covering deep (PD1, $z_{ref} = 240$ m) and very deep migration (PD2, $z_{ref} = 350$ m). Copepods characterized by PD1 ($\alpha = 1.11$, $\beta = 0.35$) and PD2 ($\alpha = 1.11$, $\beta = 0.25$) show a strong migratory response inside the phytoplankton bloom area. In contrast to the migration behaviour of other copepods simulated in the model, copepods characterized by PD2 show a vertical night-time distribution which is not centred within but near the bottom of the phytoplankton enriched surface layer ($z_{min} = 100$ m). PD2 may characterize the migration behaviour of the copepod species *Metridia lucens* during EIFEX. The α and

β coefficients of PD2 are derived with respect to the upper edge of the scattering layer, which merged into at a diffuse persistent deep-scattering layer at the deepest daytime residence (Fig. 4) .

In addition to shallow and deep migration, we simulate the behaviour of copepods with an intermediate migration amplitude, which is defined arbitrarily by the DVM parameter set PI1 ($z_{ref} = 180$ m, $\alpha = 1$, $\beta = 0.375$) assuming a semi-moderate migratory response inside the phytoplankton bloom area. Pl1 may characterize the migration behaviour of the copepod species *R. gigas* (see below).

Please note that due to the difference between $chla_{ref}$ and the outpatch surface chlorophyll concentration used in all simulations (0.56 μg chla L^{-1}), the maximal day time migration depth outside the fertilised area is about 5% less than z_{ref} in case of PS1, PS2, PS3 and PI1 (Tab.1).

The migration behaviour of the various copepod species is modelled under different environmental conditions, representing the EisenEx and the EIFEX situation. These involve use of the stationary EisenEx and EIFEX flow field, respectively, which are superimposed by inertial oscillations with a constant amplitude $V_H = 0.2$ m s^{-1} and simulation of the specific patch dynamic (Fig. 1b). The profiles of inertial oscillations depend on the mixed layer depth (z_{mt}) in the model. Two different mixed layer depth settings of 60 m and 80 m are used for the EisenEx simulations. A deep mixed layer of 80 m is assumed during all EIFEX simulations.

The proportion of migrating animals of *R. giga*s and *M. lucens* increased with increasing phytoplankton concentration. We simulate this behaviour under EisenEx and EIFEX condition ($z_{mt} = 80$ m), using the DVM parameter PI1 and PD2 and assuming a characteristic κ_a weight of 0.15 and a basic ascend probability $p_{ba} = 0.3$ for both species (see *DVM participation*).

3 Results

Reported changes in the horizontal distribution of copepods refer to the number of individuals within the total water column (abundance per unit area). Changes in abundance are given relative to the initial horizontal homogenous copepod distribution. The term relative abundance is used, as a relative measure of the local copepod abundance relative to the initial abundance. The characteristic relative abundance outside the bloom area (N_{out}) is thus 1.

The different copepod species are divided by their maximum migration depth into a group of shallow migrating animals which reside near the food-enriched surface

layer even under the condition of low phytoplankton concentration (PS1, PS2, PS3), and secondly into a group of deep migrating animals (PD1, PD2).

Parameter set PI1 describes a vertical migration pattern with medium amplitude and semi-moderate response to the surface chlorophyll concentration. This parameter set was used for two reference simulations, during which we prescribed the patch dynamics and stationary flow field of EisenEx and EIFEX, respectively. During both simulations a mixed layer depth of 80 m was assumed, to force the same fluctuations of the flow field due to inertial oscillations superimposed on the stationary flow. These reference simulations were also used for assessing the individual food gain due to the migratory response to the ambient chlorophyll concentration (see *Individual food gain*).

3.1 Reference simulations

In the reference EisenEx simulation the copepods increase 1.8 fold at the patch centre within 3 weeks after fertilisation (Fig. 6 a-d, Fig. 7 d). The changes in the horizontal distribution of copepods follow the progression and horizontal distribution of the chlorophyll concentration until the phytoplankton bloom declines (after day 30). The maximum abundance increase is at the patch centre and vanishes within the patch margin (Fig. 6a-d) where local abundance minima are formed upstream. The interference of inertial oscillations and DVM leads to fluctuations in the local number of copepods and to a periodic displacement of the horizontal copepod distribution relative to the patch centre (see periodic short-term fluctuation in Fig. 7d).

With the reference migration behaviour PI1 the copepods increase up to 2.8 fold in the patch centre under EIFEX condition. The major pattern of abundance increase and decrease and the effects of inertial oscillations are similar to the EisenEx reference run (Fig. 6e-h, Fig. 7d).

Simulations with reference settings but different mixed layer depth and without inertial oscillations

In two additional simulation we simulate a flow field without inertial oscillation and a shallower extent of inertial oscillation ($z_{mt} = 60$ m), respectively, using otherwise unchanged settings of the reference run (PI1) under EisenEx condition. At $z_{mt} = 60$ m the increase in abundance of copepods within the central patch area (chlorophyll concentration $\geq$ 1 μg chl a L^{-1}) and in the patch centre ($r \leq 1000$ m) is lower than during the EisenEx reference simulation after day 14 (Fig. 7d). The simulation

results are very similar to the simulation results using a stationary EisenEx flow field without inertial oscillations (Fig. 7d). The copepods show similar abundances in the patch centre during bloom termination in the EisenEx reference simulation, in the simulation with a mixed layer depth of 60 m and in the EisenEx simulation without superimposed inertial oscillation (Fig. 7d).

3.2 Shallow migrating copepods

The shallow migrating copepod species show maximum increase in abundance under EisenEx condition. At a mixed layer depth of 60 m, these copepods show about 1.8 (PS1), 1.9 (PS2) and 1.3 (PS3) fold increase in the patch centre at day 21 and 1.9, 2.3 and 1.5 fold increase at day 40, respectively (Fig. 7a-c). The DVM behaviour PS2 and PS3 leads to a fast abundance increase within 6 (PS3) to 14 days (PS2). The abundance remains high till bloom termination in case of PS2; it decreases after the second week in case of PS3 (Fig. 7b,c). In both cases, the number of copepods in the patch centre increases again during the termination of the phytoplankton bloom. Copepods characterized by PS1 show a steadily increasing abundance until day 30 and minor changes thereafter until day 40 (Fig. 7a).

At a mixed layer depth of 80 m, the DVM behaviour PS1 and PS2 leads to a fast abundance increase in the patch centre within the first week in case of PS2 and within the second week after fertilisation in case of PS1. Copepod abundance remains quite constant till the bloom peak, and increases further during bloom decline (Fig. 7a,b). Contrary to PS1 and PS2, copepods migrating accordant to PS3 show a steady but weak increase in abundance (Fig. 7c). The number of shallow migrating copepods is increased by 1.9 (PS1), 1.5 (PS2) and 1.15 (PS3) in the patch centre at day 21. The respective abundance increase is 2.3, 1.7 and 1.25 at day 40 (Fig. 7a-c).

Without inertial oscillations, the abundance of the shallow migrating copepods increases steadily in the patch centre. They show about 1.3 (PS1), 1.3 (PS2) and 1.15 (PS3) fold increase at day 21, and 1.6, 1.5 and 1.25 fold increase, respectively, at day 40 (Fig. 7a-c).

In the simulations the shallow migrating copepods show less abundance increase under EIFEX than under EisenEx conditions. In the EIFEX simulations with a mixed layer depth of 80 m, their abundance increases by 1.5 (PS1), 1.3 (PS2) and 1.1 (PS3) in the patch centre at day 21, and 2.3, 1.6 and 1.2, respectively, at day 40 (Fig. 7a-c). DVM behaviour PS1 and PS2 leads to a fast initial increase in copepod abundance and gradual increase thereafter (Fig. 7a,b). The very shallow migrating

copepods (PS3) show steady but weak increase in abundance at the patch centre (Fig.7c).

Most of shallow migrating copepods show fast abundance increase inside the phytoplankton bloom area in the simulations. These copepods show a complex horizontal distribution relative to the patch centre and periodic changes in the local copepod abundance, caused by an interference of inertial oscillations and DVM. Transient local maxima are formed inside the phytoplankton bloom area which can exceed the abundance at its centre. A distinct local minimum in copepod abundance circulates periodically around the phytoplankton patch during the first three weeks after fertilisation (not shown).

3.3 Deep migrating copepods

Copepods characterized by the DVM parameter sets PD1 and PD2 show maximal migration depths of 240 and 350 m, respectively. Both species increase about 1.5 fold in the patch centre within the first three weeks under EisenEx condition (Fig. 7e,f). The abundance increase is much less affected by differences in inertial oscillations. The abundance of copepods migrating accordant to PD1 increases by 1.7 ($z_{mt} = 60$ m), 1.7 ($z_{mt} = 80$ m) and 1.8 (no inertial oscillations) until day 40 (Fig. 7e). Copepod abundance shows pronounced variability during decline of the bloom in case of PD2, increasing approximately 1.7 fold until day 40 in all EisenEx simulations (Fig. 7f).

The deep migrating copepods show maximum abundance increase under EIFEX conditions. In the EIFEX simulation ($z_{mt} = 80$ m), the copepods characterized by PD1 increase 1.8 fold at day 21 and increase 2.2 fold until day 40 (Fig. 7e). The DVM behaviour PD2 causes 1.5 fold increase at day 21. The copepods show peak abundance in the patch centre during the bloom termination which is 1.8 fold higher than the abundance outside the bloom area. Their relative abundance is 1.6 at day 40.

3.4 Individual food gain

A copepod individual gains nutritional benefit by its migratory response that increases its retention time in the phytoplankton rich area. The individual nutritional benefit may be assessed by comparing the food intake of individuals which show a migratory response to ambient food concentration to those with no response. In the following, the nutritional benefit is expressed in terms of the ratio of the cumulative

food intake of responding and non-responding individuals since they entered into the phytoplankton bloom area. The food intake is assumed to be restricted to the night time and to be linearly dependent on the diatom carbon concentration. The horizontal and vertical diatom distribution in the model domain and its progression is defined and discussed in detail in Krägefsky et al. (in press).

Individuals which were initially located at a distance of 15 to 20 km west of the patch centre are representative for a larger number of copepods which will enter the food patch within a time frame of days to two weeks after bloom initialisation. During the reference simulation these copepod individuals increase their food intake up to 2.2 times until the bloom declines (day 30) and up to 2.6 times until day 40, respectively, relative to individuals showing no shallowing of the daytime residence depth in the food rich area (Fig. 8a). Copepods which show the reference DVM behaviour (PI1) under EIFEX condition increase their food gain up to 2.5 times until the bloom decline (day 30) and up to 2.6 times until day 40, respectively, relative to non-responding animals (Fig. 8b).

After the individuals entered the food patch, the individuals with a migratory response show a decrease of their drift relative to the phytoplankton patch and their path diverges increasingly from the path of their non-responding counterparts. Likewise different retention is evidenced in the path of responding individuals that are exposed to different food concentrations. Their path is illustrated by a sequence of their horizontal positions at intervals of 2 days (Fig. 8a,b). The wobbling of the surface layer, which is caused by inertial oscillation, leads to a circular path of individuals relative to the phytoplankton patch when they reside below the mixed layer (Fig. 8a).

The actual pattern of the path of a copepod individual depends on its drift magnitude due to the stationary flow and its depth and time dependent drift due to inertial oscillations which cause periodic fluctuations of the flow field with a period of 16 h at the experimental site, while the copepods perform diel vertical migration. In the reference simulation the copepods shift their residence depth at day towards the bottom of the mixed layer, and thus within a zone with strong vertical gradients of the amplitude of inertial oscillations. This causes a distinct bending of the path within the high food area (see *Discussion*).

3.5 Changing proportion of migrating *Metridia lucens* and *Rhincalanus gigas*

Changing DVM participation of *M. lucens* and *R. gigas* during EIFEX is simulated, assuming that parameter set PD2 and PI1, respectively, characterizes the DVM pattern and the shallowing response of these copepod species.

Within 21 days, *M. lucens* increases less in abundance inside the phytoplankton bloom area in the EIFEX simulation but more in the EisenEx simulation if the copepods show triggered DVM participation compared to the standard simulations with un-triggered DVM participation (Fig. 9a). The differences each amount to about 5% of the characteristic copepod abundance outside (N_{out}). *R. gigas* shows substantially higher abundance increase within 21 days with triggered DVM participation in the EisenEx simulation compared to standard simulation (Fig. 9c). The differences amount to 5-10% of N_{out} in the central patch area ($\geq$ 1 μg chl a L^{-1}) under EisenEx conditions and to more than 20% of N_{out} towards the patch centre under EIFEX conditions.

M. lucens shows almost equally large increases till bloom termination (day 30) with triggered and un-triggered DVM participation in the respective EIFEX simulations (Fig. 9b). *M. lucens* shows substantially higher increase with triggered compared to a un-triggered DVM participation under EisenEx condition, amounting to 10-20% of N_{out}. *R. gigas* abundance increases to substantially higher values with un-triggered compared to a general DVM participation under EisenEx and EIFEX conditions (Fig. 9c,d). The differences amount to more than 20% (EisenEx) and 40% (EIFEX) of N_{out} towards the patch centre.

4 Discussion

The model study assesses the magnitude of changes in horizontal copepod distribution as solely caused by changing DVM pattern in response to the environmental phytoplankton concentration during EisenEx and EIFEX. The migration behaviour was observed with acoustic measurements, while the net samples allow only for basic identification of shallow and deep migrating copepods due to the vertical and temporal sampling resolution.

It is assumed that the acoustically detected migration response of shallow migrating zooplankton reflects the migration behaviour of *C.citer* and *C. simillimus*, which clearly dominated the shallow migrating zooplankton in the net samples. *C.*

citer was highly abundant, but is small and a very weak scatterer of sound. The acoustic observations in the upper water column suggest a wide migratory response of different species including larger zooplankton which may have responded directly to changing phytoplankton concentration or indirectly by following responding copepods as prey organisms. It is not unlikely that the backscattering signals of larger predatory zooplankton have contributed significantly to the sound scattering which would have largely increased the acoustic detectability of the migration response of small, directly responding zooplankton they prey upon. Thus, the displacement of the sound scattering layer of shallow migrating species may well reflect the migration response of small copepods like *C. citer* indirectly through their predators. Furthermore, in view of the overall migratory response of shallow and deep migrating species it can be assumed that the acoustic observations characterize the migration behaviour of a wide range of copepods including those species and stages that contribute minor to the sound scattering due to their smallness or low abundance.

Given the limitations due to the net sampling resolution, the effects of the observed migration responses are investigated systematically covering the range of shallow, intermediate and deep migrating copepodites and adults copepods. Effects of growth (recruitment from naupliar stages into copepodites) and mortality are not accounted for in the model.

We assume a general DVM participation and vertical distribution of all individuals within a dispersion range I_z around the preferential residence depth, $z_{pref}(t,\ chla)$, in the standard simulations. In the field, however, not all copepod individuals leave the surface layer during day or migrate towards the surface during night. The assumption of a general DVM participation may significantly overestimate the abundance increase in the bloom area of those copepods which show a high proportion of non-migrating individuals in the field under low and high phytoplankton concentration (but see *Triggered DVM participation*).

The basic diel migration behaviour is described by the same normalised migration pattern ($f_{nDVM}(t)$) irrespective of the maximum migration depth, while in fact the shallow migrating species showed slower descend and ascend compared to the deep migrating species. Sensitivity tests (EisenEx conditions) which take this particular DVM pattern into account show similar abundance increases compared to simulations with standard DVM pattern. In view of the likely much stronger effects of other model simplifications, we use the same f_{nDVM} for shallow, intermediate and deep migrating species. The simulated flow field and the circular shape of the phytoplankton bloom area are further model simplifications. The possible effects of these

simplifications are discussed below.

4.1 Shallow migrating copepods and effects of inertial oscillation

The phytoplankton concentration strongly affects the underwater light field in the open ocean. A displacement of the phytoplankton enriched surface layer relative to the deeper water column, like its wobbling which is caused by inertial oscillations, gives rise to local changes in intensity and spectral composition of the underwater irradiance. Copepods located within the horizontal phytoplankton gradient in the bloom area or at its border sense these changes at their actual day-time residence in the deeper water column.

The clear dependency of the day-time residence on actual surface chlorophyll concentration which is observed particularly for the more coherent scattering layer (e.g. PD1) implies its adjustment by net up- or downward movement of the copepods in response to changing phytoplankton concentration in the surface. This adjustment happens gradually in the model, because copepod swimming is predominantly random within the depth range $\pm I_z/2$ around the preferential residence depth, z_{pref}, and shows full vertical directionality only at the border of their dispersion range (I_z).

Slow migration response is sufficient to allow for adjustment of the residence depth to gradual changes in surface chlorophyll concentration, for example, due to inertial oscillations. Gradual adjustment of the residence depth of shallow migrating copepods entrains them into the wobbling movement of the surface layer which causes a net displacement of animals along the horizontal phytoplankton abundance gradient. The magnitude of the relative drift of surface and deeper layer allows for substantial short term increase in the abundance of copepods in the phytoplankton rich area (Fig. 7a-c). Their potential abundance increase is determined by the radius of inertial oscillations (ca. 1850 m in the simulation) and the extent of the phytoplankton patch.

Shallow migrating copepods increase less in abundance during EIFEX simulations compared to the EisenEx simulations, which is mainly a consequence of the initial larger extent of the fertilised area. The model simplification of a circular phytoplankton patch, however, may introduce significant bias towards underestimating the abundance increase in the field for EIFEX. This bias is due to the fact that the net displacement of copepods can take place along smallest dimension of

a non-circular food patch, because of the circular relative motion of deep-dwelling copepods and surface. The phytoplankton patch has a variable, elongated shape in the field and a smaller patch width than given by the patch radius in the simulation. The simulated abundance increase in the central patch area is in fact similar to the increase shown during the EisenEx simulations, if e.g. an elliptical phytoplankton patch is simulated under EIFEX condition with a semimajor axis identically to $r_p(t)$ and a semiminor axis of length $3/4\, r_p(t)$ (Fig. 7b).

During EisenEx and EIFEX inertial motion showed periods of intensification and decay, forced by a sequence of strong wind events which set the water in motion, that continues to move in a circular trajectory subject to the Coriolis force. The mixed layer depths settings define the depth range of the upper water column which is affected by inertial oscillations in the simulation. This depth range was variable in the field during EisenEx and EIFEX, with a temporal trend towards an increasing extent with deepening of the mixed layer during storm events during EisenEx. A constant mixed layer depth of 60 m or 80 m is assumed during the simulations, which is likely a characteristic upper and lower limit, respectively, of the variable vertical extent of inertial oscillations in the field.

PS1 show maximum abundance increase at the patch centre during the EisenEx simulation with a mixed layer depth of 80 m. PS2 shows nearly the same maximum abundance increase with a mixed layer depth of 60 m. Given the variability of the surface currents in the field (e.g. the variable depth range of inertial oscillations), PS1 and PS2 should cause similar abundance increase in the central area of a phytoplankton patch of similar dimensions during EisenEx and EIFEX. The simulation results imply comparable, up to 2-fold increase in the abundance of *C. citer* and older copepodite stages of *C. simillimus* in phytoplankton rich area during EisenEx and EIFEX, if corrected for the bias due to the simplified shape of the phytoplankton patch in the model (Fig. 7b).

In case of *C. simillimus* it has to be assumed that a high proportion of about 35% of CIV and younger copepepodites did not leave the surface layer during daytime. Accounting for this high number of non-migrating individuals, the abundance increase caused by PS2 is still large if the above discussed conditions are assumed (elliptical phytoplankton patch, $z_{mt} = 60\,m$), and shows a maximum 1.8-fold increase at the patch centre after 3 weeks (ca. 1.65-fold at day 40). The copepod abundance is increased by more than 1.6-fold till the peak of the bloom in the area with chlorophyll concentrations $> 1.5\,\mu g\,L^{-1}$ (not shown).

4.2 Comparision with observations

Multi-Net sampling covered only the first half of EisenEx. Samples were taken at 6 stations inside and 2 stations outside the fertilised area till day 11 after fertilisation. The median abundance of *C. simillimus* was ca. 23,000 m^{-3} initially, and was ca. 40,000 m^{-3} (0 - 150 m) during the second week (Krägefsky et al. in prep.). Smaller copepods like *C. citer* were sampled during the whole experiment with Niskin bottles at discrete depths between 10 m and 150 m at 11 stations inside the fertilised area. These data show ca. 3- fold increase in the abundance of *C. citer* inside the patch, which, however, is an uncertain assessment of the actual increase due to the sampling method and the high abundance variability (Henjes et al. 2007).

During EIFEX, *C. citer* and *C. simillimus* were sampled with a Mulit-Net at 18 stations inside and 6 stations outside the fertilised area till the end of the experiment which lasted for 37 days. *C. citer* shows about 2.3-fold increase in abundance in the bloom area from initially 95,000 ind. m^{-2}. Most of the increase is reached within the first 2 - 3 weeks of EIFEX (Krägefsky et al. in prep.).

C. simillimus shows a similar abundance increase in total (copepodite stages CI-CVI), increasing 2.1 fold in the bloom area from initially 15,000 ind. m^{-2}. No increase, however, is observed in the number of early copepodites CI and CII. Strong increase is shown within the stages CIII, CIV and CV, whereas the strongest increase is observed for CIV. Adults occur at very low number with a median abundance of 110 females m^{-2} and 14 males m^{-2}. Their abundance shows no clear temporal trend. A shift towards an older average copepodite stages from C3 to C4.5 is observed outside the bloom area, but no increase in the total abundance of copepodites and adult C. *simillimus* (Krägefsky et al. in prep.). The long duration of EIFEX may have allowed for significant development from earlier to older developmental stages. Growth likely has affected the abundance pattern of the single copepodite stages over the course of EIFEX. However, the stage-distribution of *C. simillimus* and *C. citer* did not indicate substantial recruitment from naupliar in copepodites.

Changes caused by growth or mortality interfere with the accumulation of copepod individuals of the different stages inside the bloom area which is caused by their vertical migration. Combined effects of stage specific vertical migration behaviour, which cause weaker increase of early *C. simillimus* stages according to the simulation results, and development of individuals into older copepodite stages, may have lead to the observed increase pattern of the different copepodite stages inside the bloom area during EIFEX.

There is good agreement between the observations and the basic simulation results. However, stronger abundance increase of shallow migrating species *C. citer* and *C. simillimus* was observed in the field compared to the simulations. *C. citer* and *C. simillimus* show high abundance variability in the samples outside the fertilised area like all other copepod species, which imply a general patchiness in their horizontal distribution that affected the pattern of their abundance increase in the phytoplankton-rich area. The very limited number of net samples outside the fertilised area does not allow a proper assessment of this patchiness. It is thus unknown to which extent the assessed abundance increases are affected by initial differences between in- and outside the fertilised area.

The major simplification of the flow field at the experimental sites in the simulation likely contributed significantly to differences between simulation results and field observations. In the field, the local increase in the abundance of shallow migrating copepods inside the bloom area and the decrease in the surrounding was sensitive to any, for example, wind-driven currents, causing a relative drift between the phytoplankton enriched surface and the deeper water column. Thus the actual flow field at the experimental sites may have caused somewhat higher abundance increase than in the simulation. However, in the simulation the vertical distribution of the different species is approximated by a simplified time- and chlorophyll dependent distribution, while their distribution is actually much more variable in the field. The variability in the surface flow and animal distribution should have been caused more complex horizontal redistribution of particularly shallow migrating species compared to the simulation. Thus the modelling results should be regarded more as an assessment of the magnitude rather than an exact evaluation of the abundance increase caused by the migration response of shallow migrants.

Deep migrating copepods are less affected by periodic fluctuations of the surface flow field. Their increase in the phytoplankton rich area is mainly affected by the vertical shear of the stationary flow field (Fig. 7d-f). Deep migrating copepods show strong abundance variability in the Multi-net samples during EisenEx. Their abundance development cannot be assessed properly.

During EIFEX, *M. lucens* dominated the deep migrating copepod species, but with strong variability. Significant abundance increase was shown in the fraction of older stages CIII-CVI, increasing 2.0 fold from 26,000 ind. m^{-2} initially. Linear regression show a non-significant decrease in abundance of CII by ca. 100 ind. d^{-1} from 12,000 individuals initially and by ca. 300 ind. d^{-1} for stages CI-CII, including however CI stages of *Pleuromamma sp.* and *Metridia sp.* which were grouped

without species identification for the earliest copepodite stage (CI). Corrected for possible recruitment by 100 - 300 ind. d^{-1} from young into older stages, the development in abundance of older stages (CIII-CVI) would imply a 1.9 fold to 1.6 fold increase due to their vertical migration behaviour (Krägefsky et al. in prep.).

M. lucens shows up to 1.8-fold increase at the highest phytoplankton concentration in the simulation with a triggered DVM participation (Fig. 9b), which is in closer agreement with the corrected field increase. Nevertheless, the strong abundance variability did not allow proper assessment of the actual recruitment from early to older copepodites of *M. lucens* during EIFEX.

R. gigas was an order of magnitude less abundant than *M. lucens* and showed 2.3 fold increase (CII-CVI) excluding the first copepodite stage and 3.5 fold including CI. *R. gigas* showed a pronounced shift in stage distribution during EIFEX. The average copepodite stage decreased gradually inside the fertilised patch from CV toward CIII. Growth and differential stage-specific mortality may have affected these changes. Except for one station, however, only younger stages with an average stage of ca. C3 were found outside the fertilised patch. The increasing convergence of the average copepodite stage inside and outside the phytoplankton rich area shown over the course of EIFEX is consistent with the assumption that most of the signal was due to the inflow and retention of individuals from the surrounding of the fertilised area.

The migration behaviour of *R. gigas* during EIFEX may differ from PI1 and between single copepodite stages. Simulations under EIFEX condition show similar increase in abundance of copepods for a range of maximum migration depths (z_{ref} = 150 - 240, $\alpha = 1$; $\beta = 0.375$) around $z_{ref} = 180$ m given by PI1 during the first 3 weeks. After the third week stronger abundance increase is observed with smaller z_{ref}, increasing ca. 3.0-fold ($z_{ref} = 150$ m) compared to 2.2- fold with $z_{ref} = 240$ m (not shown). A much shallower migration behaviour would be described by parameter set PS1. However, in view of the variability of the real flow field, the migration behaviour of *R. gigas* may be well approximated with parameter set PI1. The simulations show up to 2.8-fold increase for *R. gigas* with a triggered DVM participation (Fig 9d) which agree well with the field observations.

4.3 Triggered DVM participation

The proportion of deep-dwelling individuals of *R. gigas* and *M. lucens* decreases strongly with increasing phytoplankton concentration from a high proportion in

phytoplankton-poor areas. A general upward displacement of individuals may have added to this signal, but its contribution can not be assessed properly due to the very restricted vertical and temporal resolution of the net samples. Nevertheless, the findings suggest dependency of the ascend behaviour of *R. gigas* and *M. lucens* on the surface phytoplankton concentration. Compared to individuals with daily ascend, deep-dwelling individuals with triggered DVM participation drift larger distances relative to the rare food in the surface layer, increasing the probability for copepods to be subsequently exposed to a food rich environment in areas with patchy food distribution (see below).

The energetic requirements of a copepod may be reduced substantially during deep-dwelling periods, e.g. saving the energetic costs of vertical migration (Morris et al. 1985). However, the lower food supply in the deeper layer causes a food shortage and the copepod needs to re-ascend periodically into the food-enriched surface layer to gain net benefit by their migration behaviour. The proportion of deep-dwelling individuals of both species suggests a re-ascend every second to third day in the phytoplankton-poor area during EIFEX.

The deep-dweeling behaviour of copepods should be affected by the feeding selectivity of the different species. Probable differences between *R. gigas*, which is a predominantly herbivorous species (Atkinson 1998), and *M. lucens*, however, cannot be addressed with the limited number of net samples.

4.4 Migratory behaviour in the Southern Ocean

The predator-evasion hypothesis has gained wide acceptance, which supposes visual predation to be the driving force in evolution of diel vertical migration shown by widely diverse animal species (Hays 2003). Migration out of the well-illuminated surface layer is assumed to substantially decrease mortality of descending animals relative to their non-migrating counterparts by reducing the risk of being detected by visually hunting predators.

Different studies have addressed proximate factors in terms of mechanisms at the animals disposal to perceive and respond to environmental stimuli to realise DVM behaviour. These studies explore the ability of copepods to detect absolute or relative light intensities, to perceive chemical cues like predator exudates, or to sense predators by tactile or visual cues, and investigate the particular behavioural response (Stearns & Forward 1984, Bollens et al. 1994, Cohen & Forward 2005).

In total, findings reveal high plasticity of the DVM behaviour of single copepods,

with the ability of fast flexible response to abiotic (Buchholz et al. 1995) and biotic factors, like food abundance and vertical food distribution (Harris 1988) and presence of visual (Bollens & Frost 1991) or tactile predators (Ohmann et al. 1983, Neill 1990). Initiation of reverse diel vertical migration may be triggered in relation to the vertical distribution of tactile predators in the water column (Irigoien et al. 2004). Few studies have addressed individual variability and demonstrated the influence of body condition on DVM behaviour (Bollens & Frost 1991b ,Tarling et al. 1999, Hays et al. 2001).

The abundance of fish and fish larvae is low in the Southern Ocean (Morales-Nin et al. 1995, Hoddell et al. 2000) and the predation impact on copepods is dominated by carnivorous and omnivorous macrozooplankton. Chaetognaths and euphausiids account for most predation mortality (Pakhomov et a. 1999) and thus the predation risk basically arise from tactile or predominantly tactile predators. Absence of a reverse DVM pattern may be explained by the non-periodic migration behaviour of chaetognaths in the Southern Ocean (Johnson & Terazaki 2004). Given the energetic costs associated with vertical migration (Morris et al. 1985), however, we are faced with the question why copepods undertake normal DVM, while being exposed to modest visual predation risk.

Southern Ocean copepods drift through a strongly seasonal, patchy food environment. Transient mesoscale phytoplankton blooms strongly increase the phytoplankton concentration locally in the growth season and cause high horizontal patchiness of the food environment (Smetacek et al. 1990). Diel vertical migration periodically reintroduces animals into the relatively food-enriched surface layer, but effects divergent drift between migrating copepod individuals and food items drifting with the flow in the upper water column.

The observed DVM behaviour amplifies the drift divergence in food-poor areas, whereas the shallowing response effects an increasingly uniform drift of phytoplankton and copepods with increasing phytoplankton concentration. It causes a relative increase of retention and individual nutritional gain inside mesoscale food patches up to 2-3 fold according to the model results (Fig. 8b). The observed DVM behaviour thus should maximise the total food intake gained during the life-cycle of a copepod individual, and have minor effect on visual predation risk, as the shallowing magnitude is in the order of or less than the shift in isolume depth caused by increased phytoplankton concentration.

In fact, the field results indicate limiting food supply outside the bloom area and nutritional benefit inside. This, for example, is evidenced by a strong reproduc-

tive response of *Rhincalanus gigas* individuals (Jansen et al. 2006), increasing the percentage of egg-producing females from about 0 to 90% towards the end of the phytoplankton bloom during EIFEX.

4.5 Conclusion

The acoustic measurements show an overall response of shallow and deep migrating species, which is investigated systematically covering shallow, intermediate and deep migration. The coarse net sampling resolution does not allow to derive the particular migration behaviour of the different copepod species and their stages from the net samples, which is a major limitation of this study. The results of the simulation study show that the observed migratory response to the increased phytoplankton concentration can explain the abundance development and most of the large increase of shallow and deep migrating copepods inside the phytoplankton bloom area of EIFEX. A copepod individual should gain strong nutritional benefit by this migration behaviour.

Acknowledgements

We grateful acknowledge the professional and friendly support of the colleagues and the crew of the RV Polarstern during EisenEx and EIFEX. We thank C. Klaas for provding Chl *a* and R. Bellerby for providing pCO_2 data for the EIFEX cruise. V. Strass, H. Leach and B. Cisewski kindly provided flow field data.

identifier	z_{ref}	α	β	I_z	z_{min}	$z_{max}(Chl_0)$	charcteristic for
PS3	70	1	0.50	30	25	66	early copepodites of Calanus simillimus (EIFEX)
PS2	100	1	0.46	30	25	94	Ctenocalanus citer and Calanus simillimus (EIFEX)
PS1	125	1	0.46	30	25	118	Ctenocalanus citer and Calanus simillimus (EisenEx)
PI1	180	1	0.38	30	50	168	Rhincalanus gigas
PD1	240	1.11	0.35	30	50	246	deep migrating species
PD2	350	1.11	0.25	30	100	355	Metridia lucens

Table 1: Parameter sets describing the DVM pattern of different copepod species (see Eq. 9 - 11) and maximal migration depth ($z_{max}(chl_0)$) in the non-fertilised area ($Chl_0 = 0.56\ \mu g\ Chl\,a\ L^{-1}$).

Parameter	Definition	Units	Value
α	shallowing response weight	dimensionless	1.0 - 1.11
β	retentive weight	dimensionless	0.248 - 0.5
I_z	dispersion range	m	30
z_{ref}	maximum migration depth outside the patch	m	70 - 350
z_{min}	residence depth at night	m	25 - 100
f_{nDVM}	normalised migration pattern	dimensionles	0 - 1
p_A	ascend probabiliy	dimensionless	0 - 1
κ_a	food weight ascend	$(\mu g\ Chla)^{-1}$ L	0 - 0.15
p_{ba}	basic ascend probability	dimensionless	0.3 - 1
V_A	Swimming speed of copepod	m s^{-1}	0.01 - 0.06
ϑ	zenith	rad	0 - π
φ	azimuth	rad	0 - 2π
V_H	Velocity amplitude of inertial oscillation	m s^{-1}	0.2
Ω	Angular velocity of rotation of earth	rad s^{-1}	7.29×10^{-5}
lat	Latitude	$^\circ$	-48
h_t	slope factor	m	15
z_{mt}	mixed layer depth	m	60-80

Table 2: Definition and parameter range

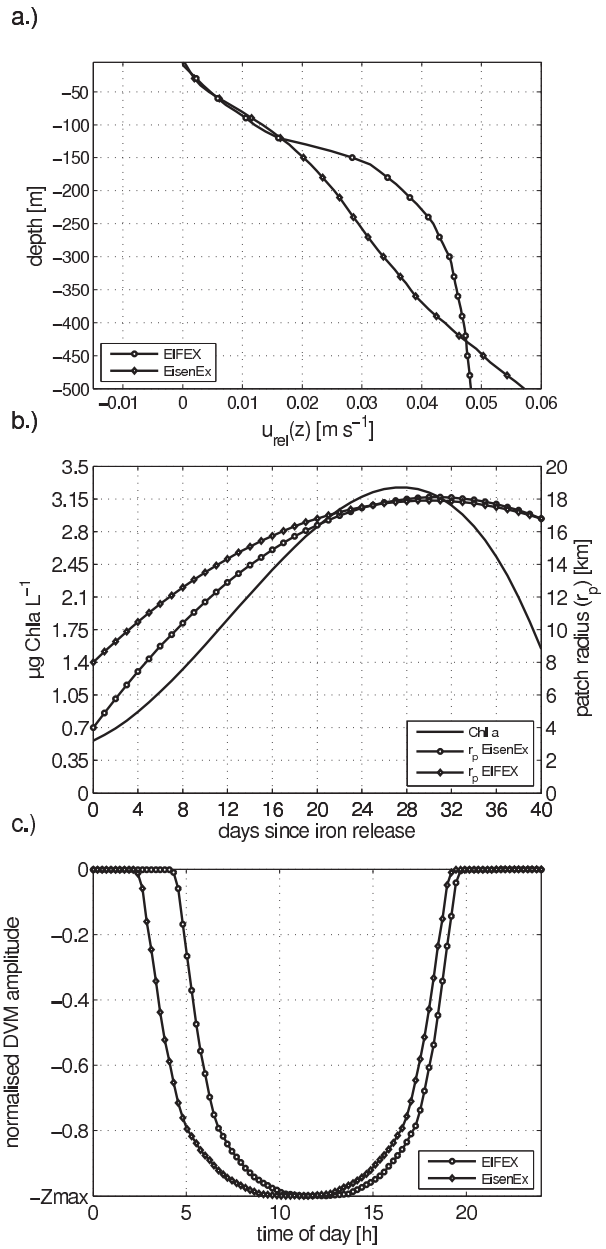

Figure 1: a.) Drift velocity of copepods relative to the upper patch centre ($u_{rel}(z)$) due to the stationary flow. b.) Temporal development of the chlorophyll a concentration at the patch centre and the progression of the patch radius (r_p) for the EisenEx and EIFEX model runs. c.) Normalised DVM amplitude used in EisenEx and EIFEX simulations, respectively.

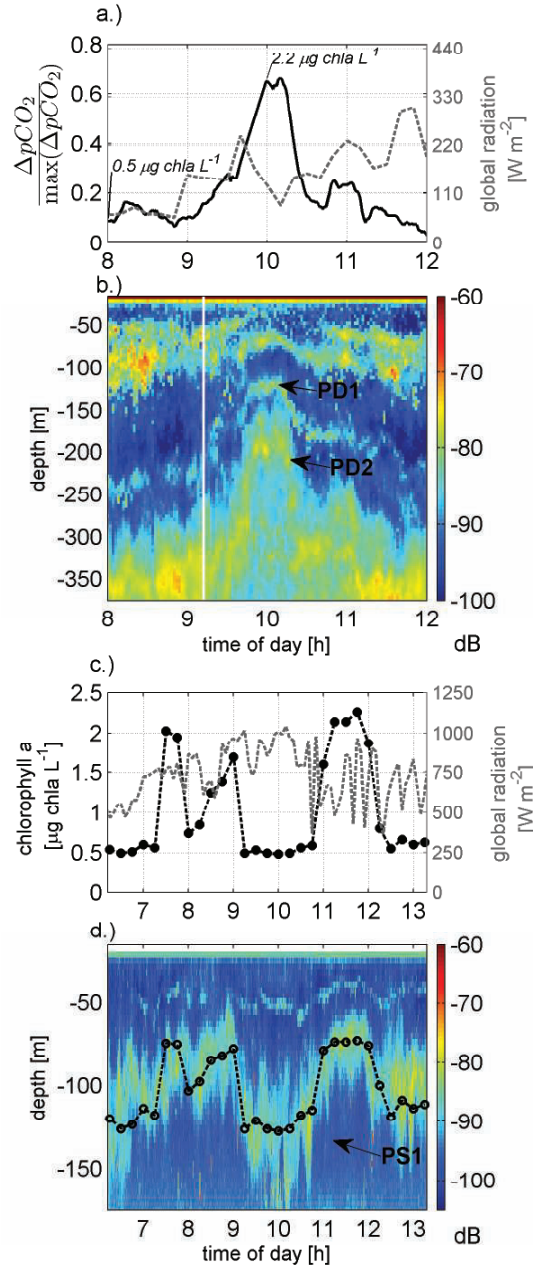

Figure 2: Overall response of shallow and deep migrating species with strong shallowing of their daytime residence towards the centre of the bloom area shown by the vertical displacement of different sound scattering layers in Echogram (b) for a transect through the phytoplankton bloom area of EIFEX . Normalised measurements of pCO2 drawdown (Bellerby et al. 2005) along the transect are shown (a, solid line) as a tracer indicating measurements outside (low values) and the location within the bloom area (increasing values towards the centre). The migratory response is widely independent of actual changes in solar irradiation (a, dashed line). Echogram d) shows the response of shallow migrating species during EisenEx to the surface chlorophyll concentration (c, filled circles), which also seems to be widely independent of changes in solar irradiation during daytime (c, dashed line). Open circle in (d) indicate the expected residence depth accordant response model PS1.

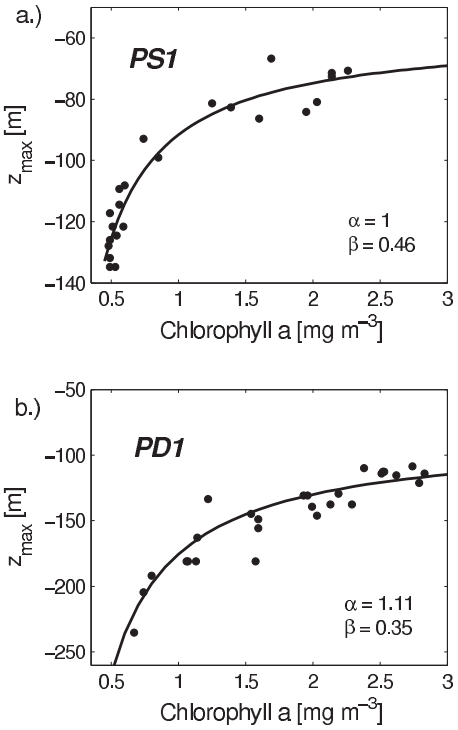

Figure 3: Chlorophyll depedent changes in the amplitude of DVM of shallow (PS1) and deep (PD1) migrating species derived from acoustic measurements during transects through the bloom area and the surrounding. DVM parameter sets are derived by curve fitting solving for α and β according Eq. 6, adjusting the shallowing response weight for PD1 from $\alpha = 1.15$ to $\alpha = 1.11$.

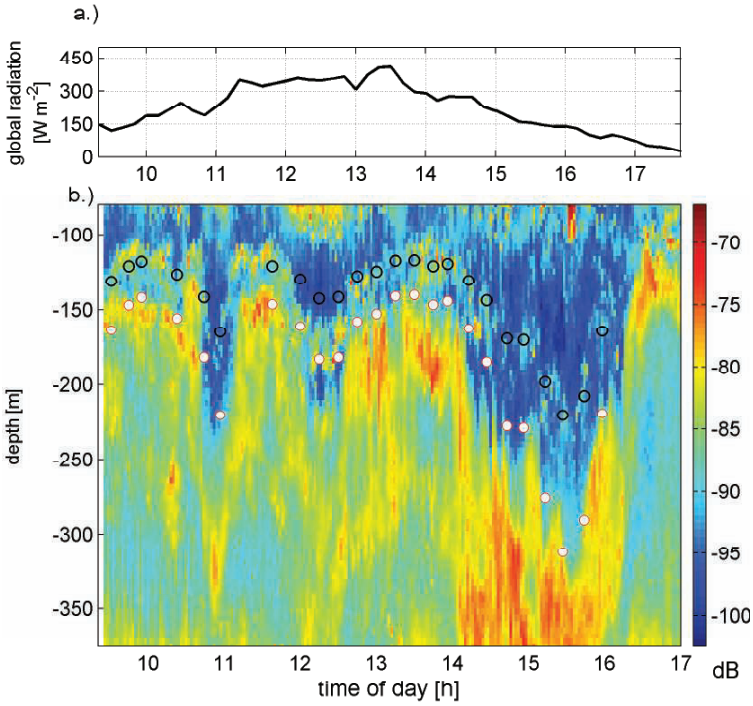

Figure 4: Echogram showing the vertical displacement of sound scattering layers during daytime of species whose migration behaviour is characterized by the response model PD1 and PD2 during a transect with variable surface chlorophyll concentration. Open black circles in (b) indicate the expected residence depth accordant PD1 and red-white circles indicate the expected residence depth accordant PD2. The actual global radiation is shown in (a).

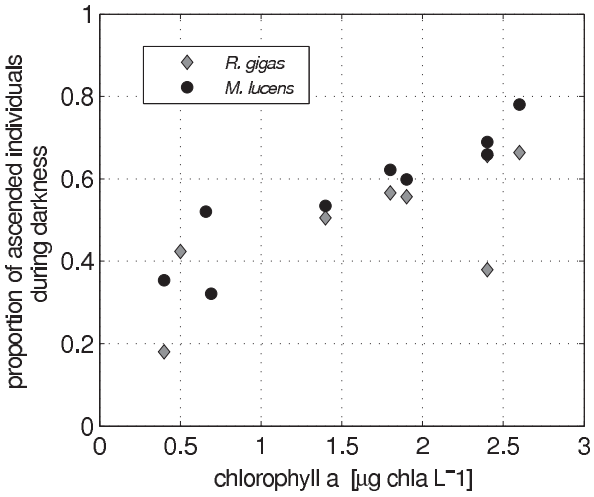

Figure 5: Proportion of individuals of *Rhincalanus gigas* (grey squares) and *Metridia lucens* (circles) found during night in the upper 100m and 160 m, respectively, depending on the surface chlorophyll concentration.

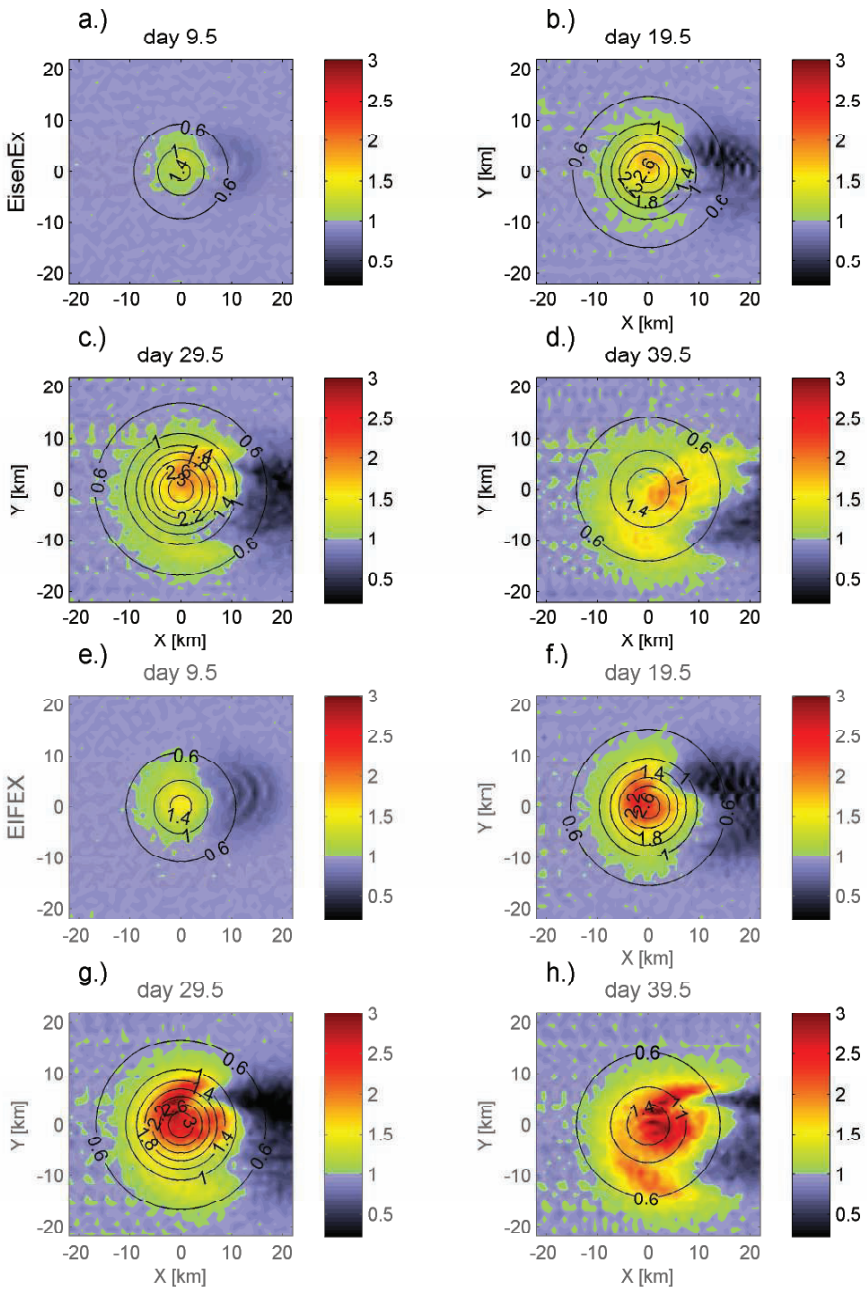

Figure 6: *R*esults of the reference simulation (PI1) under EisenEx (a-d) and EIFEX condition (e-h), respectively. Each set of figures shows the progression of the horizontal copepod distribution given in terms of the colour-coded relative copepod abundance (m^{-2}) at day 10, 20, 30 and 40 after fertilisation. Chlorophyll a surface concentration [μg Chla L^{-1}] is indicated by black isolines. Stationary flow relative to the surface is from the left to the right

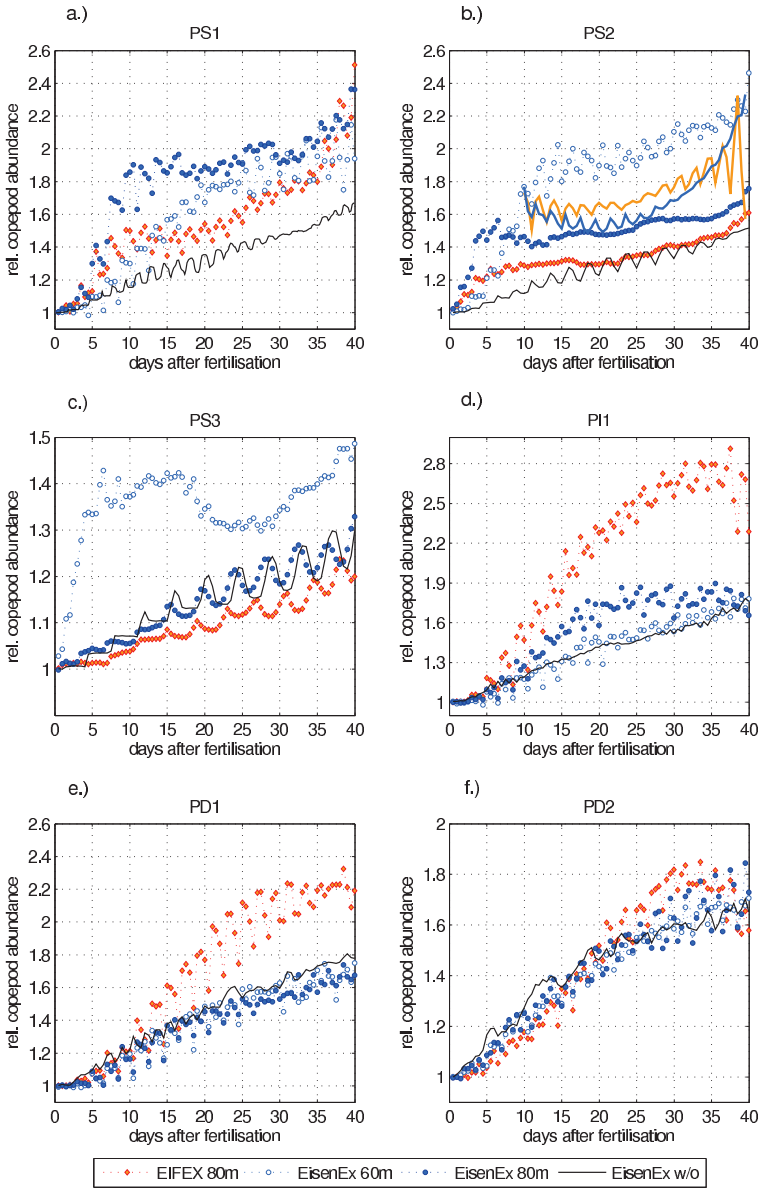

Figure 7: Temporal increase in the abundance of copepods in the patch centre during EisenEx simulation with a mixed layer depth of 60 m (open blue circle) and 80 m (filled blue circle), without inertial oscillation (black solid line) and during EIFEX simulation with a mixed layer depth of 80 m (red diamonds). DVM behaviour PS1(a), PS2 (b), PS3 (c), PI1 (d) PD2 (e) and PD2 (f) are simulated assuming general DVM participation. The mean copepod abundance found inside the bloom area at chlorophyll concentration $> 1.5\ \mu g$ chla L^{-1} during an extra simulation (PS2) with an elliptical shape of the phytoplankton patch (a/b = 4/3) under EIFEX condition and a mixed layer depth of 60 m is shown in Fig. 7b (orange solid line). The respective mean abundance during the EisenEx simulation (z_{mt}) is shown for comparison (blue solid line, 7b).

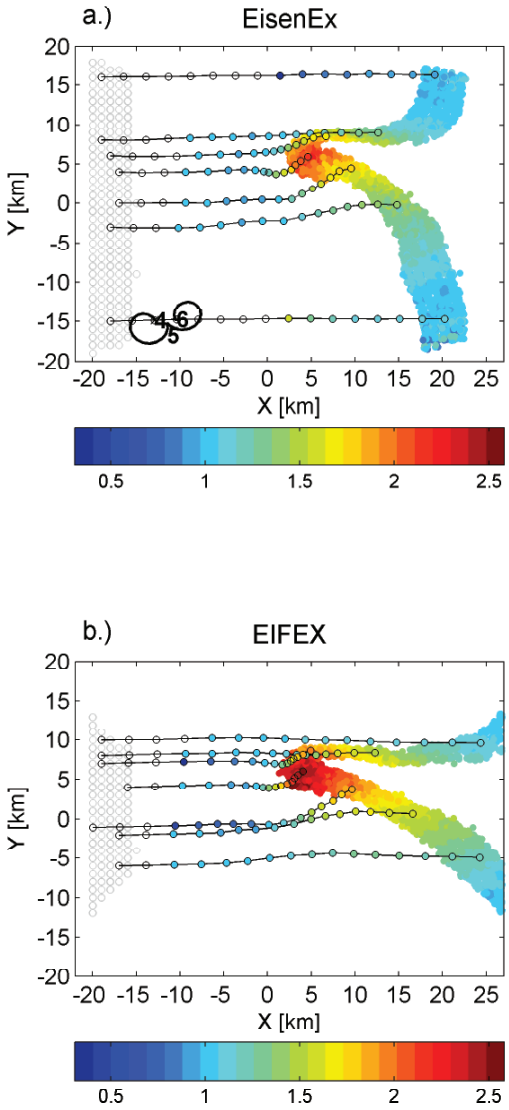

Figure 8: llustration of the effects of migratory response of *Rhincalanus gigas* individuals on food gain during EisenEx (a) and EIFEX (b). Initial location of a subset of individuals is indicated by grey circles (day 0). Their horizontal position at day 30 after fertilisation is marked by coloured dots, which code for the relative increase in individual food gain relative to non-responding individuals. Paths of single individuals are tracked and the relative food gain is given at 2 day intervals. Full path of an individual within a two-day interval is given by a solid black line, numbers indicate the respective position at midnight at day 4, 5 and 6, respectively in (a).

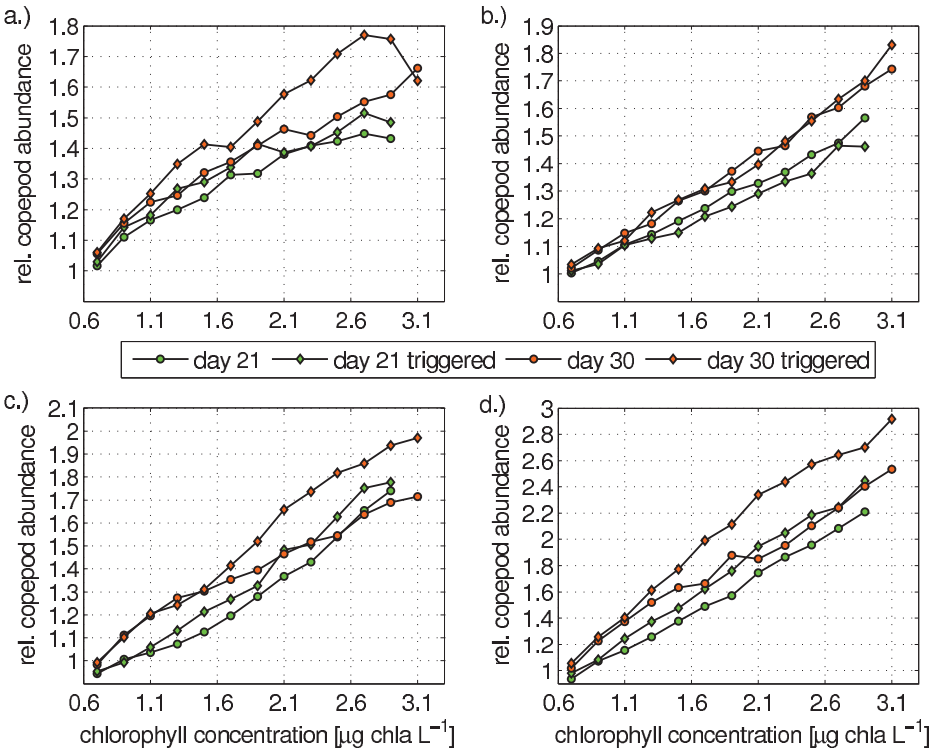

Figure 9: Effects of changing DVM participation triggered by the phytoplankton concentration. a.) Increase in abundace of *Metridia lucens* during the EisenEx simulation at a given chlorophyll concentration inside the patch with triggered (squares) and general DVM participation (circle) within 21 days (green) and within 30 days (orange). b.) Respective abundance increase of *Metridia lucens* during the EisenEx simulation. c, d.) Respective abundance increase of *Rhincalanus gigas* during the EisenEx (c) and EIFEX (d) simulations.

References

[1] Platt, T., Sathyendranath, S., White III, G. N., and Ravindran, P. Attenuation of visible light by phytoplankton in a vertically structured ocean: solutions and applications. *J. Plankton Res.*, 16:1461–1487, 1994.

[2] Assmy, P., Henjes, J., Klaas, C., and Smetacek, V. Mechanisms determining species dominance in a phytoplankton bloom induced by iron fertilization experiment EisenEx in the Southern Ocean. *Deep-Sea Res Part I*, 54:340–384, 2007.

[3] Atkinson, A. Life cycle strategies of epipelagic copepods in the Southern Ocean. *J Mar Syst*, 15(1-4):289–311, 1998.

[4] Batchelder, H. P., Edwards, C. A., and Powell, T. M. Individual-based models of copepod populations in costal upwelling regions: implications of physiologically and evironmentally influenced diel vertical migration on demograhic success and nearshore retention. *Prog Oceanogr*, 53:307–333, 2002.

[5] Bellerby, R., Neil, C., Mkatshawa, L., and Balt, C. CO2-System measurements during EIFEX. *Reports on Polar and Marine Research*, 500:66–69, 2005.

[6] Bollens, S.M. and Frost, B.W. Diel vertical migration in zooplankton: rapid individual response to predators. *J Plankton Res*, 13:1359–1365, 1991.

[7] Bollens, S.M. and Frost, B.W. Ovigerity, selective predation, and variable diel vertical migration in *Euchaeta elongata* (Copepoda: Calanoida). *Oecologia*, 87:155–161, 1991.

[8] Bollens, S.M., Frost, B.W., and Cordell, J.R. Chemical, mechanical and visual cues in the vertical migration behaviour of the marine planktonic copepod *Acartia hudonica*. *J Plankton Res*, 16:555–564, 1994.

[9] Bosch, H. F. and Taylor, W. R. Diurnal vertical migration of an eustuarine cladoceran *Podon polyphemoides* in the Cheasapeake Bay. *Mar Biol*, 10:172–181, 1973.

[10] Boyd, P. W., Jickells, T., Law, C. S., Blain, S., Boyle, E. A., Buesseler, K. O., Coale, K. H., Cullen, J. J., de Baar, H. J. W., Follows, M., Harvey, M., Lancelot, C., Levasseur, M., Owens, N. P. J., Pollard, R., Rivkin, R. B., Sarmiento, J.,

Schoemann, V., Smetacek, V., Takeda, S., Tsuda, A., Turner, S., and Watson, A. J. Mesoscale Iron Enrichment Experiments 1993-2005: Synthesis and Future Directions. *Science*, 315(5812):612–617, 2007.

[11] Cisewski, B., Strass, V. H., and Prandke, H. Upper-ocean vertical mixing in the Antarctic Polar Front Zone. *Deep-Sea Res Part II*, 52(9-10):1087–1108, 2005.

[12] Cohen, J.H. and Forward Jr, R.B. Photobehaviour as an inducible defense in the marine copepod *Calanopia americana*. *Limnol Oceanogr*, 50:1269–1277, 2005.

[13] Emsley, S. M., Tarling, G. A., and Burrows, M. T. The effect of vertical migration strategy on retention and dispersion in the Irish Sea during spring-summer. *Fish Oceanogr*, 14(3):161–174, 2005.

[14] Gervais, F., Riebesell, U., and Gorbunov, M.Y. Changes in primary production and chlorophyll a in response to iron fertilisation in the Southern Polar Frontal Zone. *Limnol. Oceanogr.*, 47(5):1324–1335, 2002.

[15] Hardy, A. C. and Gunther, E. R. The plankton of the South Georgia whaling grounds an adjacent waters, 1926-1927. *Discovery Report*, 11:1–456, 1935.

[16] Harris, R.P. Interactions between diel vertical migratory behaviour of marine zooplankton and the subsurface chlorophyll maximum. *Bull. Mar. Sci.*, 43:663–674, 1988.

[17] Hays, G.C. A review of the adaptive significance and ecosystem consequences of zooplankton diel vertical migrations. *Hydrobiologia*, 503:163–170, 2003.

[18] Hays, G.C., Kennedy, H., and Frost, B.W. Individual variability in diel vertical migration of a marine copepod: Why some individuals remain at depth when others migrate. *Limnol Oceanogr*, 46:2050–2054, 2001.

[19] Henjes, J., Assmy, P., Klaas, C., Verity, P., and Smetacek, V. Response of microzooplankton (protists and small copepods) to an iron-induced phytoplankton bloom in the Southern Ocean (EisenEx). *Deep-Sea Res Part I*, 54:363–384, 2007.

[20] Hill, A.E. Diel vertical migration in stratified tidal flows: Implications for plankton dispersal. *J Mar Res*, 56:1069–1096, 1998.

[21] Hoddel, R.J., Crossley, A.C., Williams, R., and Hosie, G.W. The distribution of Antarctic fish and larvae (CCAMLR division 58.4.1). *Deep-Sea Res Part II*, 47:2519–2541, 2000.

[22] Irigoien, X., Conway, D.V.P., and Harris, R.P. Flexible diel vertical migration behaviour of zooplankton in the Irish Sea. *Mar Ecol Prog Ser*, 267:85–97, 2004.

[23] Isaac, J.D., Tont, S.A., and Wick, G.L. Deep Scattering Layers: vertical migration as a tactic to finding food. *Deep-Sea Res*, 21:651–656, 1974.

[24] Jansen, S., Klaas, C., Krägefsky, S., Harbou, L.v., and Bathmann, U. Reproductive response of the copepod *Rhincalanus gigas* to an iron-induced phytoplankton bloom in the Southern Ocean. *Polar Biol*, 29:1039–1044, 2006.

[25] Johnson, T.B. and Terazaki, M. Chaetognath ecology in relation to hydrographic conditions in the Australian sector of the Southern Ocean. *Polar Biosci.*, 17:1–15, 2004.

[26] Kaartvedt, S., Olsen, E. M., and Jørstad, T. Effects of copepod foranging behaviour on predation risk: An experimental study of the predatory copepod Paraeuchaeta norvegica feeding on *Acartia claus*i and *A. tonsa* (Copepoda). *Limnol Oceanogr*, 42(1):164–170, 1996.

[27] Kimmerer, W. J. and McKinnon, A. D. Zooplankton in a marine bay. II. Vertical migration to maintain horizontal distribution. *Mar Ecol Prog Ser*, 41:53–60, 1987.

[28] Krägefsky, S., Bathmann, U., Strass, V., and Wolf-Gladrow, D. Response of small copepods to an iron-induced phytoplankton bloom - a model to address the mechanisms of aggregation. *Mar Ecol Prog Ser*, -:–, in press.

[29] Krägefsky, S., Harbou, L. v., Jansen, S., and Bathmann, U. Copepod response to iron-induced diatom blooms in the Southern Ocean (EisenEx and EIFEX). -:–, in prep.

[30] Moore, J. K. and Abbott, M. R. Surface chlorophyll concentrations in relation to the Antarctic Polar Front: seasonal and spatial patterns from satellite observations. *J Mar Syst*, 37(1-3):69–86, 2002.

[31] Morales-Nin, B., Palomera, I., and Schadwinkel, S. Larval fish distribution in the Antarctic Peninsula region and adjacent waters. *Polar Biol*, 15:143–154, 1995.

[32] Morris, M.J., Gust, G., and Torres, J.J. Propulsion effenciency and cost of transport for copepods: a hydromechanical model of crustacean swimming. *Mar Biol*, 86:283–295, 1985.

[33] Neil, W.E. Induced vertical migration in copepods as a defence against invertebrate predation. *Nature*, 345:524–526, 1990.

[34] Ohmann, M.D., Frost, B.W., and Cohen, E.H. Reverse diel vertical migration - an escape from invertebrate predators. *Science*, 220:1404–1407, 1983.

[35] Pakhomov, E.A., Perissinotto, R., McQuaid, C.D., and Froneman, P.W. Zooplankton structure and grazing in the Atlantic sector of the Southern Ocean in late austral summer 1993. Part 1. Ecological zonation. *Deep-Sea Res Part I*, 47:1663–1686, 2000.

[36] Peterson, W. T., Miller, C. B., and Hituchinson, A. Zonation and maintenance of copepod populations in the Oregon upwelling zone. *Deep-Sea Res*, 26A:467–494, 1978.

[37] Rollwagen Bollens, G. C. and Landry, M. R. Biological response to iron fertilization in the eastern equatorial Pacific (IronEx II). II. Mesozooplankton abundance, biomass, depth distribution and grazing. *Mar Ecol Prog Ser*, 201:43–56, 2000.

[38] Russel, F. S. The apparent importance of light intensity as a controlling factor in the behaviour of certain species in the plymouth area. *J Mar Biol Ass U K*, 14 (2):415–440, 1926.

[39] Schminke, H. K. Entomology for the copepodologist. *J. Plankton Res.*, 29:i149–i162, 2007.

[40] Smetacek, V., Scharek, R., and Nöthig, E. M. Seasonal and regional variation in the pelagial and its relationship to the life history cycle of krill. In K. Kerry and G. Hempel, editors, *Antartic ecosystems: Egologycal change and conservation*, pages 103–114. Springer Verlag, Berlin, 1990.

[41] Smetacek, V., Strass, V. H., Klass, C., Assmy, P., Cisewski, B., Savoye, N., Henjes, J., Bathmann,U., Bellerby, R., Berg, G. M., Croot, P., Friedrich, L., Gonzalez, S., Harbou, L. v., Herndl, G. J., Hoffmann, L., Jansen, S., Krägefsky, S., Latasa, M., Leach, H., Losch, M., Mills, M. M., Montresor, M., Neill, C., Passow, U., Peeken, I., Röttgers, R., Scharek, R., Terbrüggen, A., Webb, A., and Wolf-Gladrow, D. Massive carbon flux to the deep sea from an iron-fertilized phytoplankton bloom in the Southern Ocean. *in prep.*, -:–, 2008.

[42] Stearns, D.E. and Forward, R.B. Photosensitivity of the calanoid copepod *Arcatia tonsa*. *Mar Biol*, 82:85–89, 1984.

[43] Strass, V., Cisewski, B., Gonzalez, S., Leach, H., Loquay, K-D., Prandke, H., Rohr, H., and Thomas, M. The physical setting of the European Iron Fertilisation experiment 'EIFEX' in the Southern Ocean. *Reports on Polar and Marine Research*, 500:15–46, 2005.

[44] Tiselius, P. and Jonsson, P. R. Foranging behaviour of six calanoid copepods: observations and hydromechanic analysis. *Mar Ecol Prog Ser*, 66:23–33, 1990.

[45] Visser, A. W. Hydromechanical signals in the plankton. *Mar Ecol Prog Ser*, 222:1–24, 2001.

[46] Voronina, N.M. Comparative abundance and distribution of major filter-feeders in the antarctic pelagic zone. *J Mar Syst*, 17(1-4):375–390, 1998.

7 Manuscript 3

Copepod response to iron-induced diatom blooms in the Southern Ocean (EisenEx and EIFEX)

S. Krägefsky[1]*, L. v. Harbou, S. Jansen, U. Bathmann

Alfred Wegener Institute for Polar and Marine Research, Am Handelshafen 12, 27570 Bremerhaven, Germany

Copepod abundance, biomass, species composition and ingestion rates were measured inside and outside iron-fertilised areas during the two mesoscale fertilisation experiments EisenEx and EIFEX. Additionally, the detailed stage composition of copepods was determined during EIFEX. The vertical and horizontal zooplankton distribution was surveyed by net sampling and by acoustic measurements. Strong vertical migration response of copepods was observed during both experiments in the areas with the induced phytoplankton blooms resulting in an aggregation of copepods. Their migration behaviour allows copepods to utilise the vertical sheared flow field of their oceanic environment to find food and to cope with the patchy, mostly poor food environment of the Southern Ocean. The amount of phytoplankton production which was grazed over the course of the experiments exceeded by far the increase in phytoplankton standing stock. Copepod grazing has to be considered as a mechanism which can significantly alter carbon and nutrient fluxes after iron fertilisation in the Southern Ocean.

*Corresponding author: Soeren.Kraegefsky@awi.de

1 Introduction

The Southern Ocean is a high nutrient low chlorophyll (HNLC) area. Macronutrients are perennially high, but the phytoplankton production is limited by iron availability (Martin et al. 1990). The phytoplankton biomass and production show a high temporal and spatial heterogeneity. Blooms of large phytoplankton cells, whose occurrence are regionally and seasonally restricted, strongly increase the phytoplankton biomass locally (Smetacek et al. 1990). These are typically mesoscale blooms and develop and decay on the time scale of weeks (Moore & Abbott 2002). The main consumers of such blooms are copepods. These small crustaceans dominate the zooplankton communities of the Southern Ocean in terms of numbers and biomass (Voronina 1998; Pakhomov et al. 2000), and are obviously able to cope with the cold and mostly food-poor environment with a very patchy food distribution.

Their grazing alters the carbon and nutrient fluxes during natural phytoplankton blooms, and those artificially induced by mesoscale iron fertilisation. Studying the response of copepods during iron fertilisation experiments thus is crucial to assess the potential carbon dioxide sequestering effects of an increased phytoplankton productivity caused by iron enrichment (Martin et al. 1990). Furthermore, as the artificial are similar to natural mesoscale phytoplankton blooms, mesoscale iron fertilisation experiments can deliver highly valuable insight in the behavioural strategies of copepods which allow for their success also in the Southern Ocean.

In this article, we report and discuss observations of two iron fertilisation experiments in the Southern Ocean, the Eisen-Experiment (EisenEx) and the European iron fertilization experiment (EIFEX). Results of EIFEX will be presented in detail, while widely published results of EisenEx are summarized. The discussion also refers to two simulation studies investigating the vertical migration behaviour of diurnal and non-diurnal migrating copepods, respectively, observed during EisenEx and EIFEX (Krägefsky et al. in press, Krägefsky et al., to be submitted).

2 Methods

2.1 EisenEx setting

The iron fertilisation experiment EisenEx was conducted in the Atlantic Sector of the Southern Ocean (21°E, 48°S) during the cruise ANT XVIII/2 of R.V. Polarstern in austral spring (6–29 November 2000). The experiment was carried out in La-

grangian manner within a cyclonic eddy (approximately 120 km wide) shed by the Antarctic Polar Front (APF). An area of about 40 km^2 around a drifting buoy was fertilised with 4 tonnes of acidified iron sulphate solution ($FeSO_4$) on three occasions at intervals of 8 days (Cisewski et al. 2005). Sulphurhexafluoride (SF_6) was added as an inert tracer to the first iron infusion in order to relocate the iron fertilised patch. A diatom bloom developed in response to the iron fertilisation (Gervais et al. 2002). Methods used in studying the copepod response during EisenEx are described in Schultes (2004), Schultes et al. (2006) and Henjes et al. (2007).

2.2 EIFEX setting

The European iron fertilisation experiment EIFEX was also conducted in the Atlantic sector of the Southern Ocean on RV Polarstern (2° E, 49° S), but took place later in the year during summer/autumn (21 January 2004–25 March 2004) compared to EisenEx (austral spring). Like EisenEx, the experiment was carried out in Lagrangian manner within a cyclonic eddy of a diameter of nearly 100 km, which was shed from the APF (Cisewski et al. 2008). The centre of the eddy was marked with a drifting buoy and an area of ca. 150 km^2 around the buoy was fertilised with seven tons of $FeSO_4$ solution. A second fertilisation was made 14 days later. On board measurements of in situ phytoplankton photosynthetic efficiency (Fv/Fm) and later measurements of the partial pressure of CO_2 (pCO_2) served as markers of the fertilised patch (Röttgers et al. 2005, Bellerby et al. 2005). Sampling was carried out within the eddy, inside and outside the fertilised patch throughout the duration of the experiment (38 days). In response to the iron fertilisation, a diatom dominated bloom developed.

2.2.1 Zooplankton abundance and biomass

During EIFEX, zooplankton was collected with a vertically towed opening/closing Multi-Net (MN), equipped with 100 µm mesh. Five successive depth layers were sampled over the entire course of the experiment at standard sampling intervals (0 - 25, 25 - 50, 50 - 100, 100 - 160 and 160 - 400 m). Different from the standard, zooplankton at the first four stations were collected at the sampling intervals 0 - 20, 20 - 40, 40 - 80, 80 - 160, 160 – 360 m (Tab. 1). Sample volumes were estimated by multiplying the net opening area (0.25 m^2) by the towing distance. After retrieval, samples were fixed with hexamine-buffered formalin (4% final concentration) and stored at 4°C in the dark until further handling.

In the home laboratory, zooplankton was counted following standard protocols. Important copepod species (see Tab. 1) were identified and counted according to copepodite stages. Different from the larger copepod species, the determination of stage composition of the small copepod *Ctenocalanus citer* was only done for a subsample of 9 stations. Less abundant copepod species were grouped as diverse copepods into length classes at 0.5 mm intervals. Non-copepod zooplankton was grouped on a higher taxonomic level (e.g. amphipoda, euphausiacea etc.).

Carbon biomass of copepods was estimated from own measurements during the cruise (data not shown) and literature values for the carbon weight (Shreeve at al. 2002) or dry weight (Mayzaud 2002a and reference therein) of single copepodite stages of the different species. Dry weight values from literature were converted into carbon weight assuming a carbon content of 50% by weight for *C. citer* (Schultes 2004) and 40% for other species. Carbon weight of younger stages of *Calanus simillimus* and *Pleuromamma robusta* were estimated by scaling the measured carbon weight of older stages caught during EIFEX according the dry weight – developmental stage relation found by Atkinson et al. (1996).

2.2.2 Acoustic zooplankton survey

Multifrequency acoustic backscatter data were collected during EIFEX (38, 70, 120 and 200 kHz) at an interval of ca. 2 seconds with a Simrad EK60 echosounder. No calibration with standard calibration spheres could be performed (Foote et al. 1987) due to logistic reasons. The acoustic measurements thus gave relative, and not absolute backscattering values. The measurements were initially echo-integrated over 6 seconds with a vertical resolution of 1 m using EchoView. Noise-corrupted data were removed column-wise (ping ensemble) using custom MATLAB-routines. Mean volume backscattering strength was computed for 2 min intervals with 1 m vertical resolution for further data analysis.

The effective vertical range for the acoustic measurements decreases with increasing frequency, and was restricted to about 400 m and 250 m for the measurements with 70 kHz and 120 kHz and to less than 80 m for 200 kHz. The ability to detect zooplankton, on the other hand, decreases with decreasing frequency. For this reasons, data analysis in the following is restricted to the acoustic measurements with 70 and 120 kHz. In view of the dominance of weakly scattering zooplankton and the presence of an isolated zooplankton community within the eddy circulation we apply a normalisation to the acoustic data to detect shifts in zooplankton distribution, as

described in the following.

A norm mean volume backscattering strength ($Sv_{norm}(f, z, t)$) is defined with dependency on depth and time of the day for different frequencies. $Sv_{norm}(f, z, t)$ is the median value (in the linear domain) of all backscattering strength measurements at a particular depth within a 10 m interval and particular time of the day within a time-frame of ±15 minutes (Fig. 1). The difference between Sv and Sv_{norm} in the logarithmic domain gives the normalised Sv value (nSv):

$$nSv(f, z, t) = Sv(f, z, t) - Sv_{norm}(f, z, t) \quad (1)$$

In the linear domain, nSv equates to a relative change in backscatter quantity or biomass of organisms with identically backscattering characteristics, and is referred to as normalised backscatter (NBS) in the following:

$$NBS = 10^{(nSv/10)} \quad (2)$$

The nSv values of -3, 0 or 3 dB, for example, correspond to NBS values of 0.5, 1 and 2, and thus to 50%, 100% and 200% of the norm, respectively. Changes in NBS were surveyed over sufficiently large depth ranges to exclude small scale patchiness, e.g. within the food-enriched surface layer.

During EIFEX, the concentration of chlorophyll *a* (chl a) at the surface was measured at regular time intervals (all 15 - 120 min; n = 731) during grid surveys. Median NBS is calculated including acoustic measurements ±15 minutes around the chlorophyll sampling time within the depth intervals 25 – 160 m and 160 – 400 m.

A high number of Multi-Net hauls at standard depths during EIFEX allows relating NBS to zooplankton biomass. Net samples within the depth range 25 – 160 m (70 and 120 kHz) and 160 – 400 m (70 kHz) are compared with acoustic measurements in the particular depth interval during up- and downcast, 20 min before to 20 min after the net reached maximum depth (400 m). The median of the NBS values is used in order to exclude extreme backscattering values due to noise or a local aggregation of stronger backscattering organisms.

2.2.3 Copepod grazing

In order to estimate grazing rates, gut evacuation experiments with different abundant copepod species were conducted. Zooplankton for experiments was collected outside and inside the fertilised patch during night and day with a Bongo net (100 µm and 300 µm) towed vertically from depth between 150 and 20 m to the surface

at a maximum speed of 0.3 $m\,s^{-1}$. After retrieval of the net, the content of the cod end was transferred into a cooler with 20 litres GF/F filtered sea water at in situ temperature. Still on deck, sub-samples of the zooplankton were retrieved from the diluted catch on a piece of fine mesh for determination of the initial gut pigment content (G0). The mesh was packed in aluminium foil and was shock frozen at -80°C. A time series for estimation of gut evacuation rate was established from subsequent samples taken typically after 1, 2, 4, 6, 10, 20 and 30 min, respectively. Frozen samples were thawed and copepods sorted in a cooled Petri dish under a stereomicroscope and dim light. 1 to 20 individuals of a given species were placed in a 20 ml PE centrifuge vial, covered with 5 ml 90% aqueous acetone and left for extraction of pigments for a period of 24 hours in a fridge. Pigment concentration was measured with a Turner fluorometer before and after acidification. A correction factor for pigment destruction to non-fluorescent components was included by multiplying the concentration of phaeopigments by a factor 1.5 (Dam & Peterson 1988). Calculation of the gut clearance coefficient, k, and the gut passage time (GPT), was based on the exponential model following the method of Dam & Petersen (1988):

$$k = (\ln(G0) - \ln(G(t)))/t \tag{3}$$

and GPT = 1/k with G0 representing the initial gut content (ng pigment ind^{-1}) and G(t) the gut content at a given time t. The quotient of 1/k represents the gut passage time (GPT) in minutes. Daily ingestion (ng pigment $ind^{-1}d^{-1}$) is derived from initial gut content G0 and k according to the following equation:

$$I = G0 \times k \times 60 \times 12 \tag{4}$$

A grazing period of 12 hours was assumed, to account for the observed periodicity in the migration and likely feeding behaviour of the copepods. Ingestion rates were obtained by multiplying the initial gut content with the according gut clearance rate that was experimentally determined at the same station. Pigment concentrations were converted to phytoplankton carbon (PPC) using a C:chl a ratio of 30 (Smetacek et al. in prep.)

For estimation of the grazing rates, PPC ingestion was referred to copepod carbon weight and expressed as percentage of body carbon ingested per day (daily ration). Constant daily rations were assumed, as discussed below. Estimates for the different species were based on findings during the two the experiments, EisenEx and EIFEX, and additionally on literature values.

3 Results

The results of EisenEx will be summarized in two separate paragraphs in the discussion section, as these are widely published results. In the following we present the results of EIFEX.

3.1 Copepod abundance and biomass

Copepods ($\gtrsim$ 1 mm) were dominated in number by *Ctenocalanus citer* followed by *Metridia lucens*, *Calanus simillimus* and *Rhincalanus gigas*. Other copepods species (*Pleuromma robusta*, *Calanoides acutus*, *Heterorhabdus austrinus*, *Paraeuchaeta biloba*, *Paraeuchaeta antarctica* and *Calanus propinquus*) occurred in low abundances with minor contribution ($<$ 1 %) to the total number of copepods (Tab. 2, Fig. 2 a-b).

Regarding to the copepod biomass, *R. gigas* showed highest percentage contribution inside the fertilised area (39%) followed by *C. simillimus* (21%) and *C. citer* (18%). *C. simillimus* contributed most to copepod biomass outside the fertilised area (50%) (Fig. 2). In the upper 0 - 160 m, the shallow diel migrating copepod species *C. citer* and *C. simillimus* accounted for ca. 50% of the copepod biomass inside and ca. 80% of copepod biomass sampled outside the fertilised area except of St. 509 at day 11 with extreme abundance of *C. simillimus*, identified as outlier (Grubbs 1969; see also Fig. 5).

Copepods in the depth range 160 - 400 m were dominated by *M. lucens* in terms of number, accounting for about 70% of larger copepods ($>$ 2 mm) caught in the deep layer. Copepod biomass within this depth range was dominated by *R. gigas* outside the fertilised area (ca. 50%). Inside the fertilised area, the percentage contribution of *R.gigas* to the copepod biomass (160 - 400 m) declined from initially 80% to about 25% towards the end of EIFEX.

Generally, the number of copepods ($\gtrsim$ 1 mm) increased approximately 2-fold inside the phytoplankton bloom area from initially ca. 170,000 copepods m^{-2} (0 - 400 m) to ca. 330,000 copepods m^{-2} after 5 weeks (Fig. 3a). Accordingly, their carbon biomass increased 1.8-fold from ca. 2.4 g C m^{-2} to ca. 4.3 g C m^{-2} over the course of the experiment (Fig. 3b). An even higher relative abundance increase was observed for larger copepods ($>$ 2 mm), which increased more than 3-fold in the bloom area from initially ca. 19,000 copepods m^{-2} to ca. 60,000 copepods m^{-2} at the end of EIFEX (Fig. 3c). Carbon biomass within the size fraction $>$ 2 mm increased 1.8 fold from ca. 1.8g C m^{-2} to 3.2 g C m^{-2} (Fig. 3d).

In contrast to the inpatch situation, the abundance of copepods ($\gtrsim$ 1 mm) sampled outside the fertilised area was higher at the first stations compared to the last stations, while the copepod biomass remained at the same level (Fig. 3a-b). The peak abundance and biomass at day 11 after fertilisation is due to the extreme high abundance of *C. simillimus* at this station mentioned above. Larger copepods ($\gtrsim$ 2 mm) occurred in the non-fertilised area at similar abundances at the start and towards the end of EIFEX, while their biomass was higher towards the end (Fig. 3c-d). Median abundance and biomass was ca. 90,000 copepods m^{-2} and 1.9 g C m^{-2} for total copepods ($\gtrsim$ 1 mm) and 24,000 copepods m^{-2} and 1.7 g C m^{-2} for larger copepods ($>$ 2 mm).

3.1.1 Species and stage specific abundances

The dominant copepod species *C. citer* increased ca. 2.3-fold in total copepodites (CI-CVI) abundance in the phytoplankton bloom area from 95,000 ind. m^{-2} initially to ca. 220,000 ind. m^{-2} ($N(t) = 3215 \times t + 95000$; $r^2 = 0.42$) over the course of EIFEX (Fig. 4a-b). The stage composition of *C. citer* was determined for a subsample of stations, and showed no temporal trend. Mean and median abundance of *C. citer* sampled outside the fertilised area was 44,750 and 41,700 ind. m^{-2}, respectively. Lowest abundances were observed at the last two stations, while the mean and median abundance was 62,850 and 53,500 ind. m^{-2}, respectively, at the first three stations.

In the same time, *C. simillimus* increased 2.1 fold in total copepodites (CI-CVI) over the course of EIFEX in the phytoplankton bloom area from ca. 15,000 ind. m^{-2} initially to ca. 31,000 ind. m^{-2} ($N(t) = 430 \times t + 14832$; $r^2 = 0.37$), excluding station 513 as an outlier from regression analysis (Fig 5a-b). No increase, however, was observed in the abundance of early copepodites CI and CII. Large increase was shown within the stages CIII, CIV and CV, with strongest increase in CIV. Adults occurred at very low number with a median abundance of 110 females m^{-2} and 14 males m^{-2}. Their abundance showed no clear temporal trend. Average copepodite stage increased slightly inside the fertilised area, but shifted from initially CIII to CIV-CV outside the fertilised area (Fig. 5a), without temporal trend in the abundance of total copepodites (Fig. 5b). The abundance of *C. simillimus* outside was similar to the initial abundance in the fertilised area, except for day 11 with an extreme high number of *C. simillimus* observed (Fig. 5b).

M. lucens showed strong variability of abundance and no statistically signifi-

cant increase of total copepodites in the fertilised area (Fig. 6a-c). Large abundance increase was shown by the later copepodite stages CIV-CVI, increasing by ca. 700 copepodites d^{-1} inside the bloom area ($N(t) = 692 \times t + 11566$; $r^2 = 0.44$). No trend was observed for copepodites CIII, while the abundance of copepodites CII showed a decreasing tendency. The slope of decrease observed for CII is strongly biased by high abundances considered as outlier which were sampled at two casts of the same station at the beginning of the experiment. Excluding this station, linear regression analysis shows a decrease in CII by approximately 100 copepodites d^{-1} and by about 300 copepodites d^{-1} for CI and CII copepodites, yet the regressions are not statistically significant. Moreover, counts of the earliest copepodite stage CI include copepodites of the related species *Pleuromamma sp.* and *Metridia sp.* (Metridinidae), which were grouped for CI without species identification (Fig. 6c). However, a number of 100 - 300 copepodites d^{-1} may be nevertheless assumed as a rough estimate for possible recruitment from younger stages into older stages.

The older stages CIII-CVI of *M. lucens* increased 2-fold over the course of the experiment inside the bloom area ($N(t) = 695 \times t + 25613$; $r^2 = 0.25$) (Fig. 6c). Corrected for the possible recruitment by 100 - 300 copepodites d^{-1}, the abundance development in CIII-CVI imply a 1.6 fold to 1.9 fold increase due to other mechanism discussed below.

At the stations outside the fertilised area, the mean and median abundance of *M. lucens* (CII-CVI) was 21,150 and 17,450 ind. m^{-2}. At the first three outpatch stations the abundance was similar to the abundance encountered initially inside the fertilised area, but was lower at the two outpatch stations towards the end of the experiment (Fig. 6c).

The copepod *R. gigas* showed a pronounced temporal shift in stage distribution inside the fertilised area. The average copepodite stage decreased gradually from CV towards CIII (Fig. 7a), while a relatively young average copepodite stage of CIII was found throughout in the outpatch except one station. In abundance, *R. gigas* (CI-CVI) increased 3.4-fold inside the bloom area over the course of EIFEX ($N(t) = 88 \times t + 1421$; $r^2 = 0.62$) (Fig. 7b) and 2.3-fold (CII-CVI) excluding the first copepodite stage CI ($N(t) = 50 \times t + 1554$; $r^2 = 0.61$).

The respective contribution of other copepod species to total copepod abundance in the bloom area was less than 1%. Of these less abundant species, *P. robusta* (CII-CVI) ($N(t) = 38.5 \times t - 0.17$; $r^2 = 0.49$) and *C.acutus* (CI-CVI) ($N(t) = 23 \times t + 455$ $r^2 = 0.37$) showed a significant abundance increase.

3.1.2 Abundance of other mesozooplankton

Non-copepod crustaceans were sampled in very low abundances during EIFEX in- and outside the bloom area (Tab. 3). Mainly small amphipods (thorax length $\varnothing$ 1.5 mm) occurred with a median abundance of ca. 0.7 ind. m^{-3} (0 - 400 m). Juvenile and adult euphausids showed median abundance of ca. 0.3 and 0.1 ind. m^{-3} in- and outside the bloom area, while the median abundance of furcilia stages was ca. 1.0 and 1.2 ind. m^{-3}. Salp abundance was low with 0.4 inpatch and 1.1 ind. m^{-3} outpatch. Chaetognaths were mainly small and their median abundance was 8 (inpatch) and 6 (outpatch) ind. m^{-3}. The median abundance of polychaets was calculated to be 1.4 inside and 1.3 ind. m^{-3} outside the fertilised area.

3.2 Acoustic survey EIFEX

Acoustic measurements are available for 17 Multi-Net Stations with standard sampling intervals. However, station 509 and station 552 are excluded from further data analysis. The copepod biomass sampled at station 509 is an outlier compared to all other net samples taken outside and according the externally studentized residuals (R-student) of the regression analysis between NBS measurements (70 kHz and 120 kHz) and copepod biomass. The high copepod biomass sampled may be due to small scale patchiness in copepod distribution. However, the NBS – copepod biomass relation may also be biased by the small coverage with acoustic measurements due to strong interference with noise at this time. Station 552 was situated at the edge of the eddy, and the acoustic measurements show unusual backscattering signals. The high NBS measured at this station at 70 kHz and 120 kHz are identified as outliers (Grubbs 1969).

3.2.1 NBS - Copepod biomass relation and copepod distribution

Linear regression analysis shows a high correlation ($r^2 = 0.76$) between NBS measurements at 120 kHz and biomass of copepods ($\gtrsim$ 1 mm) sampled in the upper 25 - 160 m. The correlation slightly increases by excluding copepods smaller 2 mm ($r^2 = 0.79$; Fig. 8a). NBS measurements at 70 kHz show marked correlation with the biomass of copepods (>2.5 mm) in the upper 25 – 160 m ($r^2 = 0.45$; Fig 8b) and within 160 – 400 m ($r^2 = 0.43$; Fig 8c).

Iron fertilisation was performed at the centre of an eddy after a short initial survey (3 days). The eddy was mapped on a larger scale after iron supply for about 9 days,

before the fertilised area was revisited. NBS shows no correlation with the surface chlorophyll concentration measured prior iron fertilisation and during the larger scale mapping, which were generally low and ca. 0.7 μg chla L^{-1} on average. The NBS measurements during the larger scale mapping outside the fertilised area show also no temporal trend within the upper water column (25 - 160 m). Linear regression analysis shows weak negative correlation with time for NBS measurements at 70 kHz in the depth range 160 - 400 m. However, no such trend is observed for the respective measurements after the eddy mapping and in total.

NBS shows pronounced variability but a clear increase with increasing chlorophyll concentration within the upper 25 – 160 m at both 70 and 120 kHz for the measurements after revisiting of the fertilised area (at day 9) and for the total measurements (Fig. 9). NBS (25 – 160 m) increase from 1.05 at low chlorophyll concentration to 2.0 at high chlorophyll concentration found at the patch centre for the measurements at 120 kHz (Fig. 9a) and from 1.15 to 2.6 at 70 kHz (Fig. 8b). This increase translates to approximately a doubling in biomass according to the relation found for the NBS measurements at 120 kHz and the biomass of copepods ($\gtrsim$ 1 mm) as well as of the copepods ($>$ 2 mm) (Fig. 8a, 9a) in the upper 25-160 m. For the measurements at 70 kHz the NBS increase translates to a 1.6-fold increase in biomass of copepods $>$ 2.5 mm (Fig. 8b, 9b).

NBS (70 kHz) in the deep layer (160 - 400m) shows weak negative linear correlation with the chlorophyll *a* concentration in the surface, decreasing from 1.3 to 1.0 from low to high chlorophyll concentration (Fig 9c). According to the relation found for NBS measurements at 70 kHz and copepod biomass ($>$ 2.5 mm) within this layer (Fig 8c), this decrease translates to a decline in biomass of copepods ($>$ 2.5 mm) by 10%. It would amount to 15% of their biomass increase in the upper 25 - 160 m derived from the NBS measurements at 70 kHz (Fig 9b).

3.3 Grazing impact

Estimated phytoplankton carbon ingestion, faecal pellet production and respiratory needs of total copepods are based on copepod abundances in the upper 0 - 160 m, in order to exclude permanently deep-dwelling individuals. Grazing rates on phytoplankton were estimated with the gut fluorescence method for *C. simillimus* and *R. gigas*. Average GPT was 22.1 min ($\pm$16.4) and 15.1 min ($\pm$6.9) for *C. simillimus* and *R. gigas*, respectively. The determined grazing rates showed no statistically significant increase with increasing chlorophyll concentration for *R. gigas*, resulting in an

overall average phytoplankton carbon ingestion rate of 51 μg C copepod d^{-1}. Grazing rates determined for *C. simillimus* increased with increasing chlorophyll concentration up to 1.5 μg chla L^{-1}, but declined sharply at chlorophyll concentration $>$ 1.85 μg chla L^{-1}, resulting in an average ingestion rate of 17.4 μg C copepod d^{-1}. Such decline in grazing rate of *C. simillimus* is not confirmed by the results of the faecal pellet production experiments, which show steady increase in FP production of *C. simillimus* with increasing chlorophyll concentration (Jansen et al. submitted).

The average daily ration for *C. simillimus* was 15.7% and 9.1% for *R. gigas* both referenced to the respective weights of copepodites CV. An average daily ration of 37% for small copepods $<$ 2 mm (but mainly larger than *Oithona spp.*) was determined during EisenEx. This copepod fraction was dominated by *C. citer* during both experiments, EisenEx and EIFEX.

Due to the unclear relationship between chlorophyll concentration and grazing rates found in the gut fluorescence experiments, we assume a constant daily ration (Tab. 2). Considering EisenEx and EIFEX findings, daily rations of 15% are assumed for the species *C. simillimus*, *M. lucens*, *P. robusta*, *H. austrinus*, *C. propinquus* and other copepods, while half of this daily ration (7.5%) is assumed for *C. acutus* (Schnack-Schiel et al. 1991). A daily ration of 35% is assumed for the small copepod species *C. citer*. In view of lower daily ration reported for *R.gigas* in the literature (Atkinson et al. 1996b, Dubischar & Bathmann 1997, Mayzaud et al. 2002b) and derived during EisenEx (Schultes 2004), the assumed daily ration is reduced to 6% for a more conservative estimate compared to 9.1% derived from GF measurements for this large copepod.

The estimated phytoplankton carbon ingestion by copepods($\gtrsim$ 1 mm) increased from initially 0.2 g C m^{-2} d^{-1} to 0.5 g C m^{-2} d^{-1} (0-160m) inside the fertilised area over the course of EIFEX (Fig. 10a), while the diatom carbon concentration increased from ca. 3.5 g C m^{-2} initially to 7.5 – 8 g C m^{-2} (0 – 100 m) at the peak of the bloom (Smeatcek et al. in prep.). Thus, the estimated grazing impact is quite stable over the course of the experiment, due to the concurrent increase in phytoplankton carbon concentration and copepod standing stock and the assumed constant daily rations. The estimated grazing impact of copepods ($\gtrsim$ 1 mm) amount to ca. 6.5 % of the phytoplankton carbon stock per day on average. During the bloom period, this grazing impact amounts to ca. 30% of the primary production (PP), which increased from 0.7 - 0.8 initially to ca. 1.5 g C m^{-2} d^{-1} after day 10 of the experiment (Smeatcek et al. in prep.). Estimated phytoplankton carbon ingestion of copepods ($\gtrsim$ 1 mm) amounted to ca. 15 g C m^{-2} in total over the course of

EIFEX.

Daily FP production by the local copepod stock was calculated based on FP production estimates from experiments and by allometric scaling of the experimental results to estimate the FP production of young stages and the small species *C. citer* (Jansen et al. submitted). The estimated total faecal production of copepods ($\gtrsim$ 1 mm) increased from 0.03 g C m^{-2} d^{-1} towards 0.4 g C m^{-2} d^{-1} (0 - 160 m), and would have amounted in total to 8-9 g C m^{-2} over the course of EIFEX (Fig. 10b).

According to the relation between body carbon of zooplankton and respiration rate found by Dagg et al. (1982), copepod respiration makes up a carbon need of ca 6.5% of the copepod carbon standing stock per day on average. Hence, the respiratory carbon needs of copepods ($\gtrsim$ 1 mm) increased from 0.06 g C m^{-2} d^{-1} towards 0.2 g C m^{-2} d^{-1} (0 - 160 m) inside the phytoplankton bloom area, and would have amounted to 5-6 g C m^{-2} over the course of EIFEX (Fig. 10b). Faecal pellet production and respiration needs are not balanced by the estimated phytoplankton carbon ingestion after the 3 week of EIFEX.

4 Discussion

In the following we summarize widely published results of the iron fertilisation experiment EisenEx for later discussion. The development in copepod abundance and their grazing is treated in two separate paragraphs.

4.1 Copepod abundance and biomass during EisenEx

During EisenEx larger copepods (>1.5 mm) were sampled with a Multi-net at 6 stations inside and 2 stations outside the fertilised area between day -2 and day 10 with different vertical sampling intervals (Schultes et al. 2006). Estimates of the copepod standing stock (copepods m^{-2}) in the upper 0-150 m are based on the mean abundances estimated for according depth strata assuming a homogeneous distribution of individuals.

Copepods (>1.5mm) were clearly dominated by *C. simillimus*. All species showed a high variability in abundance, but higher numbers of copepods (0 - 150 m) were observed at the last two stations (day 7, day 10) inside the bloom area relative to the initial abundance and the abundances outside (Fig. 11a). This apparent abundance increase was dominated by *C. simillimus*. Mean and median abundance of *C. simillimus* was 19,221 and 23,168 copepods m^{-2} (0-150m) at the (initial)

stations with still low phytoplankton concentration at day -2, 0 and 3, excluding data from a station at day 2 for which the extreme high abundance value of *C. simillimus* was identified as outlier (Grubbs 1969). Abundance of *C. simillimus* was substantially higher at the last two Multi-net stations with a mean abundance of 40,883 copepods m^{-2}. *R. gigas* and *C. acutus* seem to increase in abundance in- and outside the fertilised area, but show strongest increase inside. The mean and median abundance of total copepods (>1.5 mm) at the stations at day -2, 0 and 3 was 40,110 and 39,696 copepods m^{-2} (0 - 150m), respectively, and was 67,345 copepods m^{-2} on average at the last two stations (Fig. 11a).

Copepods were not counted into copepodite stages and were grouped in size classes with 0.5 mm size intervals. Estimates for carbon standing stock are based on dry weight values reported in the literature (Mayzaud 2002a) for copepodite stages likely found in the different size classes, assuming a carbon content of 40% by weight. Mean and median of the estimated carbon standing stock (0 - 150m) of copepods (>1.5mm) was ca. 2.0 g C m^{-2} and 2.2 g C m^{-2}, respectively, at the stations at day -2, 0 and 3 and was on average 4.7 g C m^{-2} at the last two stations (Fig.11b).

C. citer was sampled with Niskin bottles over the entire course of EisenEx at the discrete depths of 10, 20, 40, 60, 80, 100 and 150 m at 5 stations outside and 13 stations inside the fertilised area (Henjes et al. 2007). Estimates of the standing stock of *C. citer* (m^{-2}) are based on trapezoidal integration of the abundance estimates at the discrete sampling depths over the upper 0-150 m, and show 3-fold increase in abundance of *C. citer* inside the phytoplankton bloom area over the course of EisenEx ($N(t) = 188550 + 19725 \times t$; $r^2 = 0.31$).

Acoustic backscatter data were collected at an interval of 2.5 seconds with a Simrad EK60 (38, 70, 120, 200 kHz) without calibration (Foote et al. 1987). Data were echo-integrated with a vertical resolution of 3.5 m and 30 seconds. The acoustic record was strongly affected by noise (e.g. due rough sea conditions). The measuring range was effectively restricted to the upper 200 m even for measurements with 70 kHz. The acoustic measurements suggest increase in zooplankton inside the fertilised area during EisenEx particularly for the upper water column (25 - 100m), but the number of comparable net hauls was not sufficient to correlate NBS values with biomass or abundance of zooplankton. Thus shifts in the horizontal distribution of zooplankton during the experiment cannot be revealed with the acoustic measurements, which were affected to an unknown degree by a horizontal NBS gradient observed inside the eddy and changing noise floor levels during strong wind periods. However, the acoustic record allow for surveying the vertical migration response of

diel migrating zooplankton inside the bloom area during EisenEx (see below).

4.2 Acoustic survey of the horizontal zooplankton distribution during EIFEX

Basic sound scattering properties of copepods are not known properly (Chu and Wiebe 2005). Copepods, however, are very weak scatterers of sound (Stanton and Chu 2000). During EIFEX as well as during EisenEx they occurred at very high abundances, in the order of 10^4 Ind. m^{-3} in the size range $<$ 1mm (e.g. *Oithona*), 10^3 Ind. m^{-3} in size range $\sim$ 1 mm (e.g. *C. citer*) and hundreds of larger copepods ($>$ 2 mm) m^{-3}. Nevertheless, the correlation between the acoustic measurements (NBS) and copepod biomass found during EIFEX is unexpectedly high, and suggests that basic sound scattering pattern are from copepods.

Larger crustacean, like amphipods and euphausids were found at very low numbers, but were probably undersampled due to net avoidance and a patchy distribution. Particularly during day-time larger zooplankton seems to have added significantly to the acoustic backscattering in the upper water column. In the deep water column a persisent sound scattering layer was observed during EIFEX between 300 and 400 m. The sound scattering within this layer was likely from an assemblage of different zooplankton, whose variable distribution contributed to the variability of the NBS measurements. On average, the backscattering strength was reduced to 75% of the day time value (linear domain) during night, which imply a dominant contribution of non-migrating animals to the sound scattering within this layer. However, also within the deep layer (160 - 400 m) the normalised acoustic data, which reveal changes in backscattering relative to a depth and daytime dependent norm, were markedly correlated with changes in copepod biomass (Fig. 8c).

In contrast to the Multi-net sampling which was mostly restricted to the central area of the phytoplankton bloom, the acoustic measurements allow monitoring of the horizontal copepod distribution with a high resolution. The NBS measured at 70 and 120 kHz in the upper 160 m strongly increases with increasing chlorophyll concentration during EIFEX (Fig. 8a,b). This increase in NBS translates to an increase in copepod biomass by up to 2-fold according the observed NBS – copepod biomass relation and agrees well with the findings of the net sampling.

4.3 Vertical migration behaviour of zooplankton

During EisenEx and EIFEX, the acoustic measurements gave insight into the vertical migration behaviour of the zooplankton, which migrated towards a deeper day-time and re-ascend towards a shallow night-time residence. The acoustic survey showed a response of shallow and deep migrating species to the increased phytoplankton concentration inside the bloom areas. Their migration response was surveyed by tracking shifts in the vertical position of different sound scattering layers during the day-time along transects through the bloom area and the surrounding. The acoustic measurements were effectively restricted to the upper 200 m of the water column during EisenEx even for measurements with 70 kHz, while the effective measuring range was down to about 400 m (70 kHz) during EIFEX and gave the ability to survey properly the migratory response of deep migrating species.

The acoustic survey shows a decrease of the diurnal vertical migration (DVM) amplitude of shallow migrating species by tens of metres inside the phytoplankton bloom area during EisenEx and EIFEX. The sound scattering layer of shallow migrating species was highly patchy due to the superposition of backscattering signals of different, apparently also larger species and showed occasionally a two-layer structure during EIFEX. Clear observations of migratory response were restricted to measurements along transects with a steep horizontal gradient in surface chlorophyll concentration after the phytoplankton had reached high concentrations inside the bloom areas of EisenEx and EIFEX. Deep migrating species showed the largest shifts in their day-time residence and reduced their DVM amplitude by up to more than 150 metre. Particularly for the deeper sound scattering layers, which were less affected by a superposition of different backscattering signals, the acoustic measurements show a clear dependency of the day-time residence of copepods and possible other zooplankton to the actual surface phytoplankton concentration, which implies its gradual adjustment by net up- or downward movement (Krägesfky et al. to be submitted).

The acoustic observations in the upper water column suggest a wide migratory response of different species including larger zooplankton which may have responded directly to changing phytoplankton concentration or indirectly by following responding copepods as prey organisms. It is not unlikely that the backscattering signals of larger predatory zooplankton have contributed significantly to the sound scattering which would have largely increased the acoustic detectability of the migration response of small, directly responding zooplankton they prey upon. Furthermore, in

view of the overall migratory response of shallow and deep migrating species it can be assumed that acoustic observations reflects the migration behaviour of a wide range of copepod species including those species that contribute minor to the sound scattering (e.g. small or low abundant copepods).

In the vertical sheared flow field of the ocean, the diel vertical migration causes a divergent drift of migrating zooplankton and the surface layer. Already Hardy and Gunther (1935) addressed this as a mechanism at disposal of planktonic animals to drift great distances relative to the surface, which they cannot achieve by own horizontal movements. The deepening of the day-time residence in areas with low phytoplankton concentration and the shallowing in the bloom area, which was observed during EisenEx and EIFEX, effect a transport out of unproductive regions and maintenance in the phytoplankton-rich area.

During EIFEX, the migratory response of shallow migrants occurred mainly within the net sampling interval 50 - 100 m, while the depth range of the daytime residence of the deep migrating species was only covered by a single sampling interval (160 - 400 m). Thus the net sampling resolution allows a basic identification of shallow and deep migrating species but do not allow to derive phytoplankton dependent changes of the daytime residence of the different copepod species and stages from the net samples. For this reasons, the effects of the acoustically observed migration responses on the individual food gain and the local copepod abundance were investigated systematically in a simulation study covering the range of shallow, intermediate and deep migration (Krägefsky et al., to be submitted).

The results of the simulation study show that the acoustically observed migration behaviour can explain the abundance development and most of the large abundance increase of copepods inside phytoplankton bloom during EIFEX (Krägefsky et al., to be submitted). It might also explain the abundance increase of *C. citer* and the apparent increase of *C. simillimus* during EisenEx. A direct migratory reponse of larger zooplankton to the increased phytoplankton concentration should have increased their abundance substantially, but such increase could only observed for small (thorax length < 1.5 mm), very low abundant amphipods, which may have doubled in abundance inside the bloom area to approximately 250 ind. m^{-2} over the course of EIFEX.

Stage specific vertical migration behaviour and initial differences in the stage composition between inside and outside the fertilised area can cause a selective aggregation of particular copepodite stages in the bloom area, which interfere with changes in the stage composition caused by growth and mortality. In case of *C. simillimus*,

for example, the pattern of increase of the different copepodite stages during EIFEX may have been caused by combined effects of a stage-specific migration behaviour, caused weaker increase of younger copepodite stages, and growth into older stages. A stage specific aggregation might often be a dominant process effecting shifts in the stage composition over the course of a phytoplankton bloom and may strongly bias growth signals. For instance, only a small part of the 2-fold increase in abundance of older copepodite stages CIII-CVI of *M.lucens* can be explained by recruitment from younger stages, while most increase have to be caused by an active aggregation due to their vertical migration behaviour. Initial differences between in and outside the fertilised area seems to have strongly influenced the development in the stage distribution observed for *R. gigas*. The increasing convergence of the average copepodite stage inside and outside the phytoplankton rich area over the course of EIFEX suggests that most of the observed shift towards younger copepodite stages inside was due to the inflow and retention of individuals from the surrounding.

The observed DVM behaviour effects a relative increase of retention and individual nutritional gain inside mescoscale food patches up 2-3 fold according to simulation results (Krägefksy et al. to be submitted). It thus should maximise the total food intake gained during the life-cycle of a copepod individual, and have minor effect on visual predation risk, as the shallowing magnitude is in the order of or less than the shift in isolume depth caused by increased phytoplankton concentration. In summary, this migration behaviour can be considered as a food finding strategy.

4.4 Copepod grazing impact

4.4.1 Results from EisenEx

Copepod grazing during EisenEx was estimated with the gut fluorescence method and with incubation experiments (Schultes 2004, Schultes et al. 2006). Correcting for grazing periodicity (12h/24h) and pigment destruction (ca. 30%) as described above, a daily ration of 9.9% was derived for *C. simillimus* with the gut fluorescence method compared to 6.6 % in terms of phytoplankton carbon and 1.9% from additional carbon sources estimated with incubation experiments. Respective estimates for *R. gigas* were 3.4% with the gut fluorescence method and 0.5% (phytoplankton) and 0.4% (other food sources) with incubation experiments. For copepods < 2 mm a daily ration of 37% was derived from the gut fluorescence measurements and 2.6% (phytoplankton) and 4.7% (other food sources) with the incubation method (Schultes 2004, Schultes et al. 2006). Ingestion rates derived from incubation did not

balance respiratory needs determined during EisenEx, thus ingestion rates derived with the gut fluorescence method are used for the grazing estimates.

Based on the estimated copepod standing stock (>1.5 mm) in the upper 0 - 150 m and assuming daily rations of 3.5% for *R. gigas*, 5% for C. acutus and 10% for *C. simillimus* and other copepod species, the carbon ingestion of copepods (> 1.5mm) doubled from ca. 0.2 g C m^{-2} d^{-1} towards 0.4 g C m^{-2} d^{-1} at day 10 inside the fertilised area (Fig. 11c). The standing stock of *C. citer* might be overestimated by a trapezoidal integration due to the low vertical sampling resolution, but assuming a daily ration of 35%, the carbon ingestion of *C. citer* amounts to 0.2 g C m^{-2} d^{-1} additionally. The estimated carbon ingestion equates to 18 - 25% of the phytoplankton carbon stock on day 10, but 60-85% of the estimated primary production of ca. 0.7 g C m^{-2} d^{-1}.

4.4.2 Grazing impact during EisenEx and EIFEX

For EisenEx, the zooplankton sampling did not allow for proper assessment of the development of abundance and biomass and thus grazing impact of copepods inside the fertilised area. The counting into size classes introduces additional uncertainty for biomass and grazing estimates. At the last MN station on day 10 the estimated carbon ingestion by copepods ($\gtrsim$ 1 mm) equates up to 85% of the primary production, even excluding grazing by very small copepods (e.g. *Oithona*). This is an unrealistic estimate of the grazing impact, but might well be biased by an underestimated primary production. The estimated integrated primary production for EisenEx was little less than the observed net uptake of dissolved inorganic carbon (DIC) over the course of the experiment (Gervais et al. 2002), suggesting an underestimation if a substantial recycling and respiration in the surface layer is assumed. Carbon ingestion rates obtained from incubation are much lower than from gut fluorescence experiments for *R.gigas* and copepods (< 2 mm), yet those are below their minimum respiratory carbon needs determined during EisenEx. Daily rations from both methods are in closer agreement for *C. simillimus* (Schultes 2004).

The gut passage times measured in gut fluorescence experiments during EisenEx (Schultes 2004) and EIFEX are fast compared to GPT values of Southern Ocean copepods reported in the literature (e.g. Tirelli & Mayzaud 1999). For EIFEX, the experimental faecal pellet production rates (FPR) allow for an indepedent estimate of the gut passage time. The FPR derived at increased chlorophyll concentration inside the patch during EIFEX suggest gut passage times of 24-45 minutes and 32-

72 minutes for *C. simillimus* and *R. gigas*, respectively (Jansen et al. submitted). These are mean values for the 24 h duration of the experiments, which likely covered periods of active and less active feeding. Thus the results seem to confirm the fast GPT estimates of 22.1 (±16.4) min derived in the gut fluorescence experiments for *C. simillimus* but showed lower GPTs for *R. gigas*.

The daily rations derived during EisenEx and EIFEX from measured GPTs and initial gut contents are in the medium-range of literature values for *C. simillimus* (e.g. Atkinson et al. 1996b, Bernard & Fronemann 2003), while the EIFEX estimate for *R.gigas* is high compared to the EisenEx estimate and to daily rations in the range of less than 1% to 7% reported in the literature (Atkinson et al. 1996b, Dubischar & Bathmann 1997, Mayzaud et al. 2002b). A lower daily ration of *R. gigas* (6% compared to 9.1%) closer agrees with literature values and is used to actually estimate the phytoplankton carbon ingestion during EIFEX. Constant daily rations are also assumed for all other copepod species, as no clear relation between chlorophyll concentration and ingestion rates was found in the gut fluorescence experiments although this might be an artefact. In the bloom situation, a strong aggregation of long-chained diatoms in the cod end and more complicated handling in the gut fluorescence experiments due to this aggregation have increased the stress to copepods. A premature egestion caused by the stress could explain the rapid decreasing ingestion rates derived for *C. simillimus* at high phytoplankton concentration. Thus the assumption of constant daily rations may overestimate the food intake under phytoplankton poor but may underestimate the grazing impact of copepods in the bloom situation.

Their minimum food requirement is defined by respiration and carbon egestion. While the latter can be estimated from experimental derived faecal pellet production rates, their daily respiratory carbon requirements are estimated according to Dagg et al. (1982) for EIFEX. After the third week of EIFEX, the assessed minimum food requirement is not balanced by the estimated phytoplankton carbon ingestion. This imbalance may be partly due to the assumption of constant daily rations. However, imbalance between derived ingestion rates and measured metabolic demands was observed for both EisenEx and EIFEX and is a longstanding observation, mainly for incubation experiments (e.g. Atkinson 1994) but also using the gut fluorescence method (Zeldis 2001). The development of the faecal pellet carbon standing stock compared to the estimated faecal pellet production suggest a turnover in the order of 1 d^{-1}, which thus imply no overestimation of the carbon egestion. If a minimum estimate of the respiratory carbon needs is applied using lower values reported e.g.

by Mayzaud (2002a) compared to Dagg et al. (1982), the estimate for the total carbon respiration by copepods (>1 mm) reduce to 3 - 4 g C m^{-2} over the course of EIFEX. Still in this case, the assessed minimum food requirements are sparsely balanced by phytoplankton carbon ingestion after the third week of the experiment.

Ingestion rates derived with the incubation and gut fluorescence method are systematically biased by limiting normal copepod behaviour (bottle effects) and cascading effects (Nejstgaard et al. 2001), and by pigment degradation in the gut (Dam & Peterson 1988, Tirelli & Mayzaud 1998), respectively. The gut fluorescence method, more fundamentally, allows only for an estimate of the phytoplankton ingestion while most copepods show omnivore feeding behaviour. Microzooplankton thus may have contributed significantly to the copepod diet.

Microzooplankton biomass remained low and quite stable during EIFEX, while their grazing impact on phytoplankton estimated from serial dilution experiments was 8.8 g C m^{-2} over the course of the experiment (Smetacek in prep.). Thus up to 3.5 g C m^{-2} of the primary production could have been channelled through a short link from phytoplankton via microzooplankton to the copepods, assuming a high gross growth efficiency of microzooplankton of 40% (Straile 1997). Some carbon may have also been channelled from the recycling pool to the copepods through feeding of microzooplankton on bacteria and detritus.

Grazing on microzooplankton include the feeding by the very small copepods, mainly of *Oithona similis*, which are not included in the above given estimate of the minimum food requirement of the copepods ($\gtrsim$ 1 mm). Assuming a daily ration similar to *C. citer*, grazing impact of *Oithona* alone would have amounted to about 0.1 – 0.2 g C m^{-2} d^{-1} during EIFEX and to 0.15 g C m^{-2} d^{-1} at the end of EisenEx. However, their actual grazing impact remains widely unknown.

Oithona is a very abundant copepod, but is not sampled adequately with plankton nets with commonly used mesh sizes (Gallienne & Robins 2001). Sampling with Niskin bottles is more efficiently but allows only for a very sparse sampling of the water column (Henjes et al. 2007). *Oithona* is known to feed on a wide variety of food items including phytoplankton, microzooplankton, and nauplii of other copepods (e.g. Hopkins 1985) and is discussed to retard the flux of zooplankton faecal material by coprophagous feeding (Gonzales & Smetacek 1994, Reigstad et al. 2005). Alterations in the grazing behaviour and impact of *Oithona* in response to changes in the food environment are likely but are sparsely investigated.

During EisenEx, *Oithona* responded with an upward migration towards the progressively phytoplankton enriched surface inside the bloom area. Similar to the

above discussed behaviour of diel migrating copepods, the non-diurnal vertical migration behaviour of *Oithona* may be considered as a food finding strategy that have caused the strong abundance increase of *Oithona* during EisenEx (Krägefsky et al. in press). Less attraction by the dominant diatom species with long spines which likely prevent an effective feeding by *Oithona* may have caused the absence of significant vertical migration response of *Oithona* during EIFEX (Henjes, unpublished results). The response of *Oithona* during EisenEx seems to imply a switch in diet composition from heterotrophic prey and other food to diatoms. Such a switch could explain differences in development in microzooplankton stock during EisenEx (increase; Henjes et al. 2007) and EIFEX (quite constant; Smetacek in prep.), but additional increased grazing pressure on diatoms during EisenEx.

4.5 Conclusion

Copepods showed strong vertical migration response in the phytoplankton bloom areas of EisenEx and EIFEX. Their vertical migration behaviour causes an increased drift out of areas with dilute food concentration but increases the retention inside phytoplankton-rich areas. The observed migration behaviour can be considered as a food finding strategy to cope with an extreme environment, which is characterized by strongly seasonal and horizontal patchy food supply (Smetacek et al. 1990). Limiting food supply outside and strong nutritional benefit inside the phytoplankton bloom area e.g. is evidenced by a reproductive response of *R. gigas*, increasing the percentage of egg-producing females from about 0 to 90% towards the end of EIFEX (Jansen et al. 2006). These findings are in agreement with findings for other copepods in the Southern Ocean (e.g. Shreeve et al. 2002, Ward and Hirst 2007).

The strong difference between the phytoplankton stock increase (4.5 g C m^{-2}), net DIC uptake (21 g C m^{-2}) and estimated integrated primary production (49 g C m^{-2}) over the course of EIFEX (Smetacek in prep.) confirm a substantial grazing impact on the phytoplankton. The development in faecal pellet stock in the surface layer and the accumulation of biogenic silica and diatom carbon at extreme molar ratio of ~ 1.3 suggest not only a strong faecal pellet recycling but also a faecal pellet production likely higher than estimated (Jansen et al. in prep.). Most of the organic faecal matter seems to be decomposed and respired in the surface layer. However, the incorporation of the remains of disintegrated faecal pellets in sinking aggregates particularly of senescent diatoms after the peak of the EIFEX bloom may have contributed to the flux of silica shell debris and non-respired organic faecal matter

to the deep sea. The fate of faecal matter during EisenEx is widely unknown.

The observed migration behaviour is triggered by increased phytoplankton concentration and causes a co-increase of copepods and phytoplankton. This co-increase likely allows phytoplankton to reach bloom concentration, though copepods and other zooplankton exert substantial grazing pressure. Their grazing determines a species specific mortality environment and thus structures the phytoplankton species composition. However, gut content analyses showed that heavily silicified frustules (*Fragilariopsis kerguelensis*) or long spike-like setae (*Chaetoceros spp.*), had no deterring effects on larger copepods during EIFEX (S. Kruse et al. submitted), but they likely prevent effective grazing by smaller copepods.

The massive increase in copepod biomass in the phytoplankton bloom area of EIFEX was predominately due to an active aggregation of copepods. This aggregation causes a mixture of individuals with different nutritional histories over the course of the bloom and biases the growth signals. Furthermore, growth and mortality signals are strongly masked for those species with stage specific migration behaviour or initial horizontal differences in stage composition. However, in total, the data suggests rather low individual growth compared to the ingested food.

In summary, the lagrangian iron fertilisation experiments EisenEx and EIFEX revealed remarkable migration behaviour of copepods. They apparently utilise the vertical sheared flow field of their oceanic environment to find food and cope with the patchy, mostly poor food environment of the Southern Ocean. As during other iron-fertilisation experiments except of SeedsII (Tsuda et al. 2007), the phytoplankton escaped grazing pressure and built up bloom concentration when relieved of iron limitation. However, the amount of phytoplankton production which was grazed over the course of the experiment by far exceeded the increase in phytoplankton standing stock. Copepod grazing (on phyto- and microzooplankton) thus has to be considered as a mechanism that can significantly alter carbon and nutrient fluxes after iron fertilisation also in the Southern Ocean.

Acknowledgements

We grateful acknowledge the professional and friendly support of the colleagues and the crew of the RV Polarstern during the two cruises. We especially thank T. Stadtlander for assistance of zooplankton collection during EIFEX and S. Grabbat for the counting of zooplankton net samples. C. Klaas kindly provided Chl *a* data for the EIFEX cruise.

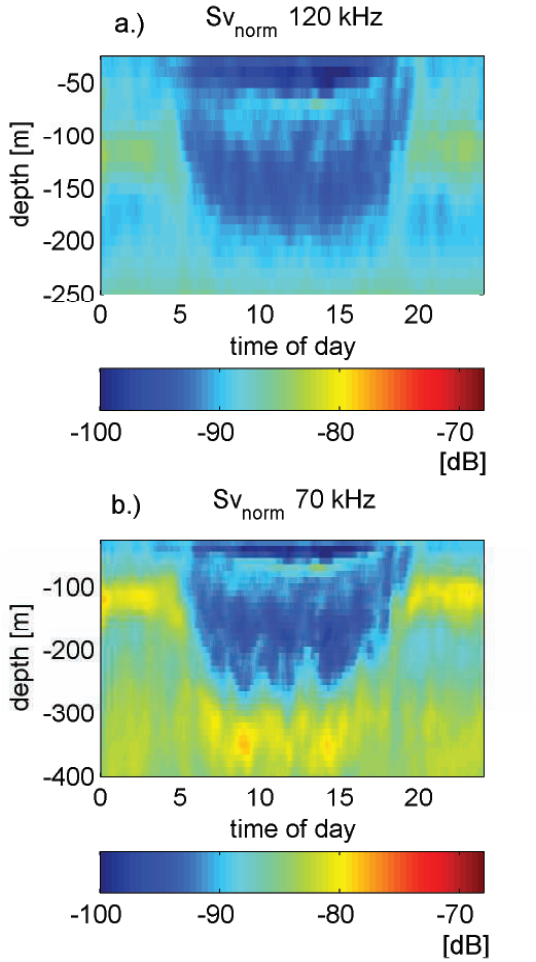

Figure 1: Norm mean volume backscattering strength (Sv_{norm}) of the acoustic measurements during EIFEX at 120 kHz (a) and 70 kHz (b).

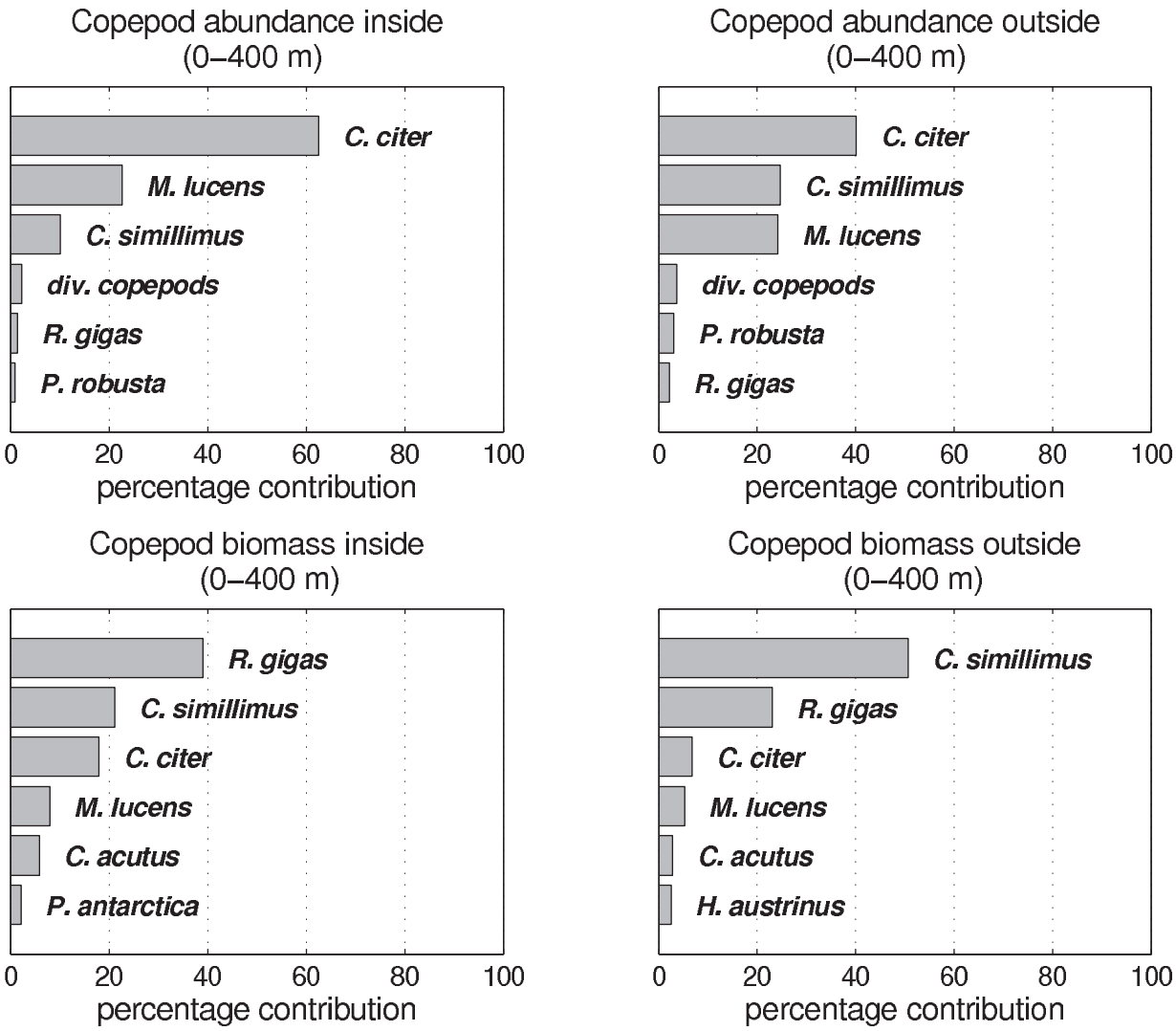

Figure 2: Percentage contribution of the six most important copepod species in terms of abundance (a, b) and biomass (c, d) contribution in- and outside the fertilised area of EIFEX, respectively.

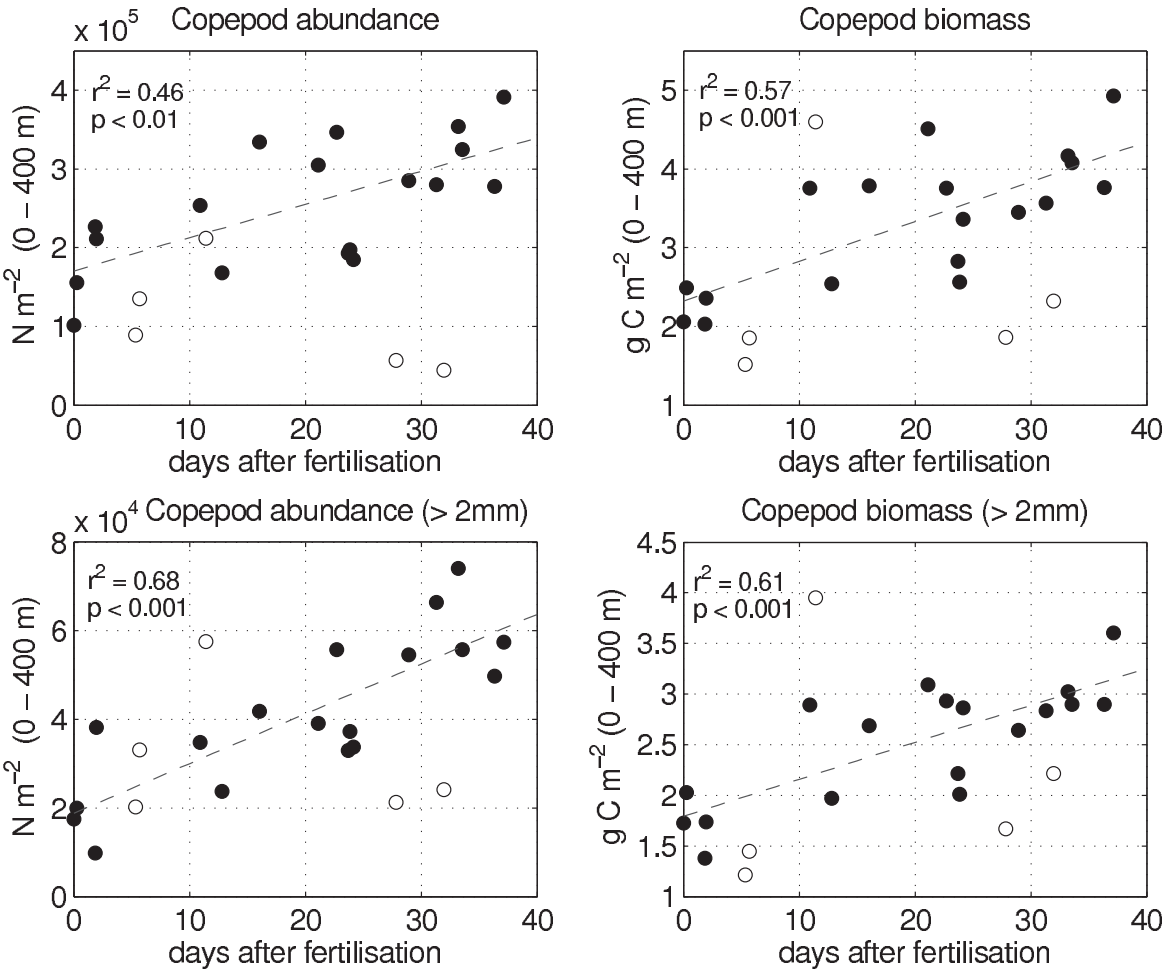

Figure 3: Abundance (a, c) and biomass (b, d) of copepods $\gtrsim 1$ mm (upper graphs) and copepods > 2 mm inside (filled circles) and outside (open circles) the fertilised area of EIFEX. Linear regressions are given for the inpatch data (dashed lines).

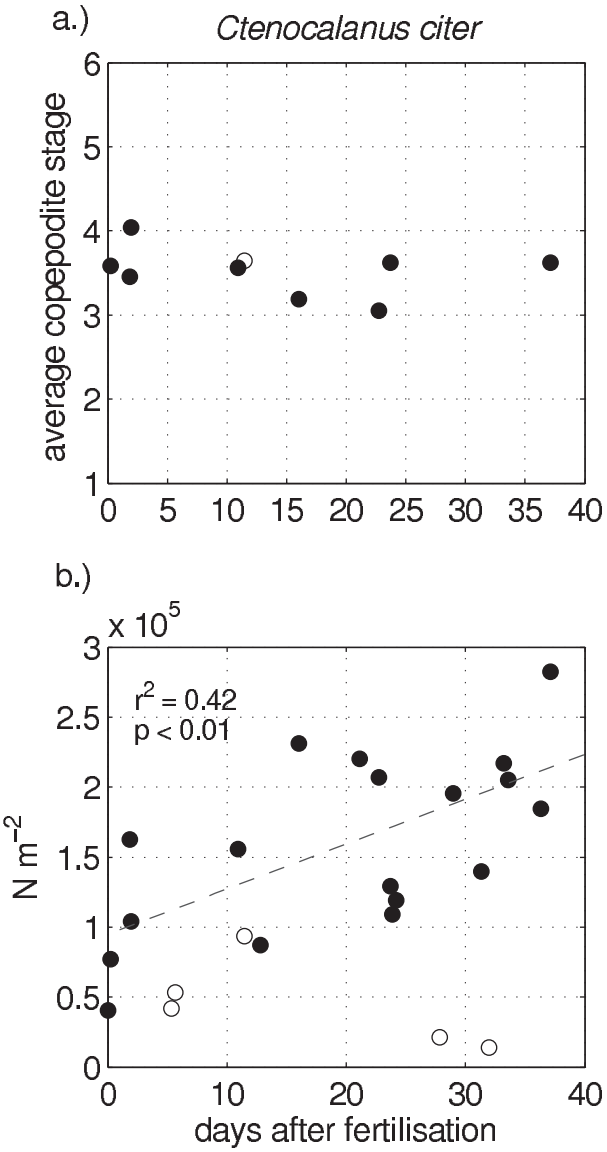

Figure 4: Average copepodite stage (a) and abundance (b) of *Ctenocalanus citer* inside (filled circles) and outside (open circles) the fertilised area of EIFEX. Linear regression for inpatch abundance data is shown by a dashed line.

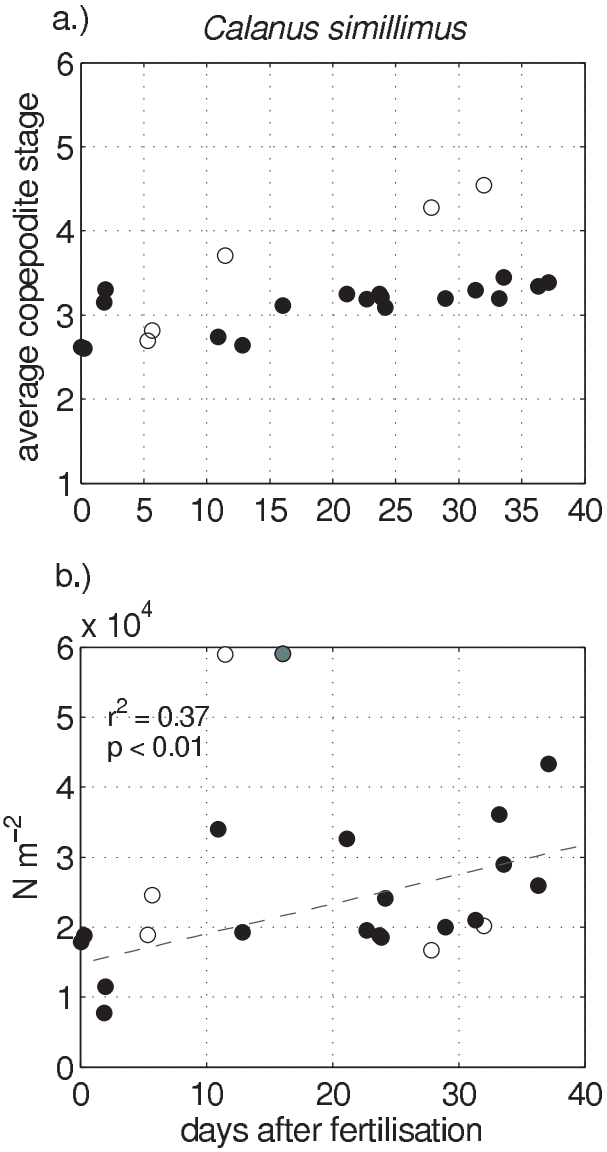

Figure 5: Average copepodite stage (a) and abundance (b) of *Calanus simillimus* inside (filled circles) and outside (open circles) the fertilised area of EIFEX. Linear regression for inpatch abundance data is shown by a dashed line. Station 513 is excluded as an outlier from regression analysis and is marked in gray.

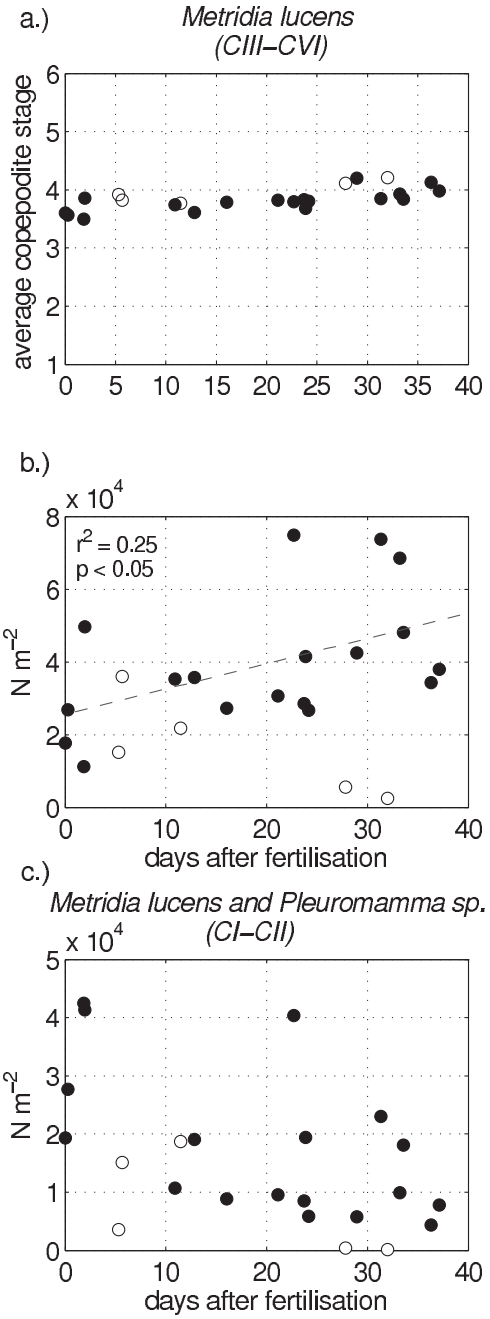

Figure 6: Average copepodite stage (a), abundance (b) of *Metridia lucens* (CIII-CVI) and abundace of *Metridia lucens* CII and earliest copepodite stage (CI) of *Metridia spp.* and *Pleuromamma sp.* inside (filled circles) and outside (open circles) the fertilised area of EIFEX. Linear regression for inpatch abundance data of CIII-CVI is shown by a dashed line in (b).

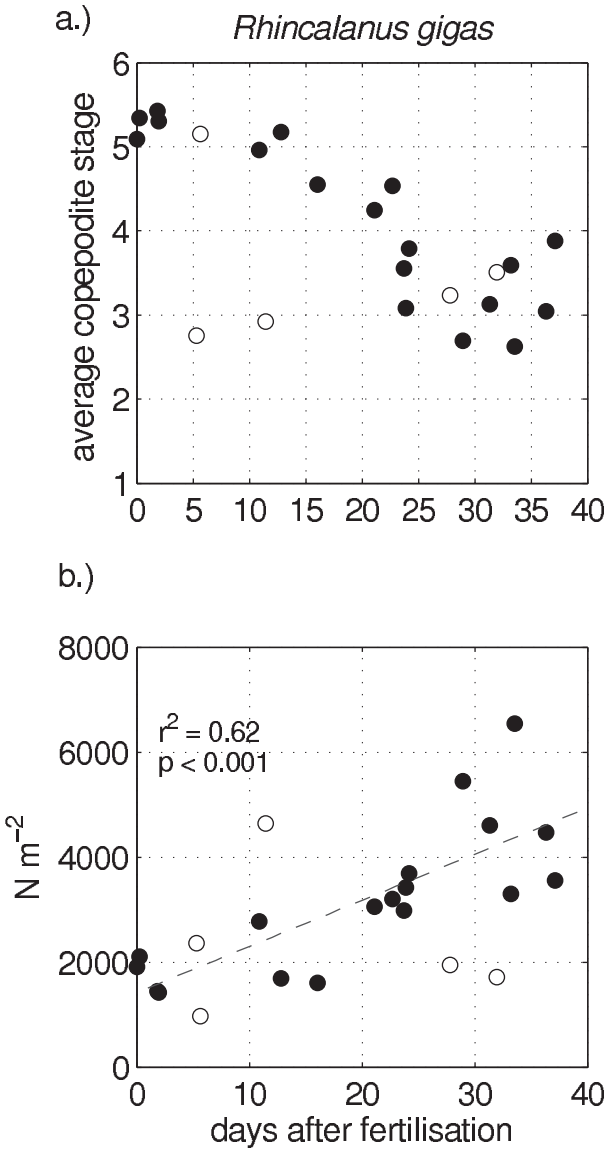

Figure 7: Average copepodite stage (a) and abundance of *Rhinalanus gigas* inside (filled circles) and outside (open circles) the fertilised area of EIFEX. Linear regression for inpatch abundance data is shown by a dashed line.

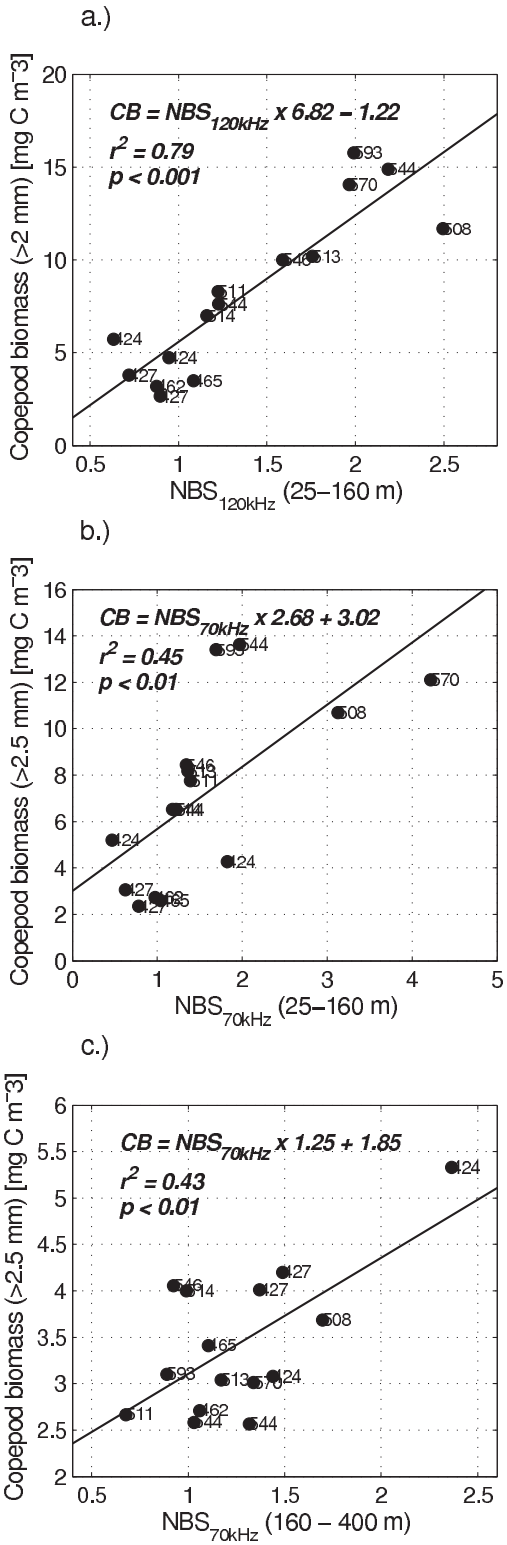

Figure 8: Correlation between NBS measured at 120 kHz (a) and 70 kHz (b, c) and biomass of copepods in the depth range 25 - 160 m (a, b) and 160 - 400m (c).

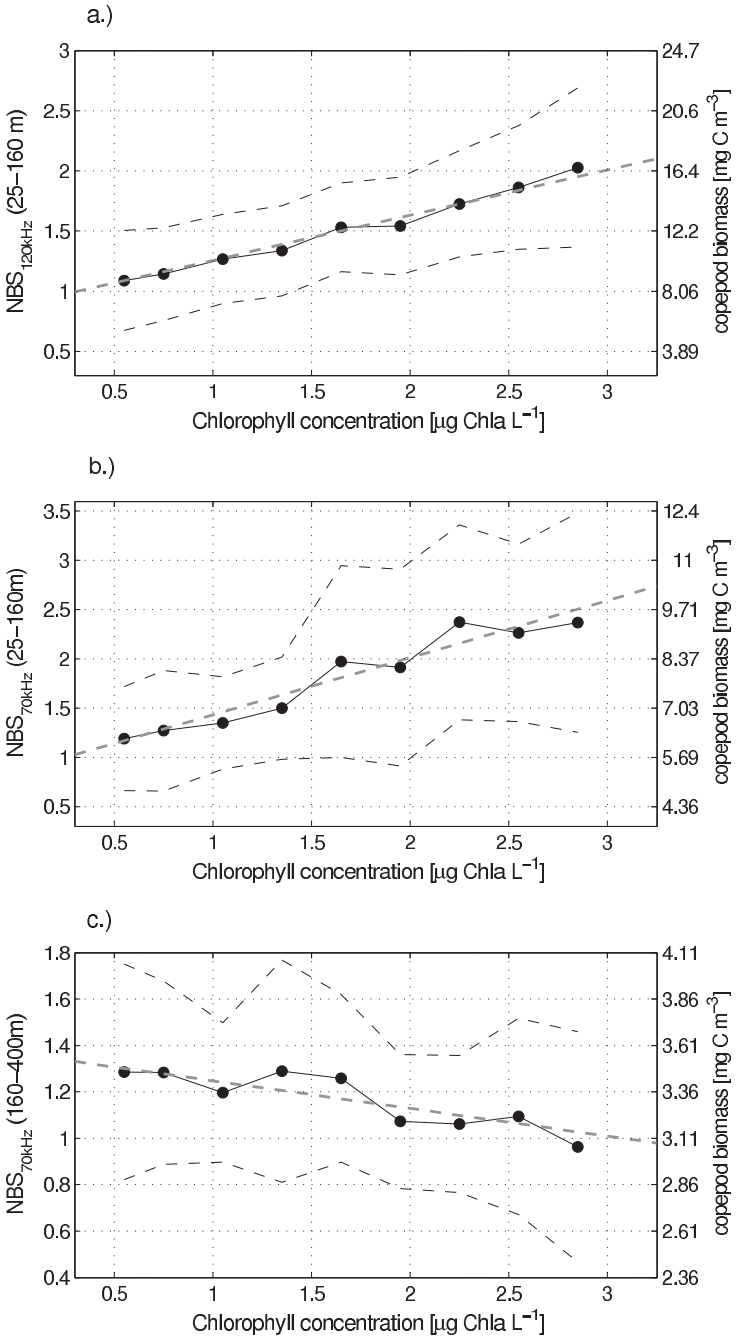

Figure 9: Relation between surface chlorophyll concentration and NBS measured at 120 kHz (a) and 70 kHz (b, c) in the depth range 25 - 160 m (a, b) and 160 - 400m (c) for total measurements inside the eddy (experimental site). Black circles show the mean NBS at chlorophyll concentration in the given range, upper and lower dashed lines show the standard deviation. A gray dashed line show the regression line derived from regression anlysis between the single NBS and cholorophyll measurements. Outliers are removed according the David-Hartley-Pearson-Test and R-student. The axis on the left hand side indicate the biomass of copepods $\gtrsim 1$ mm (a), > 2.5 mm (b) and > 2.5 mm (c) according the observed NBS – copepod biomass relation.

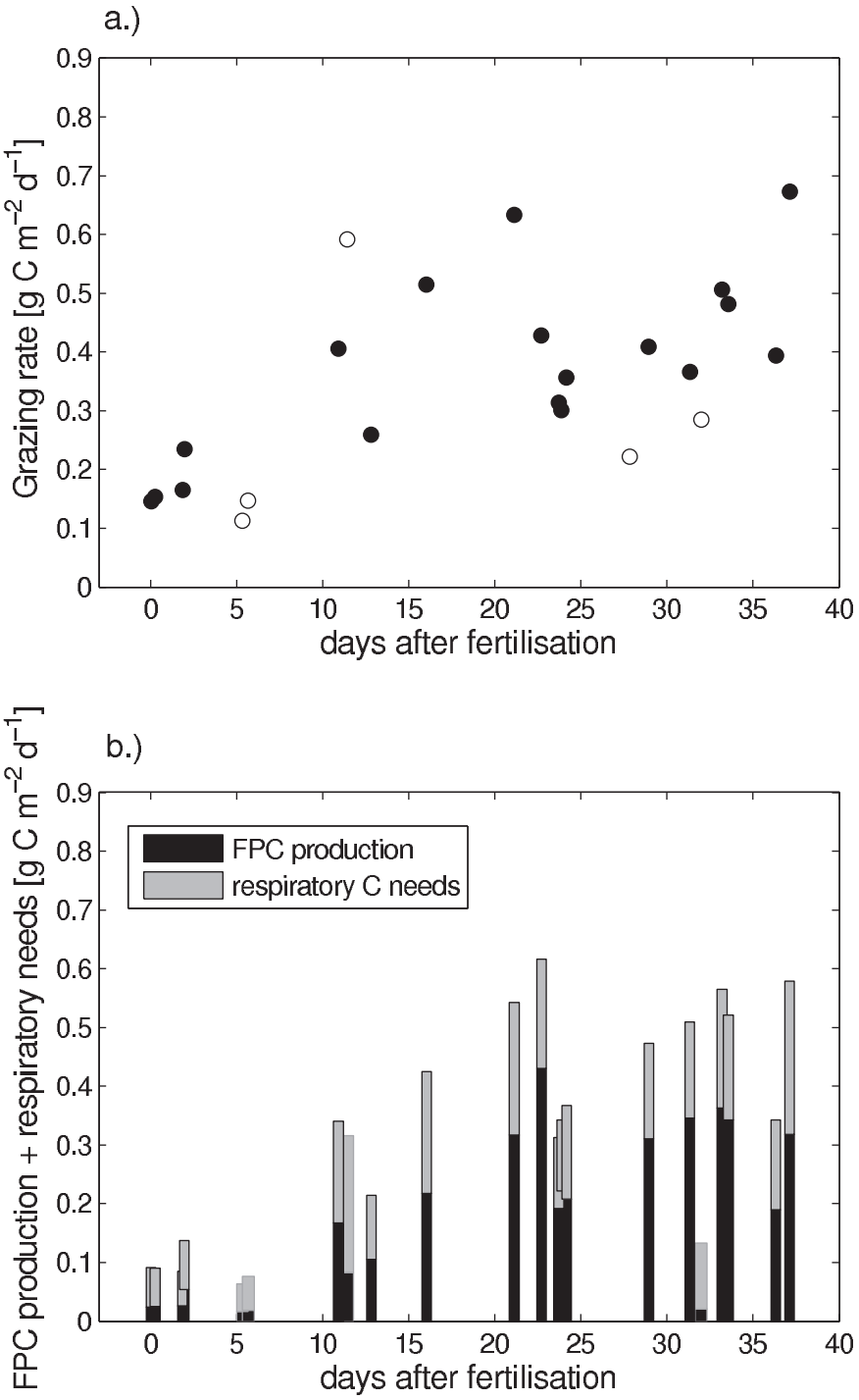

Figure 10: Phytoplankton carbon ingestion rate of copepods ($\gtrsim$ 1 mm) during EIFEX (a) inside (filled circles) and outside the fertilised area (open circles), and estimated daily fecal pellet production and respiratory carbon needs (b). Bars without a black frame in the lower graph are the outside estimates.

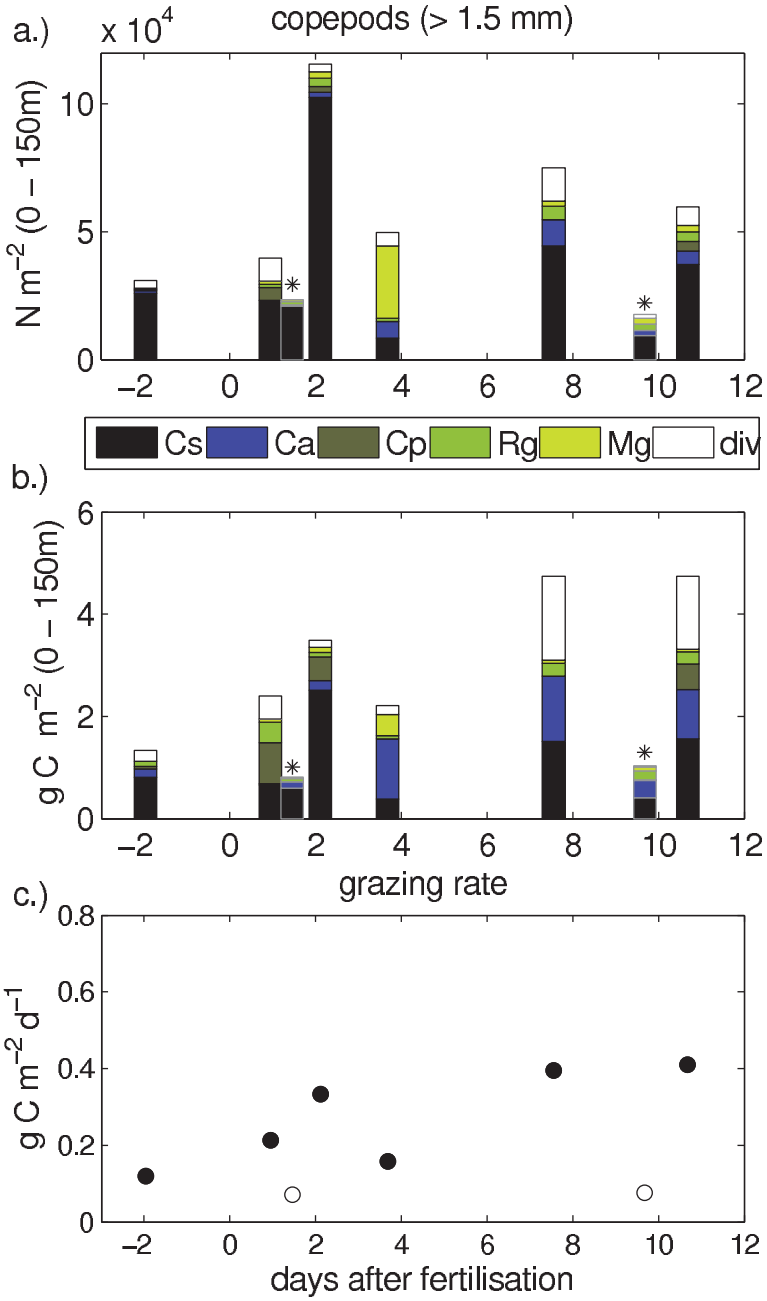

Figure 11: Abundance (a), biomass (b) and estimated grazing rate (c) of copepods >1.5 mm during EisenEx. Stacked bar plots show the relative contribution of the different copepod species. Abbrevations used in the legend: Cs = *Calanus simillimus*; Ca = *Calanoides acutus*; Cp = *Calanus propinquus*; Rg = *Rhincalanus gigas*; Mg = *Metridia lucens* and div = diverse copepods. Stations outside the fertilised area are marked with asterisk (a,b) and open circle (c).

MN Station-Cast	Days after iron release	time at depth	position	depth intervals (m)
424-14	0	00:28	IN	0 - 20, 20 - 40, 40 - 80, 80 - 160, 160 - 360
424-21	0	06:11	IN	0 - 20, 20 - 40, 40 - 80, 80 - 160, 160 - 360
427-4	1	20:18	IN	0 - 20, 20 - 40, 40 - 80, 80 - 160, 160 - 360
427-8	1	22:59	IN	0 - 20, 20 - 40, 40 - 80, 80 - 160, 160 - 360
462-2	5	07:43	OUT	0 - 25, 25 - 50, 50 - 100, 100 - 160, 160 - 400
465-1	5	15:51	OUT	0 - 25, 25 - 50, 50 - 100, 100 - 160, 160 - 400
508-20	10	21:37	IN	0 - 25, 25 - 50, 50 - 100, 100 - 160, 160 - 400
509-8	11	10:20	OUT	0 - 25, 25 - 50, 50 - 100, 100 - 160, 160 - 400
511-3	12	19:45	IN	0 - 25, 25 - 50, 50 - 100, 100 - 160, 160 - 400
513-11	16	00:23	IN	0 - 25, 25 - 50, 50 - 100, 100 - 160, 160 - 400
514-8	17	20:36	OUT	25 - 50, 50 - 100, 100 - 160, 160 - 400
543-3	21	02:48	IN	0 - 25, 25 - 50, 50 - 100, 100 - 160, 160 - 400
544-4	22	16:47	IN	0 - 25, 25 - 50, 50 - 100, 100 - 160, 160 - 400
544-27	23	16:47	IN	0 - 25, 25 - 50, 50 - 100, 100 - 160, 160 - 400
544-33	23	20:44	IN	0 - 25, 25 - 50, 50 - 100, 100 - 160, 160 - 400
544-45	24	03:47	IN	0 - 25, 25 - 50, 50 - 100, 100 - 160, 160 - 400
546-16	26	22:21	?	0 - 25, 25 - 50, 50 - 100, 100 - 160, 160 - 400
552-4	27	19:35	OUT	0 - 25, 25 - 50, 50 - 100, 100 - 160, 160 - 400
553-8	28	22:21	IN	0 - 25, 25 - 50, 50 - 100, 100 - 160, 160 - 400
570-6	31	07:27	IN	0 - 25, 25 - 50, 50 - 100, 100 - 160, 160 - 400
576-2	31	23:17	OUT	0 - 25, 25 - 50, 50 - 100, 100 - 160, 160 - 400
580-5	33	04:30	IN	0 - 25, 25 - 50, 50 - 100, 100 - 160, 160 - 400
580-15	33	13:15	IN	0 - 25, 25 - 50, 50 - 100, 100 - 160, 160 - 400
591-2	36	07:30	IN	0 - 25, 25 - 50, 50 - 100, 100 - 160, 160 - 400
593-8	37	02:34	IN	0 - 25, 25 - 50, 50 - 100, 100 - 160, 160 - 400

Table 1: Sampling details for standard casts with the Multi Net

copepod species	abundace [%] inside	abundance [%] outside	biomass [%] inside	biomass [%] outside	grazing estimate daily ration [%]
Ctenocalanus citer	62.5	40.1	17.9	6.8	35
Metridia lucens	22.5	24.1	7.9	5.3	15
Calanus simillimus	10	24.7	21.1	50.7	15
div. copepods	2.2	3.7	1.4	1.4	15
Rhincalanus gigas	1.3	2.2	39.0	23.0	6
Pleuromma robusta	0.8	3.1	1.89	2.3	15
Calanoides acutus	0.4	0.5	5.8	2.8	7.5
Heterorhabdus austrinus	0.2	0.5	1.5	2.5	15
Paraeuchaeta biloba	0.1	0.8	0.3	1.5	15
Paraeuchaeta antarctica	0.1	0.3	2	2.3	15
Calanus propinquus	0.1	0.2	1.4	1.4	15

Table 2: Percentage contribution of copepod species to abundance and biomass of copepods in- and outside the fertilised area during EIFEX, and their daily ration assumed in grazing estimates.

taxonomic group	abundance [ind. m^{-3}] inside	abundance [ind. m^{-3}] outside
Amphipoda (⌀ 1.5 mm thorax length)	0.67 (0.68)	0.69 (0.69)
Euphausiacea, juveniles + adults (⌀ 8.5 mm)	0.33 (0.28)	0.26 (0.11)
Euphausiacea, furcilia (⌀ 4.0 mm)	1.44 (1.04)	1.81 (1.20)
Euphausiacea, calyptopis (⌀ 2.0 mm)	0.26 (0.22)	0.36 (0.22)
Chaetognatha (⌀ 9 mm)	8.28 (7.93)	5.64 (5.71)
Polychaeta (⌀ 1.5 mm)	1.52 (1.43)	1.74 (1.28)
Salps	0.42 (0.21)	1.06 (0.84)

Table 3: Mean and median abundance (in parenthesis) of different non-copepod zooplankton (≥ 1.5 mm) collected during EIFEX in - and outside the fertilised area.

species	GPT [min]	number of experiments	phytoplankton carbon ingestion rate [μg C copepod^{-1}d^{-1}]	daily ration (CV) [%]
C. simillimus	22.1 ($\pm$16.4)	9	17.4 ($\pm$13.5)	15.7 ($\pm$12.2)
R. gigas	15.1 ($\pm$6.9)	9	57($\pm$29)	9.1 ($\pm$5.2)

Table 4: Gut passage time (GPT), phytoplankton carbon ingestion rate and daily ration derived from gut fluorescence experiments during EIFEX for *C. simillimus* and *R. gigas*.

References

[1] Atkinson, A. Diets and feeding selectivity among epipelagic copepod community near south georgia in summer. *Polar Biol*, 14:551–560, 1994.

[2] Atkinson, A., Shreeve, R.S., Pakhomov, E.A., Priddle, J., Blight, S.P., and Ward, P. Zooplankton response to a phytoplankton bloom near South Georgia, Antarctica. *Mar Ecol Prog Ser*, 144:195–210, 1996.

[3] Atkinson, A., Ward, P., and Murphy, E. J. Diel periodicity of Subantarctic copepods: relationships between vertical migration, gut fullness and gut evacuation rate. *J Plankton Res*, 18:1387–1405, 1996.

[4] Bellerby, R., Neil, C., Mkatshawa, L., and Balt, C. CO2-System measurements during EIFEX. *Reports on Polar and Marine Research*, 500:66–69, 2005.

[5] Bernard, K.S. and Fronemann, P.W. Mesozooplankton community structure and grazing impact in the Polar Frontal Zone of the south Indian Ocean during austral autumn 2002. *Polar Biol*, 26:268–275, 2003.

[6] Chisholm, S. W. and Morel, F. M. M. What controls phytoplankton production in nutrient-rich areas of the open sea? *Limnol Oceanogr Special Issue*, 36:1507–1511, 1991.

[7] Chu, D. and Wiebe, P. H. Measurements of sound-speed and density contrasts of zooplankton in antarctic waters. *ICES J Mar Sci*, 62:818–831, 2005.

[8] Cisewski, B., Strass, V. H., Losch, M., and Prandke, H. Mixed layer analysis of a mesoscale eddy in the antarctic polar front zone. *J. Geophys. Res.*, 113:1–19, 2008.

[9] Cisewski, B., Strass, V. H., and Prandke, H. Upper-ocean vertical mixing in the Antarctic Polar Front Zone. *Deep-Sea Res Part II*, 52(9-10):1087–1108, 2005.

[10] Dagg, M. J., Vidal, J., Whitledge, T. E., Iverson, R. L., and Goering, J. J. The feeding, respiration, and excretion of zooplankton in the Bering Sea during a spring bloom . *Deep-Sea Res*, 29:45–63, 1982.

[11] Dam, H. G. and Peterson, W. T. The effect of temperature on the gut clearance rate constant of planktonic copepods. *J Exp Mar Biol Ecol*, 123:1–14, 1988.

[12] Dubischar, C.D. and Bathmann, U.V. Grazing impact of copepods and salps on phytoplankton in the Atlantic sector of the Southern Ocean . *Deep-Sea Res. Part II*, 44:415–433, 1997.

[13] Foote, K.G., Knudsen, H.P., Vestnes, G., MaxLennan, D.N., and Simmonds, E.J. Calibration of acoustic instruments of fish density estimation: a practical guide. *Co op Res Rep int Counc Explor Sea*, 144:1– 69, 1987.

[14] Gallienne, C.P. and Robins, D.B. Is *Oithona* the most important copepod in the world's oceans? *J Plankton Res*, 23:1421–1432, 2001.

[15] Gervais, F., Riebesell, U., and Gorbunov, M.Y. Changes in size-fractionated primary productivity and chlorophyll a in response to iron fertilization in the southern Polar Frontal Zone. *Limnol Oceanogr*, 47(5):1324–1335, 2002.

[16] Gonzales, H.E. and Smetacek, V. The possible role of the cyclopoid copepod Oithona in retarding the flux of zooplankton faecal material. *Mar Ecol Prog Ser*, 113:233–246, 1994.

[17] Grubbs, F. E. Procedures for detecting outlying observations in samples. *Technometrics*, 11(1):1–21, 1969.

[18] Henjes, J., Assmy, P., Klaas, C., Verity, P., and Smetacek, V. Response of microzooplankton (protists and small copepods) to an iron-induced phytoplankton bloom in the Southern Ocean (EisenEx). *Deep-Sea Res Part I*, 54:363–384, 2007.

[19] Hopkins, T.L. Food web of an Antarctic midwater ecosystem. *Mar Biol*, 89:197–212, 1985.

[20] Jansen, S., Henjes, J., Friedrichs, L., Krägefsky, S., and Bathmann, U. Fate of copepod faecal pellets during an iron induced phytoplankton bloom (EIFEX) in the Southern Ocean. *submitted*, 0:0, 2008.

[21] Jansen, S., Klaas, C., Krägefsky, S., Harbou, L. v., and Bathmann, U. Reproductive response of the copepod *Rhincalanus gigas* to an iron-induced phytoplankton bloom in the Southern Ocean. *Polar Biol*, 29:1039–1044, 2006.

[22] Krägefsky, S., Bathmann, U., and Wolf-Gladrow, D. On the diel vertical migration behaviour of diel migrating copepods during two iron-fetilisation experiments (EisenEx and EIFEX). -, -:–, to be submitted.

[23] Krägefsky, S.K., Bathmann, U., Strass, V., and Wolf-Gladrow, D. Response of small copepods to an iron-induced phytoplankton bloom - a model to address the aggregation causes. *Mar Ecol Prog Ser*, -:–, in press.

[24] Kruse, S., Jansen, S., Krägefsky, S., and Bathmann, U. Gut content analyses of three dominant Antarctic copepod species during an induced phytoplankton bloom (EIFEX). *Mar Ecol*, 0:0, submitted.

[25] Martin, J. H., Gordon, R. M., and Fitzwater, S.E. Iron in Antarctic waters. *Nature*, 345:156–158, 1990.

[26] Martin, J.H., Coale, K.H., Johnson, K.S., Fitzwater, S.E., Gordon, R.M., Tanner, S.J., Hunter,C.N., Elrod, V.A., Nowicki, J.L., Coley,T.L., Barber, R.T., Lindley, S., Watson, A.J., Vanscoy, K., Law, C.S., Liddicoat, M.I., Ling, R., Stanton, T., Stockel, J., Collins, C., Anderson, A., Bidigare, R., Ondrusek, M. and Latasa, M., Millero, F.J., Lee, K., Yao, W., Zhang, J.Z., Friederich, G., Sakamoto, C., Chavez, F., Buck, K. and Kolber, Z., Greene, R., Falkowski, P., Chisholm, S.W., Hoge, F., Swift, R., Yungel, J., Turner, S., Nightingale, P., Hatton, A., Liss, P., and Tindale, N.W. Testing the iron hypothesis in ecosystems of the Equatorial Pacific Ocean. *Nature*, 371:123–129, 1994.

[27] Mayzaud, P., Razouls, S., Errhif, A. and Tirelli, V., and Labat, J. P. Feeding, respiration and egg production rates of copepods during austral spring in the indian sector of the antarctic ocean: role of the zooplankton community in carbon transformation. *Deep-Sea Res I*, 49:1027–1048, 2002a.

[28] Mayzaud, P., Tirelli, V., Errhif, A., Labat, J. P., Razouls, S., and Perssionotto, R. Carbon intak eby zooplankton. Importance and role of zooplankton grazing in the Indian sector of the Southern Ocean. *Deep-Sea Res II*, 49:3169–3187, 2002b.

[29] Moore, J. K. and Abbott, M. R. Surface chlorophyll concentrations in relation to the Antarctic Polar Front: seasonal and spatial patterns from satellite observations. *J Mar Syst*, 37(1-3):69–86, 2002.

[30] Nejstgaard, J. C., Naustvoll, L-J., and Sazhin, A. Correcting for underestimation of microzooplankton grazung in botlle incubation experiments with mesozooplankton. *Mar Ecol Prog Ser*, 221:59–75, 2001.

[31] Pakhomov, E. A., Perissinotto, R., McQuaid, C. D., and Froneman, P. W. Zooplankton structure and grazing in the Atlantic sector of the Southern Ocean in late austral summer 1993: Part 1. Ecological zonation. *Deep-Sea Res I*, 47:1663–1686, 2000.

[32] Reigstad, M., Wexels Riser, C., and Svensen, C. Fate of copepod faecal pellets and the role of *Oithona spp. Mar Ecol Prog Ser*, 304:265–270, 2005.

[33] Rollwagen Bollens, G. C. and Landry, M. R. Biological response to iron fertilization in the eastern equatorial Pacific (IronEx II). II. Mesozooplankton abundance, biomass, depth distribution and grazing. *Mar Ecol Prog Ser*, 201:43–56, 2000.

[34] Röttgers, R., Colijn, F., and Dibbern, M. Algal pyhsiology and biooptics . *Reports on Polar and Marine Research*, 500:82–88, 2005.

[35] Schnack-Schiel, S. B., Hagen, W., and Mizdalski, E. Seasonal comparison of *Calanoides acutus* and *Calanus propincus* (copepoda: Calanoida) in the southeastern Weddel Sea, Antarctica. *Mar Ecol Prog Ser*, 70:17–27, 1991.

[36] Schultes, S. *The Role of zooplankton grazing in the biogeochemical cycle of silicon in the Southern Ocean.* PhD thesis, University Bremen, 2004.

[37] Schultes, S., Verity, P. G., and Bathmann, U. Copepod grazing during an iron-induced diatom-bloom in the Antarctic Circumpolar Current (EisenEx): I. Feeding patterns and grazing impact on prey populations. *J Exp Mar Biol Ecol*, 338:16–34, 2006.

[38] Shreeve, R. S., Ward, P., and Whitehouse, M. J. Copepod growth and development around South Georgia: relationships with temperature, food and krill. *Mar Ecol Prog Ser*, 233:169–183, 2002.

[39] Smetacek et al. Massive carbon flux to the deep sea from an iron-fertilized phytoplankton bloom in the southern ocean. *in prep.*, 0:0, 2008.

[40] Smetacek, V., Scharek, R., and Nöthig, E. M. Seasonal and regional variation in the pelagial and its relationship to the life history cycle of krill. In K. Kerry and G. Hempel, editors, *Antartic ecosystems: Egologycal change and conservation*, pages 103–114. Springer Verlag, Berlin, 1990.

[41] Smetacek, V., Strass, V. H., Klass, C., Assmy, P., Cisewski, B., Savoye, N., Henjes, J., Bathmann,U., Bellerby, R., Berg, G. M., Croot, P., Friedrich, L., Gonzalez, S., Harbou, L. v., Herndl, G. J., Hoffmann, L., Jansen, S., Krägefsky, S., Latasa, M., Leach, H., Losch, M., Mills, M. M., Montresor, M., Neill, C., Passow, U., Peeken, I., Röttgers, R., Scharek, R., Terbrüggen, A., Webb, A., and Wolf-Gladrow, D. Massive carbon flux to the deep sea from an iron-fertilized phytoplankton bloom in the Southern Ocean. *in prep.*, -:–, 2008.

[42] Stanton, T. K. and Chu, D. Review and recommendations for the modelling of acoustic scattering by fluid-like elongated zooplankton: euphausiids and copepods. *ICES J Mar Sci*, 57:793–807, 2000.

[43] Straile, D. Gross growth efficiencies of protozoan and metazoan zooplankton and their dependence on food concentration, predaor-prey weight ratio, and taxonomic group. *Limnol Oceanogr*, 42:1375–1385, 1997.

[44] Tirelli, V. and Mayzaud, P. Gut pigment destruction by the copepod textitAcartia clausi. *J Plankton Res*, 20:1953–1961, 1998.

[45] Tirelli, V. and Mayzaud, P. Gut evacuation rates of antarctic copepods during austral spring. *Polar Biol*, 21:197–200, 1999.

[46] Tsuda, A. et al. Evidence for the grazing hypothesis: Grazing reduces phytoplankton responses of the HNLC ecosystem to iron enrichment in the western subarctic pacific (SEEDS II) . *J Oceanogr*, 63:983–994, 2007.

[47] Voronina, N.M. Comparative abundance and distribution of major filter-feeders in the antarctic pelagic zone. *J Mar Syst*, 17(1-4):375–390, 1998.

[48] Ward, P. and Hirst, A.G. *Oithona similis* in a high latitude ecosystem: abundance, distribution and temperature limitation of fecundity rates in a sac spawning copepod. *Mar Biol*, 151:1099–1110, 2007.

[49] Zeldis, J. Mesozooplankton community composition, feeding and export production during SOIREE. *Deep-Sea Res II*, 48:2615–2634, 2001.

8 Manuscript 4

Polar Biol (2006) 29: 1039–1044
DOI 10.1007/s00300-006-0147-0

ORIGINAL PAPER

Sandra Jansen · Christine Klaas · Sören Krägefsky
Lena von Harbou · Ulrich Bathmann

Reproductive response of the copepod *Rhincalanus gigas* to an iron-induced phytoplankton bloom in the Southern Ocean

Received: 3 January 2006 / Revised: 2 April 2006 / Accepted: 3 April 2006 / Published online: 5 May 2006

Abstract The reproductive response of *Rhincalanus gigas* to the build up of a phytoplankton bloom in the Southern Ocean was studied during the European iron fertilization experiment (EIFEX). Egg production experiments were conducted over a period of approximately 5 weeks during development of a diatom dominated bloom. *R. gigas* showed a clear response to increasing chlorophyll *a* concentrations and the total egg production of the *R. gigas* population was highest just after the peak of the bloom at day 29 after fertilization. The average peak production was 50 eggs female^{-1} day^{-1}. The percentage of egg producing females increased from about 0 to 90% during the course of the experiment. Accordingly, the maturation of the gonads reflected the positive response towards enhanced chlorophyll *a* concentrations. The fast reproductive response indicate that *R. gigas* was food limited during the period of this study in the Antarctic Polar Front region (APF).

Introduction

The Southern Ocean is known as a high nutrient—low chlorophyll (HNLC) ecosystem where production is generally low, even though macronutrients like nitrate and phosphate are available all year round (Martin et al. 1990). In recent years, it has been shown that primary production in the Southern Ocean is limited by iron availability (Martin et al. 1990). Large scale artificial iron fertilization experiments of HNLC waters have induced phytoplankton blooms (e.g. Boyd et al. 2000; Gervais et al. 2002; Coale et al. 2004). Copepods dominate the zooplankton communities of the Southern Ocean in terms of numbers and biomass (Voronina 1998; Pakhomov et al. 2000), but our understanding of copepod population dynamics in this area is still poor. As a consequence of the short growth season and low primary production, zooplankton growth and reproduction in the Southern Ocean may be limited by food availability. A productive area within the Southern Ocean is associated with the Antarctic Polar Front (APF) where blooms are frequently reported (Laubscher et al. 1993). In the Atlantic sector of the APF *Rhincalanus gigas* is one of the most abundant large copepod species (e.g. Ommanney 1936; Atkinson 1991; Pakhomov et al. 2000), and is known to have a protracted period of recruitment through the summer into the autumn (Ommaney 1936). In recent years it has become more and more apparent, that growth and development of populations of large calanoid copepods within the Southern Ocean depend on the availability of food (Ward and Shreeve 1999; Shreeve et al. 2002). However, most of the reported studies give only snapshot results where temporal development is not taken into consideration.

The European iron fertilization experiment (EIFEX) provided an unique opportunity to follow the reproductive response of *R. gigas* during the entire development of a diatom dominated phytoplankton bloom. This Lagrangian type experiment made it possible to study the same zooplankton assemblage for 38 consecutive days, which has so far not been achieved for the Southern Ocean.

S. Jansen (✉) · C. Klaas · S. Krägefsky · L. von Harbou
U. Bathmann
Alfred Wegener Institute for Polar and Marine Research,
Am Handelshafen 12, 27570 Bremerhaven, Germany
E-mail: sjansen@awi-bremerhaven.de
Tel.: +49-471-48311442
Fax: +49-471-48311049

Material and methods

Study location

The iron fertilization experiment EIFEX was carried out during austral autumn (21 Jan 2004–25 Mar 2004) in the Atlantic sector of the Southern Ocean on *RV* Polarstern. We choose a cyclonic eddy (extending over

60 × 100 km) for our experiment, embedded in a meander of the APF and centred at approximately 49.5°S and 02°E (Strass et al. 2005). On the 10th of February the centre of this eddy was marked with a drifting buoy and an area of 150 km^2 around the buoy was fertilized with seven tons of iron sulphate solution ($FeSO_4$). The first indication of algal response to iron enrichment was a small but detectable increase in the photosynthetic efficiency (F_v/F_m) after about 24 h (Röttgers et al. 2005). On board measurements of in situ phytoplankton F_v/F_m and later measurements of the partial pressure of CO_2 (pCO_2) served as markers of the fertilized patch. Sampling was carried out within the eddy, inside and outside the fertilized patch throughout the duration of the experiment (38 days).

Egg production experiments

Net samples from the upper 50 m of the water column were taken with Bongo nets (100 µm mesh size) around dusk. Net catches were diluted in 20 l of surface water. Sub-samples were transferred to a Petri dish and sorted under a binocular. For the egg production experiments, healthy *R. gigas* females were handpicked individually and transferred to 100 ml beakers filled with filtered seawater. The females were incubated individually at in situ temperature in the dark. Depending on how many females were present in the net haul, 12–36 parallel incubations were set up (Table 1). After 24 h, the females were removed from the beakers and eggs in the beakers were counted immediately under the binocular. For each station the average egg production rate was derived using data from all incubations, including those where females did not spawn.

Carbon mass (CM) analyses

Rhincalanus gigas females for carbon analysis were handpicked from additional Bongo net catches (100 µm mesh size; 50–0 m). Females were kept in filtered seawater for 24 h before the carapace length was measured under a binocular. Subsequently, animals were transferred individually onto pre-combusted GFF-filters and stored at −80°C. Back on land, samples were dried overnight at 60°C and analysed for carbon and nitrogen on a C/N-Analyser (Carlo Erba NA-1500).

Maturation of the gonads

Zooplankton was sampled using a Mulitnet (100 µm mesh size) at five depth intervals: 400–160, 160–100, 100–50, 50–25 and 25–0 m, respectively. The samples were preserved in buffered formaldehyde (4% final concentration) and stored at 4°C until further analysis. Between 40 and 60 *R. gigas* females from selected stations were examined to determine the stage of the ovarian development. Stations were selected to give good temporal coverage, irrespective of the time of the day at capture. Gonad maturation stages can be established from whole preserved specimens without staining (Niehoff and Runge 2003) in copepods with transparent carapaces. This is the case for female *R. gigas*. Therefore, gonads of whole, unstained animals were studied under a dissecting microscope and five developmental stages (GS) were distinguished (Table 2; modified after Niehoff and Hirche 1996; Niehoff and Runge 2003).

Results

Before fertilization near-surface (8 m depth) chlorophyll *a* distribution in the eddy was patchy with concentrations ranging from 0.5 up to 1.2 µg chlorophyll *a* l^{-1}. During the course of the experiment samples outside the fertilized patch showed high variability with chlorophyll *a* values ranging from 0.3 µg l^{-1} up to about 1 µg l^{-1}. Inside the fertilized patch, chlorophyll *a* concentrations increased and maximum integrated values (0–100 m depth) were found around day 30. Because of the patchy chlorophyll *a* distribution within the eddy, clear differences between in-patch and out-patch values were not observed until about day 10 after fertilization when in-patch chlorophyll *a* concentrations exceeded those found outside the fertilized patch. Throughout the experiment the phytoplankton assemblage was dominated by chain-forming (*Chaetoceros* spp., *Fragilariopsis kerguelensis*, *Pseudo-nitzschia* spp.) and large single

Table 1 Mean (± SE) egg production rates (EPR) of *Rhincalanus gigas* inside and outside the fertilized patch (out). Station numbers are given with corresponding average chlorophyll *a* concentrations over the upper 60 m of the water column (mg m^{-3}). *n* number of incubated females

Station	*t* (day after fertilization)	Chl *a*	*n*	Mean EPR ± SE
424	0	0.76	20	0
508	10	1.7	36	23.7 ± 3.6
513	15	1.97	12	28 ± 8.1
514 out	17	0.61	12	0
544	23	2.45	20	22 ± 5.4
560	29	2.7	18	49.8 ± 10
561 out	29	1.02	20	0.3 ± 0.3
579	32	1.65	20	15.4 ± 4.3
593	36	2.05	15	8 ± 4.8

Table 2 Classification of the gonad developmental stage (GS) based on macroscopic criteria, modified for *Rhincalanus gigas* after Niehoff and Hirche (1996) and Niehoff and Runge (2003)

GS 1	Oocytes present in the ovary; oviduct empty or only with single, transparent, small oocytes
GS 2	Transparent oocytes in the oviduct in one or maximal two layers
GS 3	Transparent oocytes in the oviduct in several layers; all oocytes similar in size; no nucleus visible
GS 3.5	Oocytes in the oviduct in several layers, all similar in size; ventral row with visible nucleus, but still transparent
GS 4	Several rows of oocytes in the oviduct; oocytes increase in size in ventral direction, ventral row is larger, darker and with visible nucleus

celled diatoms (*Thalassiothrix antarctica*, *Corethron inerme*, *Proboscia* spp., *Rhizosolenia* spp.; P. Assmy, personal communication).

Temperature profiles taken inside and outside the fertilized patch over the duration of the experiment indicated that the mixed layer often extended down to 100 m, temperatures between 3.5 and 4.5°C were stable within the nearly closed eddy circulation (V. Strass, personal communication).

Egg production and CM analyses

Figure 1 shows the egg production rates of *R. gigas* over the course of the experiment. First measurements were conducted at the time of iron release and represent conditions before fertilization. *R. gigas* did not produce eggs at this time. Egg production and the proportion of egg producing females increased significantly inside the fertilized patch with increasing chlorophyll *a* concentrations (Table 1). At day 29 after fertilization an average of 50 eggs female^{-1} day^{-1} were produced, with about 90% of the incubated females producing eggs. The highest individual egg production rate (153 eggs female^{-1} day^{-1}) was also observed at day 29 after fertilization. Outside the fertilized patch, the number of egg producing females as well as egg production rates remained close to zero (Fig. 1, Table 1).

Carbon content of *R. gigas* varied considerably from 220 to 1,780 µg C female^{-1} (Table 3). The mean carbon content of the females did not change significantly over the course of the fertilization experiment (ANOVA: $F = 6.22$, $P = 0.067$), although a slight increase in carbon content was observed.

Maturation of the gonads

The proportion of females in the different gonad developmental stages (GS 1–GS 4) is shown in Fig. 2. The corresponding integrated chlorophyll *a* values for the upper 100 m of the water column are indicated. Until day 12 after fertilization, females in all GS were present in changing proportions with no significant difference between in- and out-patch stations. From day 16 on, about 90% of the *R. gigas* females were in GS 4 at all in-patch stations. In the out-patch stations the relative contribution of GS 4 females remained low (about 10%).

Discussion

Several studies have examined the relationship between reproduction of *R. gigas* and chlorophyll *a* as an indicator of food availability. Published results show high variability in the correlation between egg production rates and surface chlorophyll levels (Ward and Shreeve 1995; Ward et al. 1996; Shreeve et al. 2002). However, although chlorophyll *a* concentration may represent actual food availability it does not give information on past feeding conditions or food quality. Hence, interpretation of the correlation found in previous studies can be problematic. The EIFEX cruise presented an unique opportunity to study the complete build up of a phytoplankton bloom with the corresponding reproductive response of the copepods investigated.

Egg production in relation to food

Although maturing females require food supply for oocyte maturation and egg production, some studies have shown that temperature rather than food controls egg production rates for different species (e.g. Kiørboe et al. 1988; White and Roman 1992). Our survey of the reproductive response of copepods within an iron fertilized patch and non-fertilized water in a nearly closed eddy allows us to separate the temperature effect from that of food supply. Temperature changes were only minor during the experiment (± 1°C) and the temperature field was the same within the eddy. During the present study, females started to produce eggs within the fertilized patch and egg production rate increased concurrent with increasing chlorophyll *a* concentrations (Fig. 1a). In contrast, at the two out-patch stations where female *R. gigas* could be obtained for egg production experiments, chlorophyll *a* values and egg production remained low (Table 1, Fig. 1a). The average egg production of *R. gigas* during the course of the experiment showed a significant positive relationship with chlorophyll *a* concentrations ($r^2 = 0.714$; $P < 0.005$; Fig. 1b). Although the present study was a Lagrangian experiment, some of the *R. gigas* sampled may have just recently turned into adult females or immigrated into the patch (S. Krägefsky, unpublished data). Both factors could affect the correlation between egg production rates and chlorophyll *a*, and may lead to the relatively high variability observed between and within each station (Fig. 1b).

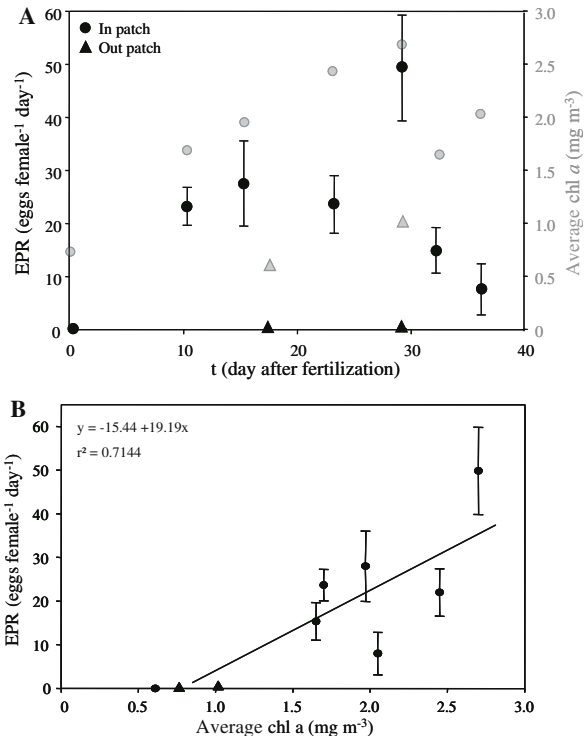

Fig. 1 Mean (± SE) egg production rates (EPR) of *Rhincalanus gigas* after iron fertilization, **a** inside the fertilized patch (*black circles*) and outside the fertilized patch (*black triangles*), with corresponding average chlorophyll *a* concentrations over the upper 60 m of the water column (*grey symbols*). **b** Mean (± SE) egg production rates (EPR) of *Rhincalanus gigas* in relation to the average chlorophyll *a* concentration (0–60 m). Regression line fitted ($P < 0.005$)

In this study we found no saturation level for egg production rate as a function of chlorophyll *a*. It is therefore possible that with even higher chlorophyll *a* the egg production rate may exceed the maximum of ~50 eggs female^{-1} day^{-1}. Indeed, the highest daily egg production rate by a single female was 153 eggs female^{-1} day^{-1}, exceeding the number of ripe eggs counted in preserved females with full oviducts. Consequently, under conditions of abundant food supply, the spawning cycle may take even less than 24 h. This has also been observed for another Antarctic copepod species, *Calanoides acutus*, during a study in Gerlache Strait (Lopez et al. 1993). Assuming a carbon content of 420 ng C per egg (Ward and Shreeve 1999) and an egg production rate of 153 eggs female^{-1} day^{-1}, this corresponds to a daily rate of 5–11% of measured body carbon for day 29 after fertilization. The high variability in the carbon content of adult females found in this study is within the range given by Shreeve et al. (2002; 288–1,791 µg C female^{-1}). Given the high variability of results and the small amount of samples analysed, no significant changes in body carbon could be found during this study.

Gonad maturation with increasing chlorophyll *a* concentration

Different gonad stages for *R. gigas* were already described and illustrated by Ommanney (1936). Similar to the increase in egg production rates, gonad maturation took place concurrent with increasing chlorophyll *a* concentrations (Fig. 2). Females in GS 4 were also found at the beginning of the fertilization experiment and at the out-patch stations which may indicate favourable past feeding conditions for these animals. Consequently, no significant differences between the stages of gonad development between in- and out-patch were found until day 12 (Fig. 2). In contrast, the out-patch station at day 17 after fertilization and all following days show significant differences in *R. gigas* gonad development compared to the in-patch stations where almost all females were found in GS 4. The fact that all other GS stages were more or less absent in the in-patch stations after day 17, show that it took at most 1 week for *R. gigas* to use the increasing food availability during the present study for the completion of the gonad maturation.

The reproductive flexibility of *R. gigas* depending on food conditions, as shown in this study, can be seen as a behavioural response to the episodic and patchy food supply in the Southern Ocean environment.

Table 3 Carbon and nitrogen analyses of *Rhincalanus gigas* females during the European iron fertilization experiment (EIFEX)

Station	*t*	Carapax length (µm)	CM (µg)	C:N	*n*
424	0	7,140 (6,720–7,600)	245 (220–267)	3.97 (3.71–4.16)	4
508	10	7,965 (6,743–10,600)	1,034 (636–1,656)	4.89 (2.67–6.79)	23
513	16	7,400 (6,560–8,080)	790 (352–1,780)	6.43 (4.2–9.46)	45
514 out	17	7,300 (6,975–7,518)	760 (519–1,083)	4.38 (3.17–5.95)	5
544	22	6,975 (6,433–7,363)	847 (657–906)	4.82 (4.25–5.73)	6
560	29	7,380 (7,200–7,500)	877 (576–1,218)	4.77 (3.62–5.62)	5
579	33	7,392 (6,975–7,750)	1,102 (899–1,399)	5.13 (4.56–5.73)	8

Mean values of the carapace length, carbon mass (CM) and carbon to nitrogen mass ratio (C:N) are shown, with their range in parentheses
n number of analysed individuals, *t* number of days after the first iron addition

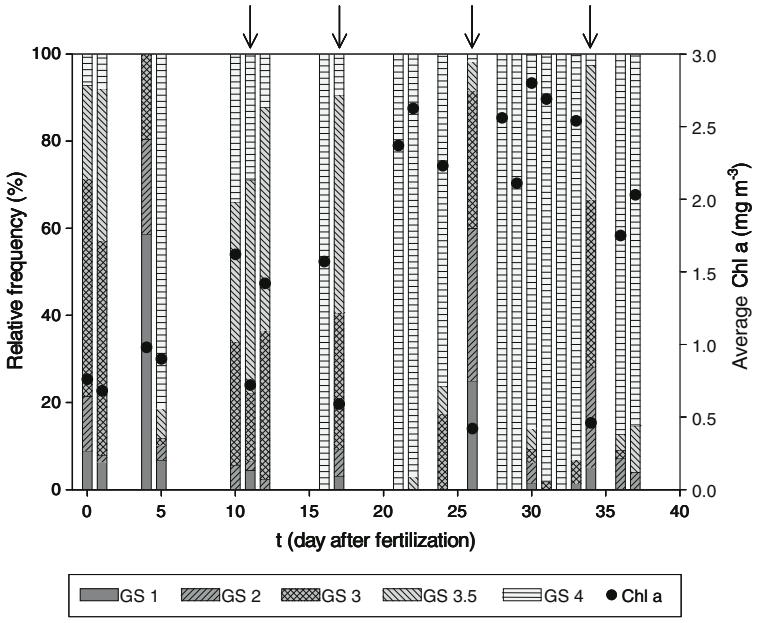

Fig. 2 Percent composition of *Rhincalanus gigas* female population gonad development stages (GS) from multinet samples with corresponding average chlorophyll *a* concentrations over the upper 100 m of the water column (*black dots*). *Arrows* mark the out-patch stations

Acknowledgements We would like to thank the captain and the crew of the RV "Polarstern" for their support. T. Stadtlander helped with the zooplankton collection during the cruise. M. Schmidt and A. Terbrüggen helped with Chl *a* analysis. C/N values from station 424 and 513 were provided by S. Kruse. Helpful comments by V. Smetacek, C. Wexels Riser, B. Niehoff and two anonymous referees are highly appreciated.

References

Atkinson A (1991) Life cycles of *Calanoides acutus*, *Calanus simillimus* and *Rhincalanus gigas* (Copepoda: Calanoida) within the Scotia Sea. Mar Biol 109:79–91

Boyd PW, Watson AJ, Law CS, Abraham ER, Trull T, Murdoch R, Bakker DCE, Bowle AR, Buesseler KO, Chang H, Charette M, Croot P, Downing K, Frew R, Gall M, Hadfield M, Hall J, Harvey M, Jameson G, LaRoche J, Liddlcoat M, Ling R, Maldonado MT, McKay RM, Nodder S, Pickmere S, Pridmore R, Rintoul S, Safl K, Sutton P, Strzepek R, Tanneberger K, Turner S, Walte A, Zeldis J (2000) A mesoscale phytoplankton bloom in the polar Southern Ocean stimulated by iron fertilization. Nature 407:695–702

Coale KH, Johnson KS, Chavez FP, Buesseler KO, Barber RT, Brzezinski MA, Cochlan WP, Millero FJ, Falkowski PG, Bauer JE, Wanninkhof RH, Kudela RM, Altabet MA, Hales BE, Takahashi T, Landry MR, Bidigare RR, Wang X, Chase Z, Strutton PG, Friederich GE, Gorbunov MY, Lance VP, Hilting AK, Hiscock MR, Demarest M, Hiscock WT, Sullivan KF, Tanner SJ, Gordon RM, Hunter CN, Elrod VA, Fitzwater SE, Jones JL, Tozzi S, Koblizek M, Roberts AE, Herndon J, Brewster J, Ladizinsky N, Smith G, Cooper D, Timothy D, Brown SL, Selph KE, Sheridan CC, Twining BS, Johnson ZI (2004) Southern Ocean iron enrichment experiment: carbon cycling in high- and low-Si waters. Science 304:408–414

Gervais F, Riebesell U, Gorbunov MY (2002) Changes in primary productivity and chlorophyll a in response to iron fertilization in the Southern Polar Frontal Zone. Limnol Oceanogr 47:1324–1335

Kiørboe T, Møhlenberg F, Tiselius P (1988) Propagation of planktonic copepods: production and mortality of eggs. Hydrobiologia 167/168:219–225

Laubscher RK, Perissinotto R, McQuaid CD (1993) Phytoplankton production and biomass at frontal zones in the Atlantic Sector of the Southern Ocean. Polar Biol 13:471–481

Lopez MDG, Huntley ME, Lovette JT (1993) *Calanoides acutus* in Gerlache Strait, Antarctica. I. Distribution of late copepodite stages and reproduction during spring. Mar Ecol Prog Ser 100:153–165

Martin JH, Gordon RM, Fitzwater SE (1990) Iron in Antarctic waters. Nature 345:156–158

Niehoff B, Hirche H-J (1996) Oogenesis and gonad maturation in the copepod *Calanus finmarchicus* and the prediction of egg production from preserved samples. Polar Biol 16:601–612

Niehoff B, Runge JA (2003) A revised methodology for prediction of egg production *Calanus finmarchicus* from preserved samples. J Plankton Res 25:1581–1587

Ommanney FD (1936) *Rhincalanus gigas* (Brady) a copepod of the southern macroplankton. Discov Rep 13:277–384

Pakhomov EA, Perissinotto R, McQuaid CD, Froneman PW (2000) Zooplankton structure and grazing in the Atlantic sector of the Southern Ocean in late austral summer 1993: Part 1. Ecological zonation. Deep Sea Res I 47:1663–1686

Röttgers R, Colijn F, Dibbern M (2005) Algal physiology and biooptics. In: Smetacek V, Bathmann U, Helmke E (eds) The expedition ANTARKTIS XXI/3-4-5 of the research vessel Polarstern in 2004. Reports on Polar and Marine Research, 500, pp 82–88

Shreeve R, Ward P, Whitehouse MJ (2002) Copepod growth and development around South Georgia: relationships with temperature, food and krill. Mar Ecol Prog Ser 233:169–183

Strass V, Cisewski B, Gonzalez S, Leach H, Loquay K-D, Prandke H, Rohr H, Thomas M (2005) The physical setting of the European Iron fertilization Experiment EIFEX in the Southern Ocean. In: Smetacek V, Bathmann U, Helmke E (eds) The expedition ANTARKTIS XXI/3-4-5 of the research vessel Polarstern in 2004. Reports on Polar and Marine Research, 500, pp 15–46

Voronina NM (1998) Comparative abundance and distribution of major filter-feeders in the Antarctic pelagic zone. J Mar Syst 17:375–390

Ward P, Shreeve RS (1995) Egg production in three species of Antarctic Calanoid Copepods during austral summer. Deep Sea Res I 42:721–735

Ward P, Shreeve RS (1999) The spring mesozooplankton community at South Georgia: a comparison of shelf and oceanic sites. Polar Biol 22:289–301

Ward P, Shreeve RS, Cripps GC, Trathan PN (1996) Mesoscale distribution and population dynamics of *Rhincalanus gigas* and *Calanus simillimu*s in the Antarctic Polar Open Ocean and Polar Frontal Zone during summer. Mar Ecol Prog Ser 140:21–32

White JR, Roman MR (1992) Egg production by the calanoid copepod *Acartia tonsa* in the mesohaline Chesapeake Bay: the importance of food resources and temperature. Mar Ecol Prog Ser 86:239–249

9 Manuscript 5

Gut content analyses of three dominant Antarctic copepod species during an induced phytoplankton bloom (EIFEX)

S. Kruse[1*], S. Jansen[1], S. Krägefsky[1],U. Bathmann[1]

Alfred Wegener Institute for Polar and Marine Research, Am Handelshafen 12, 27570 Bremerhaven, Germany

The diet of three Antarctic copepods, *Calanus simillimus*, *Rhincalanus gigas* and *Pleuromamma robusta*, was studied from samples collected during the European iron fertilization experiment (EIFEX) in austral autumn 2004. The diet has been investigated by microscopical gut content analysis. The food spectra of the three copepod species showed a clear overlap. The pennate diatom *Fragiliariopsis kerguelensis* was commonly found in all guts. A high amount of cells was fractured, but some were found complete when arranged as chains. The same was true for the genus *Chaetoceros*, a centric diatom, of which even their long and complete setae as well as some apparently intact cells could be observed. In general the ingested food particles extented over a wide size range up to a few hundred mm. The copepod *C. simillimus* e.g. fed on large foraminiferans and swallowed them as a whole. However, *P. robusta* was the protozoan feeding species among the copepods under investigation. This copepod ingested a higher diversity of hard shelled protozoans

*Corresponding author: Svenja.Kruse@awi.de

including tintinnids, radiolarians and acantharians, whereas the gut content of *C. simillimus* and *R. gigas* was mainly diatom dominated.

1 Problem

The Southern Ocean is known as a high nutrient-low chlorophyll (HNLC) ecosystem. Despite the availability of essential macronutrients like nitrate and phosphate the primary production is low. In recent years, several iron fertilization experiments elucidated the crucial role of iron as limiting factor of primary production in the Southern Ocean (e.g. Boyd et al. 2000, Coale et al. 2004). Since copepods dominate the zooplankton community of the Southern Ocean in terms of number and biomass (Pakhomov et al. 2000), they are one of the main consumers of a phytoplankton bloom. To accomplish times of phytoplankton shortage, Antarctic copepods may switch to a more omnivorous (Froneman et al. 1996) or even carnivorous diet (Pasternack & Schnack-Schiel 2001a). Especially during the winter months the pelagic copepods of the Southern Ocean have to cope with harsh environmental conditions and must therefore adjust their life cycle strategies to the highly seasonal primary production. The diet of Antarctic copepods have yet been studied by analyzing gut contents (Pasternack & Schnack-Schiel 2001a), and by measuring feeding rates using gut fluorescence (e.g. Atkinson et al. 1992, Drits et al. 1993, Pasternack et al. 1994). Moreover, grazing experiments and studies on feeding selectivity have been conducted (Perissinotto 1992, Atkinson 1994, Schultes et al. 2006) to provide information on the trophic relations in the copepod community of the Southern Ocean. Beyond this general framework of trophic relations, more and more studies focused on the responses of copepods to environmental variability during the last decade (e.g. Pasternack & Schnack-Schiel 2001b, Schultes et al. 2006). However, less attention has been paid to the qualitative aspects of the ingested food, which is important to understand the feeding behavior and the usability of prey by copepods.

The European iron fertilization experiment (EIFEX) provided therefore the opportunity to have a look at the diet composition and on the food item quality under two different environmental conditions. The main focus will lie on the quality of the food particles ingested by the three abundant copepod species *Calanus simillimus*, *Rhincalanus gigas* and *Pleuromamma robusta*.

2 Material and Methods

2.1 Study location and iron fertilization

The European in situ iron fertilization experiment EIFEX was carried out in the Atlantic Sector of the Southern Ocean (∼49° S, 2° E) during the cruise ANT XXI/3 of RV Polarstern from late austral summer to early austral fall (21.01.–25.03.2004, Bathmann 2005). A cyclonic eddy was chosen as experimental site to follow the development of an iron induced phytoplankton bloom. The center of the eddy was marked with a drifting buoy and an area of 150 km^2 around the buoy was fertilized twice with seven tons of iron sulphate solution ($FeSO_4$). The developing plankton bloom was followed by monitoring photosynthetic efficiency (Fv/Fm), pCO_2 and derived Fe measurements (Smetacek et al. 2005, Cisewski et al. in press). In response to the iron fertilization, a diatom dominated bloom developed. The chlorophyll *a* (Chl *a*) concentrations in the cyclonic eddy were constantly higher than at the stations outside the patch (Hoffmann et al. 2006). During the course of the experiment the Chl *a* concentration increased in the fertilized area more than fivefold. 26 days after fertilization a peak value of 2853 ng Chl *a* L^{-1} was reached. A significant differentiation of "in patch" and "out patch" on the basis of Chl *a* was possible after day 10 of fertilization.

2.2 Copepod sampling

Sampling of copepods was performed inside and outside the fertilized patch throughout the duration of the experiment (Tab. 1). The samples for gut content were taken during night with a bongo net of 500 μm mesh size at eight stations in the upper 50 m of the water column. On deck, the net catch was diluted in 10 L of surface water. A subsample was directly concentrated on mesh (100 μm) and immediately stored at -80° C for later analysis. The time span between the net retrieval and the freezing of the samples never exceeded five minutes.

2.3 Gut content analysis

In the home laboratory, *Calanus simillimus*, *Rhincalanus gigas* and *Pleuromamma robusta* CV and females from the frozen samples were analyzed regarding their gut content. Diet components were obtained through microscopic analysis. Therefore, the frozen samples were carefully flushed down the mesh and washed with filtered

sea water (0.7 μm filter pore size) in order to remove the phytoplankton attached to the animals. Individual copepods were then identified to developmental stage, and placed in iced petri-dishes. The subsequent dissection of the copepod gut was conducted under a constant temperature of 0° C to slow down the melting process. The gut was separated from the surrounding tissue, then carefully squished and the content was transferred to a counting chamber according to Utermöhl (1958). The gut content settled over night at room temperature. Particles were identified and counted, using inverted light microscopy (Zeiss, Axiovert 135, 200 – 400 times magnification). Complete and broken food items were listed separately. Generally, all food items larger than 5 μm were counted and identified if possible.

2.4 Scanning Electron Microscopy

High numbers of copepods in the sample caught at station 513 (16 days after first iron addition) allowed examination of individual copepod gut contents by means of scanning-electron-microscopy (SEM). Therefore, guts were dissected as described before. Samples were then prepared as described in Wexels Riser et al. (2003).

3 Results

3.1 Gut content composition

Generally, 92% of all food fragments identified within the analyzed copepod guts comprised of diatoms (Fig. 1), with pennate diatoms and their fragments as the most frequent items. The number of non-diatom components adds with a maximum of 9% to the average gut content. Nineteen different genera and species of pennate diatoms and twenty species of centric diatoms were found and determined in the guts of the three copepod species investigated (Tab. 2, 3). As identifiable non-diatom components, eight different tintinnid species, some radiolarians, dinoflagellates, silicoflagellates, foraminiferans and acantharians were found in the copepod guts (Tab. 4).

Remarkably, within all copepod guts analyzed, the diatom *Fragilariopsis kerguelensis* was observed, either complete or in fragments (Tab. 1). This pennate diatom is characterized by its heavily silicified frustules. The second most abundant species seen in the copepod guts was the slightly smaler and less silicified *F. rhombica* and/or *F. separanda*, which is generally hard to disdinguish under the light micro-

scope. Namely, 71 to 85% of all individual copepod guts investigated contained this species. The elongated diatom *Pseudonitzschia lineola* has been ingested by a similar percentage of copepods. Among the centric diatoms the discoid *Thalassiosira gracilis* was the most frequently found species, observed in 84 to 89% of all guts analyzed. The fragments of the large cylindrical diatom *Dactyliosolen antarcticus* were identified in about 70% of the copepod guts. All other centric diatoms occurred in less than 50% of the individuals.

Within the non-diatom fraction, the rounded cells of the dinoflagellate *Prorocentrum sp.* and the hexagonal-shaped silicoflagellate *Dictyocha speculum* were counted at highest rates. Tintinnids, radiolarians, foraminiferans and acantharians were less frequently found food components.

Besides these similarities, there were distinct differences between the three copepod species. A comparatively lower amount of *C. simillimus* individuals ingested the four pennate diatom species of the genus *Pseudonitzschia*. Except the species *P. prolongatoides*, 18% less individuals of *C. simillimus* ingested this genus compared to *R. gigas* and *P. robusta*. The same applies to the lanceolate species *Navicula sp.*, the centric diatoms *Thalassiosira lentiginosa* and *Rhizosolenia sp.* The needle-like pennate diatom *Thalassiothrix antarctica* was not represented at all in the guts of *C. simillimus*. Among the protozoans, tintinnids occurred less frequently whereas complete radiolarians of the group Polycystina as well as acantharians were absent.

Differences in the pennate diatom uptake between the copepod species were represented by the species *Cylindrotheca closterium* and the group of Membraneis and Manguinea, which were consumed by a higher number of individuals of *R. gigas*. Furthermore *R. gigas* was the only copepod which fed on the three spiny *Chaetoceros* species *C. convolutus*, *C. criophilus* and *C. debilis*, although to a low extent (1 to 3% of total diatoms consumed). Tintinnids were more frequently found in *R. gigas* guts than in *C. simillimus*. This was especially true for the two tintinnid species *Codonellopsis pusilla* and *Stenosomella sp.* In this aspect *R. gigas* even outcompetes *P. robusta*.

P. robusta is the copepod species which can be best distinguished from the two other copepod species in terms of gut content. It shows the highest occurrence frequency of several diatom and non-diatom species. Among the pennates *F. obliquecostata*, *Thalassionema nitzschoides* and *T. n. var. lancolatum* as well as *Haslea sp.* were frequently found. The centric diatoms *Thalassiosira oliverana*, *T. bulbosa* and *Actinocyclus sp.* were observed at comparatively higher percentages as well. *Thalassiosira tumida* and *Asteromphalus hookeri* were exclusively found in *P. robusta*

guts. However, *P. robusta* was the only species where neither *Chaetoceros aequatorialis* nor *C. peruvianus* were found in the gut. Compared to the two other copepod species, complete *Chaetoceros* cells occurred generally less frequently in *P. robusta*. Every second gut of *P. robusta* contained the bowl cap-shaped tintinnid *Cymatocylis calyciformis*, every third radiolarian fragments and every fifth dinoflagellate fragments and complete foraminiferans. The group Phaeodaria within the radiolarians has only been observed in the guts of *P. robusta*. Moreover the dinoflagellate *Protoperidinium* occurred at a higher percentage in this copepod species than in *C. simillimus* and *R. gigas*.

3.2 Food item condition

A small number of food items in the copepods' guts like the diatom *Dactyliosolen* could be observed only fragmented or in case of the foraminiferans only complete. However, most of the diatom and non-diatom food could be found either complete or broken (Tab. 5). Comparing the fertilized and unfertilized situation, there seems to be a slightly, but not significant difference between the ratio of broken components to complete cells/specimens. Outside the fertilized patch a larger proportion of ingested food was fragmented. There were 8% more broken pennate diatoms outside than inside the fertilized area in *C. simillimus* guts. Centric diatom fragments in the guts of *R. gigas* were even 13% more abundant in the unfertilized area (26% compared to 39%). Furthermore for *R. gigas* the ratio of fragments to complete cells/specimens was the largest for centric diatoms. In general only few centric cells (< 5 %) were complete compared to the pennates ($> 20\%$) in all *R. gigas*' guts analyzed.

Overall there were no distinct differences concerning the condition of ingested diatoms between the three copepod species. In terms of diatom ingestion the feeding preferences can be generalized in the following for all copepods investigated. However, some differences among the non-diatom food shall be highlighted, thereafter.

3.2.1 Pennate diatoms

Of all food items, the pennate diatom *Fragilariopsis kerguelensis* was most frequently found as mentioned before. A remarkable number of complete chain-forming cells of this species could be observed in the guts (Fig. 3E). The same applied to other *Fragilariopsis* species like *F. rhombica* and the genera *Pseudonitzschia* (Fig. 3A), of which broken and complete single cells were found. *Pseudonitzschia* was also often found in chains of two or three cells. *F. kerguelensis* often exceeded ten cells

building one chain in the guts. Of the remaining *Fragilariopsis* species mostly single cells were observed, although all species usually occur in chains within the water column. Due to the high degree of fragmentation, some of the *Fragilariopsis* pieces could not be related to certain species. The species *Thalassiothrix antarctica* was always fragmented, whereas the smaller genus *Thalassionema* was also found in its full length. The genera *Cylindrotheca*, *Navicula* as well as *Haslea*, *Membraneis* and *Manguinea* were always complete in the guts or at least no fragments could be assigned to them.

3.2.2 Centric diatoms

Complete single cells of the centric diatom *Chaetoceros* were only rarely found. Exceptions are the species *C. aequatorialis*, *C. bulbosus*, *C. criophilus* and *C. peruvianus* which only appeared as single cells or in short chains, although even these species were often fragmented. In most of the cases *C. dichaeta* and *C. atlanticus* were only intact when ingested as a chain of two to five cells (Fig. 3B), most likely snaped off a longer chain. Even the setae of some *Chaetoceros*-chains were then complete. However, there was still a high proportion of broken *Chaetoceros* cells. Broken cells of *C. dichaeta* or *C. atlanticus* occurred twice as much as complete cells in the guts of *R. gigas*. Moreover, the gut content of *C. simillimus* contained some optical intact cells of the discoid diatom *Thalassiosira lentiginosa* with full cell content (Fig. 3D). *P. robusta* ingested sparse cells of *T. oliverana*, carrying even intact looking chloroplasts. A main characteristic of the genus *Thalassiosira* is colony formation by threads, but only single cells occurred in the guts. *Dactyliosolen antarcticus*, *Corethron pennatum* and *Rhizosolenia sp.* as well as the aforementioned pennate diatom *Thalssiothrix antarctica* belong to the largest diatoms being ingested. Except for *Corethron pennatum* these cells are all elongated and can reach a length of up to several hundreds μm. The three large centrics were eaten by all three copepod species, but fragmented into small pieces. As not only *Asteromphalus sp.* was more frequently found broken than complete, a high amount of broken centrics could be observed overall in the guts, hiding numerous cells of the genera *Thalassiosira* and *Actinocyclus* (Fig. 2C, D, E).

3.2.3 Non-diatom food

In addition to diatoms, in particular tintinnids were identified in considerable numbers as complete individuals, but also as fragments. The largest tintinnid being

ingested was *Cymatocylis calyciformis* with a size of up to 520 μm and only the aboral horn was left in some cases. *Prorocentrum sp.* was ingested by all copepod species and was the best-preserved dinoflagellate found in the guts. Nevertheless there were some differences. Unbroken foraminiferans and silicoflagellates occurred more often in the guts of *P. robusta* than in the ones of *C. simillimus* and *R. gigas*. Acantharians (Fig. 3F) were observed mostly in the guts of *P. robusta*, as well as a couple of complete radiolarians (Fig. 3G). If the foraminiferans and radiolarians were found complete, their outer appearance, i.e. condition and colour, led to the conclusion, that they must have been still alive after ingestion. However, the radiolaria Phaeodaria was only intact in *P. robusta*. The only acantharian found in a *R. gigas*' gut was in a bad state as most of its spines were broken. In *C. simillimus*' and *R. gigas*' guts only fragments of radiolarians could be counted.

4 Discussion

Copepods are known to feed on a high variety of food from small suspended particles to zooplankton of equal size (Verity & Smetacek 1996). Observations by Atkinson (1994) show maximum filtration rates of small copepods on cells < 100 μm, whereas the large grazers clear the largest cells (usually long diatoms) at maximum rates. All three copepod species investigated comprised a broad range of pennate and centric diatoms as well as protozoan species in their guts. As the gut content analysis is based on hard shelled remains, this method can therefore only give information on the identifiable components of the diet, particularly diatoms. As already mentioned by Marshall (1973) soft bodied organisms or those without a skeleton were rarely recognized and consequently underestimated. The identification of protozoans in copepod guts is therefore rather difficult, as many protists have soft tissued bodies. However, protists are known to be an important part of the microplankton (Garrison 1991) and may therefore be an important part of the food spectrum of copepods. This can not be determined based on microscopy techniques performed during this study. Therefore, we focused on the qualitative aspects of the hard shelled identified food items within the guts of the three Antarctic copepod species *Calanus simillimus*, *Rhincalanus gigas* and *Pleuromamma robusta* sampled during the induced phytoplankton bloom.

Some food items were commonly found in nearly all copepod guts. The best example for such a food item is the diatom *Fragilariopsis kerguelensis*. Despite their mechanical resistibility (Hamm et al. 2003), a high number of frustules of

F. kerguelensis were broken, which leads to the conclusion that mandibles of the adult and subadult larger copepods are hard enough to break even this heavily silicified diatom frustules. Such mechanism of evolving fortification and evolution in breaking mechanics is named "arms race" in the plankton (Smetacek 2001). Nevertheless a remarkable number of complete single and chain-forming cells of this species could be observed in the guts. Jansen & Bathmann (2007) made the same observation, as they found broken and complete cells in copepod faecal pellets. These authors concluded therefore that the combination of chain forming and strong frustules may protect against destruction of cells. Chains of up to ten cells and more were not unusual food items in the guts. In the water column most chains consist of up to ten cells, fewer of even up to 60 cells (Julia Hager personal communication), assuming that chains were not fractured due to the applied sampling method (Niskin bottles). Therefore we assume that a complete chain could be ingested by the copepods under investigation, however a high portion might be bitten off from a longer chain.

Pseudonitzschia was a frequently ingested pennate diatom as well, which has been eaten despite the elongation by chain-forming. A chain of *P. lineola* can easily reach a length of 1000 μm in the water column and is too long to be ingested completely. Therefore the copepods probably bite off parts of a chain, since mainly chains with only two to three cells were detected within the guts. *Pseudonitzschia* and its chains have been found in the guts under fertilized and unfertilized conditions. Furthermore, the cell morphology of some cells of *Pseudonitzschia* and *Thalassiosira* gives an indication that they are still intact within the guts. Several studies reported signs of intact (Bathmann & Liebezeit 1986, Wexels Riser et al. 2003) and even viable (Fowler & Fisher 1983, Jansen & Bathmann 2007) cells in faecal pellets. Fowler & Fisher (1983) reported that it is evident that a variety of different algal species, particularly diatoms, can pass unharmed through the gut of zooplankters. The observed intact and chlorophyll containing cells in this study may resist digestion as well, but a physiological proof is missing.

All three copepods fed on the centric diatom *Chaetoceros*, although *R. gigas* did it to a higher extent than the other two copepod species. Copepods feed on *Chaetoceros* to some degree (Marshall & Orr 1955, Schnack 1979, Pasternack & Schnack-Schiel 2001b), however some studies have shown that it has not been readily ingested due to the spiny setae (Parsons et al. 1967, Hargrave & Geen 1970, Voronina & Sukhanova 1977, Perissinotto 1992). In this study we observed that the genus *Chaetoceros* is part of all copepods' diet, while complete *Chaetoceros* chains seemed to be more

frequently in the guts of the copepods caught in the fertilized region. The spike-like setae seem to be no obstacle, because even optical intact cells with complete setae were ingested (Fig. 3B for *C. simillimus*). It is not clear, whether the setae from *Chaetoceros* species protect these diatoms to some extent from being ingested by copepods. It might be that they act as a protection in case of the two smaller copepod species *C. simillimus* and *P. robusta*. Both copepods did not feed on *C. convolutes*, *C. criophilus* and *C. debilis*. These three *Chaetoceros* species are chain forming and have long setae. Although *C. atlanticus* has also setae of up to 200 μm length, it was eaten completely by *C. simillimus* and *P. robusta*. Consequently it still remains uncertain, whether the setae are really a limiting factor for ingestion.

Findings of complete and apparently intact individuals of foraminiferans in all three copepod species are astonishing, particularly because of their size of a few 100 μm. *C. simillimus* did swallow them as a whole without fragmenting them. Presumably the calcitic and multi-chambered shells were not broken by this copepod's mouthparts. Radiolarians being in the same size range as foraminiferans were never eaten completely by *C. simillimus* and *R. gigas*, although radiolarians have a stable siliceous skeleton. This observation has not been made before. The stability of the prey items does not seem to be decisive in this case. Consequently food uptake or food selection is rather complex and not only depending on one factor. Table 2 and 3 show that there is no pattern between the relation of food item occurrence and cell/specimen size.

Besides size and stability the condition of the food items found within the copepod guts has to be discussed along with the availability of food. The observed lower amount of fragments in copepod guts inside the fertilized area may indicate an increased uptake-frequency of complete cells/specimens when food supply is sufficient. It could be hypothesized that the copepods under investigation reduce the effort spend on handling and processing of a single food item in a food rich environment. This would mean a kind of "superfluous" feeding. There are different opinions on the "superfluous feeding" theory, which has been discussed in detail by Turner & Ferrante (1979): Beklemishev (1962) suggested that the available food may be in excess of that required for nutrition when phytoplankton concentration is high. This could lead to a "superfluous feeding" with reduced assimilation rates. Since several studies (Marshall & Orr 1955, Conover 1966, Butler et al. 1970) did disprove this theory, Steele and Mullin (1977) assumed that it is just a myth.

In our study the fragments of the genera *Pseudonitzschia*, *Thalassionema*, *Thalassiothrix* and fragments of the species *Corethron pennatum*, *Rhizosolenia sp.* and

Cymatocylis calyciformis were not counted due to their high degree of fragmentation and variable fragment size. Therefore the microscopical analysis of gut content can give only limited information on superfluous feeding, as the ratios (fragments/complete cells) are probably underrepresented here and a significant difference between the fertilized and unfertilized area hardly exists, particularly with regard to the pennate diatoms.

4.1 Differences among species

Calanus simillimus has been described as an omnivorous species (Atkinson 1998). However, studies on the food composition of *C. simillimus* and in particular with respect to changes in environmental conditions are scarce. A detailed observation on feeding was conducted in a subantarctic area near South Georgia (Atkinson 1996). It has been suggested that *C. simillimus* prefers protozoans when phytoplankton is limited. Protozoans seem at least to be a welcome additional food source, as these were identified as part of their diet. During an iron induced bloom in 2000 (EisenEX) Schultes et al. (2006) reported from their feeding experiments a diet composition consisting of diatoms, silicoflagellates, heterotrophic dinofalgellates and ciliates for *C. simillimus*. Diatoms were the most important carbon source. However, they showed only little change in food composition in response to the induced phytoplankton bloom.

The number of species like *Pseudonitzschia lineola* (length up to 112 μm) or *Cymatocylis calyciformis* (lorica length 125-520 μm), which were found broken in the guts, indicate that size does play a role during food uptake (ratio broken/complete) in the case of this copepod species. Size might be the reason why *C. simillimus* did not ingest *Thalassiothrix antarctica* in contrast to the two other copepod species. A cell length of up to 5600 μm is limiting in this case, although all copepods are known to feed on a wide size range. However, Schultes et al. (2006) observed *C. simillimus* to be a spezialized harvester of large and carbon rich diatoms during EisenEx. A predator:prey size ratio of 3:1 up to 180:1 (as equivalent spherical diameter) has been observed by several authors (reviewed by Hansen et al. 1994). The optimal particle size ratio for copepods is expected to be 18:1 (Hansen et al. 1994).

R. gigas is generally considered as a herbivorous or omnivorous species (Schnack-Schiel & Hagen 1994), depending largely on season. In spring and autumn (before and after a bloom) diatoms are the main food, although protozoans, crustaceans and detritus are ingested additionally compared to feeding in summer (Atkinson

1998). Hopkins and Torres (1989) described 77 % of phytoplankton and 16 % of protozoans as a characteristical gut content for *R. gigas* in Antarctic autumn. Pasternak and Schnack-Schiel (2001a) observed however, that the contribution of proto- and metazoan prey is negligible in summer and autumn. Schultes et al. (2006) reported a switch in diet composition from mainly heterotrophic prey to diatoms in response to the induced phytoplankton bloom. This dominance of diatoms when food supply is sufficient can be seen in our observations as well. Nevertheless *R. gigas* did feed on hard shelled protozoans. This copepod species ingested spiny and large items like acantharians. The question is, whether *R. gigas* really selected the acantharians, e.g. because of their high carbon content (i.e. to fulfill the nutrient requirements), or whether it was a matter of random grazing. The fact that the morphology of its gnathobases indicates a feeding on both phyto- and zooplankton (Michels & Schnack-Schiel 2005) argues for an intended uptake of protozoans. *R. gigas* fed on large and spiny genera like *Corethron* and *Chaetoceros* in this study as well, whereas the two other copepod species did it to less degree (only half of the copepods in case of *Corethron*).

Pleuromamma robusta showed some differences in its diet compared to the other two species investigated. In contrast to *C. simillimus* and *R. gigas*, *P. robusta* seem to be a more omnivorous species, because of the higher diversity of protozoans and in particular hard shelled protozoans in its guts. Hopkins (1985) already confirmed that diatoms, dinoflagellates and tintinnids are the main food sources for *P. robusta* in late summer and autumn. Although Hopkins also found *Euphausia superba* debris, copepods, coelenterates and *Pelagobia longicimata* in *P. robusta* guts, such remains were not seen during this study. Foraminiferans, radiolarians and acantharians were ingested to a higher proportion compared to the two other copepod species, though. *P. robusta* did feed on a high number of diatoms and showed some differences e.g. in the uptake frequency of the genera *Fragilariopsis* or *Pseudonitzschia*. However, it is the quantity and quality of protozoans within the guts which distinguishes this copepod species clearly from the other two. Especially foraminiferans and radiolarians were well preserved in its guts. In any case it is obvious that this copepod species favors protozoans more than the other two.

4.2 Conclusions

All three copepods under investigation were capable of ingesting similar particles of almost the same size and showed therefore a fair amount of overlap in ingested

prey items. However, each species did also show distinct differences. *Pleuromamma robusta* e.g. fed more frequently on *Thalassiosira oliverana* and *Actinocyclus sp.* than the two other copepod species. Furthermore the diet of *P. robusta* was more characterized by protozoans compared to the other two species under investigation. The spiny *Chaetoceros* cells though were favored by *Rhincalanus gigas*, whereas C. simillimus ingested more or less a bit of everything. The condition of food items, e.g. of the diatoms *Chaetoceros* and *Pseudonitzschia* or the foraminiferans, was most astonishing and raises several new questions in the face of food item selection and feeding behavior.

Overall, the ability to ingest a diversity of food items, ranging from small to large sized particles (Atkinson 1995, Verity & Smetacek 1996), allows the copepods to retrieve all nutritional requirements and consequently to optimize secondary production (Kleppel 1993). Moreover, being able to select a very wide food spectrum might be a necessary adaptation to Antarctic seasonality and therefore to changing food availability.

Acknowledgements

We would like to thank the captain and the crew of the RV "Polarstern" for their support. Many thanks to P. Assmy, J. Henjes and R. Crawford for providing assistance with the identification of diatoms and protozoans and to F. Hinz for helping with the scanning electron microscopy.

Station	Date	t	Time (UTC)	Latitude	Longitude	Depth[m]
424-11	11.02.04	0	22:50	49°24.06'S	2° 15.50'E	155
508-19	22.02.04	10	21:02	49° 12.14'S	2° 0.43'E	50
513-10	27.02.04	16	23:40	49° 35.75'S	2° 4.09'E	50
514-11 out	29.02.04	17	21:25	49° 17.79'S	2° 20.32'E	50
544-41	07.03.04	25	01:38	49° 28.23'S	1° 56.92'E	50
546-17 out	09.03.04	27	22:53	49° 27.61'S	2° 7.59'E	50
587-6 out	17.03.04	35	22:00	49° 31.87'S	2° 6.91'E	50
593-4	20.03.04	38	00:03	49° 27.81'S	2° 26.10'E	50

Table 1: List of stations sampled for gut content analyses and abundance investigations of the copepods *Calanus simillimus*, *Rhincalanus gigas* and *Pleuromamma robusta* during the European Iron Fertilization Experiment (EIFEX). Station number, date and time are shown as well as the position of the station and the sampled depth. t days after first iron addition. Out – location of station outside the fertilization patch.

	C. simillimus	*R. gigas*	*P. robusta*
No. of guts analyzed	**150**	**72**	**46**
Cell size < 80 μm			
Fragilariopsis kerguelensis	99	100	98
F. kerguelensis fragments	100	100	98
F. rhombica/separanda	71	82	85
F. rhomb./sep. fragments	47	56	54
F. ritscheri	16	28	28
F. cylindrus	7	11	15
F. pseudonana	19	25	28
F. fragments	75	75	87
P. prolongatoides	1	6	9
Cell size < 150 μm			
F. obliquecostata	3	6	20
Pseudonitzschia lineola	71	89	96
P. turgiduloides	54	72	80
P. heimii	13	35	30
Navicula sp.	26	49	46
Cell size < 600 μm			
Cylindrotheca closterium	9	21	13
Thalassionema nitzschoides	39	58	78
T. n. var. lanceolatum	5	7	17
Haslea sp.	14	19	30
Membraneis/Manguinea sp.	5	10	2
Cell size 420-5680 μm			
T*halassiothrix antarctica*	0	3	4

Table 2: List of pennate diatoms found in the guts of the copepods *Calanus simillimus*, *Rhincalanus gigas* and *Pleuromamma robusta* during the European Iron Fertilization Experiment (EIFEX). Percentage of all guts/individuals analyzed are shown, in which the diatoms where found. For counting details see material and methods.

	C. simillimus	*R. gigas*	*P. robusta*
No. of guts analysed	**150**	**72**	**46**
Cell size < 80 μm			
Thalassiosira gracilis	84	86	89
T. oliverana	27	26	41
T. bulbosa	6	7	17
Asteromphalus hookeri	0	0	11
A. hyalinus	1	3	7
Asteromphalus fragments	43	40	57
Chaetoceros aequatorialis	1	7	0
C. aequatorialis fragments	1	6	0
C. atlanticus	6	11	4
C. atlanticus fragments	6	22	17
C. bulbosus	0	0	0
C. bulbosus fragments	3	10	7
C. castracanei	0	1	2
C. castracanei fragments	1	3	2
C. convolutus	0	0	0
C. convolutus fragments	0	1	0
C. criophilus	0	3	0
C. criophilus fragments	0	0	0
C. debilis	0	1	0
C. debilis fragments	0	0	0
C. dichaeta	11	26	9
C. dichaeta fragments	15	43	26
C. peruvianus	1	6	0
C. peruvianus fragments	1	7	0
Chaetocersos sp. fragments	8	25	13
Other centric diatoms	7	10	13
Centric diatom fragments	99	99	100
Cell size < 150 μm			
Thalassiosira lentiginosa	17	28	39
T. lentiginosa fragments	7	11	20
T. tumida	0	0	4
Actinocyclus sp.	10	19	48
Dactyliosolen antarcticus fragments	70	71	67
Cell size < 600 μm			
Corethron pennatum	11	29	15
Rhizosolenia sp.	8	24	33

Table 3: List of centric diatoms found in the guts of the copepods *Calanus simillimus*, *Rhincalanus gigas* and *Pleuromamma robusta* during the European Iron Fertilization Experiment (EIFEX). Percentage of all guts analyzed are shown, in which the diatoms where found.

	C. simillimus	*R. gigas*	*P. robusta*
No. of guts analysed	**150**	**72**	**46**
Tintinnids (< 180 μm)			
Codonellopsis gaussi	1	11	9
C. pusilla	9	26	17
Codonellopsis sp.	0	1	0
Cymatocylis antarctica	7	18	13
C. calyciformis (< 520 μm)	7	29	48
Acanthostomella norvegica	7	15	22
Stenosemella sp.	3	15	9
Salpingella sp. (< 250 μm)	3	7	4
Tintinnid fragments	9	17	22
Other ciliates	2	3	13
Radiolarians (< 100 μm)			
Phaeodaria	0	0	9
Polycystina	0	0	11
Radiolarian fragments	13	4	30
Dinoflagellates			
Prorocentrum sp. (< 80 μm)	63	58	63
Protoperidinium sp. (< 150 μm)	5	4	15
Mesoporus perforatus (ca. 21 μm)	2	6	2
Other dinoflagellates	8	17	20
Dinoflagellate fragments	5	13	20
Silicoflagellates			
Dictyocha speculum (< 80 μm)	59	61	76
D. speculum fragments	57	78	61
Foraminiferans (< 180 μm)	5	3	20
Acantharians (< 150 μm)	0	3	7

Table 4: List of protozoans found in the guts of the copepods *Calanus simillimus*, *Rhincalanus gigas* and *Pleuromamma robusta* during the European Iron Fertilization Experiment (EIFEX). Percentage of all guts analyzed are shown, in which the protozoans where found.

	Pennate diatoms	Centric diatoms	Non-diatoms
Complete	*Cylindrotheca*		Ciliates (without tintinnids)
	Navicula		Foraminiferans
	Haslea		Acantharians
	Membraneis/Manguinea		
Complete and	*Fragilariopsis*	*Thalassiosira*	Tintinnids
Fragmented	*Pseudonitzschia*	*Asteromphalus*	Radiolarians
	Thalassionema	*Actinocyclus*	Dinoflagellates
		Chaetoceros	Silicoflagellates
Fragmented	*Thalassiothrix*	*Corethron*	
		Dactyliosolen	
		Rhizosolenia	

Table 5: List of food items, which were found complete, complete and fragmented or only fragmented in the guts of the copepods *Calanus simillimus*, *Rhincalanus gigas* and *Pleuromamma robusta* during the European Iron Fertilization Experiment (EIFEX).

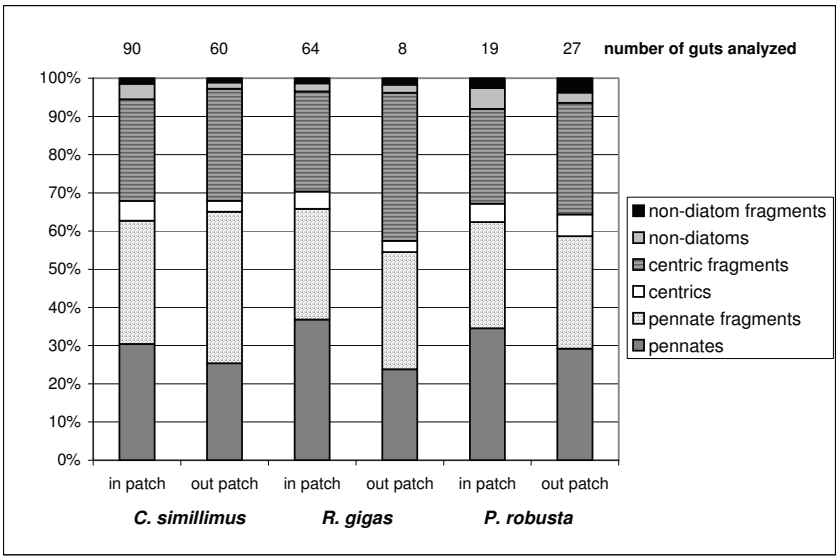

Figure 1: Mean diet composition of the three copepod species analyzed. "In patch" presenting the data in the fertilized area and "out patch" outside this area.

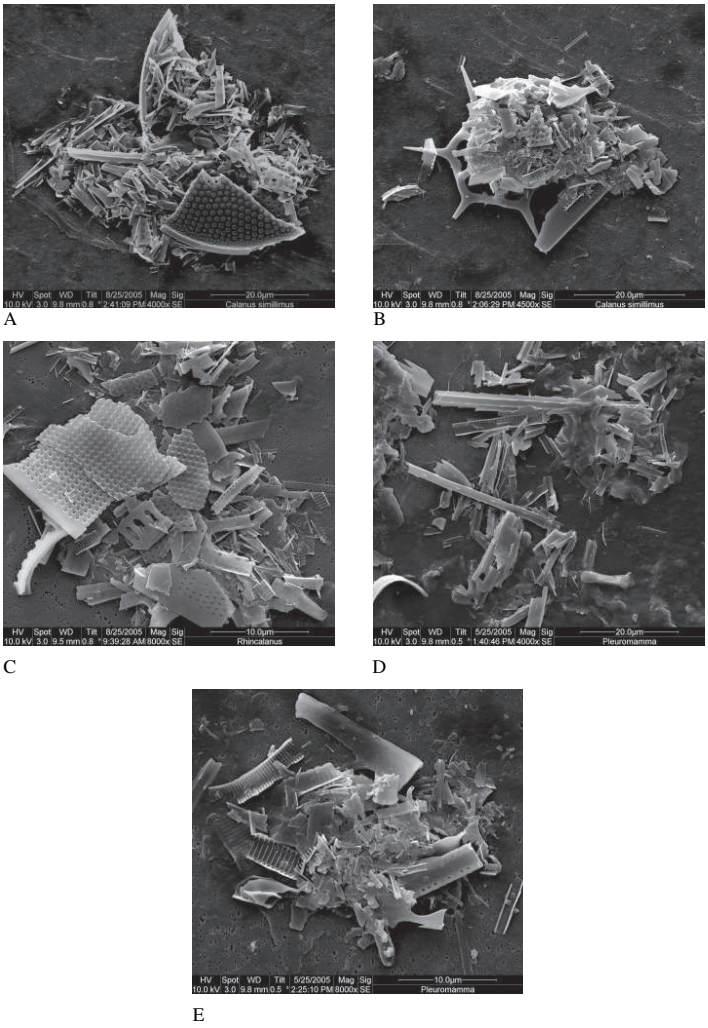

Figure 2: Scanning electron micrographs of food items ingested by *C. simillimus* (A,B), *R. gigas* (C) and *P. robusta* (D,E). A, C-E: fragments of pennate and discoid diatoms, B: diatom fragments with the silicoflagellate *Dictyocha speculum*.

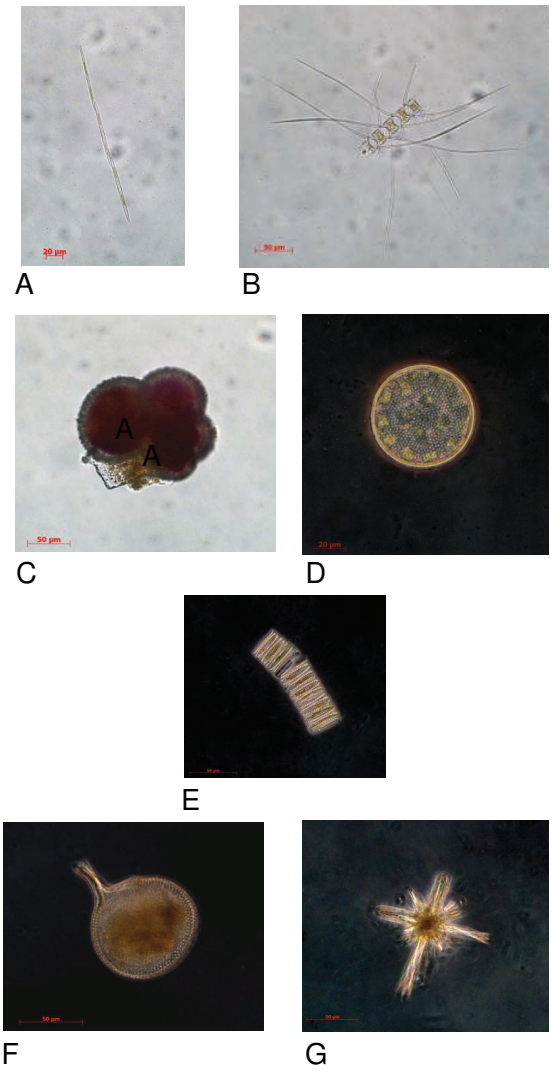

Figure 3: Light micrographs of food items ingested by *C. simillimus* (A-D), *R. gigas* (E) and *P. robusta* (F, G). A: chain of *Pseudonitzschia turgiduloides* (station 587), B: *Chaetoceros atlanticus* (station 508), C: foraminiferan (station 508), D: *Thalassiosira lentiginosa* (station 513), E: chain of *Fragilariopsis kerguelensis* (station 544), F: radiolarian (Phaeodaria; station 546), G: acantharian (station 546).

References

[1] Atkinson A. . Subantarctic copepods in an oceanic, low chlorophyll environment: ciliate predation, food selectivity and impact on prey populations. *Marine Ecology Progress Series*, 130:85–96, 1996.

[2] Atkinson A. Diets and feeding selectivity among the epipelagic copepod community near South Georgia in summer. *Polar Biology*, 14:551–560, 1994.

[3] Atkinson A. Omnivory and feeding selectivity in five copepod species during spring in the Bellingshausen Sea, Antarctica. *ICES Journal of Marine Science*, 52:385–396, 1995.

[4] Atkinson A. Life cycle strategies of epipelagic copepods in the Southern Ocean. *Journal of Marine Systems*, 15:289–311, 1998.

[5] Atkinson A., Ward P., Williams R., Poulet S.A. Diel vertical migration and feeding of copepods at an oceanic site near South Georgia. *Marine Biology*, 113:583–593, 1992.

[6] Bathmann U. Ecological and biogeochemical response of Antarctic ecosystems to iron fertilization and implications on global carbon cycle. *Ocean and Polar Research*, 27:231–235, 2005.

[7] Bathmann U., Liebezeit G. Chlorophyll in copepod fecal pellets: changes in pellet numbers and pigment content during a decline Baltic spring bloom. *Marine Ecology -pubblicazioni della stazione zoologica di napoli*, 7:59–73, 1986.

[8] Boyd P.W., Law C.S., Wong C.S., Nojiri Y., Tsuda A., Levasseur M., Takeda S., Rivkin R., Harrison P.J., Strzepek R., Gower J., McKay R.M., Abraham E., Arychuk M., Barwell-Clarke J., Crawford W., Crawford D., Hale M., Harada K., Johnson K., Kiyosawa H., Kudo I., Marchetti A., Miller W., Needoba J., Nishioka J., Ogawa H., Page J., Robert M., Saito H., Sastri A., Sherry N., Soutar T., Sutherland N., Taira Y., Whitney F., Wong S.-K. E., Yoshimura T. The decline and fate of an iron-induced subarctic phytoplankton bloom. *Nature*, 428:549–553, 2004.

[9] Cisewski B., Strass V.H., Losch M., Prandke H. Mixed layer analysis of a mesoscale eddy in the Antarctic Polar Front Zone. *Journal of Geophysical Research Oceans*, in press:–, 2008.

[10] Coale K. H., Johnson K.S., Chavez F.P.,Buesseler K.O., Barber R. T.,Brzezinski M.A., Cochlan W.P., Millero F.J., Falkowski P.G., Bauer J.E., Wanninkhof R.H., Kudela R.M., Altabet M.A., Hales B.E., Takahashi T., Landry M.R., Bidigare R.R., Wang X., Chase Z., Strutton P.G., Friederich G.E., Gorbunov M.Y., Lance V.P., Hilting A.K., Hiscock M.R., Demarest M., Hiscock W.T., Sullivan K.F., Tanner S.J., Gordon R.M., Hunter C.N., Elrod V.A., Fitzwater S.E., Jones J. L., Tozzi S., Koblizek M., Roberts A.E., Herndon J., Brewster J., Ladizinsky N., Smith G., Cooper D., Timothy D., Brown S.L., Selph K.E., Sheridan C.C., Twining B.S., Johnson Z.I. Southern Ocean Iron Enrichment Experiment: Carbon Cycling in High- and Low-Si Waters. *Science*, 304:408–414, 2004.

[11] Drits A.V., Pasternak A.F., Kosobokova K.N. Feeding, metabolism and body composition of the Antarctic copepod Calanus propinquus Brady with special reference to ist life cycle. *Polar Biology*, 13:13–21, 1993.

[12] Fowler S.W., Fisher N.S. Viability of marine phytoplankton in zooplankton fecal pellets. *Deep-Sea Research*, 30:963–969, 1983.

[13] Froneman P.W., Pakhomov E.A., Perissinotto R., McQuaid C.D. Role of microplankton in the diet and daily ration of Antarctic zooplankton species during austral summer. *Marine Ecology Progress Series*, 143:15–23, 1996.

[14] Garrison D.L. . An overview of the abundance and role of protozooplankton in Antarctic waters. *Journal of Marine Systems*, 2:317–331, 1991.

[15] Hamm C.E, Merkel R., Springer O., Jurkojc P., Maier C., Prechtel K., Smetacek V. Architecture and material properties of diatom shells provide effective mechanical protection. *Nature*, 421:841–843, 2003.

[16] Hansen B., Bjornsen P.K., Hansen P.J. The size ratio between planctonic predators and their prey. *Limnology and Oceanography*, 39:395–403, 1994.

[17] Hargrave B.T., Geen G.H. Effects of copepods grazing on two natural phytoplankton populations (A. Tonsa). *Journal of the Fisheries Research Board of Canada*, 27:1395–1403, 1970.

[18] Hoffman L.J., Peeken I., Lochte K., Assmy P., Veldhuis M. Different reactions of Southern Ocean phytoplankton size classes to iron fertilization. *Limnology and Oceanography*, 51:1217–1229, 2006.

[19] Hopkins T.L. . Food web of an Antarctic midwater ecosystem. *Marine Biology*, 89:197–212, 1985.

[20] Hopkins T.L., Torres J.J. Midwater food web in the vicinity of a marginal ice zone in the western Weddell Sea. *Deep-Sea Research*, 36:543–560, 1989.

[21] Jansen, S., Bathmann, U. Algae viability within copepod faecal pellets: evidence from microscopic examinations. *Mar Ecol Prog Ser*, 337:145–153, 2007.

[22] Kleppel G.S. On the diets of calanoid copepods. *Marine Ecology Progress Series*, 99:183–195, 1993.

[23] Marshall S.M. Respiration and feeding in copepods. *Advances in Marine Biology*, 11:57–120, 1973.

[24] Marshall S.M., Orr A.P. On the biology of Calanus finmarchicus: Food uptake, assimilation and excretion in adult and stage V. *Journal of the Marine Biological Association UK*, 34:495–529, 1955.

[25] Michels J., Schnack-Schiel S.B. Feeding in dominant Antarctic copepods - does the morphology of the mandibular gnathobases relate to diet. *Marine Biology*, 146:483–495, 2005.

[26] Pakhomov E.A., Perissinotto R., McQuaid C.D., Froneman P.W. Zooplankton structure and grazing in the Atlantic sector of the Southern Ocean in late austral summer 1993. Part 1. Ecological zonation. *Deep-Sea Research I*, 47:1663–1686, 2000.

[27] Parsons T.R., Lebrasseur R.J., Fulton J.D. Some Observations on the dependance of Zooplankton Grazing on the Cell Size and Concentration of Phytoplankton Blooms. *Journal of the Oceanographical Society of Japan*, 23:10–17, 1967.

[28] Pasternak A.F., Kosobokova K.N., Drits A.V. Feeding, metabolism and body composition of the dominant antarctic copepods with comments on their life cycles. russian. *Journal of Aquatic Ecology*, 3:49–62, 1994.

[29] Pasternak A.F., Schnack-Schiel S.B. Feeding patterns of dominant Antarctic copepods: an interplay of diapause, selectivity and availability of food. *Hydrobiologia*, 453/454:25–36, 2001a.

[30] Pasternak A.F., Schnack-Schiel S.B. Seasonal feeding patterns of the dominant Antarctic copepods Calanus propinquus and Calanoides acutus in the Weddell Sea. *Polar Biology*, 24:771–784, 2001b.

[31] Perissinotto R. Mesozooplankton size-selectivity and grazing impact on the phytoplankton community of the Prince Edward Archipelago (Southern Ocean). *Marine Ecology Progress Series*, 79:243–258, 1992.

[32] Rintoul, S., Hughes, C., and Olbers, D. *The Antarctic Circumpolar Current System, In: Ocean Circulation and Climate*, chapter 4, pages 271–302. Academic Press New York, 2001.

[33] Schnack S.B. Feeding of Calanus helgolandicus on phytoplankton mixtures. *Marine Ecology Progress Series*, 1:41–47, 1979.

[34] Schnack-Schiel S.B., Hagen W. . Life cycle strategies and seasonal variations in distribution and population structure of four dominant calanoid copepod species in the eastern Weddell Sea, Antarctica. *Journal of Plankton Research*, 16:1543–1566, 1994.

[35] Schultes S., Verity P.G., Bathmann U. . Copepod grazing during an iron-induced diatom bloom in the Antarctic Circumpolar Current (EisenEx): I. Feeding patterns and grazing impact on prey populations. *Journal of Experimental Marine Biology and Ecology*, 338:16–34, 2006.

[36] Smetacek V. A watery arms race. *Nature*, 411:745, 2001.

[37] Smetacek V., Bathmann U.V., Helmke E. The Expeditions Antarktis XXI/3-4-5 of the Research Vessel Polarstern in 2004 . *Berichte zur Polar- und Meeresforschung*, 500:1–134, 2005.

[38] Turner J.T., Ferrante J.G. Zooplankton fecal pellets in aquatic ecosystems. *Bioscience*, 29:670–677, 1979.

[39] Utermöhl H. Zur Vervollkommnung der quantitativen Planktonmethodik. *Mitteilungen - Internationale Vereinigung für Theoretische und Angewandte Limnologie*, 9:1–38, 1958.

[40] Verity P.G., Smetacek V. Organism life cycles, predation, and the structure of marine pelagic ecosystems. *Marine Ecology Progress Series*, 130:277–293, 1996.

[41] Voronina N.M., Sukhanova I.N. Composition of food of massive species of herbivorous Antarctic copepods. *Oceanology*, 16:614–616, 1977.

[42] Wexels Riser C., Jansen S., Bathmann U., Wassmann P. Grazing of Calanus helgolandicus on Dinophysis norvegica during bloom conditions in the North Sea: evidence from investigations of faecal pellets. *Marine Ecology Progress Series*, 256:301–304, 2003.

10 Manuscript 6

Fate of copepod faecal pellets during an iron induced phytoplankton bloom (EIFEX) in the Southern Ocean

S. Jansen[1*], J. Henjes[1], L. Friedrichs[1],S. Krägefsky[1],U. Bathmann[1]

Alfred Wegener Institute for Polar and Marine Research, Am Handelshafen 12, 27570 Bremerhaven, Germany

A combination of faecal pellet production experiments and the analysis of the faecal pellet standing stock within the water column were carried out in the course of the European iron fertilization experiment EIFEX in the Southern Ocean in 2004. Faecal pellet production experiments with the abundant copepod *Calanus simillimus* showed that faecal pellet volume as well as faecal pellet production increased with increasing chlorophyll a values. The faecal pellet carbon (FPC) standing stock increased inside the fertilized patch in the course of the experiment. At day 37 after fertilization, FPC within the upper water column (0-150 m depth) was 13 times higher than initial values, while FPC at the out-patch stations increased sevenfold compared to the start condition. The turnover rate for faecal pellets within the upper water column could be estimated from a comparison between the expected faecal pellet production of the total copepod community and the actual faecal pellet abundance in the field and was approximately 24 hours for the

*Corresponding author: Sandra.Jansen@awi.de

in-patch stations. We assume that most of the faecal pellets were recycled within the upper water column during EIFEX. Hence, the different possible mechanisms and processes responsible for the recycling of the faecal pellets in the surface layer are discussed.

1 Introduction

Copepods are the most numerous consumers of phytoplankton in the ocean (Boxshall, 1998). With potential high sinking rates of faecal pellets from larger copepods (<100 to >1000 m d^{-1}: Komar et al., 1981), it was formerly expected that the contribution of these faecal pellets to the vertical flux is always high (e.g. Turner and Ferrante, 1979; Angel, 1984). Vertical flux studies of the recent two decades, however, showed that the contribution of faecal pellets to the vertical carbon flux is not always high but highly variable. Reported values range from less than 1% to more than 100% of particulate organic carbon (POC) flux via zooplankton faecal pellets (Bathmann et al., 1987; Gonzalez et al., 1992; Wexels Riser et al., 2000; Turner, 2002; Dagg et al., 2003; Sampei et al., 2004). In fact, it becomes more and more clear, that the main carbon transfer to the deeper water column is run by marine snow and direct sedimentation of phytoplankton blooms, especially diatoms (e.g. Smetacek, 1980, reviewed by Turner, 2002).

Different recycling mechanisms for produced faecal pellets are discussed in literature, including coprophagy and coprochaly (e.g. Lampitt et al., 1990; Noji et al., 1991). Additional studies showed that factors like food concentration, food composition or assimilation efficiency may play an important role for the density and stability of the produced faecal pellet material (Butler and Dam, 1994; Feinberg and Dam, 1998; Besiktepe and Dam, 2002). Besides these factors, microbial colonization, water temperature and chemical composition of sea water influence pellet degradation processes (Hansen et al., 1996; Olsen et al., 2005). All these factors have an impact on pellet sinking rates and on the percentage of pellets which are recycled within a given water layer and thus have an impact on the vertical carbon flux mediated by copepod faecal pellets.

In the context of an increasing atmospheric CO_2 level due to recent human influences, large scale iron fertilization experiments have become of increasing interest. The induction of large phytoplankton blooms and their subsequent export to the deep sea attracted interest as a possibility to reduce the CO_2 concentration in the atmosphere and thereby slow down global warming. The first large scale iron fer-

tilization experiments have been conducted in the nineties. The theory, that iron is the missing nutrient in the so-called HNLC (high nutrient low chlorophyll) regions, was confirmed (Boyd et al., 2004; Coale et al., 2004) and the hypothesis of Martin (Martin, 1990) has become generally accepted (Buesseler et al., 2008). Between 1993 and 2005, eleven large scale iron fertilization experiments have been conducted in HNLC regions all over the world (Boyd et al., 2007; Boyd, 2008) and all of them induced phytoplankton blooms after the addition of iron.

The response of the zooplankton to iron addition can mainly be seen as an indirect response to the fertilization, since zooplankton react on the induced phytoplankton bloom and not directly to the iron. The zooplankton, i.e. the copepods of the area can accumulate within the fertilized patch within some days (Rollwagen Bollens and Landry, 2000; Krägefsky et al., in prep.). Such an abundance increase of copepods within the area of enhanced phytoplankton concentration may result in different mechanisms. Even though it was shown, that some species can directly respond reproductively to higher phytoplankton levels (Jansen et al., 2006), there must be other, faster mechanisms to explain an increase in abundance as it was observed in some of the recent iron fertilization experiments (Rollwagen Bollens and Landry, 2000; Tsuda et al., 2005; S. Krägefsky et al., submitted). However, increased zooplankton abundances lead to enhanced grazing pressure on the bloom and subsequent higher faecal pellet production within the fertilized area. Whether such an increase in faecal pellet production may in turn lead to enhanced carbon export, is one of the major questions to estimate the fate of carbon after iron fertilization.

The duration of most of the so far conducted large scale iron fertilization experiments was less then four weeks and assumptions about the export of the induced phytoplankton bloom was in most cases questionable. EIFEX was conducted in the beginning of 2004 for an experimental duration of more than five weeks. This was the longest of all iron fertilization experiments conducted so far. In this manuscript we want to highlight the possible influence of copepods on the potential export of the iron induced phytoplankton bloom.

2 Material and Methods

2.1 Studied area

Samples were collected during the in situ European Iron Fertilization Experiment (EIFEX) conducted in the Atlantic Sector of the Southern Ocean ($\sim$ 49° S, 02° E)

in late austral summer to early austral fall (21 January - 25 March 2004) during the cruise ANT XXI-3 of RV Polarstern (Smetacek et al., 2005). EIFEX was carried out in a mesoscale cyclonic eddy which was obviously shed from the Antarctic Polar Front. The eddy water was characteristic for the Antarctic Circumpolar Current (low temperature, HNLC conditions) and showed iron depletion (0.08 - 0.2 nM: Hoffmann et al., 2006). Seven tons of iron sulphate (FeIIISO4) were added to an area of approximately 150 km^2 on February 12 - 13 (t0 / t1) after an initial sampling to determine pre-fertilization conditions. Day zero (t0) reflected the conditions one day before the iron release. A second iron fertilization was made on February 26 - 27 (t14 / t15). The outcome of the fertilization was monitored for 37 days after the initial iron release (Smetacek et al., 2005; Hoffmann et al., 2006; Jansen et al., 2006). In the course of the experiment, the "in-patch" stations were placed at the sites of highest photosynthetic efficiency (Fv / Fm) and/or lowest pCO_2 values observed, hence closest to the center of the iron-fertilized patch. In contrast, the "out-patch" stations were located in adjacent, iron-limited waters with low Fv / Fm ratios and equilibrium pCO_2 concentrations (Smetacek et al., 2005).

2.2 Faecal pellet production experiments

Faecal pellet production experiments were carried out for a rough estimate of the grazing rates and the impact of important copepod species on the carbon flux of the phytoplankton bloom as well as for content analysis of the faecal pellets. Furthermore the experiments should give an idea about size and shape of the faecal pellets of different abundant zooplankton species. Experimental water was taken from the chlorophyll a (chl a) maximum at the respective station and filled into 1 or 2 litre bottles. Adult females of the calanoid copepods *Calanus simillimus*, *Rhincalanus gigas*, *Pleuromamma robusta* and *Calanus propinquus* were taken from Bongo nets, slowly towed from 20 meter depth to surface. In the on-board laboratory healthy females were sorted out under the binocular and experiments were set up not longer than two hours after retrieval of the Bongo net. Depending on the size of the copepod species, two to four animals of the same species were transferred into three to five parallel bottles and placed on a slowly rotating plankton wheel at in situ temperature and dim light. After 24 hours, the content of the bottles was carefully sieved over 30 μm and fixed with hexamine-buffered formalin (4% final concentration) for later enumeration and size measurements. While measuring the faecal pellets under an inverted microscope, it was additionally recorded, whether

they were complete (1), broken with one end (0.5), or broken without an end (0) for determination of the faecal pellet production rates. Experiments with C. *simillimus* were carried out on six stations during EIFEX, *R. gigas* faecal pellet production rates were determined at three stations, while for the other two copepod species experiments could only be conducted at two stations (Table 1).

2.3 Faecal pellet abundance and carbon content

Water samples for determination of faecal pellet abundances in the water column were taken from eight to ten discrete depths between 10 and 550 m in the beginning of the fertilization experiment as well as at 6 in- and 3 out-patch CTD (Conductivity Temperature Depth) stations using Niskin bottles (Table 2). Additionally, samples were taken during a 48 hours station inside the fertilized patch on day 23 / 24 after the first iron release (Station 544) with about 6 hours time intervals between the different CTD-casts (Table 2). For every discrete depth sampled, the entire content of one or two Niskin bottles (12 or 24 l) depending on depth, were gently passed through a 20 μm mesh plankton net and concentrated to a final volume of 50 ml. The concentrated samples were preserved with hexamine-buffered formalin solution to a final concentration of 2% and stored at 4°C in the dark for subsequent counting. In the home laboratory, a volume of 3 ml (10 – 150 m depth) and 10 ml (250 – 550 m depth) was settled in sedimentation chambers (Hydrobios, Kiel, Germany) for 12 or 24 hours, respectively. Faecal pellets were enumerated using inverted light and epifluorescence microscopy with a magnification of 160 (Axiovert 135, Zeiss, Oberkochen, Germany), according to the method of Utermöhl (1958). Prior to counting, 35 μl of stock solution of the nuclear fluorochrome 4',6-diamidino-2-phenylindole (DAPI) (Porter and Feig, 1980) were added to the samples to stain the nucleus of ciliates and flagellates with similar shape as metazoan faecal pellets. All faecal pellets or faecal pellet fragments were photographed and measured in length and width with a Zeiss AxioCam MRc5 and the Zeiss AxioVision software 4.1 (Zeiss, Oberkochen, Germany). Faecal pellet volume (FPV) could be calculated assuming a regular geometrical shape (Hillebrand et al., 1999). For all metazoan faecal pellets a carbon conversion factor of 69.4 μg C mm^{-3} was applied (Riebesell et al., 1995). Faecal pellet abundances and biomass (number of faecal pellets m^{-2} and mg C m^{-2}, respectively) were obtained from trapezoidal integration of values from the depth intervals.

3 Results

During EIFEX, chl a concentrations increased more than fivefold by day 23 with maximal chl a concentrations of 3.16 μg l^{-1} and then decreased towards the end of the experiment with values over 2 μg l^{-1} extending down to 100 m depth (Klaas et al., 2005). Particulate organic carbon (POC) followed a similar pattern, declining after day 30 (Smetacek et al., in prep.). These findings indicate the demise of the iron-induced bloom (Hoffmann et al., 2006). The massive increase in chl a concentration was mainly due to the growth of large chain-forming diatoms (Assmy et al., in prep.). A deep and fast export of organic matter has been clearly characterized during EIFEX, as revealed by available sediment and ^{234}Th data (Sachs et al., in prep., Smetacek et al., in prep.).

3.1 Faecal pellet production experiments

C. simillimus

The number of faecal pellets produced by *C. simillimus* during EIFEX increased with increasing chl a values inside the fertilized area, while it remained low on the stations outside the fertilized area, accompanied by lower chl a values (Table 1). Mean faecal pellet production rate was measured to be 6 $\pm$ 0.5 faecal pellets copepod^{-1} day^{-1} at the out-patch Station 587 with lowest experimental chl a start concentration, while it peaked at station 513 (t16) with 59 $\pm$ 4 faecal pellets copepod^{-1} day^{-1} when chl a start concentration of the experiment was measured to be 2.47 μg l^{-1} (Table 1). Lowest individual faecal pellet production rate was determined to be about 5 faecal pellets copepod^{-1} day^{-1} at station 546 (t26), where chl a was $\sim$ 0.4 μg chl a l^{-1}, while the maximum individual value measured for *C. simillimus* was 70 faecal pellets copepod^{-1} day^{-1}, determined at station 544 (t23) with a chl a value of 2.16 μg l^{-1}. Via the size measurement of the faecal pellets, FPV was calculated and values showed as well an increase with increasing chl a concentration (Fig. 1). Generally, the calculation of FPV is the best way to compare different faecal pellet production experiments, since faecal pellet size may change due to different conditions. During EIFEX; faecal pellets of *C. simillimus* increased significantly in length (ANOVA: F = 22.44; p = 0.01) as well as in width (ANOVA: F = 13.17; p = 0.02) with increasing chl a values. Figure 2 shows the increase in FPV of single faecal pellets produced by *C. simillimus* with increasing chl a values, which is as well significant (ANOVA: F = 18.51; p = 0.01). The determined

FPV values of *C. simillimus* were subsequently transferred to FPC (Riebesell et al., 1995) and values increased with increasing chl a concentration with a slope of 2.084 μg FPC copepod^{-1} day^{-1}(μg chl a l^{-1})$^{-1}$ ($r^2 = 0.92$; $p < 0.001$).

Other species

Less experimental data are available from the other three copepod species under investigation. However, produced FPV copepod^{-1} day^{-1} for all these species increased with increasing chl a concentrations (Table 1). FPC production of total copepods in the experiments (*C. simillimus*, *R. gigas*, *P. robusta* and *C. propinquus*) increased at a slope of 1.885 μg FPC copepod^{-1} day^{-1}(μg chl a l^{-1})$^{-1}$ ($r^2 = 0.87$; $p < 0.001$).

Figure 3 shows the size distribution of faecal pellets from the four copepod species investigated. Faecal pellet sizes from R. gigas, *C. simillimus* and *C. propinquus* were determined at Station 508 (t10), where the chl a concentration was measured to be 1.68 μg l^{-1}, while the faecal pellet size of *P. robusta* was determined at Station 543 (t21; 2.44 μg chl a l^{-1}). However, neither length, nor width of the faecal pellet sizes overlapped with regard to the 95% confidence intervals.

3.2 *In situ* concentration of faecal pellets

The succession of copepod faecal pellet abundance and subsequently copepod FPC in situ was recorded outside and inside the fertilized patch (Tab. 2; Figs 4 and 5). Figure 4A shows the condition shortly after fertilization (Station 427, t1). FPC was relatively constant (~ 0.3 μg C l^{-1}) throughout the water column (0 - 350 m), without a distinct maximum. The depth distribution of FPC at the three out-patch stations investigated during the following 35 days is shown in Figure 4 (B-D). The FPC maximum at all three stations was laying between 20 and 40 m depth and the maximum values were increasing over the course of the experiment from 1.5 μg C l^{-1} to 2.8 μg C l^{-1}. FPC values were decreasing below 150 m depth to their minimum values.

The depth profiles from the eight in-patch stations generally showed a similar trend (Fig. 5). Within the upper 80 meter of the water column the calculated FPC reached its maximum, while values were decreasing below the wind mixed layer depth (Ciesewski et al., 2008). Until day 29 (Station 553) after the first iron addition, the maximum FPC value was not exceeding 2 μg C l^{-1}. After day 29 the maximum was always calculated to be higher than 4 μg C l^{-1}. The maximum FPC value for all stations was obtained at Station 580 (t33) with almost 6 μg C l^{-1} at 10 m depth.

Below the mixed layer depth, the FPC values decreased and in the lowest included water depth, values were calculated to be between 1 and 7% of the maximum value of the surface layers. Integrated FPC stocks over the upper 150 m showed a $\sim$ 13-fold increase inside the fertilized patch in the course of the experiment, whereas in outside waters a sevenfold increase could be observed, compared to Station 427 (Tab. 2).

3.3 48 hours station

Beside the determination of the in situ concentration of faecal pellets during EIFEX, faecal pellet concentration and distribution was obtained during a 48 hours station. To display a possible daily curve of the faecal pellets we calculated the barycenter distribution of metazoan faecal pellet carbon (Fig. 6). During the night casts (04:30 h and 23:32 h) the barycenter of the faecal pellet carbon was located in the upper 80 m of the water column. During the day time casts (08:37 h, 15:27 h and 18:49 h) the barycenter was below 80 m depth with its deepest value (120 m) at 15:27 h (Fig. 6). Integrated carbon stocks over the upper 150 m varied between 150 and 267 mg C m^{-2} during this 48h station whereas values in the 150-350 m depth horizon were significantly lower ranging between 7 and 92 mg C m^{-2} (Tab. 2).

4 Discussion

The present iron fertilization experiment EIFEX offered the possibility to study the built up and breakdown of an iron-induced, diatom-dominated phytoplankton bloom over a time span of 37 days. With the combination of experimental and field data we wanted to identify the role of copepod faecal pellets for the carbon export during an induced phytoplankton bloom.

4.1 Faecal pellet production experiments and faecal pellet content

Faecal pellet production experiments with the abundant copepod *C. simillimus* showed, that faecal pellet size increased with food concentration, while the maximum faecal pellet size was not reached at food concentrations of 2.5 μg chl a l^{-1} (Fig. 2). This dependency of faecal pellet size and chl a could already be shown in earlier studies, where sizes increased up to food concentration of $\sim$ 3 μg chl a l^{-1}

and remained constant at higher concentrations (Dagg and Walser, 1986). Surprisingly, the faecal pellet size measurements from different species at comparable chl a concentrations showed no size overlapping within the 95% confidence interval of the four copepod species under investigation (Fig. 3). The ideal scenario, to separate the faecal pellets collected within the field on species specific basis was, however, not accomplishable in praxis, since only faecal pellets of females were included in this measurements. Stage specific size differences of the produced faecal pellets as well as degradation processes and fragmentation causes indeterminable problems. However, in areas with little variation in copepod species and stage composition, a classification of the faecal pellets found in the field may be possible to a certain degree in close combination with laboratory experiments.

Beside the experimental determination of the faecal pellet production rate and the size measurements of the produced faecal pellets, some faecal pellets were examined with the scanning electron microscope (SEM). Generally, microscopic analysis of copepod faecal pellets can give valuable qualitative and semi-quantitative information on the copepods diet and the degree of dissolution within the pellets, since the surrounding membrane is more or less transparent (Gauld, 1957). Main phytoplankton groups, such as diatoms, plastidic thecate dinoflagellates and coccolithophores can easily be identified within faecal pellets because of their cellulose or mineral skeletons. All metazoan faecal pellets analyzed from the present experiments were coated by a membrane and contained unidentifiable amorphous material, at times intact and broken diatom frustules, thecae of dinoflagellates and loricae of tintinnid ciliates. Especially the faecal pellets from *P. robusta* often contained larger food organisms like tintinnids, dinoflagellates or diatom chains (e.g. *Fragilariopsis kerguelensis*).

Samples for content analysis with the SEM were prepared like described in Wexels Riser et al. (2003). Scanning electron micrographs showed that the faecal pellets contained mainly highly fragmented cell debris of diatoms (Fig. 7). It becomes obvious, that the quantification of diatom debris which makes up more than 50% of the frustules can hardly be correlated to faecal pellet recycling in the water column, since most of the fragments within the faecal pellets are much smaller. However, beside the cell debris, in some of the analyzed faecal pellets intact diatoms could be found (Fig. 7). Especially *Thalassiosira spp.* and *F. kerguelensis* cells were identified and observed complete within a number of analysed faecal pellets. The extreme stability of *F. kerguelensis* is known (Hamm et al., 2003) and their ability to survive the gut passage of copepods was shown in a study of Jansen and Bathmann

(2007). Therefore, the fate of the material stemming from faecal pellets recycled in the mixed layer depends on the condition of the material enclosed within the faecal pellets.

The combination of faecal pellet production experiments of important copepod species in the laboratory, the information about the copepod abundance within the field and the determination of faecal pellet standing stock within the field, offered the possibility to compare the expected faecal pellet production of the copepod community with the real faecal pellet abundances in the field. The discrepancies between these values generate the background for the following discussion of possible recycling or export mechanisms.

4.2 Copepod abundances and expected FP production of the copepod community

During the iron fertilization experiment EIFEX, calanoid copepod copepodites and adults increased in abundance, approximately doubling their initial abundance of about 170,000 individuals m^{-2} to $\sim$ 330,000 individuals m^{-2} (0 – 400 m) in the centre of the phytoplankton bloom (Kägefsky et al., to be submitted). Their carbon biomass increased 1.8-fold from $\sim$ 2.4 g C m^{-2} to $\sim$ 4.3 g C m^{-2}. The detailed development of the zooplankton community on species and stage specific levels and a discussion of the aggregation mechanism will be published elsewhere.

With the copepod abundances in the field and the on board faecal pellet production experiments, it was possible to estimate the in situ faecal pellet production of the copepod community. However, before presenting the expected faecal pellet production of the copepod community in the field, and the comparison of these values with the faecal pellets counted from the concentrated water samples, we would like to discuss a methodology comparison for the determination of the faecal pellet abundances in the field. As described, faecal pellet abundances were determined from concentrated water samples, by concentrating 12 or 24 l of water from a discrete depth over a mesh to a volume of 50 ml of which a subsample of 3 ml or 10 ml were counted. We also took non-concentrated water samples and counted the faecal pellets within 50 ml of these samples. A comparison of the results from these methods revealed a difference of the factor two ($y = 2.06$; $r^2 = 0.46$), resulting in an underestimate, when working with the values of the concentrated samples.

A linear model for the chlorophyll dependent faecal pellet production was derived by regression analysis for *C. simillimus* separately and for the copepod species in

total. The experimental determined FPV production of *C. simillimus* increased with increasing chl a concentration with a slope of 2.084 μg FPC copepod^{-1} d^{-1} (μg chl a l^{-1})$^{-1}$ (r2 = 0.92). FPV production of total copepods in the experiments (*C. simillimus*, *R. gigas*, *P. robusta* and *C. propinquus*) increased at a slope of 1.885 μg FPC copepod^{-1} d^{-1} (μg chl a l^{-1})$^{-1}$ (r^2 = 0.87). As mentioned, all experiments were conducted with female copepods only. To transfer the experimental derived pellet production rates to the field population, we assumed similar production for adults and CV stages. Presuming egestion proportional to food ingestion, the faecal pellet production rates of younger stages were estimated using the allometric function provided by Peters and Downing (1984) for the filtering rate of calanoid copepods:

$$\log(V_1/V_2) = 0.534 \log(W_1/W_2)$$

V_1 is the experimental derived faecal pellet production rate and V_2 being the faecal pellet production rate of young stages with weight W_2 , while W_1 is the reference weight of stage CV. The small but highly abundant *Ctenocalanus citer* was not included in the experiments. Their stage specific faecal pellet production was estimated using the weight of *C. simillimus* (CV) as reference weight (W_1) to scale down the faecal pellet production derived for larger copepods. Daily faecal pellet production by the local copepod stock was calculated based on the faecal pellet production estimates for the different copepod species and stages and their respective abundance sampled at a given multi-net station in the upper 0 - 160 m. Due to the unknown feeding behaviour of *Oithona spp.* and other very small copepod species, these are excluded from the estimate. Therefore, calculated in situ pellet production of all copepods must be seen as rather conservative values.

Figure 8 shows the integrated FPC values, calculated from the counted and measured faecal pellets from the concentrated water samples over the course of the experiment for the in-patch stations. An area is given between calculated values and values multiplied by 2.06 to account for the underestimation when working with concentrated water samples. The expected FPC values produced from the zooplankton community over a time span of 24 hours are indicated as well. The expected FPC produced within 24 hours, show good correlation with the FPC standing stock values, i.e. the faecal pellet standing stock and the daily faecal pellet production of the copepod community equal. Therefore, we conclude, that the faecal pellet resistance time was approximately 24 hours for the produced faecal pellets within upper layer

of the water column. Only the last station (593, t37) deviates from the otherwise significant correlation (Pearson correlation; r = 0.96; P = 0.01). The disappearance of the faecal pellets from the upper 150 m of the water column within ∼ 24 hours might result from recycling within the mixed layer or export out of this layer.

For the out patch stations the FPC values determined from the concentrated water samples were generally higher than the expected FPC values produced from the zooplankton community within 24 hours. However, comparable values are only available for two stations, which make it difficult to discuss this data. Residence time of faecal pellets at the out-patch stations was approximately twice as long as at the in-patch stations. Since the calculated faecal pellet production from the zooplankton community must be seen as very conservative values, there is evidence that the turn over rate out-patch was slower compared to the in-patch stations.

4.3 Possible fate of faecal pellets – Export or retention?

The general findings, that sinking rates for faecal pellets with diatoms are higher (Bienfang, 1980) and that faecal pellets produced under high food concentrations sink faster than faecal pellets produced under low food concentrations (Dagg and Walser, 1986), would at first glance support the export of faecal pellets during EIFEX, since we induced a diatom- dominated phytoplankton bloom with high food concentrations. However, this relatively simple correlation must be handled with care within a field study, and in fact numerous studies have shown that the contribution of copepod faecal pellets to the total material flux is highly variable (Bathmann et al., 1987; Sampei et al., 2004; Smetacek, 1980; Turner, 2002; Viitasalo et al., 1999; Wexels Riser et al., 2001), with the majority of the studies reporting relatively low faecal pellet export, as fraction of the total particulate organic carbon (POC). The relative importance of faecal pellets for recycling or vertical flux depends on various factors, which include zooplankton abundance and species composition as well as faecal pellet abundance, size, density, chemical and particulate contents (Turner, 2002). Mechanisms such as coprophagy, coprochaly or coprorhexy are thought to be important for the recycling of the pellets within the mixed layer (Lampitt et al., 1990; Noji et al., 1991; Viitasalo et al., 1999; Wexels Riser et al., 2001). *Oithona spp.* is discussed to be responsible for a considerable breakage of copepod faecal pellets due to coprophagy (González and Smetacek, 1994). New investigations challenge this hypothesis as no clear indication could be observed that feeding by *Oithona spp.* is responsible for pellet destruction or uptake (Reigstad et al., 2005). Also within

the present study, there was no (positive or negative) correlation found between the abundance and vertical distribution of *Oithona spp.* and the distribution of copepod faecal pellets in the water column. We thus conclude that *Oithona spp.* probably was not significantly involved in faecal pellet degradation during EIFEX. In place of *Oithona spp.*, other copepod species and recently the protozooplankton came in the focus of discussion to play a key role in the fragmentation of faecal pellets (Poulsen and Kiørboe, 2005; Iversen and Poulsen, 2007, Poulsen and Iversen, 2008), but a correlation is generally difficult to establish within field studies. However, the increase in zooplankton abundance inside the fertilized area may have contributed to the disintegration of faecal pellets in the upper water column. Beside mechanisms including zooplankton, other processes like microbial degradation are discussed for being mechanisms responsible for rapid faecal pellet break-up and loss (Hansen and Bech, 1996; Olsen et al., 2005).

The analysis of broken diatom frustules within the water column can be seen as an indicator for enhanced grazing and faecal pellet recycling activity. Diatom fragments were counted and identified, as long as they made up more than 50% of the complete frustule (Assmy et al., in prep). The abundance of broken fustules increased 2.5 times at maximum in the upper 100 m within the fertilized patch, whereas a slight decrease could be observed in surrounding waters. This indicates that heavy grazing pressure was exerted on the iron-induced bloom. However since smaller fragments of the diatom frustules were not quantified, an absolute quantification becomes difficult. Fragments seen within faecal pellets are often small and cell debris making up for more than 50% of the frustule are rather an exception than a rule within faecal pellets (Fig. 7). The development of the faecal pellet stock in the surface layer and the accumulation of biogenic silica and diatom carbon at extreme molar ratio of ~ 1.3 suggest strong faecal pellet recycling and faecal pellet production likely higher than estimated. However, the actual main mechanism triggering the recycling of the faecal pellets during EIFEX can only be speculated and may well be a combination of different processes.

During EIFEX a deep and fast export of organic matter has been clearly characterized, as revealed by available sediment and ^{234}Th data (Sachs et al., in prep., Smetacek et al., in prep.). The incorporation of remains of the disintegrated faecal pellets in sinking aggregates, particularly in the fast sinking diatom aggregates after the peak of the EIFEX bloom may have significantly contributed to the export of carbon and silica to the deep-sea. The actual contribution to this flux, which seems to have partly re-coupled the flux of unrespired carbon and silica debris from fae-

cal material, should critically depend on the actual mechanisms of the faecal pellet degradation.

Acknowledgments

The authors would like to thank the captain and crew of Polarstern expedition ANT XXI/3. The help from Timo Stadtlander and Kathrin Schmidt during the cruise is highly appreciated. We also would like to thank Friedel Hinz for help with the scanning electron microscope.

		Calanus simillimus			*Rhincalanus gigas*			*Calanus propinquus*			*Pleuromamma robusta*		
Station	chl a	FPR	FPV	n	FPR	FPV	n	FPR	FPV	n	FPR	FPV	n
508	1.68	32 ± 3	33.81 ± 2.29	3	25 ± 3	44.68 ± 5.37	5	23 ± 1	83.42 ± 6.65	4	no data		
513	2.47	59 ± 4	100.75 ± 11.24	3	20 ± 2	65.17 ± 2.42	3	no data			no data		
543	2.44	32 ± 4	51.91 ± 0.43	3	no data			no data			7 ± 1	32.04 ± 2.66	3
544	2.16	58 ± 7	73.91 ± 5.78	3	45 ± 1	45.47 ± 6.62	3	no data			no data		
546 (out)	0.39	8 ± 2	6.67 ± 1.73	3	no data			no data			no data		
587 (out)	0.37	6 ± 0.5	2.45 ± 0.51	5	no data			11 ± 1	8.22 ± 2.45	3	3 ± 0.5	6.08 ± 1.42	3

Table 1: Mean (±S.E.) faecal pellet production rate (FPR) [faecal pellets copepod^{-1}day^{-1}] and mean (±S.E.) faecal pellet volume (FPV) [FPV produced μm^3 copepod^{-1}day^{-1} $\times$ 10^6] produced by four copepod species during the iron fertilization experiment EIFEX. The number of parallels is indicated (n). Chlorophyll a (chl a) values [μg l^{-1}] were determined at the beginning of each experiment.

Station/cast	t	Date	Time at depth (UTC)	Latitude	Longitude	Depth sampled	FPC mg C m^{-2} (0-150 m)	FPC mg C m^{-2} (150-350 m)
427-06	1	13.02.	21:14	49° 12.53'S	2° 06.98'E	10, 20, 40, 80, 100, 150, 250, 350	35.4	50.1
508-22	10	22.02.	22:10	49° 11.64'S	2° 01.35'E	10, 20, 40, 80, 100, 150, 250, 350	115.4	54.2
509-16 (out)	11	23.02.	13:58	48° 59.76'S	2° 02.96'E	10, 20, 40, 80, 100, 150, 250, 350	136.7	73.0
514-18 (out)	17	29.02.	23:53	49° 19.78'S	2° 21.18'E	10, 20, 40, 80, 100, 150, 250, 350	189.6	71.9
544-06	22	05.03.	18:51	49° 28.92'S	2° 07.10'E	10, 20, 40, 80, 100, 150, 250, 350	156.4	25.4
544-16	23	06.03.	08:37	49° 31.04' S	2° 03.01' E	10, 20, 40, 80, 100, 150, 250, 350	163.8	20.4
544-30	23	06.03.	18:49	49° 29.50' S	1° 59.33' E	10, 20, 40, 80, 100, 150, 250, 350	186.0	21.4
544-39	23	06.03.	23:32	49° 28.65' S	1° 57.30' E	10, 20, 40, 80, 100, 150, 250, 350	150.4	7.2
544-46	24	07.03.	04:33	49° 27.38' S	1° 56.03' E	10, 20, 40, 80, 100, 150, 250, 350	221.9	16.6
544-58	24	07.03.	15:27	49° 23.87' S	1° 52.80' E	10, 20, 40, 80, 100, 150, 250, 350	266.6	91.5
553-11	29	12.03.	01:33	49° 29.89'S	2° 24.12'E	10, 20, 40, 80, 100, 150, 250, 350	185.6	31.2
580-12	33	16.03.	09:48	49° 07.53'S	2° 18.73'E	10, 20, 40, 80, 100, 150, 250, 350, 450, 550	296.0	34.4
587-14 (out)	35	18.03.	01:33	49° 30.67'S	2° 05.65'E	10, 20, 40, 80, 100, 150, 250, 350, 450, 550	254.2	30.9
590-01	35	18.03.	21:04	49° 23.80'S	2° 18.24'E	10, 20, 40, 80, 100, 150, 250, 450	432.3	49.1
593-09	37	20.03.	03:05	49° 28.74'S	2° 27.16'E	10, 20, 40, 80, 100, 150, 250, 350, 450, 550	446.3	66.5

Table 2: Station plan for the determination of the faecal pellet concentration in the water column during the European iron fertilization Experiment (EIFEX) Station and cast numbers are given, as well as the day after the first fertilization (t), the date, Latitude and Longitude and the integrated faecal pellet carbon (FPC) values [mg C m^{-2}] from 0 - 150 m and from 150 - 350 m depth. Stations written in gray indicate the 48 hours station.

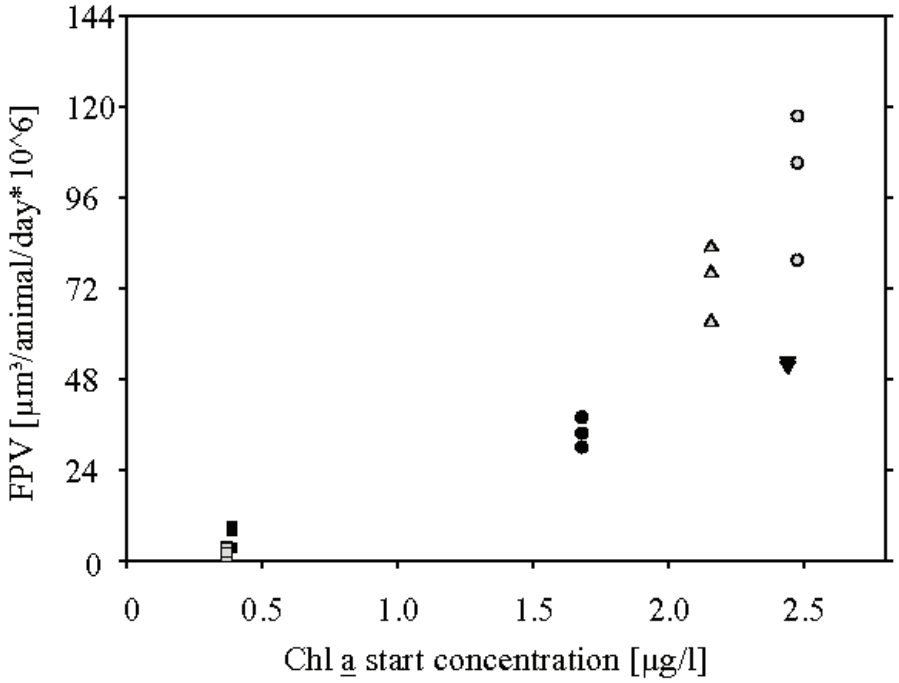

Figure 1: Faecal pellet volume (FPV) produced by *Calanus simillimus* at different chlorophyll a (chl a) start concentrations. Different symbols show parallel experiments at different stations (gray squares: station 587; black squares: station 546; black circles: station 508; gray triangles: station 544; black triangles: station 543; gray circles: station 513)

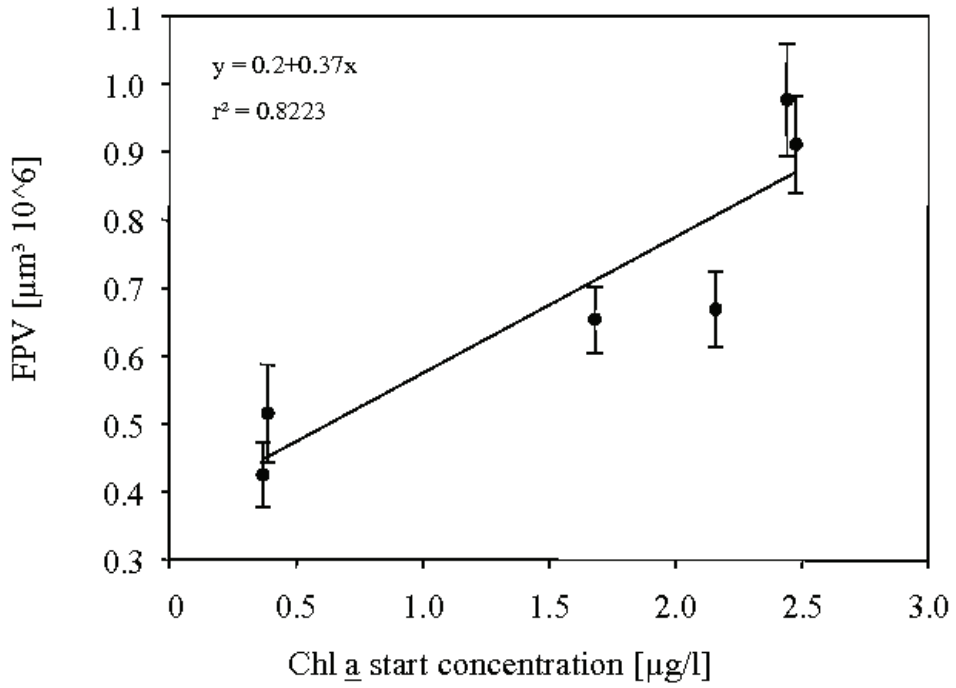

Figure 2: *Calanus simillimus* faecal pellet volume (FPV) of single faecal pellets produced in experiments with different chlorophyll a (chl a) start concentrations. The 95% confidence interval is indicated as error bars and linear regression is fitted.

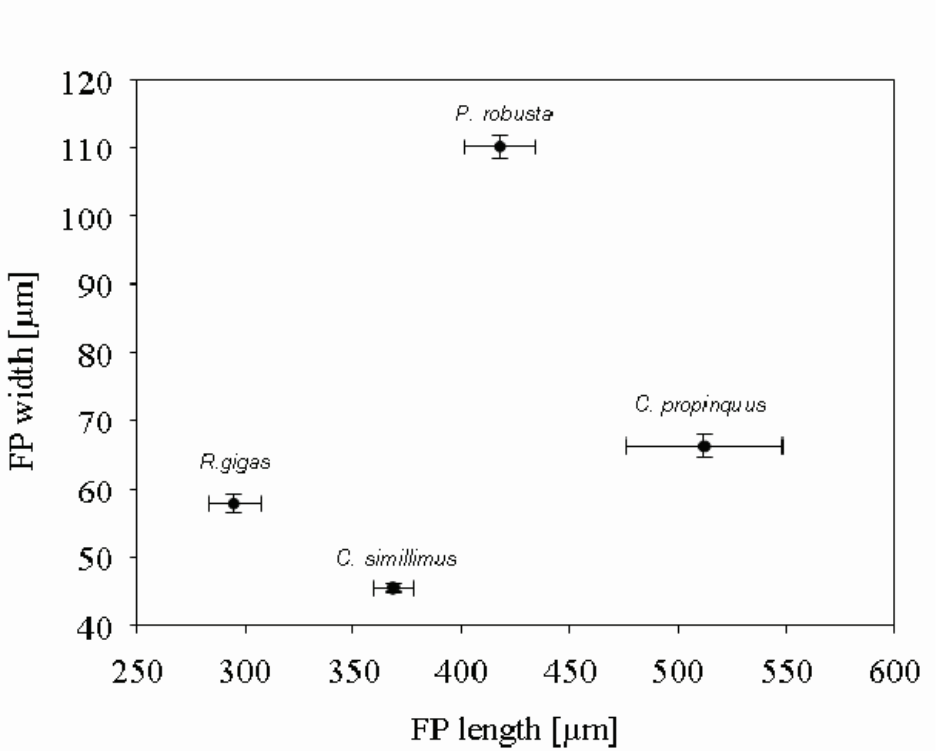

Figure 3: Faecal pellet (FP) size measurements from FP production experiments on Station 508 (1.68 μg chl a l^{-1}) from *Rhincalanus gigas* (n = 109), *Calanus simillimus* (n = 157) and *Calanus propinquus* (n = 54). *Pleuromamma robusta* (n = 58) FPs were measured after a FP production experiment on Station 543 (2.44 μg chl a l^{-1}). The 95% confidence intervals are indicated as error bars.

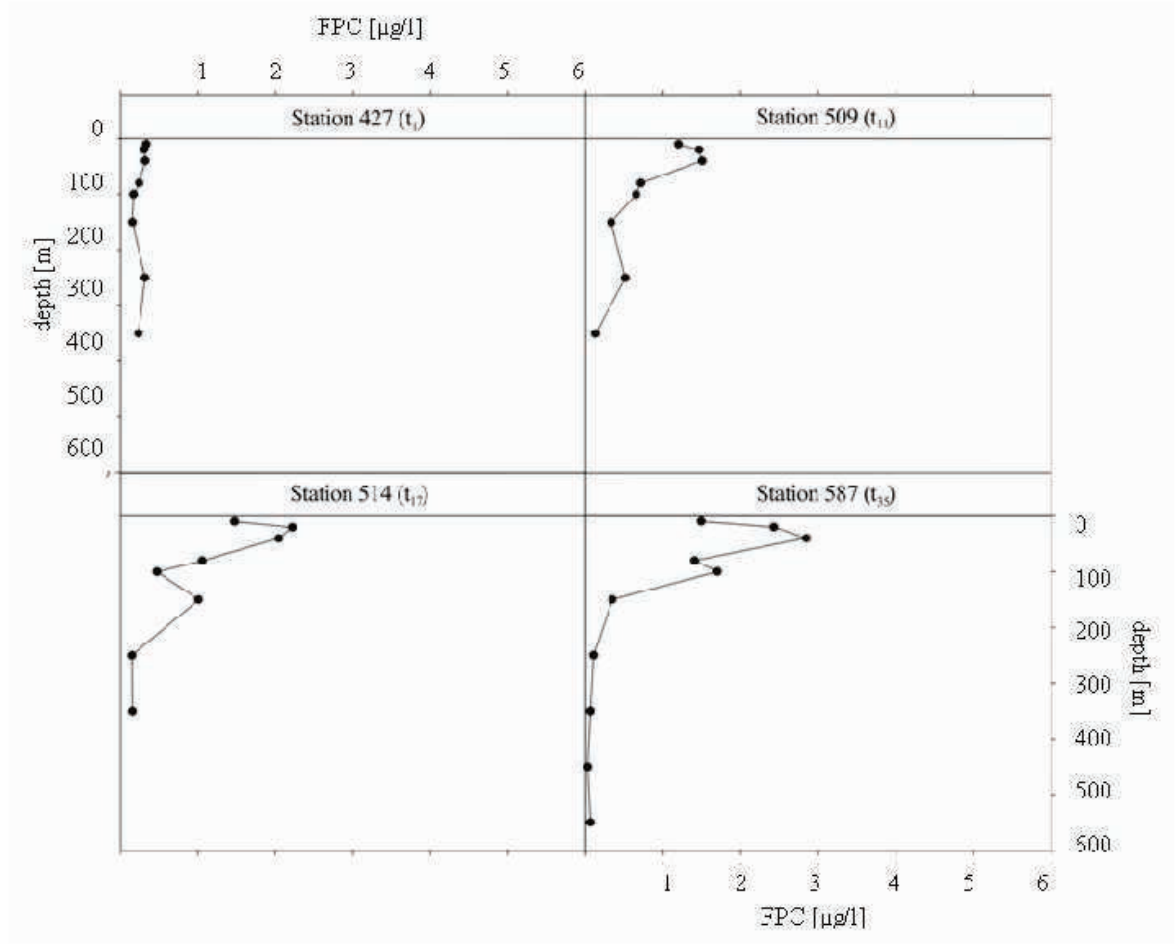

Figure 4: Faecal pellet carbon (FPC) depth profiles at the start and three out-patch stations during the European iron fertilization experiment EIFEX. Station numbers and the day after fertilization (t) are given in the graphs, respectively.

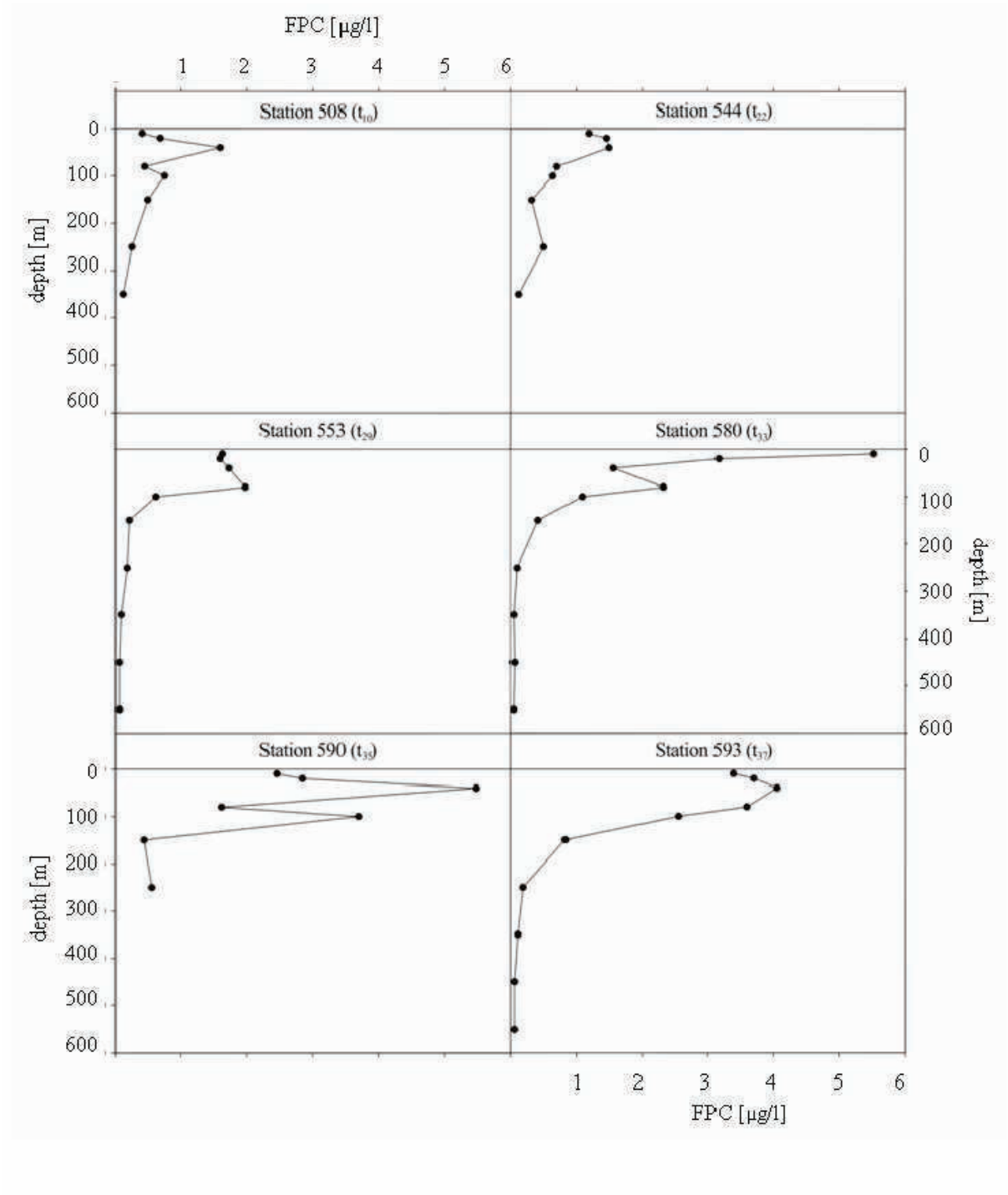

Figure 5: Faecal pellet carbon (FPC) depth profiles at the six in-patch stations during the European iron fertilization experiment EIFEX. Station numbers and the day after fertilization (t) are given in the graphs, respectively.

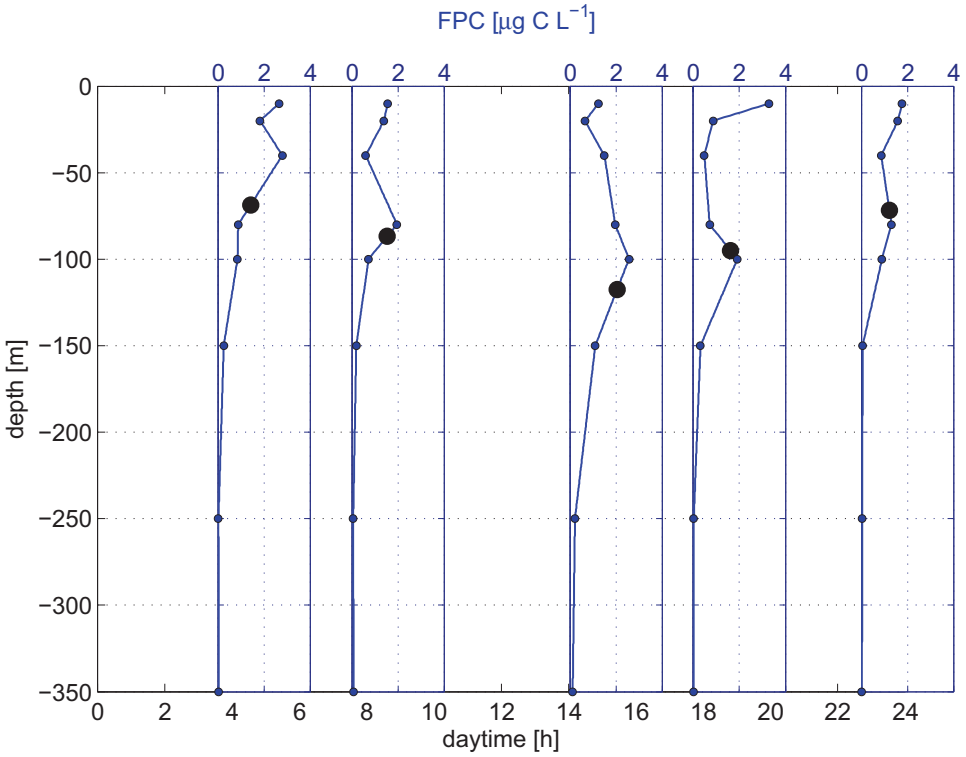

Figure 6: Fecal pellet carbon concentrations at distinct depths (blue circles) and centre of gravity of the vertical fecal pellet carbon distribution at the different stations over the course of a 24hour cycle (black circle) .

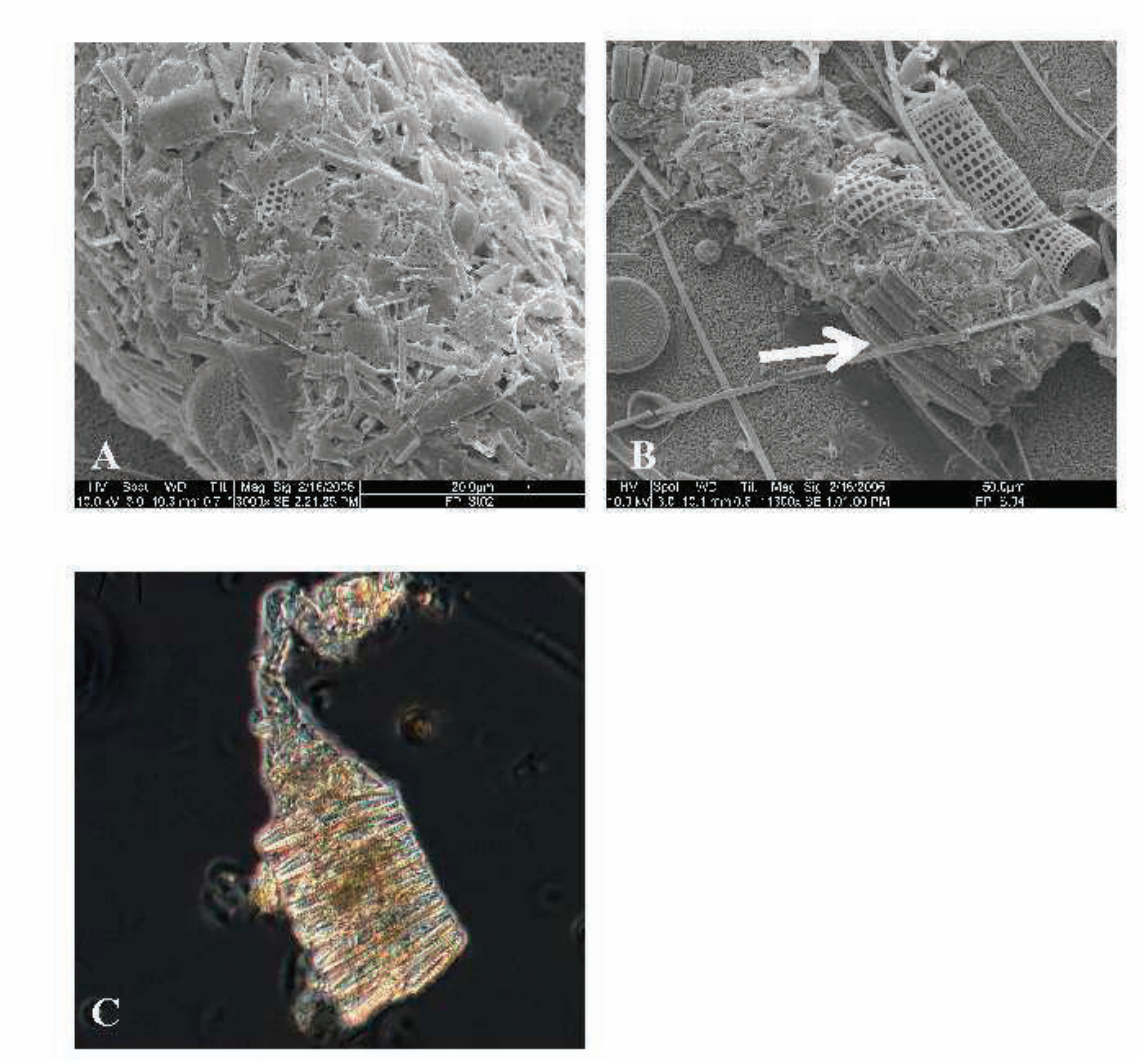

Figure 7: Faecal pellet collected at (A) Station 580 (0 – 50 m), (B) Station 590 (50 - 100 m). (C) Faecal pellet produced by *Calanus simillimus* during the faecal pellet production experiments (Station 544). Faecal pellets shown in (B) and (C) contain visible intact *Fragillariopsis kergulensis.*

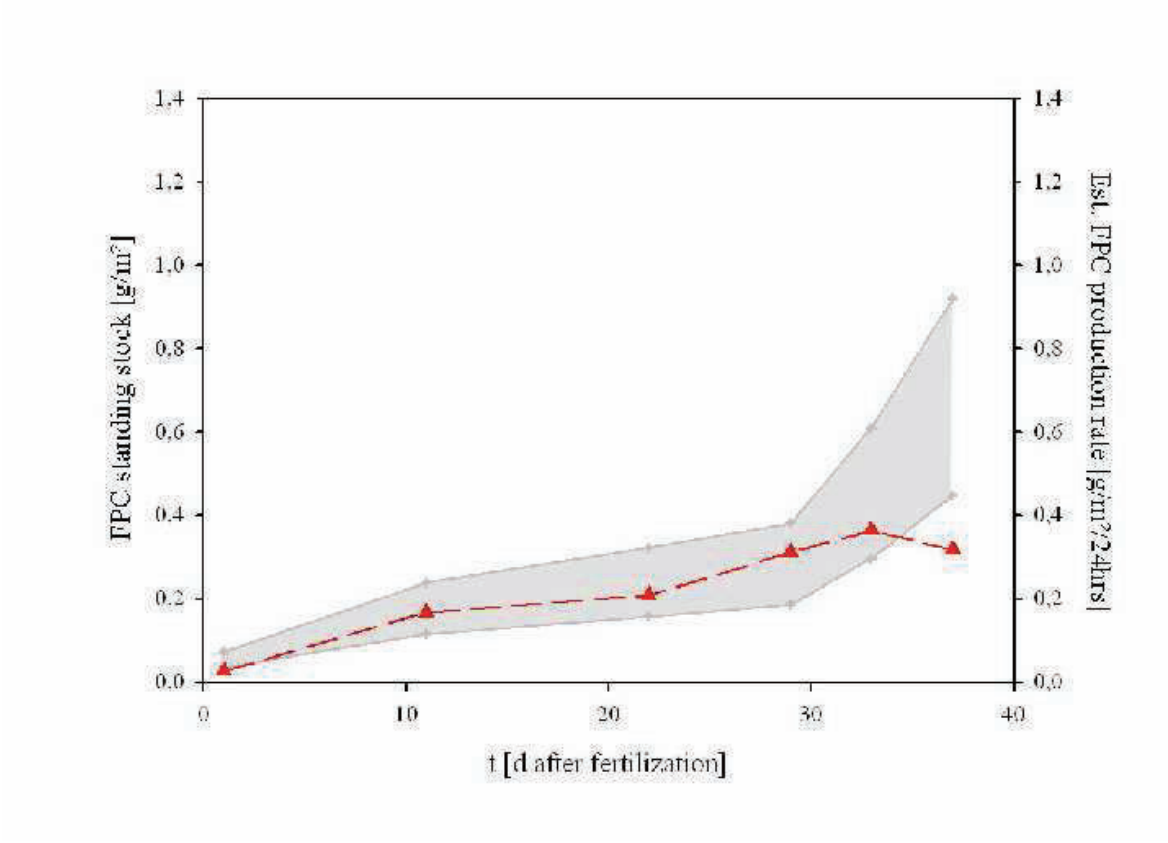

Figure 8: Estimated faecal pellet carbon (Est. FPC) production of the zooplankton community within 24 hours (red line) and ranges for the integrated FPC standing stock values in the field (gray). See text for further descriptions.

References

[1] Bathmann, U.V., Noji, T.T., Voss, M., and Peinert, R. Copepod fecal pellets: abundance, sedimentation and content at a permanent station in the Norwegian Sea in May/June 1986. *Mar Ecol Prog Ser*, 38:45–51, 1987.

[2] Bienfang, P.K. Herbivore diet affects fecal pellet settling. *Can J Fish. Aquat Sci*, 37:1352–1357, 1980.

[3] Boxshall, G.A. Preface. *Phil Trans R Soc Lond B*, 353:669–670, 1998.

[4] Boyd, P. W., Jickells, T., Law, C. S., Blain, S., Boyle, E. A., Buesseler, K. O., Coale, K. H., Cullen, J. J., de Baar, H. J. W., Follows, M., Harvey, M., Lancelot, C., Levasseur, M., Owens, N. P. J., Pollard, R., Rivkin, R. B., Sarmiento, J., Schoemann, V., Smetacek, V., Takeda, S., Tsuda, A., Turner, S., and Watson, A. J. Mesoscale Iron Enrichment Experiments 1993-2005: Synthesis and Future Directions. *Science*, 315(5812):612–617, 2007.

[5] Boyd, P.W. Implications of large-scale iron fertilization of the oceans - Introduction and synthesis. *Mar Ecol Prog Ser*, 364:213–218, 2008.

[6] Boyd, P.W., Law, C.S., Wong, C.S., Nojiri, Y., Tsuda, A., Levasseur, M., Takeda, S., Rivkin, R., Harrison, P.J., Strzepek, R., Gower, J., McKay, R.M., Abraham, E., Arychuk, M., Bartwell-Clarke, J., Crawford, W., Crawford, D., Haie, M., Harada, K., Johnson, K., Kiyosawa, H., Kudo, I., Marchetti, A., Miller, W., Needoba, J., Nishioka, J., Ogawa, H., Page, J., Robert, M., Saito, H., Sastri, A., Sherry, N., Soutar, T., Sutherland, N., Taira, Y., Whitney, F., Wong, S.-K.E., and Yoshimura, T. The decline and fate of an iron-induced subarctic phytoplankton bloom. *Nature*, 428:549–553, 2004.

[7] Buesseler, K.O., Doney,S.C., Karl, D.M., Boyd, P.W., Caldeira, K., Chai, F., Coale, K.H., de Baar, H.J.W., Falkowski, P.G., Johnson, K.S., Lampitt, R.S., Michaels, A.F., Naqvi, S.W.A., Smetacek, V., Takeda, S., and Watson, A. J. Ocean fertilization - Moving forward in a sea of uncertainty. *Science*, 319:162, 2008.

[8] Cisewski, B., Strass, V.H., Losch, M., and Prandke, H. 2008. . Mixed layer analysis of a mesoscale eddy in the Antarctic Polar Front Zone. *J Geophys Res*, 113:C05017, 2008.

[9] Dagg, M.J. and Walser, W.E. The effect of food concentration on fecal pellet size in marine copepods. *Limnol Oceanogr*, 31:1066–1071, 1986.

[10] Gauld, D. T. A peritrophic membrane in calanoid copepods. *Nature*, 179:325–326, 1957.

[11] H.E. Gonzales and V. Smetacek. The possible role of the cyclopoid copepod Oithona in retarding the flux of zooplankton faecal material. *Mar Ecol Prog Ser*, 113:233–246, 1994.

[12] Hamm, C.E., Merkel, R., Springer, O., Jurkojc, P., Maier, C., Prechtel, K., and Smetacek, V. Architecture and material properties of diatom shells provide effective mechanical protection. *Nature*, 421:841–843, 2003.

[13] Hansen, B. and Bech, G. Bacteria associated with a marine planktonic copepod in culture. I. Bacterial genera in seawater, body surface, intestines and fecal pellets and succession during fecal pellet degradation. *J Plankton Res*, 18:257–273, 1996.

[14] Hillebrand, H., Dürselen, C.-D., Kirschtel, D., Pollinger, U., and Zohary, T. Biovolume calculation for pelagic and benthic microalgae. *J Phyco*, 35:403–424, 1999.

[15] Hoffmann, L.J., Peeken, I., Lochte, K., Assmy, P., and Veldhuis, M. Different reactions of Southern Ocean phytoplankton size classes to iron fertilization. *Limnol Oceanogr*, 51:1217–1229, 2006.

[16] Iversen, M.H. and Poulsen, L.K. Coprorhexy, coprophagy, and coprochaly in the copepods *Calanus helgolandicus*, *Pseudocalanus elongatus*, and *Oithona similis*. *Mar Ecol Prog Ser*, 350:79–89, 2007.

[17] Jansen, S. and Bathmann, U. Algae viability within copepod faecal pellets: evidence from microscopic examinations. *Mar Ecol Prog Ser*, 337:145–153, 2007.

[18] Jansen, S., Klaas, C., Krägefsky, S., Harbou, L.v., and Bathmann, U. Reproductive response of the copepod *Rhincalanus gigas* to an iron-induced phytoplankton bloom in the Southern Ocean. *Polar Biol*, 29:1039–1044, 2006.

[19] Klaas, C, Schmidt, M., Terbrüggen, A., and Wolf-Gladrow, D. Chlorophyll a, particulate and dissolved carbon, nitrogen. *Reports on Polar and Marine Research*, 500:70–73, 2005.

[20] Komar, P.D., Morse, A.P., Small, L.F., and Fowler, S.W. An analysis of sinking rates of natural copepod and euphausiid fecal pellets. *Limnol Oceanogr*, 26:172–180, 1981.

[21] Krägefsky, S., Harbou, L. v., Jansen, S., and Bathmann, U. Copepod response to iron-induced diatom blooms in Southern Ocean (EisenEx and EIFEX). -, -:–, to be submitted.

[22] Lampitt, R.S., Noji, T., and Bodungen, B.v. What happens to zooplankton faecal pellets? Implications for material flux. *Mar Biol*, 104:15–23, 1990.

[23] Noji, T.T., Estep, K.W., Macintyre, F., and Norrbin, F. Image analysis of faecal material grazed upon by three species of copepods: evidence for coprorhexy, coprophagy and coprochaly. *J mar biol Ass U.K.*, 71:465–480, 1991.

[24] Olsen, S., Westh, P., and Hansen, B. Real-time quantification of microbial degradation of copepod fecal pellets monitored by isothermal microcalorimetry. *Aquat Microb Ecol*, 40:259–267, 2005.

[25] Peters, R.H. and Downing, J.A. Empirical analysis of zooplankton filtering and feeding rates. *Limnol Oceanogr*, 29:763–784, 1984.

[26] Porter, K.G. and Feig, Y.S. The use of DAPI for identifying and counting aquatic microflora. *Limnol Oceanogr*, 25:943–948, 1980.

[27] Poulsen, L.K and Iversen M.H. Degradation of copepod fecal pellets: key role of protozooplankton. *Mar Ecol Prog Ser*, 367:1–13, 2008.

[28] Poulsen, L.K. and Kiørboe, T. Coprophagy and coprorhexy in the copepods Acartia tonsa and Temora longicornis: clearance rates and feeding behaviour. *Mar Ecol Prog Ser*, 299:217–227, 2005.

[29] Reigstad, M., Wexels Riser, C., and Svensen, C. Fate of copepod faecal pellets and the role of *Oithona spp. Mar Ecol Prog Ser*, 304:265–270, 2005.

[30] Riebesell, U., Reigstad, M., Wassmann, P., Noji, T., and Passow, U. On the trophic fate of Phaeocystis pouchetii (Hariot): VI. Significance of Phaeocystis-derived mucus for vertical flux. *Neth J Sea Res*, 33:193–203, 1995.

[31] Sampei, M., Sasaki, H., Hattori, H., Fukuchi, M., and Hargrave, B.T. Fate of sinking partcles, especially fecal pellets, within the epipelagic zone in the North

Water (NOW) polynya of northern Baffin Bay. *Mar Ecol Prog Ser*, 278:17–25, 2004.

[32] Sastri, A.R. and Dower, J.F. Mesozooplankton community response during the SERIES iron enrichment experiment in the subarctic NE Pacific. *Deep Sea Res Part II*, 53:2268–2280, 2006.

[33] Small, L.F., Fowler, S.W., and Ünlü, M.Y. Sinking rates of natural copepods fecal pellets. *Mar Biol*, 51:233–241, 1979.

[34] Smayda, T.J. Some measurements of the sinking rate of fecal pellets. *Limnol Oceanogr*, 14:621–625, 1969.

[35] Smayda, T.J. The suspension and sinking of phytoplankton in the sea. *Oceanogr Mar Biol Annu Rev*, 8:353–414, 1970.

[36] Smayda, T.J. Some experiments on the sinking characteristics of two freshwater diatoms. *Limnol Oceanogr*, 19:628–6351, 1974.

[37] Smetacek, V. Annual cycle of sedimentation in relation to plankton ecology in western Kiel Bight. *Ophelia*, 1:65–76, 1980.

[38] Smetacek, V., Bathmann, U., and Helmke, E. The Expeditions ANT XXI/3-4-5 of the research vessel Polarstern in 2004. *Berichte zur Polar- und Meeresforschung*, 500:1–134, 2005.

[39] Turner, J.T. Zooplankton fecal pellets, marine snow and sinking phytoplankton blooms. *Aquat Microb Ecol*, 27:57–102, 2002.

[40] Utermöhl, H. Zur Vervollkommnung der quantitativen Phytoplankton-Methodik. *Verh Int Verein Theor Angew Limnol*, 17:47–71, 1958.

[41] Viitasalo, M., Rosenberg, M., Heiskanen, A.-S., and Koski, M. Sedimentation of copepod fecal material in the coastal northern Baltic Sea: Where did all the pellets go? *Limnol Oceanogr*, 44:1388–1399, 1999.

[42] Wexels Riser, C., Wassmann, P., Olli, K., and Arashkevich, E. Production, retention and export of zooplankton faecal pellets on and off the Iberian shelf, north-west Spain. *Prog Oceanogr*, 51:423–441, 2001.

11 General Discussion

The publications presented in this thesis investigated the response of copepods in phytoplankton blooms which were experimentally induced by iron fertilisation during two mesoscale fertilisation experiments in the Southern Ocean (EisenEx and EIFEX). The thesis addressed strategies of copepods to cope with the extreme Southern Ocean environment (manuscript 1, manuscript 2, manuscript 4) and, in doing so, how they impact the fluxes of carbon and nutrients (manuscript 3, manuscript 5, manuscript 6). Copepod behaviour was explored with special emphasis on the vertical migration pattern in response to increasing food concentration in the surface mixed layer.

11.1 Vertical migration behaviour as a food finding strategy

Southern Ocean copepods have to cope with a strongly seasonal and mostly low food supply. The food environment is also horizontally patchy distributed, as local maxima of phytoplankton biomass can develop in transient blooms. These are typically mesoscale blooms and develop and decay on the time scale of weeks (Smetacek et al. 1990, Strass et al. 2002, Moore & Abbott 2002). Phytoplankton blooms thus cover only a short period of the long generation times of Southern Ocean copepods, which are in the order of months to years (e.g. Atkinson 1998, Schnack-Schiel 2001).

Copepods drift through this environment without the ability to control their horizontal distribution by swimming against the horizontal currents. However, due to the vertical differences in the oceanic flow field, vertical movements of copepods can cause significant changes in their drift direction and speed. Vertical migration is thus a mechanism at disposal of copepods and other planktonic animals to actively affect their drift to maintain themselves in favoured regions or to enhance their transport out of regions with unfavourable conditions (Hardy & Gunther 1935). In fact, numerous studies mainly in tidal and estuarine environments have provided evidence

for such behaviour (Bosch & Taylor 1973, Isaac et al. 1974, Peterson et al. 1978, Kimmerer & McKinnon 1987, Hill 1998, Batchelder et al. 2002, Emsley et al. 2005). Also our studies in the Southern Ocean show that the vertical migration behaviour of both diel migrating copepods and of *O. similis* enhances their transport out of regions with low phytoplankton concentration in the surface layer, while it increases their retention in phytoplankton-rich areas (manuscript 1, manuscript 2).

Vertical migration behaviour of *Oithona similis*

Oithona similis is a small copepod species which is distributed world-wide, often reaching high abundances (Gallienne & Robins 2001). Ward and Hirst (2007) found the abundance and fecundity rates of *O. similis* to be strongly related to temperature and depth-integrated chlorophyll a in the Southern Ocean. Their findings suggest that *O. simillis* is food limited during long periods of its life span, which is in agreement with findings for other copepods species (e.g. Shreeve et al. 2002, Jansen et al. 2006). *O. similis* does not migrate diurnally but our study has shown that it changes its vertical distribution in response to the phytoplankton development. We found that *O. similis* abundance increased in the surface layer in the iron-fertilsed area during EisenEx, while the population showed a deeper vertical distribution outside the patch (manuscript 1). The strong upward migration of *O. similis* into the phytoplankton enriched surface layer in the fertilised area during EisenEx likely has caused a switch in diet composition from heterotrophic prey and other food items, prevailing in greater water depth, to diatoms, which dominated the bloom. This switch in grazing behaviour and the aggregation of individuals inside the bloom area may in turn have caused pronounced effects on the prey species composition and the flux of carbon and nutrients during EisenEx (see Discussion below). During EIFEX, no significant migration response of *O. similis* was detected. During this experiment, however, diatom species with long spines dominated the phytoplankton community and, likely, this copepod species was not capable of effectively feeding on these diatoms (manuscript 1).

Oithona similis is known to feed on a wide variety of food items, including nauplii of other copepod species, microzooplankton, faecel pellets, diatoms and other phytoplankton (Lampitt 1978, Hopkins 1985, Gonzales & Smetacek 1994, Atkinson 1998, Castellani et al. 2005). Thus, feeding is not directly coupled to primary production and this strategy seems to allow *O. similis* to prolong their residence in deeper waters. The deep-dwelling behaviour of *O. similis* enhances the drift out of

unproductive regions and thus increases the chance of getting advected from a low to a high food environment. Given the wide range of potential food for *O. similis*, the nutritional loss during deep-dwelling periods should be moderate compared to the food gain due to an increased probability to being subsequently exposed to a food rich environment.

Vertical migration behaviour of diel migrating copeods

Diel migration behaviour was observed for copepod species larger than *Oithona similis* such as *Ctenocalanus citer*, *Calanus simillimus*, *Rhincalanus gigas* and *Metridia lucens*. These copepods leave the surface layer during day and migrate up to hundreds of metres to a deeper daytime residence (e.g. Hays 2003, Pearre 2003). During both experiments, EisenEx and EIFEX, the acoustic survey showed that diel migrating copepods and maybe other zooplankton decreased their daytime residence inside the bloom areas. Shallow migrating species reduced their amplitude of diel vertical migration (DVM) by tens and deep migrating species by up to more than 150 metres (manuscript 2).

Acoustic measurements allow monitoring the vertical migration behaviour of the zooplankton with a very high temporal and spatial resolution. However, copepods are very weakly sound scattering organisms, and small and less abundant copepod species contribute minor to the backscattering in the water column. During EisenEx and EIFEX, copepods clearly dominated the zooplankton biomass. A reasonable comparison between net samples and acoustic measurements was only possible for EIFEX. This shows a high correlation between acoustic measurements (normalised mean volume backscattering strength measured at 70 and 120 kHz) and copepod biomass (manuscript 3), which suggests that basic sound scattering patterns originated from the copepods. Large zooplankton species were sampled in low numbers with multi nets, however, they seem to have added significantly to the acoustic backscattering and may have contributed to overall vertical migration response in the phytoplankton bloom area (manuscript 2, manuscript 3).

The low vertical and temporal resolution of the net sampling during EIFEX (0 - 25, 25 - 50, 50 - 100, 100 - 160, 160 - 400 m) did not allow to detect phytoplankton related changes of the daytime residence of the different copepod species and stages from net samples. The migratory response of shallow migrants occurred mainly within the net sampling interval of 50 - 100 m, while the depth range of the daytime residence of the deep migrating species was only covered by a single sampling interval (160 -

400 m). For this reason, the effects of acoustically observed migration responses on the horizontal copepod distribution and the individual food gain were investigated systematically in a simulation study (Individual based Model) covering the range of shallow, intermediate and deep migration patterns (manuscript 2). The results of the simulation study show large, up to 3-fold increase in copepod abundance in the bloom area and an up to 2-3 fold relative increase in the food gain of responding individuals.

Only a minority of studies addressed the diel vertical migration behaviour of zooplankton in the context of utilisation of the flow field (see above), while the predation-evasion hypothesis has gained wide acceptance (Hays 2003 and references therein). This hypothesis suggests visual predation to be the driving force in the evolution of diel vertical migration exhibited by widely diverse animal species. It is assumed that leaving the well-illuminated surface layer during daytime substantially decreases the mortality of migrating animals relative to non-migrating animals by reducing the risk of being detected by visually hunting predators. Different studies have revealed high plasticity of the DVM behaviour of zooplankton, with the ability of fast and flexible responses to abiotic (Buchholz et al. 1995) and biotic factors, such as food abundance and distribution (Harris 1988) and presence of visual or tactile predators (Ohmann et al. 1983, Neill 1990, Bollens & Frost 1991). Initiation of reverse diel vertical migration may be triggered in relation to the vertical distribution of tactile predators in the water column (Irigoien et al. 2004).

The abundance of fish and fish larvae is low in the Southern Ocean (Morales-Nin et al. 1995, Hoddell et al. 2000) and the predation impact on copepods is dominated by carnivorous and omnivorous macrozooplankton. Chaetognaths and euphausiids account for most predation mortality (Pakhomov et al. 1999) and thus the predation risk mainly arises from tactile predators. The question why Southern Ocean copepods nevertheless spend energy to undertake normal DVM while being exposed to modest visual predation risk, can be at least partly explained by the strong nutritional benefit suggested by the observations during EisenEx and EIFEX and the results of the simulation study (manuscript 2).

The diel migration periodically reintroduces animals into the relatively food-enriched surface layer, allowing the copepods to exploit the phytoplankton production efficiently. The migration into deeper water layers leads to drift with currents other than the surface currents. If food at the surface is scarce, the cycle of downward migration, drifting and upward migration should enhance the chances of finding patches of rich food supply. In phytoplankton rich areas, as in the fertilised

area during both experiments, the acoustic measurements show a strong decrease in the migration amplitude of the copepods, which cause an increased retention in these food-rich areas.

The long duration of the iron-fertilisation experiment EIFEX (38 days) may have allowed for significant recruitment from naupliar to copepodite stages. However, the stage composition as derived from net samples does not indicate a large contribution to the abundance increase shown by the copepodites of the different species inside the bloom area (manuscript 3). The abundance development of the different species suggests that the migration behaviour as derived from the acoustic observations is shown by wide range of copepods including those species, which were not or barely detected by the measurements, e.g. less abundant or small species. The simulation results shows large increase for shallow (up to 2-fold), intermediate (up to 3-fold) and deep migrating species (up to 2-fold) and can explain most of the distinct increase in abundance of diel migrating copepods during EIFEX and may explain the apparent increase during EisenEx (manuscript 2, manuscript 3). Their migration behaviour as well as that of *Oithona similis* (see above) can be considered as a food finding strategy.

11.2 Effects of copepod grazing on the prey community and on carbon and nutrient fluxes

Life cycle strategies of copepods in the Southern Ocean have been studied with different approaches over the past decades (e.g. Atkinson 1998, Schnack-Schiel 2001). Most studies investigated the horizontal and vertical distribution of copepod species and stages during different seasons in various regions of the Southern Ocean. Physiological measurements on feeding, respiration, excretion and egg production, for examples, are still rare. These investigations have revealed pronounced differences between species and suggest that *Calanoides acutus* is the only true diapausing species and over-winters at great depth. Over-wintering in the other species is flexible with parts of the population staying active in surface layer (see review in Schnack-Schiel 2001).

Copepods need to utilise a wide range of food items to survive fluctuations in food supply during their life span, which includes the long winter but also periods of food shortage in the growth season. In contrast to the classical view that copepods feed predominantly on diatoms, it is now known that copepods change their feeding behaviour in response to changes in the food environment (e.g. Kleppel 1993, Kiørboe et al. 1996). Their diet can include metazoan, protozoan, diatoms and other phytoplankton, as well as on non-living material like faecal pellets (Gonzales & Smetacek 1994, Atkinson 1996a, Pasternak & Schnack-Schiel 2001a, Pasternak & Schnack-Schiel 2001b).

Though our knowledge about feeding strategies of copepods in Southern Ocean has increased greatly over the past 20 years, information on species specific responses to a changing food regime is still limited. It is also not known how shifts in feeding behaviour structure the phytoplankton and microzooplankton community under phytoplankton rich and phytoplankton poor conditions. Particularly little is known about the feeding behaviour of small copepods like *Oithona similis*. Differences in the nutritional value of available food, prey handling time, suitability of prey size as well as differences in prey perceptibility are import factors which influence the feeding selectivity of copepods in general (Frost 1972, Paffenhöfer & VanSant 1985, DeMott 1989, Visser 2001). The prey perceptibility is not only a function of prey size and motility but depends also on the feeding mode of the copepod which may change in response to the availability of different food items (Kiørboe et al. 1996, Prince & Paffenhöfer 1986).

The ambush feeding of *O. similis* bias its prey perception ability to motile prey

and larger immobile particles (Visser 2001). Studies on the feeding biology of this species are, however, rare and contradicting, which may in part be due to the fact that different methods have been used. Gut content analyses showed that diatoms were preferred in spring, summer and autumn (Hopkins 1985, Hopkins 1987, Hopkins & Torres 1989) while a study of the fatty acid composition by Kattner et al. (2003) did not confirm feeding on diatoms in the summer. Other studies, including both gut content analyses and feeding experiments, suggest that substantial amounts of diatoms were ingested but that motile prey was preferred prior to and after the spring bloom (Atkinson 1995, Atkinson 1996). It is possible that these differences result from the influence of food quality, e.g. algal size and morphology.

The relative contribution of phytoplankton, protozoan, crustaceans and other food to the diet in general and in a particular food environment varies greatly between the copepod species and over time. Generally, the contribution of diatoms increases strongly during the growth season, even in species like *Metridia gerlachei*, which shows a pronounced carnivorous tendency (Pasternak & Schnack-Schiel 2001b). Microzooplankton largely contributes to the nutrition during periods of phytoplankton shortage but may also be an important component in a phytoplankton bloom situation (Kleppel 1993, Atkinson 1996). Atkinson (1998) considers the feeding behaviour of *O. similis* and *Calanoides acutus* as being representative for contrasting life cycle strategies of Southern Ocean copepods, with herbivorous diet in summer and diapause in winter in case of *C. acutus* and omnivorous diet during an extended period and no diapause as exhibited by *O. similis* and other species. *Rhincalanus gigas* is assumed to be intermediate between these strategies (Atkinson 1998).

A clear response with an abundance increase inside the phytoplankton bloom areas was observed for dominant copepod species, especially during EIFEX, which suggests limiting food supply outside the patch. As previously outlined for *Oithona similis*, in the fertilised area the feeding behaviour likely has also changed in diel migrating copepods from feeding primarily on heterotrophic prey and other food items, prevailing outside the patch, to diatoms, which dominated the bloom. This switch in grazing behaviour and the aggregation of individuals inside the bloom area may in turn have caused pronounced effects on the prey species composition and the flux of carbon and nutrients during EisenEx.

In incubation experiments during EisenEx, *Calanus simillimus* maintained constant clearance rates and fed predominantly on diatoms in- and outside the bloom area, while clearance and ingestion rates of diatoms increased significantly with diatom concentration in *Rhincalanus gigas* and other copepods $<$2 mm. Prey switch-

ing from dinoflagellates to diatoms was observed for *R. gigas*, however, preying on microzooplankton remained important. The diatom species specific clearance rates which were observed in the experiments suggest a size-selectivity with highest clearance rates for larger diatoms (Schultes et al. 2006).

During EIFEX, the copepod grazing was investigated by means of gut fluorescence experiments, faecal pellet production experiments and gut content analyses. None of these methods allow for the determination of grazing on soft bodied organisms such as heterotrophic microzooplankton. Thus, the following does only describe feeding on hard bodied organisms and autotrophic algae, respectively. The gut content analyses of *Calanus simillimus*, *Rhincalanus gigas* and *Pleuromamma robusta* showed no clear selectivity for specific diatom species, neither inside as nor outside the bloom area. The number of long-spined (*Chaetaoceros spp.*) or heavily silicified diatoms (*Fragilaripsis kerguelensis*) found in the guts suggest that these diatom shell features did not prevent effective intake by larger copepods (manuscript 5) as shown previously (e.g. Pasternack & Schnack-Schiel 2001b, Schultes et al. 2006). Deterring effects by spiny setae, as observed by e.g. Perissinotto 1992, were not found.

The gut content of the highly abundant small copepod *Ctenocalanus citer* was not investigated. The food items, which other studies found in the guts of *C. citer*, suggest that this copepod is a small particle feeder with diatoms as the major diet (Hopkins 1985, Hopkins 1987; Hopkins and Torres 1988, Pasternack & Schnack-Schiel 2007). The results of a recent study in the Weddel Sea region of the Southern Ocean suggest that the feeding of *C. citer* was partially decoupled from the phytoplankton bloom (Pasternack & Schnack-Schiel 2007). In contrast, *C. citer* showed a strong response in the phytoplankton bloom areas of EIFEX and EisenEx and increased more than 2-fold in abundance (manuscript 2, manuscript 3, Henjes et al. 2007). Whether these observations reflect regional differences of the feeding behaviour of *C. citer* in the Polar Front area and the Weddel Sea is unknown. However, in view of EisenEx and EIFEX, a substantial grazing impact of *C. citer* particularly on small diatoms can be assumed.

Small copepods like *Ctenocalanus citer* and *Oithona similis* ingest a large amount of food in relation to their body weight and their daily carbon ingestion often exceeds the carbon weight of their body. Their food includes phytoplankton species and phytoplankton of size classes that also microzooplankton organisms graze upon. Particularly, changes in feeding behaviour of omnivorous species like *O. similis* increase or reduce the grazing pressure on microzooplankton. This likely has marked

cascading effects, impacting the species composition and biomass of small phytoplankton (Froneman & Bernard 2004).

The different responses of *Oithona similis* during EisenEx and EIFEX suggests that migration and feeding response of *O. similis* may depend on the species composition of the phytoplankton bloom, which was dominated by long-spined diatoms during EIFEX (Smetacek et al. in prep). These differences in the response of *O. similis* may partly explain why the microzooplankton stock increased during EisenEx (Henjes et al. 2007) and while it remained quite constant during EIFEX (Smeatcek in prep.). Furthermore, grazing on microzooplankton may have allowed very small diatoms (2-8 µm) to increase their biomass inside the bloom area of EIFEX (Hoffmann et al. 2008).

Estimates of copepod grazing rates derived from different methods often vary considerably as they did during EisenEx. An imbalance between ingestion rates and measured metabolic demands is a longstanding observation, mainly for incubation experiments (e.g. Atkinson 1994, Schultes 2004) but also using the gut fluorescence method (Zeldis 2001). To assess the actual grazing impact of copepods, it is therefore important to combine different methods and to measure a large set of parameters, including primary production, net uptake of DIC and grazing rates among others. The experimental set up and the multidisciplinary investigations over the course of the experimentally induced phytoplankton blooms therefore greatly improved our knowledge on grazing impact.

During EisenEx, the zooplankton sampling did not allow for a proper assessment of the development of abundance and biomass and thus of the feeding impact of copepods over the course of the phytoplankton bloom. However, the ingestion rates measured in incubation experiments suggest that the phytoplankton mortality had reached up to 25% of the phytoplankton standing stock per day (Schultes 2006, manuscript 3). During EIFEX, the number of copepods ($\gtrsim$ 1 mm) almost doubled inside the phytoplankton bloom area (0 - 400 m) from initially ca. 170,000 copepods m^{-2} to ca. 330,000 copepods m^{-2} after 5 weeks. Accordingly, their carbon biomass increased 1.8-fold from ca. 2.4 g C m^{-2} to ca. 4.3 g C m^{-2} over the course of the experiment. The estimated carbon ingestion of copepods ($\gtrsim$ 1 mm) amounted to a total of approximately 15 g C m^{-2} over the course of EIFEX and to ca. 30% of the daily primary production during the bloom period (manuscript 3). The total carbon egestion of these copepods, estimated from faecal pellets production rates (manuscript 6), amounted to 8-9 g C m^{-2}. Respiratory carbon needs have been calculated according to Dagg et al. (1982) and amounted to 5-6 g C m^{-2} over the

course of the experiments, indicating that the miminum need for ingestion was 13-15 g C m^{-2} . The loss in carbon was, however, not balanced by the estimated phytoplankton carbon ingestion after the 3 week of EIFEX. It has therefore to be considered that there are food sources other than phytplankton, and our data suggest that the copepods have fed upon microzooplankton. Microzooplankton biomass remained low and quite stable during EIFEX, while the microzooplankton grazing impact on the phytoplankton as estimated from serial dilution experiments was 8.8 g C m^{-2} over the course of the experiment (Smetacek et al. in prep.). Assuming a high gross growth efficiency of the microzooplankton of 40% (Straile 1997), up to 3.5 g C m^{-2} of the primary production could have been channelled through a short link from phytoplankton via microzooplankton to the copepods. Some carbon may have also been channelled from the recycling pool to the copepods through feeding of microzooplankton on bacteria and detritus.

The strong difference between the phytoplankton stock increase (4.5 g C m^{-2}), net DIC uptake (21 g C m^{-2}) and estimated integrated primary production (49 g C m^{-2}) over the course of EIFEX (Smetacek et al. in prep.) confirm a substantial grazing impact on the phytoplankton.

The observed migration behaviour of the copepods was triggered by increased phytoplankton concentration. Hence, the large abundance increase of copepods and thus the strong increase in their grazing pressure on the phytoplankton community happened gradually, after the phytoplankton had already reached increased concentration inside the iron fertilised area. During EIFEX, a co-increase of phytoplankton and copepod abundance was observed, and the phytoplankton reached bloom concentration though copepods ingested large amounts of the phytoplankton over the course of the bloom.

The faecal pellet stock in the surface layer did not substantially exceed daily faecal pellet production, indicating that no accumulation of pellets had taken place. At the same time, biogenic silica and diatom carbon accumulated at an extreme molar ratio of ~ 1.3 suggesting not only a strong faecal pellet recycling but also that the faecal pellet production was higher than estimated from the experiments (manuscript 6). Most of the organic faecal matter seems to have been decomposed and respired in the surface layer. However, the incorporation of the remains of disintegrated faecal pellets in sinking aggregates, which developed from senescent diatoms particularly after the peak of the EIFEX bloom, may have contributed to the flux of silica and carbon to the deep sea. The fate of faecal matter during EisenEx is basically unknown.

The mechanisms that determine the degree of faecal pellet recycling in the surface layer are poorly known. Recent findings suggest little direct impact of copepods but a pivotal role of microzooplankton in the degradation of faecal pellets (Poulsen & Iversen 2008). A diet switch of copepods during a phytoplankton bloom, which relaxes the grazing pressure on microzooplankton, thus may indirectly result in an increasing recycling of faecal material. In contrast, if copepods are assumed to be the main pellet degraders (e.g. Gonzales & Smetacek 1994) a very different scenario would be expected. If coprophagus feeding is important for copepods when other food sources like phytoplankton are scarce, their degree of coprophagy should decrease in a phytoplankton bloom when high nutritional food is abundant. In this scenario, the recycling of faecal material decreases in a bloom situation. Though the faecal pellet production increased strongly over the course of the experiment, most of the production seems to have been recycled in the phytoplankton bloom area of EIFEX. The microzooplankton biomass, however, remained low and quite stable, and might have been controlled by grazing. Thus, the EIFEX results do not clearly support the first nor the second scenario.

In summary, the iron fertilisation experiments EisenEx and EIFEX revealed remarkable changes in the migration behaviour of copepods. Copepods apparently utilised the vertical sheared flow field of their oceanic environment to find food and, hence, to cope with the patchy, mostly poor food environment of the Southern Ocean. As during other iron-fertilisation experiments except for SeedsII (Tsuda et al. 2007), the phytoplankton escaped grazing pressure and built up bloom concentration under iron replete conditions. However, the amount of phytoplankton production which was grazed over the course of EIFEX by far exceeded the increase in phytoplankton standing stock, i.e. the gross phytoplankton production was considerably higher than net production of the phytoplankton. Copepod grazing (on phyto- and microzooplankton) thus has to be considered as a mechanism which can significantly alter carbon and nutrient fluxes after iron fertilisation also in the Southern Ocean.

11.3 Perspectives for future research

The findings of this thesis delivered new insights in behaviour of copepods, which apparently utilise the vertical sheared flow field of their oceanic environment to find food and cope with the patchy, mostly poor food environment of the Southern Ocean. The vertical resolution by the net and the Niskin bottle sampling causes

major limitations in the present study (manuscript 1, manuscript 2), however, the ability to improve the vertical resolution is strongly limited by the time constraints during field work and the effort to analyze the samples. Future research should include the combined use of net and/or Niskin bottle sampling, multi-frequency acoustical but also optical observation methods (e.g. video plankton recorder) to overcome the limitations inherent to the different sampling methods.

Observations with a video plankton recorder provide fine-scale resolution information about the vertical distribution of zooplankton and would improve the ability to identify the different sound scatterers. Optical observations would also give an estimate of the vertical distribution of very small copepods like *Oithona spp.*, which are not sampled adequately with plankton nets with commonly used mesh sizes while the sampling with Niskin bottles allows only a very sparse sampling at discrete depth.

Acoustic measurements are highly valuable to survey the migration behaviour of copepods and other zooplankton. However, basic sound scattering properties of copepods are not well known and have to be measured more extensively in the future (see Chu & Wiebe 2005). Copepods are very weak scatterers of sound and the use of higher sound frequencies would largely enhance the acoustic detectability of smaller copepods. As the effective measuring range decreases with increasing frequency, measurements with higher frequencies have to be done with towed systems, and would be most usefully deployed as a horizontal towed undulating system.

At present it is unknown if diel migrating species used phytoplankton-induced changes in light intensities per se as a cue for the migratory response or whether sensing of qualitative changes in the underwater light field was involved in the migration behaviour. Changes in the underwater light field below the mixed layer were not measured during both EisenEx and EIFEX, but should be measured during future studies. Experimental investigations in the photoreception abilities of copepods (see Goodel 2008) are highly desirable.

During EisenEx and EIFEX, the feeding behaviour of copepods was investigated with different methods (gut fluorescence experiments, incubation experiments, microscopic gut content analysis, faecal pellet production experiments). The development of molecular techniques to detect different prey organisms including soft-bodied species in the copepod guts and faecal pellets could provide an additional valuable tool to investigate in situ feeding behaviour in the future. However, only the combination of the different methods can lead to reliable estimates of copepod grazing impact on the different prey species. Particularly mesoscale iron fertilisation exper-

iments may provide further insights in the copepod feeding behaviour and response to phytoplankton blooms.

Bibliography

[1] Atkinson, A. Diets and feeding selectivity among epipelagic copepod community near south georgia in summer. *Polar Biol*, 14:551–560, 1994.

[2] Atkinson, A. Omnivory and feeding selectivity in five copepod species during spring in the Bellinghausen Sea, Antarctica. *ICES J Mar Sci*, 52:385–396, 1995.

[3] Atkinson, A. Subantarctic copepods in an oceanic, low chlorophyll environment: ciliate predation, food selectivity and impact on prey populations. *Mar Ecol Prog Ser*, 130:85–96, 1996.

[4] Atkinson, A. Life cycle strategies of epipelagic copepods in the Southern Ocean. *J Mar Syst*, 15(1-4):289–311, 1998.

[5] Batchelder, H.P., Edwards, C.A., and Powell, T.M. Individual-based models of copepod populations in costal upwelling regions: implications of physiologically and evironmentally influenced diel vertical migration on demograhic success and nearshore retention. *Prog Oceanogr*, 53:307–333, 2002.

[6] Bathmann, U. Ecological and biogeochemical response of Antarctic ecosystem to iron fertilization and implications on global carbon cycle. *Ocean and Polar Res*, 27:231–235, 2005.

[7] Bathmann, U. Polar ocean ecosystems and changing climate. *Antarctic Science*, -:–, submitted.

[8] Blain, S. and Trull, T. The natural fertilization experiment KEOPS (KErguelen Ocean Plateau Study: An overview). *Deep Sea Res Part II*, 55:559–565, 2008.

[9] Bollens, S.M. and Frost, B.W. Diel vertical migration in zooplankton: rapid individual response to predators. *J Plankton Res*, 13:1359–1365, 1991.

[10] Bosch, H.F. and Taylor, W.R. Diurnal vertical migration of an eustuarine cladoceran *Podon polyphemoides* in the Cheasapeake Bay. *Mar Biol*, 10:172–181, 1973.

[11] Boyd, P.W., Jickells, T., Law, C.S., Blain, S., Boyle, E.A., Buesseler, K.O., Coale, K.H., Cullen, J.J., de Baar, H.J.W., Follows, M., Harvey, M., Lancelot, C., Levasseur, M., Owens, N.P.J., Pollard, R., Rivkin, R.B., Sarmiento, J., Schoemann, V., Smetacek, V., Takeda, S., Tsuda, A., Turner, S., and Watson, A.J. Mesoscale Iron Enrichment Experiments 1993-2005: Synthesis and Future Directions. *Science*, 315(5812):612–617, 2007.

[12] Boyd, P.W. and Law, C.S. The Southern Ocean Iron RElease Experiment (SOIREE) - introduction and summary. *Deep Sea Res Part II*, 48:2425–2438, 2001.

[13] Bradford-Grieve, J.M. Colonization of the pelagic realm by calanoid copepods. *Hydrobiologia*, 485:223–244, 2002.

[14] Buchholz, F., Buchholz, C., Reppin, J., and Fischer, J. Diel vertical migration of *Meganyctiphanes norvegica* in the Kattegat: Comparision of net catches and measurements with Acoustic Doppler Current Profiler. *Helgol Meeresunters*, 49:849–866, 1995.

[15] Bundy, M.H., Gross, T.F., Vanderploeg, H.A., and Strickler, J.R. Perception of inert particle by calanoid copepods: behavioral observations and numerical model. *J Plankton Res*, 20:2129–2152, 1998.

[16] Buskey, E.J. and Swift, E. Behavioural responses of oceanic zooplankton to simulated bioluminiscence. *Biol Bull*, 168:263–275, 1985.

[17] Castellani, C., Irigoien, X., Harris, R.P., and Lampitt, R.S. Feeding and egg production of *Oithona similis* in the North Atlantic. *Mar Ecol Prog Ser*, 288:173–182, 2005.

[18] Chu, D. and Wiebe, P.H. Measurements of sound-speed and density contrasts of zooplankton in antarctic waters. *ICES J Mar Sci*, 62:818–831, 2005.

[19] Coale, K.H., Johnson, K.S., Chavez, F.P., Buesseler, K.O., Barber, R.T., Brzezinski, M.A., Cochlan, W.P., Millero, F.J., Falkowski, P., Bauer, J.E., Wanninkhof, R.H., Kudela, R.M., Altabet, M.A., Hales, B.E., Takahashi, T., Landry, M.R., Bidigare, R.R., Wang, X., Chase, Z., Strutton, P.G., Friederich, G.E., Gorbunov, M.Y., Lance, V.P., Hilting, A.K., Hiscock, M.R., Demarest, M., Hiscock, W.T., Sullivan, K.F., Tanner, S.J., Gordon, R.M., Hunter, C.N., Elrod, V.A., Fitzwater, S.E., Jones, J.L., Tozzi, S., Koblizek, M., Roberts, A.E., Herndon, J., Brewster, J., Ladizinsky, N., Smith, G., Cooper, D., Timothy, D., Brown, S.L., Selph, K.E., Sheridan, C.C., Twining, B.S., and Johnson, Z.I. Southern Ocean iron enrichment experiment: carbon cycling in high- and low-Si waters. *Science*, 304:408–414, 2004.

[20] Cohen, J.H. and Forward Jr, R.B. Photobehaviour as an inducible defense in the marine copepod *Calanopia americana*. *Limnol Oceanogr*, 50:1269–1277, 2005.

[21] Dagg, M.J., Vidal, J., Whitledge, T.E., Iverson, R.L., and Goering, J.J. The feeding, respiration, and excretion of zooplankton in the Bering Sea during a spring bloom . *Deep-Sea Res*, 29:45–63, 1982.

[22] de Baar, H.J.W., de Jong, J.T.M., Bakker, D.C.E., Löscher, B.M., Veth, C., Bathmann, U., and Smetacek, V. Importance of Iron for Phytoplankton Spring Blooms and CO2 Drawdown in the Southern Ocean. *Nature*, 373:412–415, 1995.

[23] de Baar, H.J.W., et al. Synthesis of iron fertilization experiments: From the Iron Age in the Age of Enlightenment. *J Geophys Res*, 110:C09S16, 2005.

[24] DeMott, W.R. Optimal foraging theory as a predictor of chemically mediated food selection by suspension-feeding copepods. *Limnol Oceanogr*, 34:140–154, 1989.

[25] Dussart, B.H. and Defaye, D. *Copepoda: Introduction to the Copepoda. Guides to the identification of the microinvertebtrates of the continental waters of the world.* SPB, Academic Publishing, Amsterdam, The Netherlands, 1995.

[26] Eisner, T. and Wilson, E.O. *The insects. Readings from Scientific American.* W.H. Freeman and Company, San Francisco, 1977.

[27] Emsley, S.M., Tarling, G.A., and Burrows, M.T. The effect of vertical migration strategy on retention and dispersion in the Irish Sea during spring-summer. *Fish Oceanogr*, 14(3):161–174, 2005.

[28] Falkowski, P.G., Barber, R.T., and Smetacek, V. Biogeochemical controls and feedbacks on ocean primary production. *Science*, 281:200–206, 1998.

[29] Fiers, F. and Ghenne, V. Cryptozoic copepods from belgium: diversity and biogeographic implications. *Belg J Zool* , 130:11–19, 2000.

[30] Franck, V.M., Brzezinski, M.A., Coale, K.H., and Nelson, D.M. Iron and silicic acid concentrations regulate Si uptake north and south of the Polar Frontal Zone in the Pacific Sector of the Southern Ocean. *Deep-See Res Part II*, 47:3315–3338, 2000.

[31] Froneman, P.W. and Bernard, K.S. Trophic cascading in the Polar. Frontal Zone of the Southern Ocean in austral autumn 2002. *Polar Biol*, 27:112–118, 2004.

[32] Frost, B.W. Effects of size and concentration of food particles on the feeding behaviour of the marine planktonic copepod *Calanus pacificus*. *Limnol Oceanogr*, 17:805–815, 1972.

[33] Gallienne, C.P. and Robins, D.B. Is *Oithona* the most important copepod in the worlds oceans? *J Plankton Res*, 23:1421–1432, 2001.

[34] Genin, A., Jaffe, J.S., Reef, R., Richter, C., and Franks, P.J.S. Swimming against the flow: a mechanism of zooplankton aggregation. *Science*, 308:860–862, 2005.

[35] Gonzales, H.E. and Smetacek, V. The possible role of the cyclopoid copepod *Oithona* in retarding the flux of zooplankton faecal material. *Mar Ecol Prog Ser*, 113:233–246, 1994.

[36] Goodel, A. *Behavioural evidence of color vision in the negligible image color eye (NICE) copepod Diaptomus nevadensis*. PhD thesis, Humboldt State University, 2008.

[37] Gran, H.H. On the conditions for the production of plankton in the sea. *Rapp Proc Verb Cons Int Explor Mer*, 75:37–46, 1931.

[38] Grimaldi, D. and Engel, M.S. *Evolution of the insects*. Cambridge University Press, 2005.

[39] Hardy, A.C. and Gunther, E.R. The plankton of the South Georgia whaling grounds an adjacent waters, 1926-1927. *Discovery Report*, 11:1–456, 1935.

[40] Harris, R.P. Interactions between diel vertical migratory behaviour of marine zooplankton and the subsurface chlorophyll maximum. *Bull Mar Sci*, 43:663–674, 1988.

[41] Hart, T.J. On the phytoplankton of the southwest Atlantic and the Bellingshausen Sea 1921-31. *Discovery Reports*, VIII:1–268, 1934.

[42] Hays, G.C. A review of the adaptive significance and ecosystem consequences of zooplankton diel vertical migrations. *Hydrobiologia*, 503:163–170, 2003.

[43] Henjes, J., Assmy, P., Klaas, C., Verity, P., and Smetacek, V. Response of microzooplankton (protists and small copepods) to an iron-induced phytoplankton bloom in the Southern Ocean (EisenEx). *Deep-Sea Res Part I*, 54:363–384, 2007.

[44] Heptner, M.V. and Ivanenko, V.N. Copepoda (crustacea: Copepoda) of hydrothermal ecosystems of the world ocean. *Arthropoda Selecta*, 11:117–134, 2002.

[45] Hill, A.E. Diel vertical migration in stratified tidal flows: Implications for plankton dispersal. *J Mar Res*, 56:1069–1096, 1998.

[46] Hoddel, R.J., Crossley, A.C., Williams, R., and Hosie, G.W. The distribution of Antarctic fish and larvae (CCAMLR division 58.4.1). *Deep-Sea Res Part II*, 47:2519–2541, 2000.

[47] Hoffmann, L.J., Peeken, I., and Lochte, K. Iron, silicate, and light co-limitation of three Southern Ocean diatom species. *Polar Biol*, 31:1067–1080, 2008.

[48] Hopkins, T.L. Food web of an Antarctic midwater ecosystem. *Mar Biol*, 89:197–212, 1985.

[49] Hopkins, T.L. Midwater food web in Mc Murdo Sound, Ross Sea, Antarctica. *Mar Biol*, 96:93–106, 1987.

[50] Hopkins, T.L. and Torres, J.J. Midwater food web in the vicinity of a marginal ice zone in the western Weddel Sea. *Deep-Sea Res*, 36:542–560, 1989.

[51] Huys, R. and Boxhal,l G.A. *Copepod evolution*. The Ray Society, London, p. 468, 1991.

[52] Irigoien, X., Conway, D.V.P., and Harris, R.P. Flexible diel vertical migration behaviour of zooplankton in the Irish Sea. *Mar Ecol Prog Ser*, 267:85–97, 2004.

[53] Isaac, J.D., Tont, S.A., and Wick, G.L. Deep Scattering Layers: vertical migration as a tactic to finding food. *Deep-Sea Res*, 21:651–656, 1974.

[54] Jansen, S., Klaas, C., Krägefsky, S., Harbou, L.v., and Bathmann, U. Reproductive response of the copepod *Rhincalanus gigas* to an iron-induced phytoplankton bloom in the Southern Ocean. *Polar Biol*, 29:1039–1044, 2006.

[55] Jickells, T.D., An, Z.S., Andersen, K.K., Baker, A.R., Bergametti, G., Brooks, N., Cao, J.J., Boyd, P.W., Duce, R.A., Hunter, K.A., Kawahata, H., Kubilay, N., la Roche, J.O., Liss,P.S., Mahowald, N., Prospero, J.M., Ridgwell,A.J., Tegen, I., and Torres, R. Global iron connections between desert dust, ocean biogeochemistry, and climate. *Science*, 308:67–71, 2005.

[56] Johnson, T.B. and Terazaki, M. Chaetognath ecology in relation to hydrographic conditions in the Australian sector of the Southern Ocean. *Polar Biosci*, 17:1–15, 2004.

[57] Kaartvedt, S., Olsen, E., and Jørstad, T. Effects of copepod foranging behaviour on predation risk: An experimental study of the predatory copepod *Paraeuchaeta norvegica* feeding on *Acartia clausi* and *A. tonsa* (copepoda). *Limnol Oceanogr*, 42(1):164–170, 1996.

[58] Kattner, G., Albers, C., Graeve, M., and Schnack-Schiel, S.B. Fatty acid and alcohol composition of small polar copepods, *Oithona* and *Oncaea*: indication on feeding modes. *Polar Biol*, 26:666–671, 2003.

[59] Kimmerer, W.J. and McKinnon, A.D. Zooplankton in a marine bay. II. Vertical migration to maintain horizontal distribution. *Mar Ecol Prog Ser*, 41:53–60, 1987.

[60] Kiørboe, T., Saiz, E., and Viitaaslo, M. Prey switching behaviour in the planktonic copepod *Acartia tonsa*. *Mar Ecol Prog Ser*, 143:65–75, 1996.

[61] Klaas, C. Spring distribution of larger (>64 μm) protozoans in the Atlantic sector of the Southern Ocean. *Deep Sea Res Part I*, 48:1627–1649, 2001.

[62] Kleppel, G.S. On the diets of calanoid copepods. *Mar Ecol Prog Ser*, 99:183–195, 1993.

[63] Lampitt, M.R. Carnivorous feeding by a small marine copepod. *Limnol Oceanogr*, 23:1228–1230, 1978.

[64] Longhurst, A. The structure and evolution of plankton communities. *Progr Oceanogr*, 15:1–35, 1985.

[65] Marcotte, B.M. Turbidity, arthropods and the evolution of perception: toward a new paradigm of marine phanerozoic diversity. *Mar Ecol Prog Ser*, 191:267–288, 1999.

[66] Martin, J.H., Gordon, R.M., and Fitzwater, S.E. Iron in Antarctic waters. *Nature*, 345:156–158, 1990.

[67] Michels, J. and Schnack-Schie, S.B. Feeding in dominant Antarctic copepods - does the morphology of the mandibular gnathobases relate to diet. *Marine Biology*, 146:483–495, 2005.

[68] Mitchell, B.G., Brody, E.A., Holm-Hansen, O., McClain, C.R., and Bishop, J. Light limitation of phytoplankton biomass and macro-nutrient utilization in the Southern Ocean. *Limnol Oceanogr*, 36:1662–1677, 1992.

[69] Moore, J.K. and Abbott, M.R. Phytoplankton chlorophyll distributions and primary production in the Southern Ocean. *J Geophys Res*, 105:28709–28722, 2000.

[70] Moore, J.K. and Abbott, M.R. Surface chlorophyll concentrations in relation to the Antarctic Polar Front: seasonal and spatial patterns from satellite observations. *J Mar Syst*, 37(1-3):69–86, 2002.

[71] Morales-Nin, B., Palomera, I., and Schadwinkel, S. Larval fish distribution in the Antarctic Peninsula region and adjacent waters. *Polar Biol*, 15:143–154, 1995.

[72] Mumm, N. Composition and distribution of mesozooplankton in the Nansen Basin, Arctic Ocean, during summer. *Polar Biol*, 13:451–461, 1993.

[73] Neil, W.E. Induced vertical migration in copepods as a defence against invertebrate predation. *Nature*, 345:524–526, 1990.

[74] Ohmann, M.D., Frost, B.W., and Cohen, E.H. Reverse diel vertical migration - an escape from invertebrate predators. *Science*, 220:1404–1407, 1983.

[75] Orsi, A.H., Whitworth III, T., and Nowlin Jr., W.D. On the meridional extent and fronts of the Antarctic Circumpolar Current. *Deep-Sea Res*, 42:641– 673, 1995.

[76] Paffenhöfer, G.A. and Van Sant, K.B. The feeding response of marine planktonic coepepods to quantity and qualitity of particles. *Mar Ecol Prog Ser*, 27:55–65, 1985.

[77] Pakhomov, E.A., Perissinotto, R., McQuaid, C.D., and Froneman, P.W. Zooplankton structure and grazing in the Atlantic sector of the Southern Ocean in late austral summer 1993. Part 1. Ecological zonation. *Deep-Sea Res Part I*, 47:1663–1686, 2000.

[78] Pakhomov, E.A., Perssinotto, R., and Froneman, P.W. Predation impact of carnivorous macrozooplankton and micronekton in the Atlantic sector of the Southern Ocean. *J Mar Syst*, 19:47–64, 1999.

[79] Pasternak, A.F. and Schnack-Schiel, S.B. Seasonal feeding patterns of the dominant Antarctic copepods *Calanus propinquus* and *Calanoides acutus* in the Weddell Sea. *Polar Biol*, 24:771–784, 2001a.

[80] Pasternak, A.F. and Schnack-Schiel, S.B. Feeding patterns of dominant Antarctic copepods: an interplay of diapause, selectivity, and availability of food. *Hydrobiologia*, 453/454:25–36, 2001b.

[81] Pasternak, A.F. and Schnack-Schiel, S.B. Feeding of *Ctenocalanus citer* in the eastern Weddell Sea: low in summer and spring, high in autumn and winter. *Polar Biol*, 30:493–501, 2007.

[82] Pearre, S.Jr. Eat and run? The hunger satiation hypothesis in vertical migration: history, evidence and consequences. *Biol Rev*, 78:1–79, 2003.

[83] Peterson, W.T., Miller, C.B., and Hituchinson, A. Zonation and maintenance of copepod populations in the Oregon upwelling zone. *Deep-Sea Res*, 26A:467–494, 1978.

[84] Platt, T., Sathyendranath, S., White III, G.N., and Ravindran, P. Attenuation of visible light by phytoplankton in a vertically structured ocean: solutions and applications. *J Plankton Res*, 16:1461–1487, 1994.

[85] Pollard, R.T., Lucas, M.I., and Read, J.F. Physical controls of biogeochemical zonation in the Southern Ocean. *Deep-Sea Res II*, 49:3289–3305, 2002.

[86] Prince, H.J. and Pfaffenhöfer, G.-A. Effects of concentrations on the feeding of a marine copepod in algal monocultures and mixtures. *J Plankton Res*, 8:119–128, 1986.

[87] Ragni, M. and D'Alcala, M.B. Light as an information carrier underwater. *J Plankton Res*, 26:433–443, 2004.

[88] Raiswell, R., Benning, L.G., Tranter, M., and Tulaczyk, S. Bioavailable iron in the Southern Ocean: the significance of the iceberg conveyor belt. *Geochem Trans*, 9:1–9, 2008.

[89] Sarmiento, J.L., Gruber, N., Brzezinsk, M.A., and Dunne, J.P. High-latitude controls of thermocline nutrients and low latitude biological productivity. *Nature*, 427:56–60, 2004.

[90] Schminke, H.K. Entomology for the copepodologist. *J Plankton Res*, 29:i149–i162, 2007.

[91] Schnack-Schiel, S.B. Aspects of the study of the life cycles of Antarctic copepods. *Hydrobiologia*, 453/454:9–24, 2001a.

[92] Schnack-Schiel, S.B., Dieckmann, G.S., Gradinger, R., Melnikov, I.A., Spindler, M., and Thomas, D.N. Meiofauna in sea ice of the Weddell Sea (Antarctica). *Polar Biol*, 24:724 – 728, 2001b.

[93] Schultes, S. *The Role of zooplankton grazing in the biogeochemical cycle of silicon in the Southern Ocean*. PhD thesis, University Bremen, 2004.

[94] Schultes, S., Verity, P.G., and Bathmann, U. Copepod grazing during an iron-induced diatom-bloom in the Antarctic Circumpolar Current (EisenEx):

I. Feeding patterns and grazing impact on prey populations. *J Exp Mar Biol Ecol*, 338:16–34, 2006.

[95] Shreeve, R.S., Ward, P., and Whitehouse, M.J. Copepod growth and development around South Georgia: relationships with temperature, food and krill. *Mar Ecol Prog Ser*, 233:169–183, 2002.

[96] Smetacek, V. EisenEx: International Team Conducts Iron Experiment In Southern Ocean. *U.S. JGOFS Newsletter*, 40482:–, 2001.

[97] Smetacek, V., Assmy, P., and Henjes, J. The role grazing in structuring Southern Ocean pelagic ecosystem and biogeochemical cycles. *Antarctic Science*, 16:541–558, 2004.

[98] Smetacek, V., Scharek, R., and Nöthig, E.M. Seasonal and regional variation in the pelagial and its relationship to the life history cycle of krill. In K. Kerry and G. Hempel, editors, *Antartic ecosystems: Ecologyial change and conservation*, pages 103–114. Springer Verlag, Berlin, 1990.

[99] Smetacek, V., Strass, V. H., Klass, C., Assmy, P., Cisewski, B., Savoye, N., Henjes, J., Bathmann,U., Bellerby, R., Berg, G.M., Croot, P., Friedrich, L., Gonzalez, S., Harbou, L.v., Herndl, G.J., Hoffmann, L., Jansen, S., Krägefsky, S., Latasa, M., Leach, H., Losch, M., Mills, M.M., Montresor, M., Neill, C., Passow, U., Peeken, I., Röttgers, R., Scharek, R., Terbrüggen, A., Webb, A., and Wolf-Gladrow, D. Massive carbon flux to the deep sea from an iron-fertilized phytoplankton bloom in the Southern Ocean. *in prep.*, -:–, -.

[100] Stearns, D.E. and Forward, R.B. Photosensitivity of the calanoid copepod *Arcatia tonsa*. *Mar Biol*, 82:85–89, 1984.

[101] Straile, D. Gross growth efficiencies of protozoan and metazoan zooplankton and their dependence on food concentration, predaor-prey weight ratio, and taxonomic group. *Limnol Oceanogr*, 42:1375–1385, 1997.

[102] Strass, V.H., Naveira Garabato, A.C., Pollard, R.T., Fischer, H.I., Hense, I., Allen, J.T., Read, J.F., Leach, H., and Smetacek, V. Mesoscale frontal dynamics: shaping the environment of primary production in the Antarctic Circumpolar Current. *Deep-Sea Res Part II*, 49:3735–3769, 2002.

[103] Sullivan, C.W., Arrigo, K.R., McClain, C.R., Comiso, J.C., and Firestone, J. Distributions of of Phytoplankton Blooms in the Southern Ocean. *Science*, 262:1832 – 1837, 1993.

[104] Tilzer, M.M., Gieskes, W.W., Heusel, N., and Fenton, R. The impact of phytoplankton on spectral water transparency in the Southern Ocean: implications for primary productivity. *Polar Biol*, 14:127–136, 1994.

[105] Timmermans, K.R., Davey M.S., Wagt, B.v d., Snoek, J., Geider, R.J., Veldhuis, M.J.W., Gerringa, L.J.A., and deBaar, H.J.W. Co-limitation by iron and light of *Chaetoceros brevis*, *C. dichaeta* and *C. calcitrans* (Bacillariophyceae). *Mar Ecol Prog Ser*, 217:287–297, 2001.

[106] Tiselius, P. and Jonsson, P. R. Foranging behaviour of six calanoid copepods: observations and hydromechanic analysis. *Mar Ecol Prog Ser*, 66:23–33, 1990.

[107] Tsuda, A. et al. Evidence for the grazing hypothesis: Grazing reduces phytoplankton responses of the HNLC ecosystem to iron enrichment in the western subarctic pacific (SEEDS II). *J Oceanogr*, 63:983–994, 2007.

[108] Vaissere, R. Morphologie et histologie comparees des yeux des crustaces copepodes. *Arch Zool Exp Gen*, 100:1–125, 1961.

[109] van Duren, L.A and Videler, J.J. Escape from viscosity: the kinematics and hydrodynamis of copepod foraging and escape swimming. *J Exp Biol*, 206:269–279, 2003.

[110] Verity, P.G. and Smetacek, V. Organism life cycles, predation, and the structure of marine pelagic ecosystems. *Mar Ecol Prog Ser*, 130:277–293, 1996.

[111] Visser, A.W. Hydromechanical signals in the plankton. *Mar Ecol Prog Ser*, 222:1–24, 2001.

[112] Voronina, N.M. Comparative abundance and distribution of major filter-feeders in the antarctic pelagic zone. *J Mar Syst*, 17(1-4):375–390, 1998.

[113] Ward, P. and Hirst, A.G. *Oithona similis* in a high latitude ecosystem: abundance, distribution and temperature limitation of fecundity rates in a sac spawning copepod. *Mar Biol*, 151:1099–1110, 2007.

[114] Yen, J. Life in transition: balancing inertial and viscous forces by planktonic copepods. *Biol Bull*, 198:213–224, 2000.

[115] Zeldis, J. Mesozooplankton community composition, feeding and export production during SOIREE. *Deep-Sea Res Part II*, 48:2615–2634, 2001.